UNIVERSITAT ROVIRA I VIRGILI

ASSEMBLY AND PROPERTIES OF POLYOXOMETALATES: A THEORETICAL POINT OF VIEW

Laia Vilà Nadal

ISBN: 978-84-694-2170-3
Dipòsit Legal: T. 1039-2011

UNIVERSITAT ROVIRA I VIRGILI
ASSEMBLY AND PROPERTIES OF POLYOXOMETALATES: A THEORETICAL POINT OF VIEW
Laia Vilà Nadal
ISBN.978-84-694-2170-3/DL:T. 1039-2011

Departament de Química Física i Inorgànica

UNIVERSITAT ROVIRA I VIRGILI

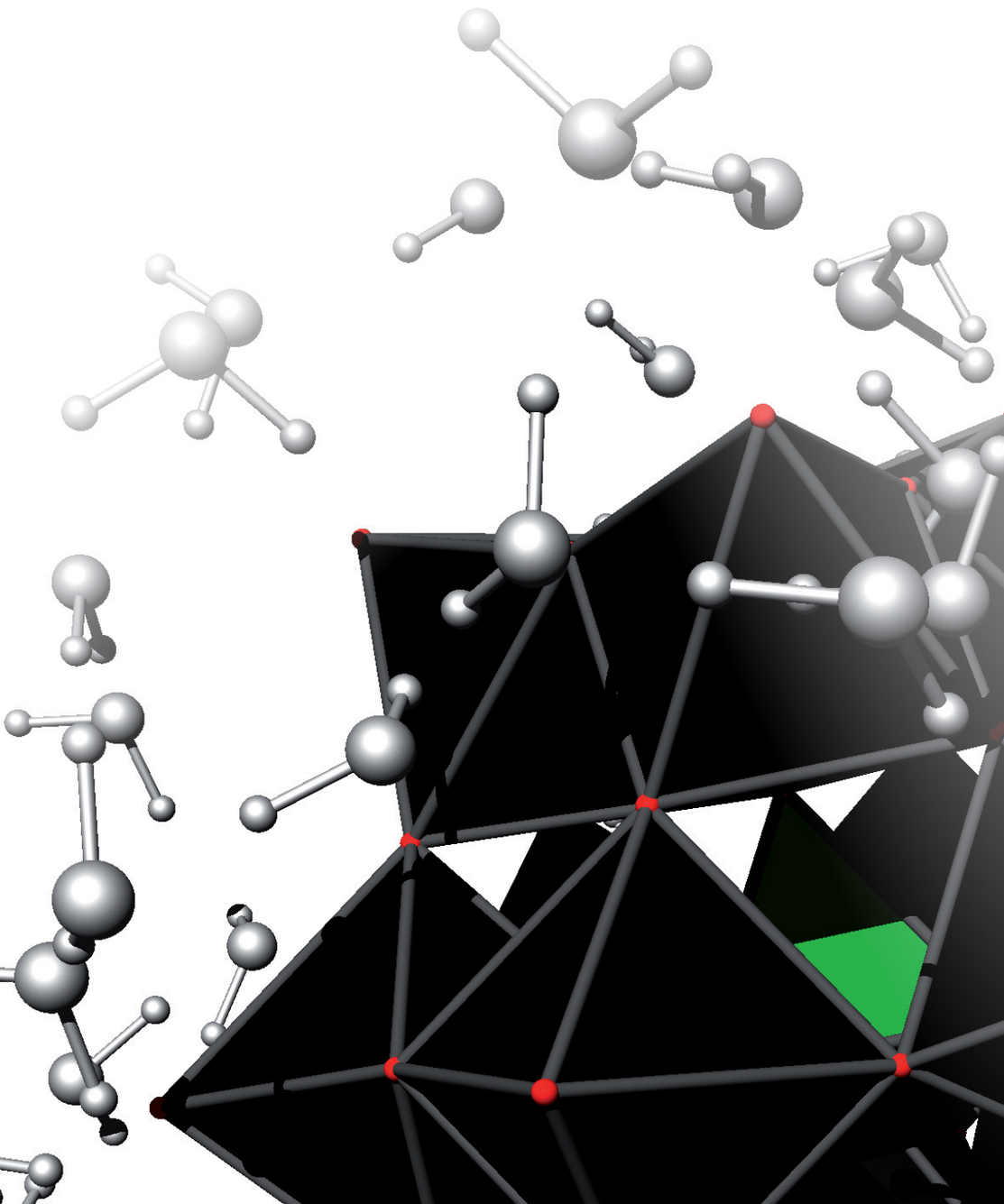

Doctoral thesis
Laia Vilà Nadal

ASSEMBLY AND PROPERTIES OF POLYOXOMETALATES:
A THEORETICAL POINT OF VIEW

Doctoral thesis

ASSEMBLY AND PROPERTIES OF POLYOXOMETALATES:

A THEORETICAL POINT OF VIEW

Laia Vilà Nadal

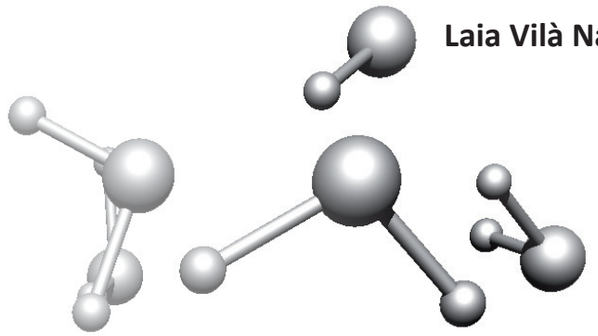

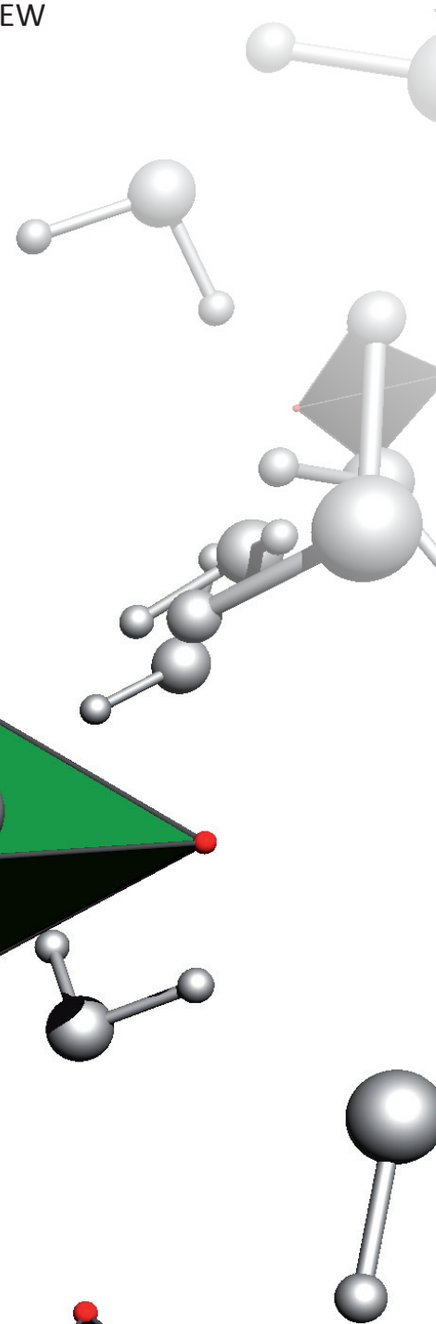

UNIVERSITAT ROVIRA I VIRGILI

UNIVERSITAT ROVIRA I VIRGILI
ASSEMBLY AND PROPERTIES OF POLYOXOMETALATES: A THEORETICAL POINT OF VIEW
Laia Vilà Nadal
ISBN.978-84-694-2170-3/DL:T. 1039-2011

UNIVERSITAT ROVIRA I VIRGILI
ASSEMBLY AND PROPERTIES OF POLYOXOMETALATES: A THEORETICAL POINT OF VIEW
Laia Vilà Nadal
ISBN.978-84-694-2170-3/DL:T. 1039-2011

UNIVERSITAT ROVIRA I VIRGILI
ASSEMBLY AND PROPERTIES OF POLYOXOMETALATES: A THEORETICAL POINT OF VIEW
Laia Vilà Nadal
ISBN.978-84-694-2170-3/DL:T. 1039-2011

Laia Vilà Nadal

ASSEMBLY AND PROPERTIES OF POLYOXOMETALATES:

A THEORETICAL POINT OF VIEW

Doctoral thesis

Supervised by

Prof. Josep Maria Poblet and Dr. Antonio Rodríguez Fortea

Departament de Química Física i Inorgànica

UNIVERSITAT ROVIRA I VIRGILI

Tarragona
Febrer 2011

UNIVERSITAT ROVIRA I VIRGILI
ASSEMBLY AND PROPERTIES OF POLYOXOMETALATES: A THEORETICAL POINT OF VIEW
Laia Vilà Nadal
ISBN.978-84-694-2170-3/DL:T. 1039-2011

UNIVERSITAT ROVIRA I VIRGILI
ASSEMBLY AND PROPERTIES OF POLYOXOMETALATES: A THEORETICAL POINT OF VIEW
Laia Vilà Nadal
ISBN.978-84-694-2170-3/DL:T. 1039-2011

Josep Maria Poblet Rius, catedràtic de Química Física i Antonio Rodríguez Fortea, investigador Ramón y Cajal, del Departament de Química Física i Inorgànica de la Universitat Rovira i Virgili,

Fem constar que la present memòria, que porta per títol:

ASSEMBLY AND PROPERTIES OF POLYOXOMETALATES:

A THEORETICAL POINT OF VIEW

que presenta Laia Vilà Nadal per a obtenir el Grau de Doctora en Química, ha estat realitzada sota la nostra direcció al Departament de Química Física i Inorgànica de la Universitat Rovira i Virgili. El treball compleix els requeriments per poder optar a Menció Europea.

Tarragona, febrer de 2011

Josep Maria Poblet Rius

Antonio Rodríguez Fortea

UNIVERSITAT ROVIRA I VIRGILI
ASSEMBLY AND PROPERTIES OF POLYOXOMETALATES: A THEORETICAL POINT OF VIEW
Laia Vilà Nadal
ISBN.978-84-694-2170-3/DL:T. 1039-2011

UNIVERSITAT ROVIRA I VIRGILI
ASSEMBLY AND PROPERTIES OF POLYOXOMETALATES: A THEORETICAL POINT OF VIEW
Laia Vilà Nadal
ISBN.978-84-694-2170-3/DL:T. 1039-2011

Agraïments

La realització d'aquesta tesi no hauria estat possible sense els consells, la paciència i la motivació per part del Prof. Josep Maria Poblet i del Dr. Antonio Rodríguez Fortea.

També vull agrair als membres del Grup de Química Quàntica que d'alguna manera o altra han estat partíceps en l'elaboració d'aquesta tesi: Prof. Rosa Caballol Lorenzo, Prof. Josep Manel Ricart, Dr. Carles Bo, Dra. Anna M. Clotet, Dr. Joan Igual, Dra. M. Del Mar Reguero, Dr. Jordi Carbó, Dr. Cornelis De Graaf, Dr. Xavier López, Dra. Maria Angels Carvajal, Dr. Nuno Guerreiro.

Una menció especial als tècnics informàtics que han estat uns excel·lents metges del meu ordinador i la meva salvació una infinitat de vegades: Elisenda Mas, Moisès Álvarez i José Carlos Ortiz.

La recerca és un món extremadament dinàmic, durant aquest quatre anys han passat pel departament moltes persones. Des d'aquí vull donar les gràcies a tots aquells que han estat els meus companys: Dra. Susana Romo, Dra Eva Santos, Dr. Benjamí Martorell, Dr. Gerard Novell, Dr. Alberto Roldán, Nadya Antonova, Yannick Mercier, Jorge A. Fernández, David Taratiel, Núria Queralt, Ramón Valencia, Xavier Aparicio, Sonia Aguado Ullate, Núria Alegret, Pablo Aparicio, Gian Giacomo Asara, Jéssica Cid, Alex Domingo, Pablo Jimenez, Alejandro Jimenez, Marc Mulet Gas, Igor Negodaev, Mireia Segado, Zahra Tabookht, John Zapata, Pere Miró. Per acabar demano disculpes per si algú s'ha sentit omès en aquests agraïments, i faig extensiu l'agraïment a totes les persones amb les qui he tingut el plaer de compartir feina, docència, conferències, cursos, seminaris, etc. A tots ells moltes gràcies.

I would also like to acknowledge here Prof. Cronin and his group for the warm welcome I received in Glasgow. I improved both my English and my research skills.

UNIVERSITAT ROVIRA I VIRGILI
ASSEMBLY AND PROPERTIES OF POLYOXOMETALATES: A THEORETICAL POINT OF VIEW
Laia Vilà Nadal
ISBN.978-84-694-2170-3/DL:T. 1039-2011

I would like to specially thank: Dr. Haralampos Miras, Dr Scott Mitchell, Mali Husby Rosnes, Thomas McGlorne and Neus Corella. I felt like a glasgowegian...

El mes de febrer de 2007 vaig tenir el plaer de compartir els Cursos de Doctorat a Santander amb uns companys excepcionals: Miquel Huix, Anna Díaz, Juan José Nogueirar, Ceila Margarita Fong, Elisa Isabel Martín, Pablo G. Jambrina y Silvia Bouzón. Com tots sabeu aquell mes va marcar un punt d'infleixó. Hubo un antes y un después...

També vull agrair als meus amics esplaierus: Rosa Martí, Joan Figuerola, Joan Bové, Marc Físico, Míriam París, Míriam Magre i Pep Ventura. Per la paciència que han tingut intentant entendre els "polioxoquè?" i tots els grans moments que hem viscut junts! Gràcies.

A Vanesa Chavarria, Patrícia Cózar, Laura Escorihuela i Lídia Vernet. Per tot el que hem compartit, per la nostra química i perquè cada vegada que ens reunim sembla que no passi el temps.

A la Gemma Marsal, gràcies per la teva amistat sincera, per les nostres xerrades i per tot el que hem compartit des d'aquelles primeres pràctiques juntes. Ja ho va dir Francis Bacon "L'amistat duplica les alegries i divideix les angoixes per la meitat."

Als meus pares Ramon i Maria Teresa per els valors que m'han transmès, perquè sempre m'han encoratjat a anar més lluny, a superar les adversitats i no tenir mai por als nous reptes.

Als meus germans Gemma i Albert per ser el millor equip i la millor afició, tots tres som més que un Club. Tampoc vull oblidar a la Maria i en Josep que ja són socis i membres de la junta de direcció.

A tu Felix, ni una sola frase està escrita sense pensar en tu, ni un sol paràgraf sense parlar de nosaltres i ni una sola pàgina és del tot meva. Junts.

UNIVERSITAT ROVIRA I VIRGILI
ASSEMBLY AND PROPERTIES OF POLYOXOMETALATES: A THEORETICAL POINT OF VIEW
Laia Vilà Nadal
ISBN.978-84-694-2170-3/DL:T. 1039-2011

A Felix

UNIVERSITAT ROVIRA I VIRGILI
ASSEMBLY AND PROPERTIES OF POLYOXOMETALATES: A THEORETICAL POINT OF VIEW
Laia Vilà Nadal
ISBN.978-84-694-2170-3/DL:T. 1039-2011

UNIVERSITAT ROVIRA I VIRGILI
ASSEMBLY AND PROPERTIES OF POLYOXOMETALATES: A THEORETICAL POINT OF VIEW
Laia Vilà Nadal
ISBN.978-84-694-2170-3/DL:T. 1039-2011

Contents

UNIVERSITAT ROVIRA I VIRGILI
ASSEMBLY AND PROPERTIES OF POLYOXOMETALATES: A THEORETICAL POINT OF VIEW
Laia Vilà Nadal
ISBN.978-84-694-2170-3/DL:T. 1039-2011

UNIVERSITAT ROVIRA I VIRGILI
ASSEMBLY AND PROPERTIES OF POLYOXOMETALATES: A THEORETICAL POINT OF VIEW
Laia Vilà Nadal
ISBN.978-84-694-2170-3/DL:T. 1039-2011

UNIVERSITAT ROVIRA I VIRGILI
ASSEMBLY AND PROPERTIES OF POLYOXOMETALATES: A THEORETICAL POINT OF VIEW
Laia Vilà Nadal
ISBN.978-84-694-2170-3/DL:T. 1039-2011

UNIVERSITAT ROVIRA I VIRGILI
ASSEMBLY AND PROPERTIES OF POLYOXOMETALATES: A THEORETICAL POINT OF VIEW
Laia Vilà Nadal
ISBN.978-84-694-2170-3/DL:T. 1039-2011

Resum

Conèixer els mecanismes de formació de compostos químics és una tasca àrdua. El camí que condueix a la formació d'un cert compost, ja sigui orgànic o inorgànic, és rarament evident. Així dons, per la majoria dels casos, és necessari un llarg treball d'investigació. Conèixer un mecanisme de reacció implica conèixer el conjunt d'etapes en les quals es desenvolupa una reacció química. Cal anar més enllà d'una reacció química expressada en forma d'equació igualada: $A+B \rightarrow C$, en la qual només estem veient el resum del procés de transformació de reactius en productes. Fent un símil quotidià: és com si veiéssim només el punt de sortida i el punt d'arribada en un viatge. Per conèixer els detalls a través dels quals la reacció va avançant, haurem d'estudiar el mecanisme. En aquesta tesi s'han estudiat els mecanismes de formació dels òxids de tungstè i molibdè, coneguts pel nom de polioxometal·lats (POMs). La Termodinàmica ens ha ajudat a descriure els aspectes energètics de les reaccions estudiades: ens ha descrit si la reacció era o no favorable, des del punt de vista energètic si era espontània o no. En aquesta tesi també s'han estudiat altres propietats rellevants dels POMs com ara els seus isòmers i la predicció de senyals de RMN (Ressonància Magnètica Nuclear). Les següents línies són una breu introducció a la química dels polioxometal·lats, així com un resum dels principals objectius de la tesi.

UNIVERSITAT ROVIRA I VIRGILI
ASSEMBLY AND PROPERTIES OF POLYOXOMETALATES: A THEORETICAL POINT OF VIEW
Laia Vilà Nadal
ISBN.978-84-694-2170-3/DL:T. 1039-2011

Un els aspectes més importants en la química del Mo i del W és la formació d'un gran nombre de poliàcids i de les seves respectives sals. Els poliàcids poden dividir-se en dos tipus, en isopoliàcids i els seus anions associats que contenen Mo o W a més a més d'oxigen; i els heteropolianions, que contenen a més a més algun altre tipus d'element.

Tots els polianions contenen grups MO_6, per tant la formació d'un polianió requereix un canvi de coordinació tetraèdrica en els productes de partida ($[MoO_4]^{2-}$ o $[WO_4]^{2-}$) a octaèdrica en el complex. L'objectiu inicial d'aquesta tesi fou l'estudi teòric del procés de formació del polianió més senzill $[W_6O_{19}]^{2-}$. També es van voler identificar les espècies més estables presents en solució. L'èxit obtingut en la primera etapa va fer que ens plantegéssim nous reptes, d'aquesta manera vam voler estudiar la formació d'altres polianions com ara $[Mo_6O_{19}]^{2-}$ i els heteropolianions $[XM_{12}O_{40}]^{q-}$ (X=P, As, M=W, Mo).

Breu perspectiva històrica

Va ser l'any 1826 quan Berzelius va descriure el primer polioxometal·lat (POM) de fórmula $[PMo_{12}O_{40}]^{3-}$. Més endavant, l'any 1862, Marignac va descriure les composicions analítiques dels compostos d'àcid tungstosilícic i les seves sals. A partir d'aquell moment i durant la primera dècada del segle XX es van poder descriure una seixantena de diferents tipus d'heteropoliàcids. Els primers intents per tal d'explicar la composició dels heteropolianions es van basar en la teoria de coordinació de Werner. Durant les primeres dècades del segle XX, es van anar desenvolupant teories per tal d'explicar la coordinació dels metalls.

L'ús de tècniques espectroscòpiques va ser clau a l'hora de caracteritzar els compostos. Als inicis de la dècada del 1930 Keggin va resoldre l'estructura de $H_3PW_{12}O_{40}\cdot 5H_2O$ mitjançant difracció de RX. Keggin va demostrar que l'estructura del

UNIVERSITAT ROVIRA I VIRGILI
ASSEMBLY AND PROPERTIES OF POLYOXOMETALATES: A THEORETICAL POINT OF VIEW
Laia Vilà Nadal
ISBN.978-84-694-2170-3/DL:T. 1039-2011

compost es basava en unitats octaèdriques de WO_6 unides compartint arestes i costats.

Avui en dia els POMs constitueixen una gran família de compostos, entre els que cal destacar els clústers formats per Mo, W o V i mescles d'aquests elements. El seu gran interès rau en la seva capacitat d'oxidar ja que fàcilment poden acceptar un o més electrons amb un mínim canvi estructural. Cal destacar també el seu ús potencial en camps com la medicina, poden ser usats com a biomolècules; en la catàlisi, són capaços de catalitzar reaccions orgàniques donant bones selectivitats i rendiments o bé el seu ús com a blanquejants de fusta i de paper.

Principals estructures dels Polioxometal·lats

L'estructura dels POMs es basa en un àtom metàl·lic central, M, rodejat per un àtom o un grup d'àtoms. El lligand més habitual és l'oxigen tot i que també hi ha alguns derivats amb lligands S, F i Br i altres elements del grup p. En general tindrem unitats MO_n, n ens indica el nombre de coordinació de M. Normalment n=6, tot i què també pot ser 4, 5 o 7. D'altra banda, en un POM a part de M i O podem tenir altres elements que els anomenarem X. Depenent de si X és o no és present podrem distingir dos tipus de POMs. Aquesta classificació és merament estructural:

Isopolianions (IPAs) $[M_nO_y]^{p-}$ (1)

Heteropolianions (HPAs) $[X_zM_nO_y]^{q-}$, on $z \leq n$ (2)

Per definició no hi ha limitacions químiques per X o M. Pel que fa X se sol anomenar element primari, central o bé heteroàtom. No hi ha cap requeriment físic per poder ocupar aquesta posició, i en general, qualsevol element pot participar com a X en un POM. La Figura 1 ens presenta l'estructura dels anions anomenats Lindqvist $[M_6O_{19}]^{q-}$, Keggin $[XM_{12}O_{40}]^{q-}$ i Dawson $[X_2M_{18}O_{60}]^{q-}$.

UNIVERSITAT ROVIRA I VIRGILI
ASSEMBLY AND PROPERTIES OF POLYOXOMETALATES: A THEORETICAL POINT OF VIEW
Laia Vilà Nadal
ISBN.978-84-694-2170-3/DL:T. 1039-2011

D'altra banda M se l'anomena element secundari, perifèric o addenda (apèndix). M és normalment Mo o W, i en menor freqüència V, Nb, Ta, o bé mescles d'aquests elements. Aquests metalls es troben amb el seu estat d'oxidació més elevat (d^0 o bé d^1). L'estructura bàsica, tot i que no la única, que trobem en els POMs és un metall coordinat quasi octaèdricament.

No hem de fer cas, però, a la simplicitat de les formules (1) i (2) ja que la composició dels clústers pot ser molt complexa, amb diversos elements M formant part de l'estructura. L'entitat estructural més important en un POM és l'àtom metàl·lic M. Com hem dit anteriorment el bloc estructural fonamental en un POM és l'unitat MO_6, on M és un metall de transició. Tot i que molts metalls poden formar compostos octaèdrics coordinant-se amb l'oxigen, no hi ha gaires metalls que puguin formar part de l'estructura d'un POM. Els principis electrostàtics i de radi iònic ens regeixen l'estabilitat de les estructures polianiòniques. Per aquesta raó només trobem uns determinats valors de càrrega/radi en els M^{n+} combinats amb lligands O^{2-} formant part dels POMs.

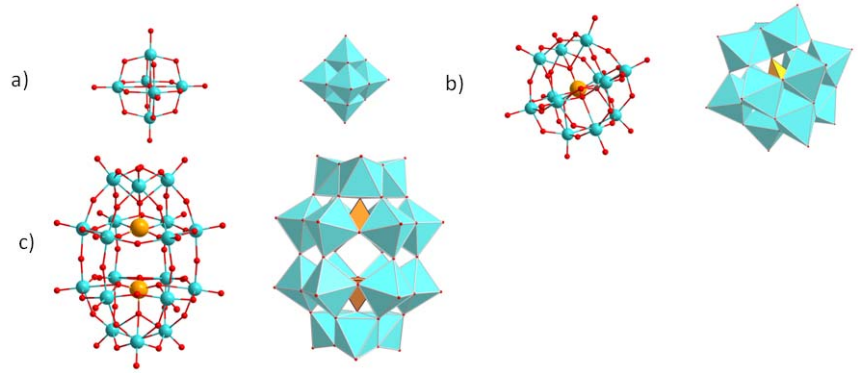

Figura 1. Representacions *ball-and-stick, esquerra* i polièdriques, dreta: a) l'anió de Lindqvist $[M_6O_{19}]^{n-}$, b) l'anió de Keggin $[\{XO_4\}M_{12}O_{36}]^{n-}$ Keggin, c) l'anió de Wells-Dawson $[\{XO_4\}_2M_{18}O_{54}]^{n-}$. (Les esferes vermelles són àtoms d'oxigen, les esferes turquesa són els centres metàl·lics i finalment l'esfera taronja representa l'heteroàtom, s'ha utilitzat el mateix codi de color per la representació polièdrica).

UNIVERSITAT ROVIRA I VIRGILI
ASSEMBLY AND PROPERTIES OF POLYOXOMETALATES: A THEORETICAL POINT OF VIEW
Laia Vilà Nadal
ISBN.978-84-694-2170-3/DL:T. 1039-2011

Unitats estrucurals

Podem caracteritzar els polioxometal·lats com a unions de políedres que comparteixen arestes, costats, i en menor freqüència, cares. De fet podem considerar els POMs com a estructures formades per unitats piramidals MO_5 i octaèdriques MO_6. Aquestes entitats són les unitats estructurals bàsiques dels POMs, d'alguna manera similars a l'unitat $–CH_2–$ en química orgànica. Tal i com podem apreciar a la Figura 2, el metall es troba desplaçat del centre geomètric del políedre cap a un dels oxígens.

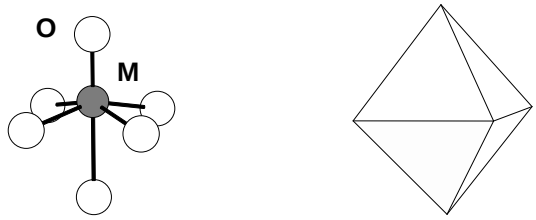

Figura 2. Unitat fonamental MO_6 representada de forma ball-and-stick esquerra i de forma polièdrica, dreta. Cada costat del políedre representa un oxigen.

Tal i com hem vist a la Figura 1, les unitats MO_6 es van unint l'una amb l'altra seguint una sèrie de normes i poden formar infinitat de formes compactes. Les unions més estables es formen quan els octàedres comparteixen costats o arestes. En aquest tipus d'unitats els ions M^{n+} es troben suficientment allunyats els uns dels altres i s'eviten repulsions. La Figura 3 presenta els models polièdrics que representen les tres possibles unions entre dues unitats octaèdriques MO_6.

UNIVERSITAT ROVIRA I VIRGILI
ASSEMBLY AND PROPERTIES OF POLYOXOMETALATES: A THEORETICAL POINT OF VIEW
Laia Vilà Nadal
ISBN.978-84-694-2170-3/DL:T. 1039-2011

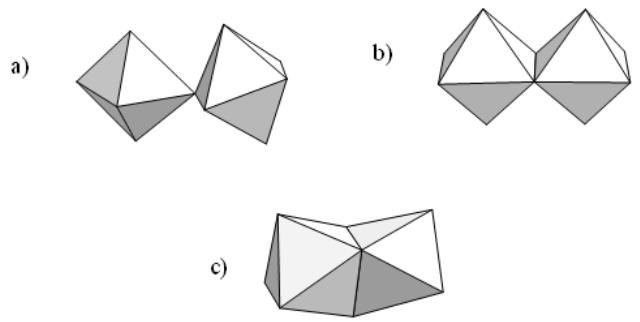

Figura 3. Representacions polièdriques dels diferents tipus d'unió entre dues unitats MO_6. a) unió compartint vèrtexs, b) unió compartint arestes, c) unió compartint cares.

Mètodes de síntesi

L'acidificació de solucions aquoses és el mètode de síntesi més comú. Per obtenir el compost desitjat només ens calen solucions aquoses dels oxoanions $[MO_n]^{m-}$ i els heteroàtoms necessaris. Aquest però no és l'únic camí possible ja que també s'han preparat i aïllat polianions en solucions no aquoses. Com a exemples de la preparativa de polioxometal·lats en solucions aquoses podem veure els següents:

Obtenció de l'anió de Lindqvist

$$6[MO_3(OH)]^- + 4\,H_3O^+ \rightarrow [M_6O_{19}]^{q-} + H_2O$$

Obtenció de l'anió de Keggin

$$12[MO_3(OH)]^- + HXO_4^{2-} + 11H_3O^+ \rightarrow [XM_{12}O_{40}]^{q-} + 23\,H_2O$$

En aquest treball hem estudiat la termodinàmica d'aquestes dues reaccions i proposat els mecanismes per a l'obtenció de Keggin i Lindqvist. Durant la síntesi s'haurà de controlar l'excés de l'heteroàtom, les condicions de pH i temperatura. També pot ser

UNIVERSITAT ROVIRA I VIRGILI
ASSEMBLY AND PROPERTIES OF POLYOXOMETALATES: A THEORETICAL POINT OF VIEW
Laia Vilà Nadal
ISBN.978-84-694-2170-3/DL:T. 1039-2011

un factor important a l'hora d'obtenir el POM desitjat l'ordre d'addició dels reactius. Per tal de precipitar els polianions i obtenir els cristalls afegiríem el contraió apropiat, normalment un metall alcalí, amoni, etc. Un cop han precipitat els cristalls es podran caracteritzar i estudiar les seves propietats.

Aspectes analitzats en la present memòria de tesi

La comprensió dels mecanismes de formació d'aquestes estructures hauria estat impossible sense la informació obtinguda dels experiments mitjançant ESI-MS (Espectrometria de Masses amb Ionització per Electroesprai). En els càlculs teòrics s'han tingut en compte els efectes del solvent en la síntesi de POMs de dues maneres: a través de models continus en els mètodes estàndard DFT (Teoria del Funcional de la Densitat) i amb molècules explícites d'aigua mitjançant les simulacions usant la metodologia descrita per Car i Parrinello (Dinàmiques Moleculars de Car–Parrinello).

Els resultats que es presenten en aquesta tesi tracten els següents tòpics:

- Anàlisi de l'efecte del pH a l'esfera de coordinació de W(VI) i Mo(VI) en els oxoanions MO_4^{2-} en solució aquosa.
- Els mecanismes de formació dels isopolianions en solució aquosa. S'ha estudiat l'anió de Lindqvist $[M_6O_{19}]^{2-}$ quan M=W i Mo.
- Els mecanismes de formació d'heteropolianions en solució aquosa. En aquest cas l'heteroàtom té un paper clau en el mecanisme de formació. Aquí hem analitzat l'anió de Keggin $[XM_{12}O_{40}]^{n-}$ quan M=W, Mo i X=P, As.
- L' isomerisme rotacional de l'anió de Wells-Dawson.
- L'estudi i predicció del desplaçament químic del nucli ^{183}W en diversos POMs.

UNIVERSITAT ROVIRA I VIRGILI
ASSEMBLY AND PROPERTIES OF POLYOXOMETALATES: A THEORETICAL POINT OF VIEW
Laia Vilà Nadal
ISBN.978-84-694-2170-3/DL:T. 1039-2011

UNIVERSITAT ROVIRA I VIRGILI
ASSEMBLY AND PROPERTIES OF POLYOXOMETALATES: A THEORETICAL POINT OF VIEW
Laia Vilà Nadal
ISBN.978-84-694-2170-3/DL:T. 1039-2011

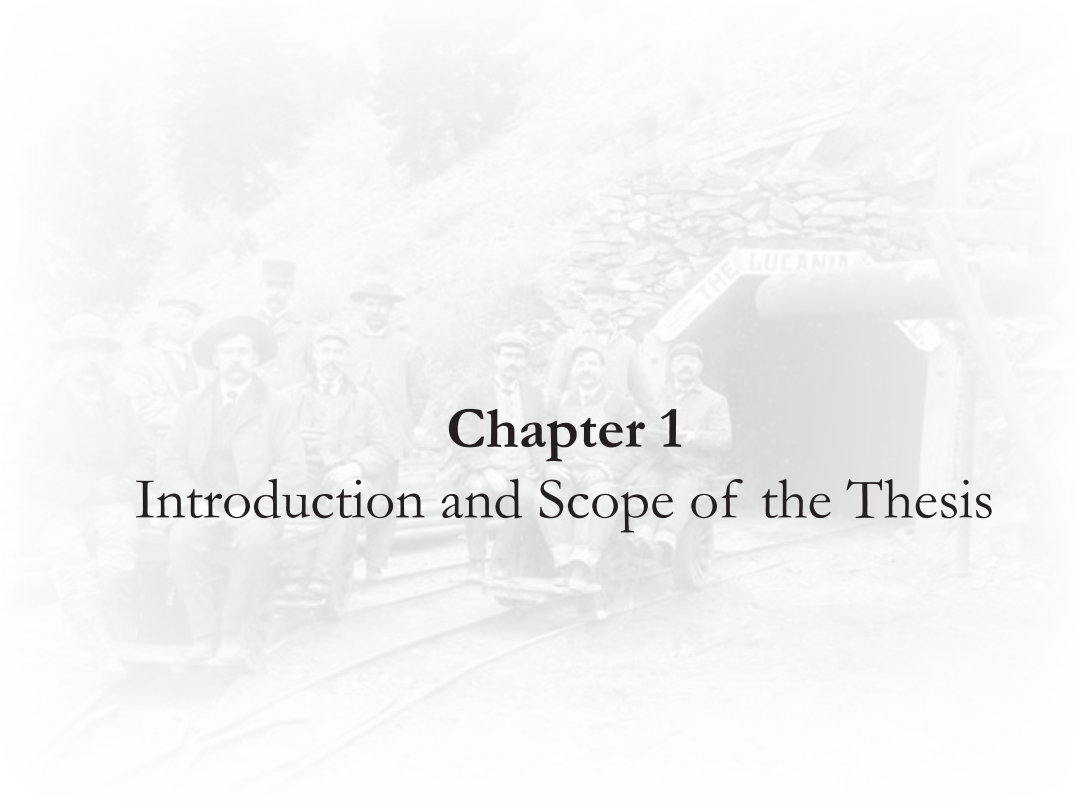

Chapter 1
Introduction and Scope of the Thesis

UNIVERSITAT ROVIRA I VIRGILI
ASSEMBLY AND PROPERTIES OF POLYOXOMETALATES: A THEORETICAL POINT OF VIEW
Laia Vilà Nadal
ISBN.978-84-694-2170-3/DL:T. 1039-2011

"...where Nature finishes producing its own species, man begins, using natural things and with the help of this nature, to create an infinity of species ..."

Leonardo da Vinci,
Disegni Anatomici, 1452-1519.

UNIVERSITAT ROVIRA I VIRGILI
ASSEMBLY AND PROPERTIES OF POLYOXOMETALATES: A THEORETICAL POINT OF VIEW
Laia Vilà Nadal
ISBN.978-84-694-2170-3/DL:T. 1039-2011

Chapter 1

Introduction and Scope of the Thesis

Inorganic metal oxygen clusters, or polyoxometalates for short, form a vast class of inorganic compounds that is unequaled in terms of their molecular and electronic structural versatility, reactivity, and relevance. From their discovery and early development in the final decades of the 19th century to their current significance in disciplines as diverse as chemistry, mathematics and medicine, these compounds continue to display surprisingly novel structures, unexpected reactivities and applications, and to attract increasing attention worldwide. Names such as Berzelius, Werner and Pauling appear in the early literature of the field. Nowadays polyoxometalates (POMs) represent a diverse range of molecular clusters with an almost unmatched type of physical properties and the ability to form dynamic structures that can range in size from the nano- to micrometer scale. Historically, the polyoxoanions of Mo(VI) and W(VI) have been the predominant species. Hundreds, if not thousands, of such complexes have been synthesized to date, and extraordinarily the field is far from exhausted. Initially this chapter will introduce the reader to the general characteristics of polyoxometalates: classification and design principles, synthetic strategies, properties and applications. The last section of the present chapter is devoted to discuss the main aims of this thesis.

UNIVERSITAT ROVIRA I VIRGILI
ASSEMBLY AND PROPERTIES OF POLYOXOMETALATES: A THEORETICAL POINT OF VIEW
Laia Vilà Nadal
ISBN.978-84-694-2170-3/DL:T. 1039-2011

1.1. Introduction

Back in the eighteenth century when the philosophy was guided by reason, science flourished in scientific academies and societies. In 1758 that stimulating environment allowed Axel Fredrik Cronstedt, Swedish chemist and mineralogist, to discover and describe an unusually heavy mineral that he called "tungsten", which is Swedish for heavy stone.[1] Tungsten is known to be the metal with the highest melting point and the most controversial name. In the autumn of 1783 Juan José de Elhuyar and his brother Fausto, Spanish Basque Chemists, discovered and isolated Tungsten, but named it Wolfram.[2] Prior to the Elhuyar brothers finding, in 1781 the famous chemist, Carl Wilhelm Scheele, succeeded in isolating the oxide (tungsten trioxide).[3] This can be thought of as the foundation of what is known today as polyoxometalates (POMs). Tungsten shares with Molybdenum the ability to form such molecular oxides. It is not by chance that some of the most famous chemists, e.g. Scheele (1742-1786), Berzelius (1779-1848), Werner (1866-1919) and Pauling (1901-1994), were interested in this field.[4] POMs are formed by transition metals in high oxidation states (e.g. W^{VI}, Mo^{VI}) surrounded by oxo-ligands, and can be called molecular metal oxides due to their molecular composition and their position between monomeric entities and bulk oxides.[5] These compounds present unique structural and electronic properties that make them attractive for applications in many fields.[6] For example, the redox activity of POMs is almost unmatched by any other general class of compounds, and this aspect has been exploited by POM applications in medicine, catalysis, material science, chemical analysis, etc.[7] POMs have been prepared and isolated from both aqueous and non-aqueous solutions whereby the polymerisation of acidified solutions of molybdenum(VI) or tungsten(VI) yields the most complicated of all the polyanion systems. In spite of the fact that the Tungsten system has been

UNIVERSITAT ROVIRA I VIRGILI
ASSEMBLY AND PROPERTIES OF POLYOXOMETALATES: A THEORETICAL POINT OF VIEW
Laia Vilà Nadal
ISBN.978-84-694-2170-3/DL:T. 1039-2011

the most intensively studied, it is still probably the least well understood.[8]

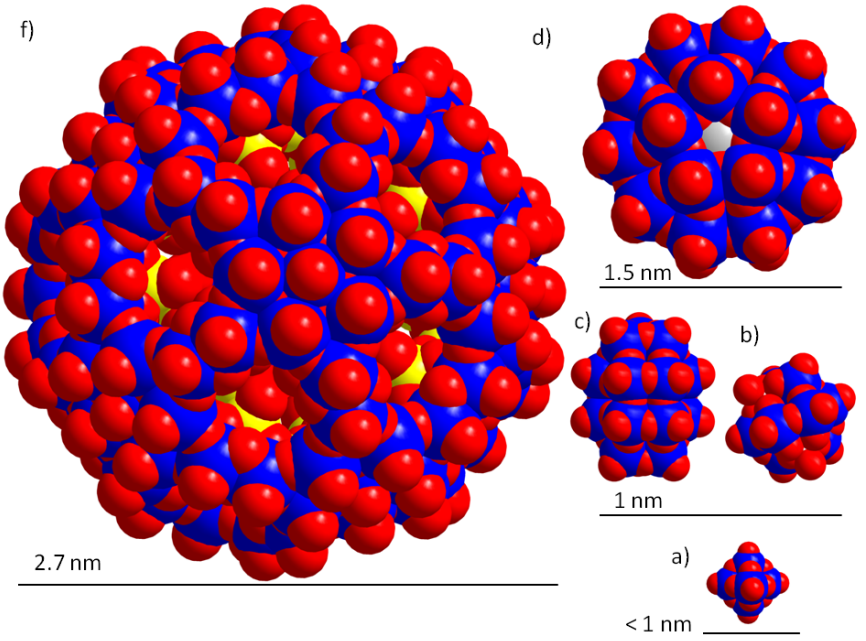

Figure 1.1. Structures of some POM clusters (space filling models M: blue, O: red, S: yellow). a) Lindqvist anion $[M_6O_{19}]^{n-}$ formed by a compact arrangement of six edge-shared MO_6 octahedra. b) The $[\{XO_4\}M_{12}O_{36}]^{n-}$ Keggin structure composed of four M_3O_{13} groups of three edge-shared MO_6 octahedra which are linked sharing corners to each other and to the central XO_4 tetrahedron. c) The $[\{XO_4\}_2M_{18}O_{54}]^{n-}$ Wells-Dawson structure made by the fusion of two Keggin fragments. d) The Preyssler anion $[NaP_5W_{30}O_{110}]^{14-}$ that presents an internal cavity. f) $\{Mo_{132}\}$ Keplerate-type structure, resulting of 'spherical disposition' of pentagonal $\{(Mo)Mo_5\}$ building blocks. The clusters are compared (to scale) to prove the wide range of sizes that POMs can achieve.

Figure 1.1 shows the dimensions of several POM clusters. With 6 metal units the smallest cluster is the well known Lindqvist anion $[M_6O_{19}]^{n-}$ (in which M=Mo, W,...).[9] Keggin (12 metal-centered) and Wells-Dawson (18 metal-centered) clusters are examples of heteropolyanions (HPAs): metal oxide clusters that

UNIVERSITAT ROVIRA I VIRGILI
ASSEMBLY AND PROPERTIES OF POLYOXOMETALATES: A THEORETICAL POINT OF VIEW
Laia Vilà Nadal
ISBN.978-84-694-2170-3/DL:T. 1039-2011

include heteroanions, such as SO_4^{2-}, PO_4^{3-}.[10] The Preyssler anion, which contains 30 W atoms and an internal cavity, was reported for the first time in 1970.[11] Finally {Mo_{132}} belongs to the family of the Keplerate[12] clusters reported by Müller and co-workers, as an example of high nuclearity clusters. Molybdenum-oxide based fragments, known as Mo-blue (MB) or Mo-brown, are reduced Mo-based POMs. Mo-based clusters display extreme structural flexibility under reducing conditions as shown by the isolation of the largest non-biologically derived molecule to date, a polyoxometalate cluster containing 368 molybdenum atoms ({Mo_{368}}, the 'Blue Lemon'), with a size of 5.4 nm –comparable to a protein– demonstrating the fascinating link between macromolecular science and POM chemistry in terms of structural complexity.[13]

1.2. Classification and Design Principles

Although new structural types of polyanions continue to be discovered, it is possible to recognize some general principles that control such structures. A very large number of polyoxometalates (most molybdates and tungstates for example) are viewed as arrangements of edge- and vertex-sharing MO_6 octahedra, each with one or two unshared vertices (terminal oxygens).[14] So, in general, the class compounds known as POMs are based upon metal oxide building blocks with a general formula $\{MO_x\}_n$ where M=Mo, W, V and sometimes Nb and x=4–7.[15] The polyanion surfaces are therefore bounded by weakly- or non-basic multiply-bonded oxygen atoms, and discourage any further polymerization. The few polyanion structures, which have recently been shown to incorporate an MO_6 octahedron with three terminal oxygens, undergo further reaction, e.g. alkylation[16], at these more basic/nucleophilic sites.

UNIVERSITAT ROVIRA I VIRGILI
ASSEMBLY AND PROPERTIES OF POLYOXOMETALATES: A THEORETICAL POINT OF VIEW
Laia Vilà Nadal
ISBN.978-84-694-2170-3/DL:T. 1039-2011

Many attempts have been made to rationalize the structures of polyoxometalates. They can be classified regarding their composition, the oxidation state of the metals or due to structural aspects. Figure 1.2 shows several structures of polyoxometalates that can be broken down into three broad subsets[17]:

1) *Heteropolyanions (HPAs)* are metal oxide clusters that include heteroanions such as SO_4^{2-}, PO_4^{3-}, AsO_4^{3-} and SiO_4^{4-}, etc. These are the most explored subset of POM clusters; much of this research has examined the catalytic properties of POMs, with great emphasis on the archetypal Keggin $[XM_{12}O_{40}]^{n-}$ and Wells–Dawson $[X_2M_{18}O_{62}]^{n-}$ anions (where M=W or Mo; X is a tetrahedral template), both anions are depicted in Figure 1.2. Tungsten-based POMs are robust, and this fact has been exploited to develop tungsten-based Keggin and Dawson anions with vacancies (most commonly with one, two, or three vacancies) that can be linked using electrophiles to larger aggregates in a predictable manner. The development of lacunary polyoxometalates based upon Keggin $\{M_{12-n}\}$ and Dawson $\{M_{18-n}\}$ is a large research area and will not be covered here in detail.[18]

2) *Isopolyanions (IPAs)* are composed of a metal oxide framework, but without the internal heteroatom/heteroanion. They are usually more unstable than their heteropolyanion counterparts.[19] However they also have interesting physical properties, such as high charges and strongly basic oxygen surfaces, which means they are attractive units for using as building blocks.[20]

3) *Molybdenum blue and molybdenum brown reduced POM clusters* are related to molybdenum blue species, which were first reported by Scheele in 1783. Their composition was largely unknown until Müller *et al.* reported the synthesis and structural characterization

in 1995 of a very high-nuclearity cluster $\{Mo_{154}\}$, which has a ring topology, that crystallized from a solution of molybdenum blue.[21] Changing the pH and increasing the amount of reducing agent along with incorporation of acetate ligands facilitates the formation of a $\{Mo_{132}\}$ spherical ball-like cluster.[22] This cluster can be formulated as $[\{Mo_2^{V}O_4(CH_3OO)\}_{30}\{(Mo)Mo_5O_{21}(H_2O)\}_{12}]^{42-}$. This class of highly reduced POM clusters is one of the most exciting developments in POM chemistry with many potential spin off applications in nanoscience.

UNIVERSITAT ROVIRA I VIRGILI
ASSEMBLY AND PROPERTIES OF POLYOXOMETALATES: A THEORETICAL POINT OF VIEW
Laia Vilà Nadal
ISBN.978-84-694-2170-3/DL:T. 1039-2011

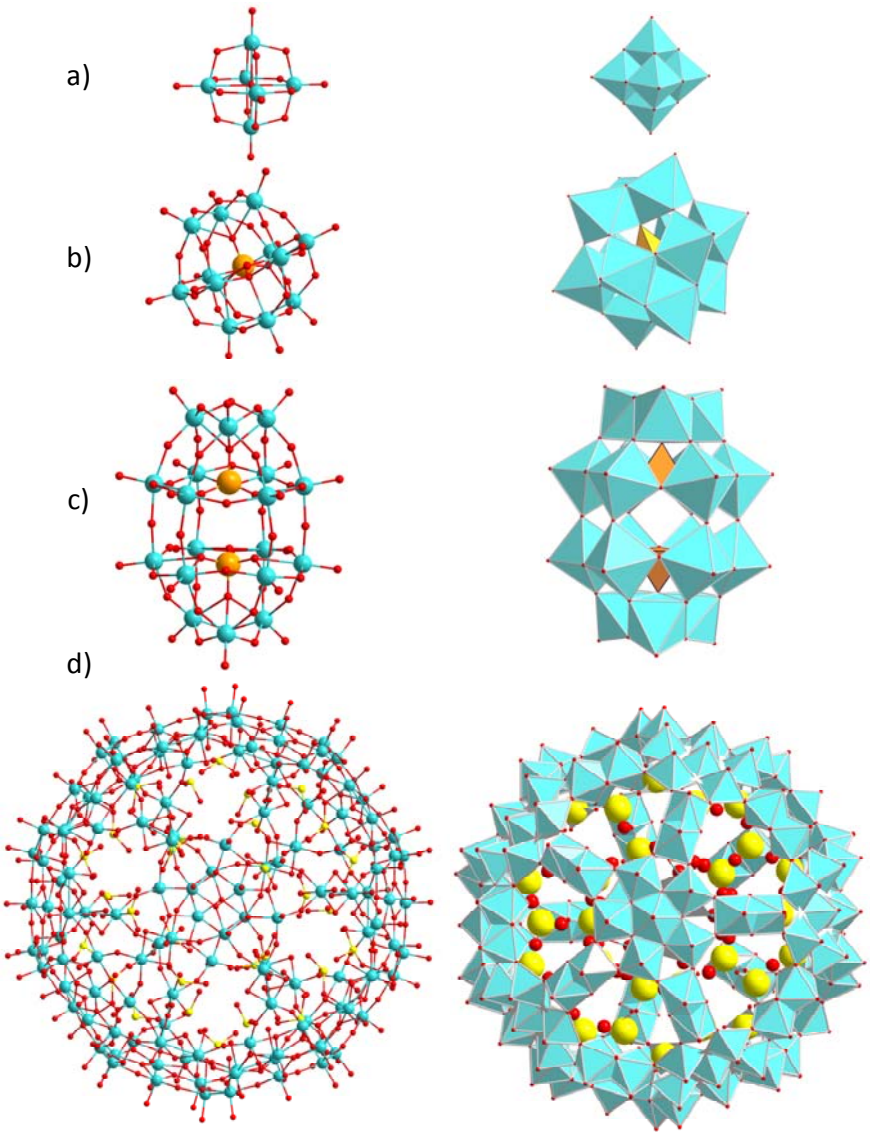

Figure 1.2. Ball-and-stick (left) and polyhedral (right) views of some POM clusters (Red spheres are oxygens, teal spheres are metal centres, orange spheres are the heteroatoms and finally yellow spheres are sulphur atoms; the same colour code has been used for polyhedral representation). a) Lindqvist anion $[M_6O_{19}]^{n-}$. b) The $[\{XO_4\}M_{12}O_{36}]^{n-}$ Keggin anion. c) The $[\{XO_4\}_2M_{18}O_{54}]^{n-}$ Wells-Dawson structure. d) $\{Mo_{132}\}$ Keplerate-type structure.

UNIVERSITAT ROVIRA I VIRGILI
ASSEMBLY AND PROPERTIES OF POLYOXOMETALATES: A THEORETICAL POINT OF VIEW
Laia Vilà Nadal
ISBN.978-84-694-2170-3/DL:T. 1039-2011

1.3. Synthetic Strategies

Native Americans gave the name "Blue Waters" to certain fountains near today's Idaho Springs (Colorado) and the Valley of the Ten Thousand Smokes (Alaska). Even after the secret of the colour was revealed some 200 years ago, the detailed molecular structures of the solutes remained unclear. In our days we know that the Native Americans observed solutions of molybdenum blue, formed by partial oxidation of molybdenite MoS_2 (leading to the mineral ilsemannite).[23] Ilsemannite, with approximate formula $Mo_3O_8 \cdot nH_2O$, can be found in the Lucania Tunnel up Fall River Road, just 5 Km from Idaho Springs. The tunnel is depicted in Fig. 1.3, just out of curiosity, constructed in the period 1907-1908 to drain the gold nearby mines.

The process of formation of POMs *de novo* remains largely a mystery and is otherwise known as "self-assembly".[24] Conversion of one formed polyoxoanion into another, or partial derivatization is a little better understood in some cases, and semi-rational syntheses of regiospecifically substituted Keggin and related structures from appropriate lacunary species have been developed.[25] Syntheses have predominantly been carried out in aqueous solutions, and the few minerals that have been found to contain polyoxoanions, notably decavanadates, the vanadoaluminate (sherwoodite)[26], and probable molybdophosphates (mendozavilite, paramendozavilite[27]) are almost certainly the result of surface weathering. Hydrothermal methods, and reactions carried out in non-aqueous solvents have also been employed for laboratory synthesis of polyoxometalates, and these methods extend the variety of complexes and structural types.

UNIVERSITAT ROVIRA I VIRGILI
ASSEMBLY AND PROPERTIES OF POLYOXOMETALATES: A THEORETICAL POINT OF VIEW
Laia Vilà Nadal
ISBN.978-84-694-2170-3/DL:T. 1039-2011

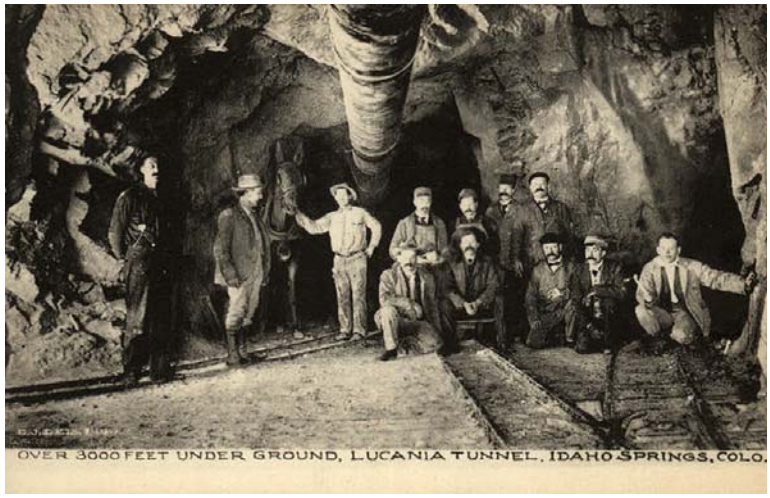

Figure 1.3. Up: miners pose on hand velocipede cars near the entrance to the Lucania Tunnel shaft in Clear Creek County, Colorado. Down: The Lucania Tunnel. "*Over 3000 feet under ground*." Old postcard.[28]

UNIVERSITAT ROVIRA I VIRGILI
ASSEMBLY AND PROPERTIES OF POLYOXOMETALATES: A THEORETICAL POINT OF VIEW
Laia Vilà Nadal
ISBN.978-84-694-2170-3/DL:T. 1039-2011

Synthetically, the routes to produce new POM clusters are often very simple synthetic manipulations requiring a small number of steps, or even just one step (one-pot synthesis). The acidification, for example, of a solution of sodium molybdate will give rise to metal oxide fragments which increase in nuclearity as the pH of the solution decreases. This means that traditionally, the aqueous synthesis of the POM cluster is the norm, and as such can be in presence of simple metal cations. However, this approach can be extended to organic cations, and the solvent system can be extended to an aqueous/organic solvent mixture; for example, water/CH_3CN. The synthetic variables of greatest importance in synthesizing such clusters are, in no particular order: 1) concentration/type of metal oxide anion, 2) pH, 3) ionic strength, 4) heteroatom type/concentration, 5) presence of additional ligands, 6) reducing agent, and 7) temperature of reaction and processing (e.g. microwave, hydrothermal, refluxing) 8) countercation type/concentration. These variables are summarized in Fig. 1.4.

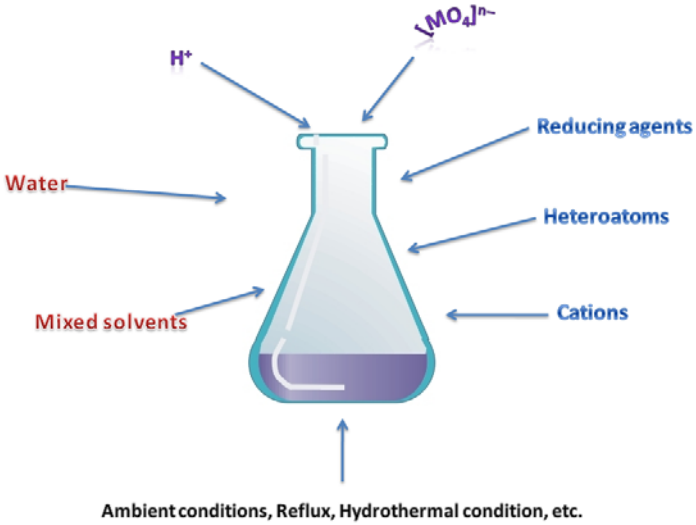

Figure 1.4. Parameters that are often adjusted in the synthesis/isolation of new POM clusters using the multi-parameter one-pot method.

UNIVERSITAT ROVIRA I VIRGILI
ASSEMBLY AND PROPERTIES OF POLYOXOMETALATES: A THEORETICAL POINT OF VIEW
Laia Vilà Nadal
ISBN.978-84-694-2170-3/DL:T. 1039-2011

1.4. Properties and Applications

POMs can be regarded as fragments of nonmolecular metal oxide lattices giving a wide distribution from insulator to superconductor in their electronic properties. As we have said previously, the principal units that make up most of polyoxometalates are MO_6 octahedra or MO_4 tetrahedra. Generally, MO_6 octahedra can be linked together by a single oxygen atom (termed corner-sharing) and two oxygen atoms (termed edge-sharing).[29] The two types of the MO_6 unit linkage afford a great variety for the anion structure. In addition, the variety of metal atoms constituting the lattice offers an interesting chance of physiochemical properties such as redox reaction, photoreaction, energy transfer, and biological activity. Polyoxometalates may be characterized by six features: (1) electrochemical or photochemical reversible multi-electron redox reaction, (2) high solubility in water and occasionally in polar organic solvents such as acetonitrile, dimethilformamide and dioxane, (3) co-ordination of large amounts of water molecules, (4) easiness of the modifications of anion size, structure, anion charge and replacement of metal atoms by other metal atoms, (5) co-ordination of a great variety of heteroatoms up to 75% of elements in the periodic table at well–defined geometric sites in the lattice, and (6) capsulation of neutral molecule (acetonitrile) or ion (carbonate and halide).[30] Due to these properties POMs can be seen as molecular device systems, Figure 1.5 shows research fields towards this direction.

The main features regarding POM chemistry have now been introduced. The following lines are devoted to give some extra details regarding some of those features, starting with the reduction processes in POMs. Despite having a negative charge POMs are known to be strong oxidising agents. This rather

counterintuitive statement can be easily understood. Remember roughly the skeleton of a POM, it is formed by metals in their highest oxidation state, d^0 and d^1 electronic configuration, bonded to O^{2-}. The valence shell of the metal centres is empty, so they are willing to accept external electrons. Of course the global charge of the POM will be a limiting point and protonations will occur. The low-lying empty d-type orbitals can accept numerous electrons without dramatic changes in the POM geometry. In a reduction process, electrons injected into polyoxometalates are usually delocalized over the MO_6 octahedra lattices. The degree of delocalization strongly depends on the configuration of the M–O–M linkage. Synthesize POMs with insulator or semiconductor properties, and also describe the trends in the reduction potentials depending on the chemical composition of a given species, as well as the behaviour of metal electrons—(de)localisation, have been major subjects of study in the previous years. [31,32]

Furthermore POMs have been shown to be effective agents for the highly selective bleaching of softwood kraft pulps.[33] They are highly selective with respect to their oxidative action, robust enough to withstand the elevated temperatures required in industrial reactions, chemically stable and capable of being regenerated in a separate stage that eliminates effluent materials and completely mineralizes the organic materials produced during bleaching.

By far the most active area of applications is catalysis, but it is remarkable that, with few exceptions, this activity has involved only a handful of well-known heteropolyanions, especially the tungsto– and molybdophospates and –silicates. Large-scale industrial processes in operation are shown in Table 1.1.[34] The potential for development of new environmentally–benign

UNIVERSITAT ROVIRA I VIRGILI
ASSEMBLY AND PROPERTIES OF POLYOXOMETALATES: A THEORETICAL POINT OF VIEW
Laia Vilà Nadal
ISBN.978-84-694-2170-3/DL:T. 1039-2011

catalytic processes based on properties of specially designed polyoxoanions is enormous, and we can expect new advances. A promising direction is the use of surface–metal–substituted polyoxometalates as robust metalloporphyrin analogs in oxidation chemistry. Control the access to high oxidation states of the incorporated metal atoms is key to catalytic success.

Perhaps the most significant general medical property of POMs is their diverse antiviral activity, but specific with efficacy *in vivo* not simply *in vitro*. The collective data available at present make a strong case that POMs can penetrate cell membranes and localize intracellularly. POMs are effective against HIV-1 *in vitro* clearly exhibiting several modes of action, despite more research will be required.[35] It is not only in the AIDS arena that POMs can play an important role. The interactions of specific vanadates and molybdates with various proteins are reported, and inhibition of acid phosphatases by certain molybdates, suggest methods of attacking parasitic virial diseases such as Leishmania, Malaria and Rocky Mountain Spotted Fever.[36]

Table 1.1. Large scale industrial processes catalized by polyoxometalates.

	Phase	Capacity (10^3t year^{-1})	Start	Remarks
Hydration of propene	liq (aq)	50	1972	First process (dil. HPA)
Oxidation of methacrolein	gas-solid	220	1982	Mo-V-P
Hydration of isobutene	liq (aq-C_4)	56	1984	C_4 separation (conc. HPA)
Hydration of n-butene	liq (aq)	40	1985	To methyl ethyl ketone
Polymerization of THF	liq (THF-aq)	2-3?	1987	Phase transfer catalysis

UNIVERSITAT ROVIRA I VIRGILI
ASSEMBLY AND PROPERTIES OF POLYOXOMETALATES: A THEORETICAL POINT OF VIEW
Laia Vilà Nadal
ISBN.978-84-694-2170-3/DL:T. 1039-2011

On a more general level, the use of heteropolytungstates as electron–dense imaging agents continues to be developed[37], and several gadolinium–containing species are being explored as relaxants for NMR imaging.[38]

Two more characteristics of POMs are remarkable: their acid strength and the effect of isomerism. Numerous acid–base equilibria have been reported in which POMs appear as polyacids. Many POMs have a p*K*a lower than 0. This denotes its strong acidity, although in very acidic media they can be protonated. Secondly the effect of isomerism in POMs is chemically subtle and it has been studied by theoretical and experimental groups.[39] From the structural point of view, POMs are highly ordered clusters with an additional richness arising from the existence of various isomeric forms in some cases, notably in the common $[XM_{12}O_{40}]^{q-}$ Keggin and $[X_2M_{18}O_{62}]^{q-}$ Wells-Dawson structures. Isomerism in POMs has been largely studied and their properties deeply analyzed experimentally and computationally, although some basic points are still not completely clear. The main interest on isomerism is related to the possibility of tuning some properties with controlled geometrical changes, such as the different location of a given atom (positional isomerism) or a rotation of a fragment of the molecule (rotational isomerism).

UNIVERSITAT ROVIRA I VIRGILI
ASSEMBLY AND PROPERTIES OF POLYOXOMETALATES: A THEORETICAL POINT OF VIEW
Laia Vilà Nadal
ISBN.978-84-694-2170-3/DL:T. 1039-2011

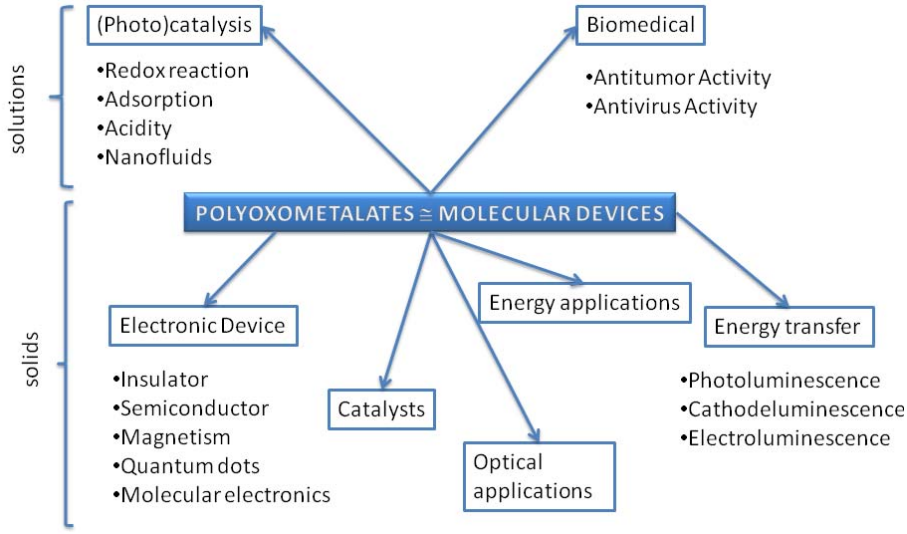

Figure 1.5. Conceptual panel summarizing applications of polyoxometalate-based molecular device systems. (modified from Ref 24, pp. 339)

1.5. Scope of the Thesis

Which is the formation mechanism a POM? One can find an answer to this question throughout the present doctoral thesis. In few words, the main objective of the present work is the elucidation of the formation mechanisms of POMs. According to this objective, several studies have been carried out and are presented in Chapters 3 to 7. In these chapters we have also included discussions about properties of POMs, i.e. isomerism and NMR shielding. The comprehension of the mechanistic processes underlying the self-assembly of POMs is not trivial, and requires fundamental contributions from several disciplines.

UNIVERSITAT ROVIRA I VIRGILI
ASSEMBLY AND PROPERTIES OF POLYOXOMETALATES: A THEORETICAL POINT OF VIEW
Laia Vilà Nadal
ISBN.978-84-694-2170-3/DL:T. 1039-2011

Information obtained by the ESI-MS[i] experiments and complementary DFT approaches *together* provide a deep insight into the formation mechanisms of POM molecular metal oxide architectures. Chapter 2 is devoted to introduce theoretical tools used throughout this thesis and also a brief discussion about the experimental techniques (i.e. ESI-MS, synthesis details,…).

The results presented here will concern the following topics:

- Analyze the effect of pH on the coordination sphere of W(VI) and Mo (VI) ions in the MO_4^{2-} oxoanions in aqueous solutions.
- Formation mechanisms in IPAs. Initially we have studied the case of the well known Lindqvist anion $[M_6O_{19}]^{2-}$ when M=W. Later we have extended this research being M=Mo.
- Formation mechanisms in HPAs. Here we have considered the effect of the heteroatom in the formation mechanism of POMs. We have analized the case of the Keggin anion, $[XM_{12}O_{40}]^{n-}$ when M=W, Mo and X=P, As.
- Analysis of ESI-MS results obtained for the Lindqvist $[W_6O_{19}]^{2-}$ and $[Mo_6O_{19}]^{2-}$ anions, and the Keggin $[PW_{12}O_{40}]^{3-}$, $[AsW_{12}O_{40}]^{3-}$, $[PMo_{12}O_{40}]^{3-}$ and $[AsMo_{12}O_{40}]^{3-}$anions.
- The rotational isomerism in the Dawson anion, α– , β–, γ–, α*– , β*– and γ*– $[X_2M_{18}O_{62}]^{n-}$, when M=W, Mo and X=P, As, S.
- Improvements in the study ^{183}W NMR chemical shifts. Here we have studied the family of the Keggin anions with formula α-$[XW_{12}O_{40}]^{q-}$, where X = B, Al, Si, P, Ga, Ge, As, Zn, the β– and γ– $[SiW_{12}O_{40}]^{4-}$ geometric

[i] Electrospray Mas Spectrometry (ESI-MS), see Chapter 2 for more details.

UNIVERSITAT ROVIRA I VIRGILI
ASSEMBLY AND PROPERTIES OF POLYOXOMETALATES: A THEORETICAL POINT OF VIEW
Laia Vilà Nadal
ISBN.978-84-694-2170-3/DL:T. 1039-2011

isomers, the derivative Dawson anion $[P_2W_{18}O_{62}]^{6-}$, the most symmetrical Lindqvist $[W_6O_{19}]^{2-}$ anion and its derivative $[W_{10}O_{32}]^{4-}$.

UNIVERSITAT ROVIRA I VIRGILI
ASSEMBLY AND PROPERTIES OF POLYOXOMETALATES: A THEORETICAL POINT OF VIEW
Laia Vilà Nadal
ISBN.978-84-694-2170-3/DL:T. 1039-2011

References and Notes

[1] E.M. Gusenius, Transactions of the Kansas Academy of Science, **1969**, 72, 476.

[2] J. Palacio-Remondo, *Juan José y Fausto de Elhuyar. Epistolario (1777-1821)*, Gobierno de la Rioja, Logroño, **1996**.

[3] a) A. Greenberg, *A Chemical History Tour: Picturing Chemistry from Alchemy to Modern Molecular Science*, John Wiley & Sons, West Sussex, **2000**. b) C.W. Sheele, *Observations sur la Physique, sur l'Historie Naturelle et sur les Arts*, **1778**, 342. c) J.J. Berzelius, *Poggend. Ann. Phys. Chem.*, **1826**, 6, 369.

[4] P. Gouzerh, M. Che, *L'actualité chimique*, **2006**, 208, 1.

[5] M.T. Pope, *Heteropoly and Isopoly Oxometalates*, Springer-Verlag, New York, **1983**.

[6] C.L. Hill (Ed.), Special issue on polyoxometalates, *Chem. Rev.*, **1998**, 98, 1.

[7] D.L. Long, E. Burkholder, L. Cronin, *Chem. Soc. Rev.*, **2007**, 36, 105.

[8] N.N. Greenwood, A. Earnshaw, *Chemistry of the elements*, Elsevier, Oxford, **2006**.

[9] I. Lindqvist, *Acta Cryst.*, **1952**, 5, 667.

[10] a) F.J. Keggin, *Nature*, **1933**, 131, 908. b) F.J. Keggin, *Proc. R. Soc. London*, **1934**, A144, 75. c) A.F. Wells, *Structural Inorganic Chemistry*, Oxford University Press, Oxford, **1945**, 344. d) B. Dawson, *Acta Crystallogr.*, **1953**, 6, 113.

[11] a) C. Preyssler, *Bull. Soc. Chim. Fr.*, **1970**, 30. b) M.H. Alizadeh, S.P. Harmalker, Y. Jeannin, J. Martin-Frère, M.T. Pope, *J. Am. Chem. Soc.*, **1985**, 107, 2662.

[12] Such spherical clusters, described with the general formula $[\{(Mo)Mo_5\}_{12}\{L\}]$ belong to the family of 'Keplerate' type molecules because of their similarity to Kepler's early model of the universe, as described in his speculative opus *Mysterium Cosmographicum*.

[13] A. Müller, H. Reuter, S. Dillinger, *Angew. Chem. Int. Ed. Engl.*, **1995**, 34, 2328.

[14] a) W.N. Lipscomb, *Inorg. Chem.*, **1965**, 4, 132. b) M.T. Pope, *Ibid*, **1972**, 11, 1973.

[15] a) M.T Pope, A. Müller, *Angew. Chem. Int. Ed. Engl.*, **1991**, 30, 34. b) A. Müller, S. Roy, *The Chemistry of Nanomaterials: Synthesis, Properties and Applications* (Editors: C.N.R. Rao, A. Müller, A.K. Cheetham), Wiley-VCH, Weinheim, **2004**.

[16] L. Ma, S. Liu, J. Zubieta, *Inorg. Chem.*, **1989**, 28, 175.

[17] D.L. Long, R. Tsunashima, L. Cronin, *Angew. Chem. Int. Ed.*, **2010**, 49, 1736.

[18] L. Cronin, *High Nuclearity Clusters: Iso and Heteropolyoxoanions and Relatives*, Comprehensive Coordination Chemistry II, Vol. 7 (Editors: J.A. McCleverty, T.J. Meyer), Elsevier, Amsterdam, **2004**.

[19] D.L. Long, L. Cronin, *Chem. Eur. J.,* **2006**, 12, 3698.

[20] D.L. Long, P. Kögerler, L.J. Farrugia, L. Cronin, *Angew. Chem. Int. Ed.*, **2003**, 42, 4180.

UNIVERSITAT ROVIRA I VIRGILI
ASSEMBLY AND PROPERTIES OF POLYOXOMETALATES: A THEORETICAL POINT OF VIEW
Laia Vilà Nadal
ISBN.978-84-694-2170-3/DL:T. 1039-2011

[21] A. Müller, E. Krickemeyer, J. Meyer, H. Bögge, F. Peters, W. Plass, E. Diemann, S. Dillinger, F. Nonnenbruch, M. Randerath, C. Menke, *Angew. Chem. Int. Ed. Engl.*, **1995**, 34, 2122.

[22] A. Müller., E. Krickemeyer, H. Bögge, M. Schimidtmann, F. Peters, *Angew. Chem. Int. Ed. Engl.*, **1998**, 37, 3359.

[23] a) Lucania Tunnel, Idaho Springs District, Clear Creek County, Colorado, USA. b) A. Müller, E. Krickemeyer, J. Meyer, H. Bogge, F. Peters, W. Plass, E. Diemann, S. Dillinger, F. Nonnebruch, M. Randerath, C. Menke, *Angew. Chem. Int. Ed. Engl.*, **1995**, 34, 2122. c) T. Liu, E. Diemann, A. Müller, *J. Chem. Edu.*, **2007**, 84, 526-532.

[24] M.T. Pope, A. Müller, *Polyoxometalates: from Platonic Solids to Anti-Retroviral Activity*, Kluwer Academic Publishers, Dordrecht, **1994**.

[25] J.P. Ciabrini, R. Cotant, J.M Fruchart, *Polyhedron*, **1983**, 2, 1229.

[26] H.T. Jr. Evans, J.A. Konnert, *Amer. Mineral.* **1978**, 63, 863.

[27] S.A. Williams, *Bol. Mineral*, **1986**, 13.

[28] a) 3000ft = 914.4 m. b) The mineral and locality database. `http://www.mindat.org/` (accessed Sep 20, 2010). c) Library of Congres Home Page, History of the American West, 1860-1920: Photographs from the Collection of the Denver Public Library. `http://photoswest.org/cgi-bin/imager?10060932+X-60932` (accessed Sep 20, 2010)

[29] a) V.W. Day, W.G. Kemplerer, *Science*, **1985**, 228, 533. b) Y. Jeannin, M. Fournier, *Pure and Appl. Chem.*, **1987**, 59, 1529.

[30] a) A. Müller, M. Penck, R. Rohlfing, E. Krickemeyer, J. Dörling, *Angew. Chem. Int. Ed. Engl.,* **1990**, 29, 926. b) P.C.H. Mitchel, *Nature*, **1990**, 348,15.

[31] a) C. Sanchez, J. Livage, J.P. Launay, M. Fournier, Y. Jeannin, *J. Am. Chem. Soc.*, **1982**, 104, 3194. b) C. Sanchez, J. Livage, J.P. Launay, M. Fournier, *Ibid*, **1983**, 105, 6817. c) T. Yamase, *Polyhedron*, **1986**, 5, 79.

[32] X. López, C. Bo, J.M. Poblet, *J. Am. Chem. Soc.*, **2002**, 124, 12574.

[33] a) I.A. Weinstock, H.R. Atalla, R.S. Reiner, M.A. Moen, K.E. Hammel, *New J. Chem.*, **1996**, 20,269. b) I.A. Weinstock, E.M.G. Barbuzzi, M.W. Wemple, J.J. Cowan, R.S. Reiner, D.M. Sonnen, R.A. Heintz, J.S. Bond, C.L. Hill, *Nature*, **2001**, 414, 191.

[34] M. Misono, N. Nojiri, *Appl. Catal.*, **1990**, 64, 1.

[35] J.T. Rhule, C.L. Hill, D.A. Judd, *Chem. Rev.*, **1998**, 98, 327.

[36] A. Saha, D.C. Crans, M.T. Pope, C. Simone, R.H. Glew, *J. Biol. Chem.*, **1991**, 266, 3511.

[37] J.F.W. Keana, Y. Wu, G. Wu, *J. Org. Chem.*, **1986**, 52, 2571.

[38] M. Mozik, J. Gilbert, J.H. Pawlow, R.J. Fiel, V. Joshi, *Abstracts of the 230rd National Meeting, Amer. Chem. Soc.*, San Francisco, **1992**, paper INOR 380.

[39] a) L.C.W. Baker, J.S. Figgis, *J. Am. Chem. Soc.*, **1970**, 92, 3794. b) G. Herve, A. Tézé, *Inorg. Chem.*, **1977**, 6, 2115. c) X. Lopez, C. Bo, J.M. Poblet, *Inorg. Chem.*, **2003**, 42, 2634. d) X. López, J.M Maestre, C. Bo, C., J.M. Poblet, *J. Am. Chem. Soc.* **2001**, 123, 9571.

UNIVERSITAT ROVIRA I VIRGILI
ASSEMBLY AND PROPERTIES OF POLYOXOMETALATES: A THEORETICAL POINT OF VIEW
Laia Vilà Nadal
ISBN.978-84-694-2170-3/DL:T. 1039-2011

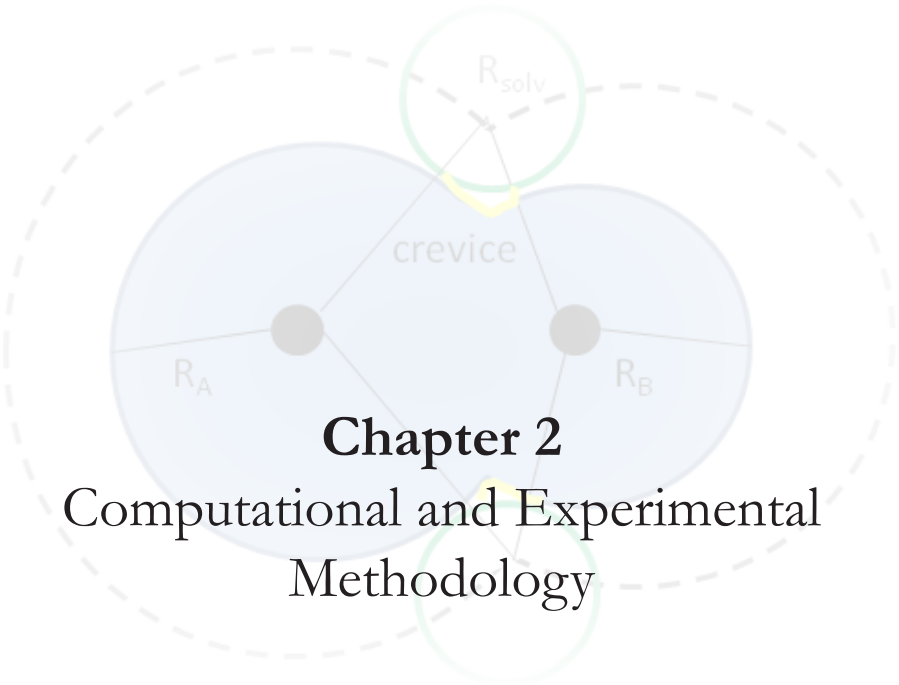

Chapter 2
Computational and Experimental Methodology

UNIVERSITAT ROVIRA I VIRGILI
ASSEMBLY AND PROPERTIES OF POLYOXOMETALATES: A THEORETICAL POINT OF VIEW
Laia Vilà Nadal
ISBN.978-84-694-2170-3/DL:T. 1039-2011

"Science is any discipline in which the fool of this generation can go beyond the point reached by the genius of the last generation."

M. Gluckman,
Politics Law and Ritual, 1965.

UNIVERSITAT ROVIRA I VIRGILI
ASSEMBLY AND PROPERTIES OF POLYOXOMETALATES: A THEORETICAL POINT OF VIEW
Laia Vilà Nadal
ISBN.978-84-694-2170-3/DL:T. 1039-2011

Chapter 2

Computational and Experimental Methodology

Prior to the 1960s theoretical chemistry was largely a pencil-and-paper endeavor. Lengthy calculations of molecular properties were either impractical, performed approximately, or made heroically on mechanical calculators. The arrival of electronic computers made calculations feasible, and the feasibility stimulated growth of new theoretical methods. Molecules are composed of atoms, and atoms are composed of nuclei and electrons. Analysis of molecular symmetry and molecular bonding requires, among other things, careful description of the electrostatic interactions among the nuclei and electrons constituting a molecule. The first barrier encountered is that if one considers all the pairwise interactions among nuclei and each electron, along with those between each pair of electrons, there is no closed-form solution to the electrostatic equations. Methods for approximating these interactions were a topic of intense interest. So, computational chemistry allows us to obtain chemical information from the structure and properties of a molecule, by examining forces that exist at the atomic level. This chapter wishes to be an overview of the techniques used in the present thesis to describe POMs. The chapter is conceptually divided into two parts, presenting all the theoretical methodologies first and leaving to the end the experimental techniques. So it starts with a conventional introduction to Quantum Chemistry. Then several aspects concerning

UNIVERSITAT ROVIRA I VIRGILI
ASSEMBLY AND PROPERTIES OF POLYOXOMETALATES: A THEORETICAL POINT OF VIEW
Laia Vilà Nadal
ISBN.978-84-694-2170-3/DL:T. 1039-2011

Density Functional Theory (DFT) are presented, followed by an introduction to Car–Parrinello Molecular Dynamics. Section 2.6 presents the physical basis of Nuclear Magnetic Resonance (NMR) and the methodological aspects for the computation of NMR shielding tensors. This section is intentionally long because aims to be an introductory lesson to NMR shielding tensor calculations described in Chapter 7. It may seem quite rare to present an experimental section in a mainly theoretically based thesis. But for a wide understanding of the results it is necessary to cover several aspects concerning ElectroSpray-Ionization Mass Spectrometry (ESI-MS) technique. So section 2.8 presents the synthetic methods to obtain several POMs and finally section 2.9 is an introduction to ESI-MS.

2.1. Foundations of Quantum Chemistry

In 1929, Dirac famously subjugated the proud and erudite discipline of chemistry into the realm of applied mathematics with two sentences. His first statement was:

"The underlying physical laws necessary for the mathematical theory of a large part of physics and the whole of chemistry are thus completely known, and the difficulty is only that the exact application of these laws leads to equations much too complicated to be soluble."[1]

The second statement followed the first and says:

"It therefore becomes desirable that approximate practical methods of applying quantum mechanics should be developed …".

The significance of these comments lies at the core of what is known today as quantum chemistry.[2] They mark, not the subjugation of a discipline, but the birth of a new one. Although

UNIVERSITAT ROVIRA I VIRGILI
ASSEMBLY AND PROPERTIES OF POLYOXOMETALATES: A THEORETICAL POINT OF VIEW
Laia Vilà Nadal
ISBN.978-84-694-2170-3/DL:T. 1039-2011

the first statement is more of a philosophical one, the second has become a practicable tenet of quantum chemistry and has divided the discipline into two main areas. The first division applies currently available approximate methods to systems that are tractable by accessible computational means. As computers have become more powerful over the last seventy years, the realm of applicability has literally exploded exponentially in a Moores' law[3] fashion. The second area develops theoretical methods that either become more accurate or scale better computationally.

This means the fundamental physical laws that Dirac speaks of, can become soluble, if a number of approximations are made. Therefore, one may attempt to build in less approximations, which usually results in a greater amount of computational effort, or refine current approximations by re-formulating them.

The readers may ask what brought Dirac to make such a resounding statement? The reason lies in the rapid development of physical laws during the first part of the 20th century, which eventually were to solve some of the fundamental mysteries of classical physics. One of the most important of these, in terms of the development of quantum mechanics, was the "ultraviolet catastrophe". The heart of this problem is the power (energy per unit time) of an ideal electromagnetic emitter. Classical Maxwellian laws predict that the power tends to infinity for shorter wavelengths of radiation. This is certainly false; otherwise, skin cancer would be the least of our worries.

The predicament was rectified by assuming that the electrons producing the radiation within a blackbody could only oscillate at fixed discrete frequencies. The successful prediction of blackbody radiation curves using this assumption led to the formulation by Bohr of a quantum theory of the electronic structure of atoms. In quick succession to this, Erwin Schrödinger formulated a wave equation, now bearing his name, which could in principle describe the electronic state of any

particular system. If this could be done then any bond–making or bond–breaking event in chemistry could be described in its entirety.

2.2. Schrödinger's Equation

Simply put, Schrödinger's equation is a boundary-valued partial-differential equation that embodies Newton's laws of motion as applied to the nuclei and electrons of atoms and molecules. The significance of the wave equation is that it describes particles, which have an associated wavelength depending on their momentum, a duality first pointed out by de Broglie.[4] The equation can be written as:

$$i\hbar\frac{\partial}{\partial t}\Psi(q,t)=H(q,t)\Psi(q,t) \tag{2.1}$$

were, $\Psi(q, t)$ is the wave function describing the state of the system, $H(q, t)$ is the time-dependent Hamiltonian operator describing the total energy of the system, and q and t are the generalized position coordinates and time coordinate, respectively. Using

$$\mathrm{H}=\frac{P^2}{2m}+V(q) \tag{2.2}$$

as the Hamiltonian operator and converting the momentum operator into the quantum mechanical form, one obtains the famous time-dependent Schrödinger equation:

$$i\hbar\frac{\partial}{\partial t}\Psi(q,t)=-\left(\frac{\hbar^2}{2m}\right)\nabla^2\Psi(q,t)+V(q)\Psi(q,t) \tag{2.3}$$

In the special case where the Hamiltonian is time-independent, the solution of equation 2.1 may be reformulated into a product of time-independent and time-dependent functions.

$$\Psi(q,t)=\Psi(q)y(t) \tag{2.4}$$

Equation 2.4 may be used to separate equation 2.1 into two ordinary differential equations, one of which contains the time-dependency, i.e.,

$$i\hbar\frac{\partial y(t)}{\partial t} = Ey(t) \tag{2.5}$$

which has solutions of the form:

$$y(t) = Ae^{-\frac{iEt}{\hbar}} \tag{2.6}$$

The equation governing the time-independent variables is known as the time-independent Schrödinger equation and is given by:

$$-\left(\frac{\hbar^2}{2m}\right)\nabla^2\Psi(q) + V(q)\Psi(q) = E\Psi(q) \tag{2.7}$$

Erwin Schrödinger detailed this result in one of four monumental papers published in the first half of 1926 marking the birth of wave mechanics (or in his words the "undulatory theory of mechanics of atoms and molecules"[5] but this may be just a poor translation) and thus quantum chemistry. To solve equation 2.7 within the theory of partial-differential equations, one needs to state the appropriate boundary condition.

For physical reasons, the condition states that the particles must be bound or confined within some region of space, i.e.,

$$\Psi(q) \to 0 \quad as \left|q\right| \to \infty \tag{2.8}$$

Imposing the boundary condition 2.8 and restricting the wave function so that it is single-valued, continuous and has continuous first derivatives gives non-trivial solutions to equation 2.7 with discrete values of E. Unfortunately for chemists, solutions to equation 2.7 subjected to the boundary condition 2.8 can only be found analytically in a small number of special cases and it is at this point Dirac's "approximate" methods must be invoked.

2.2.1. The Born–Oppenheimer Approximation

For further discussion is necessary to introduce here the well known Born-Oppenheirmer (BO) approximation. Born and Oppenheimer argued[6] that because nuclei are much heavier than electrons, the electronic response to movements by the nuclei must be nearly instantaneous. The consequence of this is a decoupling of electronic and nuclear motion. Mathematically this implies that the total wave function given in equation 2.7 can be separated into product wave functions of the electrons and nuclei, i.e., $\Psi(Q,q)= \Psi^{elec}(Q, q)\Psi^{nuc}(Q)$. Therefore one may solve equation 2.7 for the electronic wave function in the mean field of the nuclei. The total electronic energy (E_{TOT}) one finds from 2.7 then becomes the sum of the electronic energy and the coulombic repulsion of the nuclei (nuclear repulsion).

$$E_{TOT} = E_{ELEC} + E_{NR} \tag{2.9}$$

If one writes the time-independent Hamiltonian in terms of operators occurring because of electron-electron, nucleon-nucleon and electron-nucleon interactions then equation 2.7 becomes;

$$\left(-\sum_{i=1}^{N} \frac{1}{2}\nabla_i^2 - \sum_{i=1}^{N}\sum_{A=1}^{M} \frac{Z_A}{r_{iA}} + \sum_{i=1}^{N}\sum_{j>i}^{N} \frac{1}{r_{ij}} + \sum_{A=1}^{N}\sum_{B>A}^{M} \frac{Z_A Z_B}{R_{AB}} \right) \Psi^{elec}(Q,q)\Psi^{nuc}(Q)$$
$$= E_{TOT}\Psi^{elec}(Q,q)\Psi^{nuc}(Q) \tag{2.10}$$

The first term in the brackets of equation 2.10 is the kinetic energy operator for the N electrons in the system, the second term is the Coulomb attraction between the M nuclei and N electrons, the third is the Coulomb repulsion between all pairs of electrons and the final term is the Coulomb repulsion between all pairs of nuclei. Equation 2.10 introduces the use of atomic units, which are obtained by setting the mass of the electron (m_e), the charge on an electron (e) and Plank's constant divided by 2π ($\hbar$) to one. The units for energy, length and time become the Hartree, Bohr and Chronon[7], respectively. To solve the

UNIVERSITAT ROVIRA I VIRGILI
ASSEMBLY AND PROPERTIES OF POLYOXOMETALATES: A THEORETICAL POINT OF VIEW
Laia Vilà Nadal
ISBN.978-84-694-2170-3/DL:T. 1039-2011

electronic problem one separates the equation into the operations that act on the electronic wave function, and then solve it for a particular arrangement of the nuclei. In this way the electronic wave function depends parametrically on the nuclear coordinates (Q). The nuclear coordinates can be changed and the electronic problem resolved for any desired nuclear configuration so that a potential energy hypersurface is built. Each time the electronic problem is solved, a countable infinite number of solutions is obtained and each of these solutions is termed an "electronic state".

2.3. Brief Introduction to DFT

As we have said in the previous lines, the goal of most quantum chemical approaches is the -approximate- solution of the time-independent, non-relativistic Shrödinger equation.[8]

$$\hat{H}\,\Psi_i(\vec{q}_1,\vec{q}_2,..,\vec{q}_N,\vec{Q}_1,\vec{Q}_2,..\vec{Q}_M) = E_i\Psi_i(\vec{q}_1,\vec{q}_2,..,\vec{q}_N,\vec{Q}_1,\vec{Q}_2,..\vec{Q}_M) \quad (2.11)$$

Ĥ is the Hamilton operator for a molecular system consisting of M nuclei and N electrons in the absence of magnetic or electric fields.

Now that the Schrödinger equation with the molecular Hamilton operator has been presented a short introduction to density functional theory (DFT) follows.[9] This short introduction to elementary quantum chemistry is useful to introduce density functional theory (DFT). The basis for DFT is the proof by Hohenberg and Kohn[10] that the ground state electronic energy is determined completely by the electron density ρ. In other words, there exists a one-to-one correspondence between the electron density of a system and the energy.[11] Quoting from the original paper the theorem, in the words of the authors, is expressed as,

"… the external potential $V_{ext}(\mathbf{r})$ is (to within a constant) a unique functional of $\rho(\mathbf{r})$; since, in turn $V_{ext}(\mathbf{r})$ fixes H we see that the full many particle ground state is a unique functional of $\rho(\mathbf{r})$."[10]

UNIVERSITAT ROVIRA I VIRGILI
ASSEMBLY AND PROPERTIES OF POLYOXOMETALATES: A THEORETICAL POINT OF VIEW
Laia Vilà Nadal
ISBN.978-84-694-2170-3/DL:T. 1039-2011

The application of self-consistent methodology to the DFT, developed by Kohn and Sham,[12] has in the recent past emerged as an important first-principles computational method to predict chemical properties accurately and to analyse and interpret these in convenient and simple chemical terms.[13] This success is based on the suggestion that the electron kinetic energy should be calculated from an auxiliary set of orbitals used for representing the electron density.

The basic postulate in Kohn–Sham theory is that we can apply a one-electron formulation to the system of *N* interacting electrons by introducing a suitable local potential $V_{xc}(r)$ and solving the following equation. It is also required to add the Coulomb potential of the electron cloud $V_c(r)$ and, if necessary, any external potentials $V_{ext}(r)$.

$$\left(-\frac{1}{2}\nabla^2 + V_{ext}(r) + V_C(r) + V_{XC}(r)\right)\varphi_i(r) = \varepsilon_i \Phi_i(r) \qquad (2.12)$$

The functional derivative of $E_{xc}[\varrho]$ with respect to the density ϱ is the potential V_{xc}. The exact form of the exact energy density $E_{xc}(r)$ representing and incorporating all exchange and correlation (XC) effects is unknown.

Although exchange-correlation energy is the only unknown functional, luckily it represents a rather small fraction of the total energy, and can be overcome by means of approximations. The simplest one is the local density approximation (LDA), where the electron density is assumed to be slowly varying, such that the exchange-correlation energy can be calculated using formulas derived for a uniform electron density. LDA is a pretty good approximation for the special case of a uniform electron gas. But fails for inhomogeneous systems such as molecules, clusters and solids.

In these systems LDA does not provide results that are accurate enough to permit a quantitative discussion of the chemical bond in molecules.[14] In fact, LDA overestimates the bond strengths by

UNIVERSITAT ROVIRA I VIRGILI
ASSEMBLY AND PROPERTIES OF POLYOXOMETALATES: A THEORETICAL POINT OF VIEW
Laia Vilà Nadal
ISBN.978-84-694-2170-3/DL:T. 1039-2011

~100 kJ·mol^{-1}.[9] One step further is the general gradient approximation (GGA) were the first derivative of the density is included as a variable. The most popular GGA within the chemist community is BLYP (denoting the combinations of Becke's 1988 exchange functional[15] with the 1988 correlation functional of Lee, Yang and Parr).[16] Nowadays GGA give reliable results for all main types of chemical bonds: covalent, ionic, metallic and hydrogen bridge. However for van der Waals interactions common GGA and LDA fail.

The search for more accuracy in the approximations persist, and various beyond-GGA functionals have appeared, as for example meta-GGA or hybrid functionals. On one hand, the so called meta-GGA functional allow the exchange and correlation functionals to depend either on higher order derivates (Laplacian), or on orbital kinetic energy density. On the other hand, hybrid functionals try to overcome some of the deficiencies of 'pure' DFT exchange functionals by mixing in a component of the exact exchange energy from HF theory. So they combine the exact Hartree–Fock exchange with a DFT exchange term, and add a correlation functional. A popular hybrid method known as B3LYP is a combination of the LYP GGA for correlation with Becke's three-parameter hybrid functional (B3) for exchange.[17] Hybrid functionals are generally fitted to a training set of molecules and so are not *ab initio* methods in the true sense as they include some empirical input.

2.4. Conductor-like Screening Model

It is known that POMs exist in solution as negatively charged species stabilized by solvent. To be consistent with that fact, the structures discussed through this work were fully optimized in the presence of a solvent. We have used Conductor-like Screening Model (COSMO)[18] as implemented in ADF[19] program

UNIVERSITAT ROVIRA I VIRGILI
ASSEMBLY AND PROPERTIES OF POLYOXOMETALATES: A THEORETICAL POINT OF VIEW
Laia Vilà Nadal
ISBN.978-84-694-2170-3/DL:T. 1039-2011

package. In the following lines we will describe several key aspects to understand the main features concerning COSMO, for further details please consult reference 20.

The efficient construction of proper and sufficiently accurate segmentations of a molecular-shaped cavity is an important technical aspect of apparent surface charge models, because it has a strong influence on both the accuracy and speed of the calculations.

Given the coordinates and atomic numbers of all N atoms of a molecule, the usual concept for the definition of a continuum solvation model (CSM) cavity starts with the assignment of the minimum distances, R_α, for all atoms α. This assignment can either be according to the atomic numbers, using element-specific radii, or according to more details of the chemical environment, i.e., by introduction of atom-type-specific radii. The second procedure introduces more adjustable parameters, with the potential of a more accurate reproduction of experimental data, but also with the danger of loss the predictive power of the model. After assigning the radii, the union of the corresponding atom centered spheres is considered as the interior of the molecule. This is shown as the blue region in Fig. 2.1. Such cavities usually have some sharp crevices and even sharp cusps. Such crevice and cusp areas are fatal for the dielectric continuum approach, because the electrostatic field in front of a dielectric cusp becomes infinite and the boundary conditions can no longer be solved.

UNIVERSITAT ROVIRA I VIRGILI
ASSEMBLY AND PROPERTIES OF POLYOXOMETALATES: A THEORETICAL POINT OF VIEW
Laia Vilà Nadal
ISBN.978-84-694-2170-3/DL:T. 1039-2011

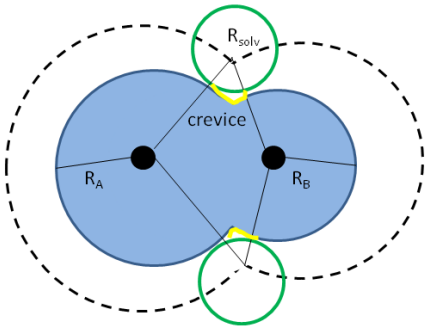

Figure 2.1. Schematic illustration of the cavity construction method.

Therefore any sphere-based CSM cavity construction requires a smoothing algorithm for such situations. In computational chemistry, a solvent radius R_{solv} is often used to define a smooth solvent-excluding surface (SES). This is made by means of the surface of a ball of radius R_{solv} rolling over the atomic spheres, as shown in Fig. 2.2.c. Of course, the surface-segment construction on the smoothing region in three dimensions is geometrically very demanding.

The solvent is handled as a dielectric medium, with a given dielectric constant (ε) that induces charge polarization on surface around the molecule (cavity-immersed in solution). To model water as a solvent we choose ε=78, to model *N,N*-dimethylformamide (DMF) ε=37. Starting from van der Waals spheres centered on the solute atoms three different kinds of molecular sufaces can be described (Fig. 2.2): the proper van der Waals surface, the solvent-accessible surface (SAS), and the solvent-excluding surface (SES). In our calculations the last two were chosen. The SAS is defined as the surface generated by the centre of a rigid probe sphere rolling on the van der Waals surface; the SES surface is the envelope of the volume extended to the probe sphere when it rolls on the van der Waals spheres centered on the solute atoms.[21]

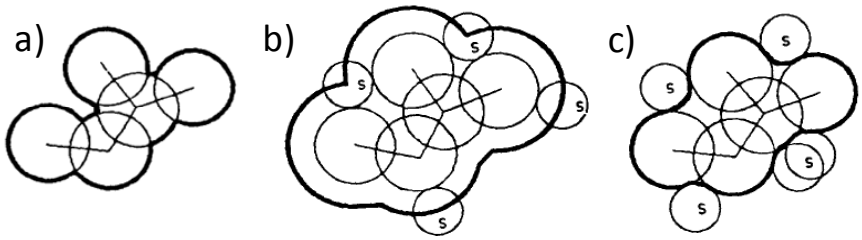

Figure 2.2. Definition of the different kinds of molecular surfaces: (a) van der Waals surface, (b) solvent-accessible surface, (c) solvent-excluding surface.

In order to obtain the electron density in solution, first it is converged in the gas phase and afterward the COSMO model is turned on to include the solvent effects variationally. So the model generates one molecular cavity, built by atom centered spheres of all atoms in molecule. Point charges are situated at the superficies of the cavity. These point charges generate a potential of interaction which is added in the calculation in vacuum and the energy of the system and the molecular orbitals are recalculated. This process is repeated until self-consistency. The ionic radii of the atoms, which define the dimensions of the cavity surrounding the molecule are chosen to be 1.26 Å for W, 0.64 for Mo, 1.52 for O, 1.20 for H, 0.85 for B, 1.20 for Al, 2.10 for Si, 1.00 for P, 1.60 for Ga, 1.22 for Ge, 0.56 for As, 1.39 for Zn, 0.78 for I and 0.81 for Te.

2.5. Car–Parrinello Molecular Dynamics

Complementary to standard DFT calculations, a description of the solute-solvent interactions by means of Car–Parrinello Molecular Dynamics has been performed. This methodology is accurate enough to describe the interactions between the solute, in our case W or Mo oxoanions, and the solvent explicit water molecules. In few words, a first-principles molecular dynamics (MD) simulation will generate a trajectory of our initial

UNIVERSITAT ROVIRA I VIRGILI
ASSEMBLY AND PROPERTIES OF POLYOXOMETALATES: A THEORETICAL POINT OF VIEW
Laia Vilà Nadal
ISBN.978-84-694-2170-3/DL:T. 1039-2011

coordinates by propagating this starting set of coordinates and velocities according to Newton's second law equation, using an "on-the-fly" calculated DFT potential energy, by a series of finite time steps. When using direct dynamics with electronic structure methods one needs a converged wave function at each time step, although this procedure is computationally expensive, i. e. so-called Born-Oppenheimer molecular dynamics. This is required to accomplish energy conservation over the whole simulation length. The improvement made by Car and Parrinello shows that it is not necessary to fully converge the wave function in each time step.[22] After having determined a converged wave function at the first point, the essence of Car–Parrinello method is to let the orbitals evolve simultaneously with the changes in nuclear positons. The computational settings of these simulations can be found elsewhere.[23] In the following lines we will give a short overview of the main features concerning Car–Parrinello MD. The reader is strongly encouraged to examine some of the excellent literature on the field.[24]

"Molecular Dynamics (MD) consists of solving numerically the classical equations of motion for the atoms or molecules of the system we want to simulate."[25]

Classical molecular dynamics using predefined potentials, force fields, either based on empirical data or on independent electronic structure calculations, is well established as a powerful tool serving to investigate many-body condensed matter systems including biomolecular assemblies.[26] At the very heart of any molecular dynamics scheme is the question of how to describe – that is in practice how to approximate– the interatomic interactions, see Fig. 2.3.

The traditional route followed in molecular dynamics is to determine these potentials in advance. Typically, the full interaction is broken up into two-body and many-body

UNIVERSITAT ROVIRA I VIRGILI
ASSEMBLY AND PROPERTIES OF POLYOXOMETALATES: A THEORETICAL POINT OF VIEW
Laia Vilà Nadal
ISBN.978-84-694-2170-3/DL:T. 1039-2011

contributions, long-range and short-range terms, electrostatic and non-electrostatic interactions, etc., which have to be represented by suitable functional forms, for detailed accounts see references.[27] So basically what is needed for a MD simulation is (i) a model describing how atoms (molecules) interact with each other, i.e. simple Lennard–Jones[28] potentials, sophisticated semiempirical potentials as CHARMM,[29] etc. (ii) an algorithm for integrating the equations of motion, i.e. Leap-Frog algorithm,[30] etc. (iii) a sensible starting configuration (positions and velocities).

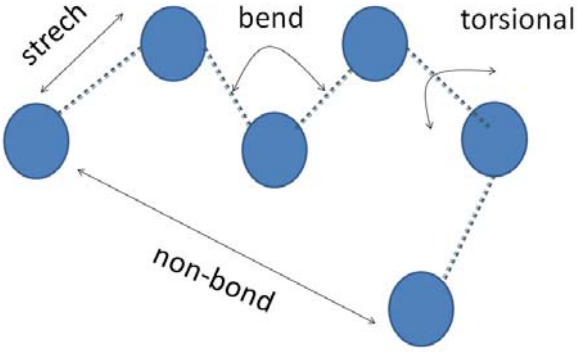

Figure 2.3. Illustration of the fundamental force-field energy terms. The force field energy is written as a sum of terms, each describing the energy required for distorting a molecule in a specific fashion. For instance, E_{str} is the energy function for *stretching* a bond between two atoms, E_{bend} represents the energy required for *bending* an angle, E_{tors} is the *torsional* energy for rotation around a bond, E_{vdw} and E_{el} describe the *non-bonded* atom–atom interactions, and finally E_{cross} describes coupling between the first three terms. Given such an energy function of the nuclear coordinates, geometries and relative energies can be calculated by optimization. Stable molecules correspond to minima in the potential energy surface and they can be located by minimizing E_{FF} as a function of the nuclear coordinates.

Coming back to Car–Parrinello MD, the basic idea underlying every *ab initio* molecular dynamics method is to compute forces acting on the nuclei from electronic structure calculations that

UNIVERSITAT ROVIRA I VIRGILI
ASSEMBLY AND PROPERTIES OF POLYOXOMETALATES: A THEORETICAL POINT OF VIEW
Laia Vilà Nadal
ISBN.978-84-694-2170-3/DL:T. 1039-2011

are performed "on-the-fly" as the molecular dynamics trajectory is generated, see Fig. 2.4 for a simplifying scheme. In this way, the electronic variables are not integrated out beforehand and represented by fixed interaction potentials, rather they are considered to be active and explicit degrees of freedom in the course of the simulation. This implies that, given a suitable approximate solution of the many-electron problem, also "chemically complex" systems, or those where the electronic structure changes drastically during the dynamics i.e. formation/breaking of bonds, can be handled easily by molecular dynamics. But this also implies that the approximation is shifted from the level of devising an interaction potential to the level of selecting a particular approximation for solving the Schrödinger equation, since it cannot be solved exactly for the typical problems at hand.

Despite its obvious advantages, it is evident that a price has to be paid for putting molecular dynamics onto an *ab initio* foundation: the correlation lengths and relaxation times that are accessible are much smaller than what is affordable in the framework of standard molecular dynamics. Happily, this discrepancy is being counterbalanced by the ever-increasing power of available computing resources.

UNIVERSITAT ROVIRA I VIRGILI
ASSEMBLY AND PROPERTIES OF POLYOXOMETALATES: A THEORETICAL POINT OF VIEW
Laia Vilà Nadal
ISBN.978-84-694-2170-3/DL:T. 1039-2011

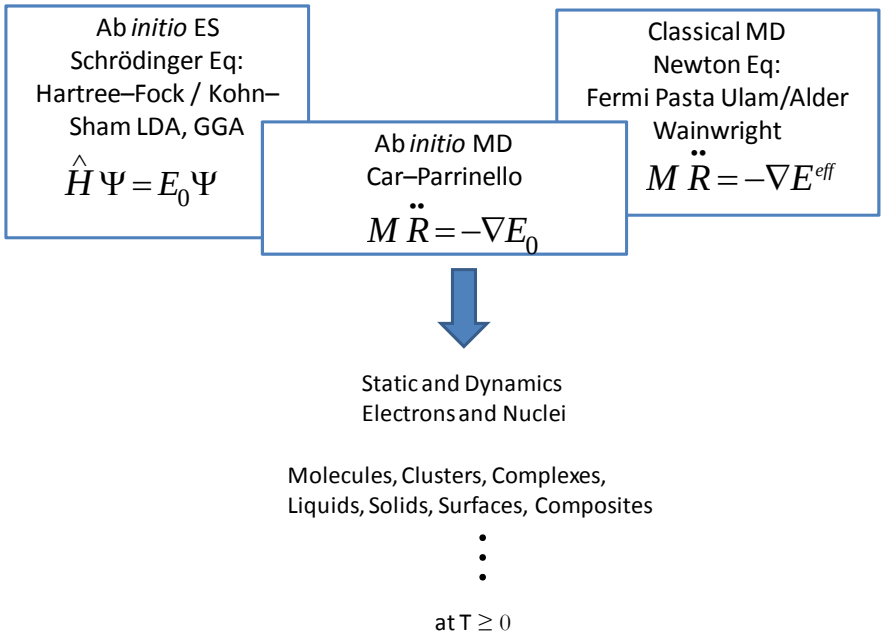

Figure 2.4. Ab inito molecular dynamics unifies approximate *ab initio* electronic structure theory (i.e. solving Schrödinger's wave equation numerically using, for instance, Hartree–Fock theory or DFT) and classical molecular dynamics (i.e. solving Newton's equation of motion numerically for a given interaction potential as reported by Fermi, Pasta, Ulam and Tsingou for a one-dimensonal anharmonic chain model of solids[31] and published by Alder and Wainwright for the three-dimensional hard-sphere model of fluids).[32]

Another appealing feature of standard molecular dynamics is less evident, namely the experimental aspect of "playing with the potential". Thus, tracing back the properties of a given system to a simple physical picture or mechanism is much harder in *ab initio* molecular dynamics, where certain interactions cannot easily be "switched off" like in standard molecular dynamics. On the other hand, *ab initio* molecular dynamics has the power to eventually map phenomena to a firm basis in terms of the underlying electronic structure and chemical bonding patterns. Most importantly, however, is the fact that new phenomena, which were not foreseen before starting the simulation, can

UNIVERSITAT ROVIRA I VIRGILI
ASSEMBLY AND PROPERTIES OF POLYOXOMETALATES: A THEORETICAL POINT OF VIEW
Laia Vilà Nadal
ISBN.978-84-694-2170-3/DL:T. 1039-2011

simply happen if necessary. All this lends *ab initio* molecular dynamics a truly predictive power. Summarizing, it can be concluded that *ab initio* molecular dynamics is the method of choice to investigate large and "chemically complex" systems.

Traditionally, direct dynamics with electronic structure methods have been done using a converged wave function at each time step. In order to fulfill energy conservation over the whole simulation length, however, such *Born–Oppenheimer dynamics* require a very tight convergence of the wave function in each time step, otherwise the electrons will create an artificial frictional term on the nuclei, and this makes the procedure computationally expensive.[33] In an elegant breakthrough by *Car and Parrinello*,[22, 34] it was shown that is not necessary to fully converge the wave function in each time step. After having determined a converged wave function at the first point, the essence of the Car–Parrinello technique is to let the wave function parameters (orbitals) evolve *simultaneously* with the changes in nuclear positions. This can be achieved by including the wave function parameters as variables with fictious "masses" in the dynamics, analogous to the nuclear positions and masses. Since this involves generalized variables, the Lagrange formulations (see eq. 2.13) for the dynamical equation is convenient. The use of such *extended Lagrange functions*[35] for describing the evolution of a system with both "real" (nuclear/electronic) and "fictious" (method parameters) degrees of freedom is quite general, and is for example also used in force field methods incorporating fluctuating charges and/or polarization.

The basic idea of the Car–Parrinello approach can be viewed as taking most direct advantage of the *quantum-mechanical adiabatic time scale separation* of fast electronic (quantum) and slow (classical) nuclear motion. Algorithmicaly this is achieved by transforming this separation into a *classical-mechanical adiabatic energy-scale separation* in the framework of dynamical systems

theory. In order to achieve this goal the two-component quantum/classical problem is mapped onto a two-component purely classical problem with two separate energy scales at the expense of losing the physical time information of the quantum subsystem dynamics. Furthermore, the central quantity, the energy of the electronic subsystem, $\langle \Psi_0 | H_e | \Psi_0 \rangle$, is certainly a *function of the nuclear positions* $\{\mathbf{R}_I\}$. But at the same time it can be considered *to be a functional of the wave function* Ψ_0 and thus of a set of orbitals $\{\phi_i\}$.

Now, in classical mechanics the force on the nuclei is obtained from the derivative of a suitable Lagrangian with respect to the nuclear positions. This suggest that a functional derivative with respect to the orbitals, which are interpreted as classical fields, might yield the correct force on the orbitals, given a suitably defined Lagrangian. In addition, possible constraints within the set of orbitals have to be imposed, such as orbital orthonormality. So after this fundamental observations we can introduce the following Lagrangian derived from Car and Parrinello approaches, eq. 2.13.

$$L_{CP} = \sum_I \frac{1}{2} M_I \dot{\vec{R}}_I^2 + \sum_i \mu_i \langle \dot{\phi}_i | \dot{\phi}_i \rangle - \langle \Psi_0 | H_e | \Psi_0 \rangle + \sum_{i,j} \Lambda_{ij} \left(\langle \Psi_i | \Psi_j \rangle - \delta_{ij} \right)$$

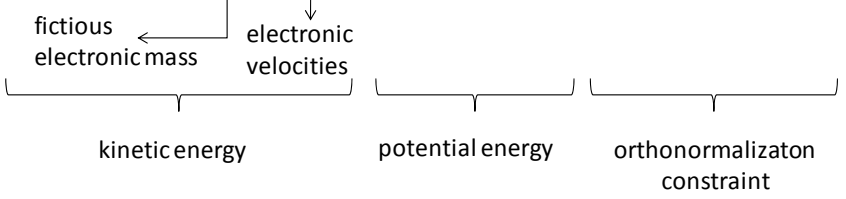

(2.13)

The corresponding Newtonian equations of motion are obtained from the associated Euler–Lagrange equations, 2.14 and 2.15,

$$\frac{d}{dt} \frac{\partial L}{\partial \dot{\vec{R}}_I} = \frac{\partial L}{\partial \vec{R}_I} \qquad (2.14)$$

UNIVERSITAT ROVIRA I VIRGILI
ASSEMBLY AND PROPERTIES OF POLYOXOMETALATES: A THEORETICAL POINT OF VIEW
Laia Vilà Nadal
ISBN.978-84-694-2170-3/DL:T. 1039-2011

$$\frac{d}{dt}\frac{\partial L}{\partial \dot{\phi}_i^*} = \frac{\partial L}{\partial \phi_i^*} \tag{2.15}$$

that is like classical mechanics, but here for both the nuclear positions and the orbitals. The nuclei evolve in time at a certain (instantaneous) physical temperature $\propto \sum_I M_I \dot{R}_I^2$, whereas a "fictious temperature" $\propto \sum_i \mu \langle \dot{\phi}_i | \dot{\phi}_i \rangle$ can be associated accordingly with the electronic degrees of freedom. In this terminology, "low electronic temperature" or "cold electrons" means that the electronic subsystem is close to its instantaneous minimum energy, $\min_{\{\phi_i\}} \langle \Psi_0 | \hat{H}_e | \Psi_0 \rangle$, i. e. close to the exact Born—Oppenheimer surface. Thus, a ground state wave function optimized for the initial configuration of the nuclei will stay close to its ground state also during time evolution if it is kept at a sufficiently low fictitious temperature.

The remaining task is to separate in practice nuclear and electronic motion such that the fast electronic subsystem stays cold also for long times but still follows the slow nuclear motion adiabatically (or instantaneously). Simultaneously, the nuclei must nevertheless be kept at a much higher temperature. This can be achieved in nonlinear classical dynamics via decoupling of the two subsystems and (quasi-) adiabatic time evolution. This is possible if the power spectra stemming from both dynamics do not have substantial overlap of their respective vibrational density of states, so that energy transfer from the "hot nuclei" to the "cold electrons" becomes practically impossible on the relevant time scales. Finally as a sum up picture, see Fig. 2.5.

UNIVERSITAT ROVIRA I VIRGILI
ASSEMBLY AND PROPERTIES OF POLYOXOMETALATES: A THEORETICAL POINT OF VIEW
Laia Vilà Nadal
ISBN.978-84-694-2170-3/DL:T. 1039-2011

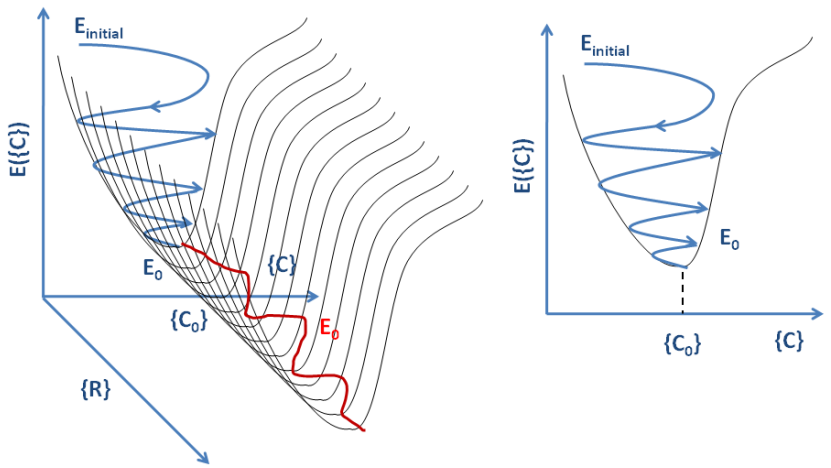

Figure 2.5. Picture showing a comparison of the Car–Parrinello MD approach, left, with BOMD, right. The Car–Parrinello MD uses fictitious dynamics for the wavefunctions (orbitals). Its nuclear and electronic degrees of freedom are propagated together. On the contrary, BOMD optimize electronic structure in each time step tightly. In the Car–Parrinello approach, the total energy is conserved during the simulation in an excellent manner, BOMD behaves not as good as Car–Parrinello MD. The iteration time step is larger in BOMD.

2.5.1. Metadynamics

Metadynamics is a novel molecular dynamics based technique aimed at enhancing the sampling of the phase space and at estimating the free energy landscape.[36, 37] The algorithm is based on a dimension reduction, defining a set of *collective variables* (s) which enclose the essential modes associated with the transitions in the analyzed process.[38]

Let us consider[37] a system of atomic coordinates x which is moving under an interatomic potential $V(x)$, see Figure 2.6. In a standard molecular dynamics simulation the system is oscillating in one of the minima of the energy surface and the crossing to the other minima is rather unlikely, because the barrier is higher than the thermal energy ($1/2\ k_bT$). In other words, the crossing is a *rare event* that cannot be observed within the typical simulation times. In order to accelerate the exploration of the

UNIVERSITAT ROVIRA I VIRGILI
ASSEMBLY AND PROPERTIES OF POLYOXOMETALATES: A THEORETICAL POINT OF VIEW
Laia Vilà Nadal
ISBN.978-84-694-2170-3/DL:T. 1039-2011

phase space we can use metadynamics. This technique is based on defining a collective variable *s* which is an explicit function of a subset of coordinates *x'* [*s* = f(*x* ')], i.e. a distance or a coordination number.

The metadynamics simulation starts in one of the minima of the energy surface. At the beginning of the simulation, the force acting on the system is given by the gradient of the potential V, see eq. 2.16:

$$f_i^V = -\frac{\partial V}{\partial r_i} \tag{2.16}$$

After a time interval *t'*, a small Gaussian-like repulsive potential term (V') is added, centered at the value of *s* at time *t'* (Figure 2.6b). This is repeated every time interval *t'* along the MD simulation, such that at a time *t* the total potential is the sum of the interatomic potential V ant the sum of the V' terms added up to that time, i.e. V_G see equation 2.17:

$$V_T = V + V_G \text{ were } V_G = \sum_{t'} w \exp\left(-\frac{\left[s(t) - s(t') \right]^2}{2(\delta s)^2} \right) \tag{2.17}$$

where *w* is the height of the Gaussian potential term, δs is its width and V_G is the *history-dependent potential* (i.e. the number of Gaussian terms added depends on the time passed). As a consequence, the force acting on the system is now the sum of two components, one coming from V and the other for V_G, equation 2.18.

$$f_i^{V_r} = f_i^V + f_i^{V_G} = -\frac{\delta V}{\delta r_i} - \frac{\delta V_G}{\delta r_i} \tag{2.18}$$

When a Gaussian potential term is added to V_G, the total potential changes and hence the system needs to be equilibrated by using a thermostat. In addition the resulting forces are also

modified, and thus the metadynamics trajectory is not an equilibrium trajectory.

The added potentials V' progressively counterbalance the underlying free energy (Figure 2.6c), thus penalizing the regions of the phase space already explored. As a result, the system tends to escape from already visited points to another energy minimum through the nearest and lowest-in-energy transition state. Hence, *metadynamics can accelerate the exploration of the phase space and the observation of rare events*. In other words, provided that the collective variables are properly chosen, the system will evolve by the same pathway that would have explored in a longer standard molecular dynamics.

Besides, *metadynamics can also be used for mapping the free energy surface (FES)* in the regions explored during the simulation as a function of *s*. The free energy surface can be estimated as the negative of the sum of the Gaussian potential terms:[36]

$$G(s) = \lim_{t \to \infty} V_G(s,t) \approx \sum_{t'} w \exp\left[-\frac{\left[s(t) - s(t') \right]}{2(\delta s)^2} \right] \qquad (2.19)$$

The quality of the FES depends on the parameters defining the history-dependent potential.[39] Large values of w and δs will allow a faster exploration of the collective variables space, although at expense of less accuracy.

UNIVERSITAT ROVIRA I VIRGILI
ASSEMBLY AND PROPERTIES OF POLYOXOMETALATES: A THEORETICAL POINT OF VIEW
Laia Vilà Nadal
ISBN.978-84-694-2170-3/DL:T. 1039-2011

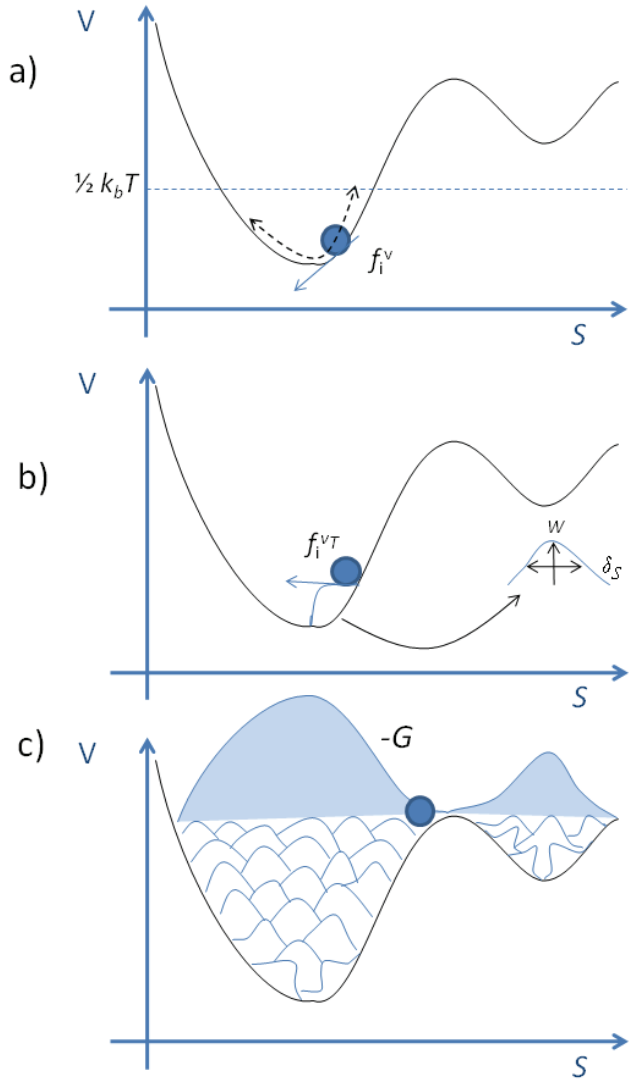

Figure 2.6. a) Standard molecular dynamics simulation. The system evolves following the interatomic potential V, and thus the force acting on the system is f_i^V (equation 2.16). b) Metadynamics simulation (i. e. a Gaussian potential term with height *w* and width δ_s is added every certain time t' centered at the value of *S* at the moment). The system evolves following the modified potential $V^T=V+V^G$, and thus the force acting on the system is f_i^{VT} (equation 2.18). c) End of metadynamics and reconstruction of the free energy surface (G, equation 2.19) Taken from reference.[40]

UNIVERSITAT ROVIRA I VIRGILI
ASSEMBLY AND PROPERTIES OF POLYOXOMETALATES: A THEORETICAL POINT OF VIEW
Laia Vilà Nadal
ISBN.978-84-694-2170-3/DL:T. 1039-2011

Collective variables

The collective variables (CVs) to be used in a metadynamics simulation have to fulfil the following requirements:[41, 42]

-They are an explicit function of a subset of coordinates of the system.

-The mathematical function that define the CVs must be continuous and derivable.

-The reaction coordinate must be a combination of the chosen CVs.

-The CVs have to clearly differentiate between the initial and final states of the process.

-All the reaction modes with relaxation times similar to those of the CVs have to be included.

In this work, we often use as CV the coordination number (CN) of one atom, or group of atoms, A, with respect to a second atom, or group of atoms, B. The CN provides information on the interaction pattern characterizing the actual atomic configuration. The analytic definition of the CN of B with respect to A reads:

$$C_{AB} = \sum_{i=1}^{N_A} \frac{1}{N_A} \left[\sum_{j=1}^{N_B} \frac{1-\left(\frac{r_{ij}}{d_{AB}}\right)^p}{1-\left(\frac{r_{ij}}{d_{AB}}\right)^q} \right] \tag{2.20}$$

where N_A and N_B are the numbers of atoms in the groups A and B, respectively. d_{AB} is a reference distance characterizing the A–B interactions. The choice of d_{AB} and of the exponents p and q determines the decay behavior of C_{AB} with the distance. In the present work, $p = 6$ and $q = 12$ are used.

UNIVERSITAT ROVIRA I VIRGILI
ASSEMBLY AND PROPERTIES OF POLYOXOMETALATES: A THEORETICAL POINT OF VIEW
Laia Vilà Nadal
ISBN.978-84-694-2170-3/DL:T. 1039-2011

2.6. Calculation of NMR Parameters

The phenomenon of nuclear magnetic resonance in solids and liquids was first observed in 1945 by two groups of physicists working independently (Purcell, Torrey and Pound at Harvard University and Bloch, Hansen and Packard at Standford University).[43] Nowadays nuclear magnetic resonance, or NMR, is widely used for structure elucidation in chemistry. The physical foundation of this technique lies in the magnetic properties of atomic nuclei. In this way a spectrum can be generated for a compound containing atoms whose nuclei have non-zero magnetic moments (^{1}H, ^{19}F, ^{13}C, ^{14}N, and many others). The significance of NMR spectroscopy in chemistry is therefore not based on its ability to differentiate between elements, but on its ability to distinguish a particular nucleus with respect to its environment in the molecule.[44-45]

What happens when a magnetic field is applied to a certain atom? The applied magnetic field, B_0, induces circulations in the electron cloud surrounding the nucleus such that a magnetic moment μ, opposed to B_0, is produced. This means that the local field at the nucleus is smaller than the applied field. This effect corresponds to a magnetic shielding of the nucleus that reduces B_0 by an amount equal to σB_0 where the σ is known as the shielding constant:

$$B_{local} = B_0(1-\sigma) \tag{2.21}$$

When a magnetic field is applied to a molecule the situation becomes more complex and the electronic circulation within the entire molecule must be considered. The value of σ in molecules then corresponds to the sum of diamagnetic and paramagnetic components of the induced electronic motion:

$$\sigma = \sigma_{dia} + \sigma_{para} \tag{2.22}$$

The presence of other nuclei within the molecule represents a perturbation of the spherical symmetry of electron distribution.

UNIVERSITAT ROVIRA I VIRGILI
ASSEMBLY AND PROPERTIES OF POLYOXOMETALATES: A THEORETICAL POINT OF VIEW
Laia Vilà Nadal
ISBN.978-84-694-2170-3/DL:T. 1039-2011

Subsequently in a molecule the diamagnetic effect is reduced. This diminution can be treated as corresponding to a paramagnetic moment that strengthens the external field B_0.

The interaction of the nuclear magnetic moment of a nucleus with an external magnetic field, B_0, leads to a nuclear energy level diagram, because the magnetic energy of the nucleus is restricted to certain discrete values E_i. The absorption of energy can be detected, amplified and recorded as a spectral line, the so-called resonance signal. In practice one usually measures the chemical shift δ, which is related to the resonance frequencies of the sample ν_s and of a reference sample ν_{ref}

$$\frac{\delta}{ppm} = 10^6 \left(\frac{\nu_s - \nu_{ref}}{\nu_{ref}} \right) \tag{2.23}$$

2.6.1. The Physical Basis of NMR Spectroscopy

In order to understand the chemical computation of NMR chemical shifts it is necessary to make an elementary presentation of the physics involved in this phenomenon. The present section deals with this question, here the basic aspects of nuclear magnetic spectroscopy are presented. This elementary section can be skipped for the readers familiar with NMR principles.

As it is known, the magnetic properties of the atomic nucleus form the basis of nuclear magnetic resonance spectroscopy.[18] Several nuclei possess *angular momentum*, P, responsible for the existence of a nuclear *magnetic moment*, μ. The two quantities are related through the expression

$$\mu = \gamma P \tag{2.24}$$

where γ, the *magnetogyiric ratio*, is a constant characteristic of the particular nucleus. Angular momentum and nuclear magnetic moment are *quantized*, according to quantum theory. The *eigenvalues* of the maximum component of the angular

UNIVERSITAT ROVIRA I VIRGILI
ASSEMBLY AND PROPERTIES OF POLYOXOMETALATES: A THEORETICAL POINT OF VIEW
Laia Vilà Nadal
ISBN.978-84-694-2170-3/DL:T. 1039-2011

momentum in the z direction of an arbitrarily chosen Cartesian coordinates system are measured in units of $\hbar$ (h/2π) and are defined by the relation

$$P_z = \hbar m_I \tag{2.25}$$

where m_I is the *magnetic quantum number* which characterizes the corresponding *eigenstates* of the nucleus. According to *quantum condition*

$$m_I = I, I-1, I-2, ..., -I \tag{2.26}$$

these magnetic quantum numbers are related to the *spin quantum number*, *I*, of the respective nucleus. The total number of possible *eigenstates* or energy levels is thus equal to $2I+1$.

If we consider the case of proton, it can exist in only two spin states. They are characterized by magnetic quantum numbers $m_I=½$ and $m_I=-½$. Moreover, for the magnitude of the magnetic moment in the z direction, we have

$$\mu_z = \gamma \hbar m_I = \pm \gamma \hbar I = \pm \gamma \hbar / 2 \tag{2.27}$$

Following the example of the proton, it can be therefore pictured as a *magnetic dipole*, whose z component, μ_z, can have a parallel or anti-parallel orientation with respect to the positive z direction of the coordinate system.

By analogy with relations that describe the magnetic properties of electrons, equation (2.27) is sometimes expressed in as

$$\mu_z = g_N \mu_N m_I \tag{2.28}$$

In equation (2.28) g_N is the nuclear g factor, characteristic of the ratio between nuclear charge and nuclear mass. The nuclear magneton is μ_N, whose value can be calculated from

$$\mu_N = eh / 4\pi m_P c \tag{2.29}$$

where e is the electronic charge, h is the Planck's constant, m_P is the mass of the proton, and c is the velocity of light. From equations (2.27) and (2.28) it follows that $\gamma \hbar = g_N \mu_N$.

In the following discussion we introduce *eigenfunctions* α and β for the proton corresponding to the m_I=½ and m_I=−½ state, respectively. They are simply provided to identify the energy levels of the proton. Both states for the nuclei of spin ½ have the same energy, i.e. they are *degenerate*. In a static magnetic field B_0 this degeneracy is destroyed as a result of the interaction of the nuclear moment μ with B_0. When the direction of B_0 coincides with the z axis, an energy difference

$$\Delta E = 2\mu_z B_0 \tag{2.30}$$

for the two spin states results, since the potential energy of a magnetic dipole in the field B_0 is $\mu_z B_0$ or $-\mu_z B_0$, depending on its orientation. The energy separation between the states produced in this way is proportional to the strength of the field B_0. It provides the necessary condition for the observation of a spectral line and thus forms the basis of the nuclear magnetic resonance experiment.

Because of its lower energy, the β state will be preferentially occupied and, according to the Bohr frequency condition, $\Delta E = h\nu$, we need an energy quantum,

$$h\nu_0 = 2\mu_z B_0 = \gamma\hbar B_0 \tag{2.31}$$

or radiation of frequency

$$\nu_0 = \frac{B_0\gamma\hbar}{h} = \frac{B_0\gamma}{2\pi} \quad \text{or} \quad (\text{with } \omega = 2\pi\nu) \quad \omega_0 = \gamma B_0 \tag{2.32}$$

in order to stimulate a transition to the state of higher energy. Equation (2.32) describes the so-called *resonance condition*, where the radiation frequency exactly matches the energy gap. The NMR signal corresponds to the arrow in Figure 2.7 and υ_0, according to equation (2.32), varies with the strength of the B_0-field employed in the experiment.

UNIVERSITAT ROVIRA I VIRGILI
ASSEMBLY AND PROPERTIES OF POLYOXOMETALATES: A THEORETICAL POINT OF VIEW
Laia Vilà Nadal
ISBN.978-84-694-2170-3/DL:T. 1039-2011

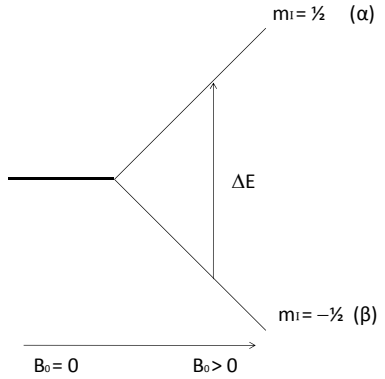

Figure 2.7. Energy separation between nuclear spin states of the proton at a given magnetic field B_0.

2.6.2. Methodological Aspects of NMR Computations

In this and the following subsections we are assuming either the knowledge of a hypothetical exact wavefunction or electron density, or when referring to existing methodology, the knowledge of an approximate wavefunction or electron density that has been determined minimizing the energy (variational approach).

NMR parameters as second-order energy perturbations

Despite this is not a necessary condition in order to calculate molecular properties in general and NMR parameters in particular, it facilitates qualitative discussions and interpretations based on wavefunction or electron density perturbations. The basic DFT theorem of Hohenberg and Kohn was formulated for a system in the absence of a magnetic field. Taking the latter into account leads to further complications, because the exchange-correlation functional should depend on the magnetic field.[46] Thus, one would need current-dependent (or magnetic-field dependent) exchange-correlation functionals. A more general report of calculations of energy derivatives can be found in more specific literature.[47]

First-principles quantum theories of molecules describe a system by its potential (nuclear coordinates and charges), by its number of electrons and by its kinematics (the form of the operators for the kinetic energy and the electronic repulsion, for instance nonrelativistic vs. relativistic expressions). The shielding tensor σ_a and indirect spin-spin coupling tensor K_{AB} second rank tensors which are obtained as double-first order perturbations of the total energy E of the molecules. In variatonal wavefuntion based methods,

$$E = \langle \Psi | \hat{H} | \Psi \rangle \tag{2.33}$$

with Ψ being the normalized wavefunction. In Kohn-Sham density functional theory (DFT),

$$E = E[\rho] \quad ; \quad \rho = \sum_{i}^{occ} \varphi_i^* \varphi_i \quad , \tag{2.34}$$

with ρ being the electron density and the φ_i the occupied Kohn–Sham molecular orbitals (MOs). For NMR calculations, the two perturbation parameters are μ_A, and μ_B or B_0, respectively, i.e.

$$\sigma_A = \left. \frac{\partial^2 E}{\partial \mu_A \partial B_0} \right|_{\mu_A=0, B_0=0} \tag{2.35}$$

$$K_{AB} = \left. \frac{\partial^2 E}{\partial \mu_A \partial \mu_B} \right|_{\mu_A=0, \mu_B=0} \tag{2.36}$$

These two equations are obtained first by deriving an expression of the molecular energy E which includes all terms in molecular quantum Hamiltonian $\hat{H}$ that are related to the nuclear magnetic moments and the external field B_0, and secondly by considering their interaction with the magnetic moments arising from the electronic spins and their motion through space. Accordingly Ψ or ρ must be understood as being dependent on μ_A, μ_B and B_0.

UNIVERSITAT ROVIRA I VIRGILI
ASSEMBLY AND PROPERTIES OF POLYOXOMETALATES: A THEORETICAL POINT OF VIEW
Laia Vilà Nadal
ISBN.978-84-694-2170-3/DL:T. 1039-2011

Taking the derivatives of E with respect to μ_A and μ_B or B_0 involves to take the derivatives of the operators that constitute the Hamiltonian $\hat{H}$ or the Kohn–Sham density functional and that are dependent on μ_A and/or μ_B and/or B_0. The presence of the magnetic perturbations in the Hamiltonian causes (small) changes in the electronic structure (i.e. ρ or Ψ) that need to be taken into account to first order so as to calculate the second–order perturbations of the energy. Therefore, derivatives of the wavefunction Ψ or the electron density ρ, with respect to at least one of the perturbations, are additionally required. Here the particular form of energy expression within different ab-initio methods, but also DFT (e.g. density vs. current-density functional), is crucial for obtaining the correct equations for these perturbations.

The Gauge-Origin problem

Computations of NMR properties with present-day DFT program codes require either the use of a finite basis set or a finite number of points on a grid, (or both) to represent the molecular orbitals. Clearly, infinite size basis sets cannot be employed, which has some important consequences for basis set calculations of σ_A, generally known as the "gauge dependence" or "gauge origin" problem. To explain in simple terms what that means, few key aspects of how magnetic properties enter the Schrödinger equations need to be introduced. The central *observable* in this context is the magnetic field B_0. However, in the *operators*, not B_0, but the related vector potential $\vec{A}$ of the field enters the appropriate equations. The connection between these two quantities is that

$$B_0 = \nabla \times \vec{A} \tag{2.37}$$

i.e, the magnetic field is defined as the *curl* of the vector potential. It should be mentioned that the curl is a particular kind of

UNIVERSITAT ROVIRA I VIRGILI
ASSEMBLY AND PROPERTIES OF POLYOXOMETALATES: A THEORETICAL POINT OF VIEW
Laia Vilà Nadal
ISBN.978-84-694-2170-3/DL:T. 1039-2011

gradient that can be applied to a vector field, for more details see references.[48] The present context makes unnecessary any in-depth discussion of what this means. However we need to put into words the following decisive point: the addition of the gradient of an arbitrary function to this vector potential $\vec{A}$ leaves the magnetic field B_0 unchanged. Or, in more graphic terms, two different choices of origin would give two alternative values of $\vec{A}$ at any point in space, while the field B_0 is of course independent of the arbitrarily chosen origin. Hence, many vector potentials give rise to *same* magnetic field and there is no unique definition for the choice of $\vec{A}$ corresponding to a particular magnetic field B_0. Since expectation values such as NMR chemical shifts only depend on the observable, i.e. B_0, the results must of course be independent of the actual choice of the vector potential $\vec{A}$ (as long as it yields B_0). It is this requirement which is meant if one states that the magnetic field is *gauge invariant*.

In all our computational strategies we are limited to approximate schemes and the use of finite one-electron basis sets. One of the outgrowths of these approximations is that gauge invariance is not fulfilled. The unpleasant consequence is that the computationally predicted magnetic properties depend on the choice of the coordinate system.

The two most widely used techniques to overcome this problem are the so-called *individual gauges for localized orbitals* (IGLO) and the *gauge-invariant atomic orbital*.[49] This second acronym (GIAO) has been criticized since orbitals are actually gauge dependent and an alternative name frequently used is *gauge-including atomic orbital*.

In the IGLO approach, gauge–dependent factors are used on localized orbitals, while in the GIAO framework the explicit field-dependence is build into the atom–centered basis functions.

UNIVERSITAT ROVIRA I VIRGILI
ASSEMBLY AND PROPERTIES OF POLYOXOMETALATES: A THEORETICAL POINT OF VIEW
Laia Vilà Nadal
ISBN.978-84-694-2170-3/DL:T. 1039-2011

Using uncoupled density functional theory in either IGLO or GIAO implementation leads in general to good agreement with experimental data in spite of the formal shortcomings of this approach. Subsequently the gauge problem is tackled with the same IGLO, GIAO or similar techniques as in wavefuction based approaches. In most current implementations, for instance *Gaussian*, *Turbomole* or *ADF* the latter is used.[8]

2.6.3. The Shielding Tensor

For simplicity reasons we will not consider any particular expression for energy E. As already mentioned, for computation of the nuclear shielding σ_A, one needs, the first-order derivative of the wavefunction with respect to the external field at μ_A=0, B_0=0. Now let us consider that Ψ_0 is the unperturbed wavefunction of the ground state of the molecule, or the reference state, for which the NMR property is to be calculated. The shielding tensor is then given by differentiating equation (2.33) in the sense of (2.35), which directly yields

$$\sigma_A = \left\langle \Psi_0 \middle| \hat{H}^{(\mu_A, B_0)} \middle| \Psi_0 \right\rangle + \left\langle \Psi^{(B_0)} \middle| \hat{H}^{(\mu_A)} \middle| \Psi_0 \right\rangle + \left\langle \Psi_0 \middle| \hat{H}^{(\mu_A)} \middle| \Psi^{(B_0)} \right\rangle$$

$$= \left\langle \Psi_0 \middle| \hat{H}^{(\mu_A, B_0)} \middle| \Psi_0 \right\rangle + 2\,\mathrm{Re}\left\langle \Psi^{(B_0)} \middle| \hat{H}^{(\mu_A)} \middle| \Psi_0 \right\rangle \qquad (2.38)$$

The first term in equation (2.38) is called the diamagnetic shielding, the second term is called the paramagnetic shielding. This subdivision refers to the nonrelativistic theory of nuclear shielding. In a relativistic theory, spin–orbit contributions are further included. As a result, NMR shielding tensor can be written as a sum of three contributions.[50]

$$\vec{\vec{\sigma}} = \vec{\vec{\sigma}}^{d} + \vec{\vec{\sigma}}^{p} + \vec{\vec{\sigma}}^{SO} \qquad (2.39)$$

Terms in Eq. (2.39) are, respectively, the diamagnetic, the paramagnetic and (relativistic) spin–orbit contributions. In the

following lines we will discuss the physical significations of these terms.

Paramagnetic shielding

The paramagnetic shielding is determined by the magnetically perturbed MOs. The leading contribution couples occupied and virtual MOs, and one can write, at least approximately

$$\sigma_{st}^{p} \propto 2\sum_{i}^{occ} n_i \sum_{\mu}^{N} u_{ai}^{(1,s)} \left\langle \psi_i \left| \left[\frac{r_N}{r_N^3} \times p \right]_t \right| \psi_a \right\rangle \tag{2.40}$$

ψ_a and ψ_i describe virtual and occupied MOs (with occupation number n_i), respectively; r_N is the electronic position operator relative to the NMR nucleus N, and p is the electronic momentum operator. The leading contribution to the first order coefficient $u_{ai}^{1,s}$ is given as

$$u_{ai}^{(1,s)} \propto -\frac{1}{2(\varepsilon_i^{(0)} - \varepsilon_a^{(0)})} \left\langle \psi_a \left| \widehat{M_S} \right| \psi_i \right\rangle \tag{2.41}$$

where $\varepsilon^{(0)}_{\mathrm{i}}$ and $\varepsilon^{(0)}_{\mathrm{a}}$ are the orbital energies of the occupied and unoccupied MOs and the integral represents the first-order magnetic coupling between the occupied and unoccupied orbitals. Paramagnetic shielding contribution depends on the electronic structure and so is sensitive to the XC functional.[51] In the GIAO formulation, *vide supra*, there are contributions to σ^p from both occupied-occupied and occupied-virtual couplings. While the former is not negligible, the major contribution of both to σ^p and to the difference between XC functional stems from the occupied-virtual terms. The coupling between occupied and virtual orbitals is due to the external magnetic field. For an energy gap, the leading contribution stems from integrals of the type

UNIVERSITAT ROVIRA I VIRGILI
ASSEMBLY AND PROPERTIES OF POLYOXOMETALATES: A THEORETICAL POINT OF VIEW
Laia Vilà Nadal
ISBN.978-84-694-2170-3/DL:T. 1039-2011

$$\left\langle \lambda_\gamma \left| \left(-\frac{r_\nu}{2} \right) \times \nabla \right| \lambda_\nu \right\rangle \tag{2.42}$$

This operator rotates the orbital λ_ν round its position R_ν; e.g., the y component rotates orbitals in the imaginary xz plane, etc. It can be then rationalized in terms of the form of the orbitals

$$r_\nu \times \nabla \Big|_y \left| p_z \right\rangle \propto \left| p_x \right\rangle \tag{2.43}$$

Paramagnetic contribution, σ^p, is always a leading contribution for heavy atoms.

Diamagnetic shielding

The diamagnetic shielding depends on the zero-order electronic density only

$$\sigma_{st}^d \propto \frac{1}{2c^2} \sum_i^{occ} n_i \sum_\mu^N d_{\mu i} \left\langle \psi_i \left| \frac{K}{r_N} \right| \lambda_\mu \right\rangle \tag{2.44}$$

Diamagnetic term is a consequence of produced shielding by the electrons close to the nuclei. Its contribution is always positive (shielding) and bigger as many electrons are next around the nuclei. It absolute value grows up with the atomic number, but it relative weight on the chemical shifts goes down. For heavy atoms, the diamagnetic shielding change is really negligible with respect to the total chemical shift range. This result is readily understandable from the fact that the core orbitals, 1s, 2s, in particular, contribute by far the largest part of the diamagnetic shielding. That is a consequence of the localized nature of the NMR shielding/chemical shift. Such core effects are largely independent from the chemical environment of the nucleus. They cancel out in relative chemical shifts.[52,53,54]

Spin-orbit shielding

The spin-orbit shielding contribution, σ_{st}^{so}, is dominated by the Fermi contact that depends on the spin polarization at the NMR nucleus

$$\sigma_{st}^{so} \propto \sigma_{st}^{FC} \propto \frac{4\pi g}{3c} \sum_{i}^{occ} \sum_{a}^{vir} u_{ai}^{1,s} \left\langle \psi_a \left| \widehat{S}_t \, \delta\left(r_N = 0\right) \right| \psi_i \right\rangle \tag{2.45}$$

where *g* is the electronic Zeeman *g–factor*, and $\widehat{S}_t$ is a cartesian component of the electronic spin operator.

The spin-orbit contribution arises from the fact that, with the electronic spin-orbit coupling present, the external magnetic field induces an electronic spin density. This spin density then causes nonvanishing shielding contributions by magnetic interactions with the nuclear-spin. The spin-orbit contribution is very sensitive not only to the atomic number of the central nuclei but to the atomic number of the atoms directly coordinated to it. Spin-orbit chemical shifts require strong s–type bonding contributions at the NMR nucleus. This explains why large spin-orbit chemical shifts are found for the ^1H NMR but less so for other nuclei. Kaupp *et al.*[55] have presented a simple but general qualitative picture of the mechanism involved. The spin-orbit operators induce spin polarization in the system. This induced spin density interacts with the nuclear magnetic moment of the NMR-active nucleus, by means of a Fermi-contact mechanism, see Figure 2.8. The SO shifts are indicated to be caused by the spin-orbit operator on the heavy atom A, which in the presence of an external magnetic field B^0 leads to a small amount of electronic spin polarization. The latter may now interact with the nuclear magnetic moments (e.g., nucleus B) in the system, mainly via an FC mechanism, and will cause a change in their nuclear shieldings.

UNIVERSITAT ROVIRA I VIRGILI
ASSEMBLY AND PROPERTIES OF POLYOXOMETALATES: A THEORETICAL POINT OF VIEW
Laia Vilà Nadal
ISBN.978-84-694-2170-3/DL:T. 1039-2011

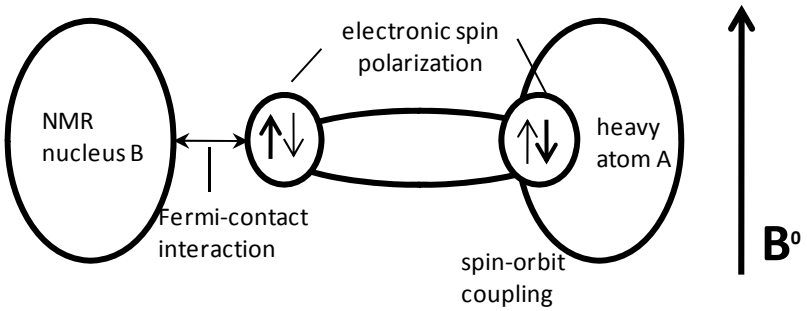

Figure 2.8. Schematic illustration of the spin–orbit effects on the shielding.

That SO shifts will depend strongly on the s-character of the bonding around the atom observed[56] by NMR spectroscopy, as the FC mechanism acts via the spherical part of the density at the nucleus. The importance of the s-character has far-reaching consequences for SO-induced heavy-atom effects on chemical shifts. Among other things, it explains why chemical shifts of main-group elements in their highest oxidation states exhibit very large SO shifts when attached to halogen or related substituents. The s-character of the bonding to the heavy-atom substituents is large in such cases, and thus there exists an efficient FC mechanism that transfers the SO-induced spin polarization to the considered NMR nucleus.

2.7. Software and Computational Details

The calculations in the present work have been performed using the DFT metodology with the program package ADF (*Amsterdam Density Functional, ADFV2004.01)*.[57] The electronic density provided by the local density approximation was improved using the X-alpha model for the exchange with Beckes's[58] gradient corrected exchange-correlation functional, and Vosko, Wilk, Nusair (VWN)[59] parametrization for correlation, corrected with

Perdew's functional[60]. The valence electrons for all atoms were described with Slater-type basis function of triple-ζ polarization quality. The inner electrons have been kept frozen. We have included scalar relativistic corrections by means of the *zeroth-order regular approximation* (ZORA)[17] formalism, via the core potential generated by subprogram called *DIRAC*.[17] All the computed stationary points have closed-shell electronic structure. The present computational settings BP86/TZP have been demonstrated to be a satisfactory methodology for describing the electronic structure of polyoxometalates.[61] Some calculations have been made at the GGA level using Becke exchange and Lee-Yang-Parr (BLYP) correlation functional.[62]

Regarding to the MD simulations, they were performed at DFT level by means of the CPMD program package.[22] The description of the electronic structure is based on the expansion of the valence electronic wave functions into a plane wave (PW) basis set, which is limited by an energy cutoff of 70 Ry. The interaction between the valence electrons and the ionic cores is treated through the pseudopotential (PP) approximation. Norm-conserving Martins-Troullier PPs are employed.[63] Nonlinear core corrections (NLCC) are included in the W PP.[64] We adopt the generalized gradient-corrected Becke-Lee-Yang-Parr (BLYP) exchange-correlation functional.[65] For the case of Mo, a semicore Mo PP was used according to the work of Boero et al.[66] and we adopt the generalized gradient-corrected functionals of Becke for the exchange and of Perdew for the correlation.[63,65] We have checked the validity of our computational settings by computing the hydration energies for tungstic and molybdic acids in the gas phase. We have compared the results with those obtained (i) using the PP approximation and a set of Gaussian functions and (ii) the frozen-core approximation and a set of Slater orbitals. The energy differences are smaller than 2 kcal mol^{-1} (less than 10 % error). In the MD simulations, the wave functions are propagated in the Car–Parrinello scheme, by

UNIVERSITAT ROVIRA I VIRGILI
ASSEMBLY AND PROPERTIES OF POLYOXOMETALATES: A THEORETICAL POINT OF VIEW
Laia Vilà Nadal
ISBN.978-84-694-2170-3/DL:T. 1039-2011

integrating the equations of motion derived from the extended Car–Parrinello Lagrangian.[22] We use a time step of 0.144 fs and a fictitious electronic mass of 700 a.u. Hydrogen atoms are substituted by deuterium atoms. The Nosé-Hoover thermostat for the nuclear degrees of freedom was used to maintain the temperature as constant as possible around 300 K. For metadynamics calculations, a simple rescaling of the atomic velocity that keeps the temperature within an interval of 50 degrees around 300 K is used.

The limited simulation time affordable by standard MD runs does not allow the observation of rare events like thermally activated chemical reactions. For this reason, we employ the metadynamics technique, which is capable of efficiently reconstructing complex reaction mechanisms and provides the free energy profile, as demonstrated in previous applications (see Chapter 3). The metadynamics simulations are based on the selection of collective variables (CV) that are suitable to describe the process.

2.8. Synthetic Methods

As we have said in the previous chapter, POM's synthetic routes are very simple and require a small number of steps, or even just one step (one-pot synthesis). Here we present the synthetic methods for the POMs studied in the present thesis: the Lindqvist $[W_6O_{19}]^{2-}$ and $[Mo_6O_{19}]^{2-}$ anions, and the Keggin $[PW_{12}O_{40}]^{3-}$, $[AsW_{12}O_{40}]^{3-}$, $[PMo_{12}O_{40}]^{3-}$ and $[AsMo_{12}O_{40}]^{3-}$ anions. For the ESI-MS experiments it was necessary to obtain the correspondent tetraalkylammonium salts such as $[(\mathbf{n}\text{-}C_4H_9)_4N]_4SiM_{12}O_{40}$ also noted $(TBA)_4SiM_{12}O_{40}$ (TBA=$[(\mathbf{n}\text{-}C_4H_9)_4N]^+$.

UNIVERSITAT ROVIRA I VIRGILI
ASSEMBLY AND PROPERTIES OF POLYOXOMETALATES: A THEORETICAL POINT OF VIEW
Laia Vilà Nadal
ISBN.978-84-694-2170-3/DL:T. 1039-2011

(A) $(TBA)_2W_6O_{19}$ was synthesized from $(TBA)_4W_{10}O_{32}$ by following the method of Klemperer and co-workers as posted here.[67] $(TBA)_4W_{10}O_{32}$ (1.5g) was refluxed in a mixture of 8 mL of CH_3CN and 30 mL of CH_3OH for 24 h. Upon cooling of the mixture to 0 ºC, a precipitate formed which was filtered and air-dried. Crystallization of this precipitate from a 60 ºC, saturated acetone solution cooled to 25 ºC yielded 0.21 g of product as clear and colorless, block-shaped crystals.

(B) $(TBA)_2Mo_6O_{19}$ used in this study was synthesized using the procedure described here.[68] A solution of 0.40 g of α-$(TBA)_4Mo_8O_{26}$ and 0.4 mL of water in 20 mL of CH_3CN was stored for 1 h. After addition of 0.05 mL of 12 N aqueous HCl, the solution volume was reduced to ca. 8 mL. Cooling of the mixture to 0 ºC yielded 0.25 g of product as yellow needles which were air-dried.

(C) $Na_3PW_{12}O_{40}\cdot 12H_2O$ was synthesized following the procedure described by Noth.[69] 1000g $Na_2WO_4\cdot 2H_2O$ and 160g $Na_2HPO_4\cdot 2H_2O$ were dissolved in 1500 mL of boiling water. While stirring, 800 mL of HCl (δ 1.18) is added drop wise. Phospotungstic acid begins to separate when about half of the acid is added. The solution is cooled and a solution of ether, free from reducting impurities is added, after shaking three layers remain. This requires about 600 ml of ether. More water may be added to dissolve the NaCl.

(D) $Na_2HPMo_{12}O_{40}\cdot 14H_2O$ was synthesized following the procedure described by Rocchiccioli-Deltcheff *et al.*[70] To 420 mL of a 2.85 M aqueous solution of Na_2MoO_4 were added successively 6.8 mL of 85% H_3PO_4 (~14.7 M) and 284 mL of 70% $HClO_4$ (~11.7 M). The disodium salt, $Na_2HPMo_{12}O_{40}\cdot 14H_2O$, precipitated from the yellow lukewarm

UNIVERSITAT ROVIRA I VIRGILI
ASSEMBLY AND PROPERTIES OF POLYOXOMETALATES: A THEORETICAL POINT OF VIEW
Laia Vilà Nadal
ISBN.978-84-694-2170-3/DL:T. 1039-2011

solution. After the mixure was cooled to room temperature, the microcrystalline powder was filtered and air-dried (250g). Recrystallization in a mixure of 40 mL Et_2O/200 mL gave 180 g of greenish microcrystals.

(E) $Na_3AsW_{12}O_{40}\cdot 12H_2O$ was synthesized following the procedure described by Rocchiccioli-Deltcheff *et al.*[62] A 20 mL quatinty of an ~2 M aqueous sodium arsenate solution (prepared with 5.42 g of 3 $As_2O_5\cdot 5H_2O$ and 3.3 g of NaOH pellets) was poured into a mixture of 100 mL of water and 165g (0.5 mol) of $Na_2WO_4\cdot 2H_2O$ (only partially dissolved). A 100 mL quantity of 1,4-dioxane was added, and the paste obtained was slowly acidified by 25 mL of concentrated (~12 M) aqueous HCl with vigorous triturating. The mixture progressively fluidized and turned into white solid suspension to which was further added 150 mL of concentrated HCl in small quantities. The stirring was continued for 30 min. The precipitate was filtered, washed with 1,4-dioxane and Et_2O, and air-dried (yield 120 g).

(F) $Li_3AsMo_{12}O_{40}\cdot 14H_2O$ was synthesized following the procedure described by Sanchez *et al.*[71] Solid MoO_3 (72 g), 6.3 g As_2O_5, and 13.2 g of solid $LiOH\cdot H_2O$ were mixed together and treated by 200 mL of hot water. The resulting solution (pH~5) was concentrated to 80 mL and 100 mL of 1,4-dioxane was added, followed by 25 mL of concentrated (12 M) HCI. The solution turned orange-yellow and after a few minutes began to precipitate. After a few hours, it was filtered and the solid was washed with dioxane and ether, giving 70 g of a crude lithium salt as a yellow powder.

Tetra-n-butylammonium salts (TBA = [(n-C4H9)4N]) of these Keggin anions were prepared by the following method: 1 mol of the relevant Keggin anion was dissolved in water and to it added 10 mol of Tetra-n-butylammonium bromide (TBABr). The

UNIVERSITAT ROVIRA I VIRGILI
ASSEMBLY AND PROPERTIES OF POLYOXOMETALATES: A THEORETICAL POINT OF VIEW
Laia Vilà Nadal
ISBN.978-84-694-2170-3/DL:T. 1039-2011

resulting precipitate was allowed to stir for 10 min and subsequently filtered by Büchner filtration. The solid products were then washed twice by the following: water, ethanol and diethyl ether before being dried in vacuo. Purification of the TBA-Keggin salts was achieved by solubilizing small quantities of the TBA-salts in acetonitrile and setting up a diethyl ether vapour diffusion crystal growth method. Single crystals of the TBA-Keggin salts appear in the acetonitrile solution within several hours. Their identities were confirmed by single-crystal X-ray diffraction and elemental analysis.

2.9. Electrospray Ionization Mass Spectrometry

Obtaining experimental information of molecular oxide clusters in solution is not an easy labour. In recent times it has been demonstrated that a combination of cation-exchange and electrospray-ionization mass spectrometry (ESI-MS) can be used as a versatile tool in various complex systems. This technique is used to elucidate the complete cluster formula including all protons, as well as determining the relative proportions of the cluster species present in solution. In fact polyoxometalate clusters should be ideal candidates to be examined using high-resolution mass spectrometry since they are intrinsically charged and have characteristic isotopic envelopes which can be precisely fitted to determine the exact formula. For instance, ESI-MS has been used extensively to investigate many types of POMs including vanadates,[72] niobates,[73] tantalates,[74] chromates,[72] molybdates,[75] tungstates,[76] and rhenates.[77] Howarth *et al.* investigated aqueous solutions of isopolytungstates, peroxotungstates, and heteropoly-molybdates, detecting the $[W_6O_{19}]^{2-}$ and $[W_2O_7]^{2-}$ species in aqueous solution for the first time.[78] Mixed-metal heteropolyanion species were also investigated and the series of $[H_xPW_nMo_{12-n}O_{40}]^{(3-x)-}$ species

UNIVERSITAT ROVIRA I VIRGILI
ASSEMBLY AND PROPERTIES OF POLYOXOMETALATES: A THEORETICAL POINT OF VIEW
Laia Vilà Nadal
ISBN.978-84-694-2170-3/DL:T. 1039-2011

reported. Here just the basic principles of this technique will be discussed.[79] Several excellent tutorials on ESI-MS can be found elsewhere.[80]

The essence of the electrospray process can be described with simplicity. In ESI-MS, a dilute solution of analyte is pumped through a capillary at a very low flow rate (0.1–10 mL/min). A high voltage (2–5 kV) is applied to the capillary. This voltage can be either negative or positive, depending on the analytes chosen. The applied voltage provides the electric field gradient required to produce charge separation at the surface of the liquid. As a result, the liquid protrudes from the capillary tip in what is known as a "Taylor cone" (Fig. 2.9). When the solution that comprises the Taylor cone reaches the Rayleigh limit[81] (the point at which Coulombic repulsion of the surface charge is equal to the surface tension of the solution), droplets that contain an excess of positive or negative charge detach from its tip. These droplets move through the atmosphere towards the entrance to the mass spectrometer, and generate charged analyte molecules (ions) by one of several proposed mechanisms.[82]

The Coulomb fission mechanism assumes that the increased charge density due to solvent evaporation causes large droplets to divide into smaller and smaller droplets, which eventually consist only of single ions.[83] A second mechanism, known as ion evaporation, assumes that the increased charge density that results from solvent evaporation eventually causes Coulombic repulsion to overcome the liquid's surface tension, resulting in a release of ions from droplet surfaces.[84] Regardless of the mechanism by which they are produced, the ESI process generates vapor phase ions that can be analyzed for mass-to-charge ratio within the mass spectrometer.

UNIVERSITAT ROVIRA I VIRGILI
ASSEMBLY AND PROPERTIES OF POLYOXOMETALATES: A THEORETICAL POINT OF VIEW
Laia Vilà Nadal
ISBN.978-84-694-2170-3/DL:T. 1039-2011

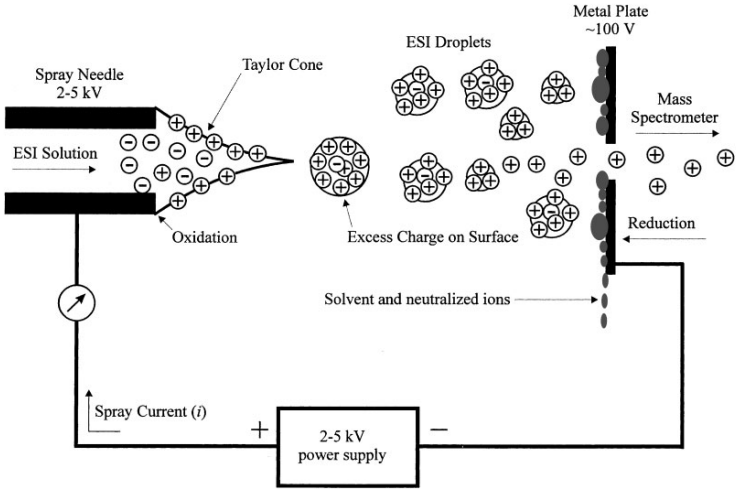

Figure 2.9. Schematic representation of the electrospray ionization process. The analyte solution is pumped through a needle to which a high voltage is applied. A Taylor cone with an excess of positive charge on its surface forms as a result of the electric field gradient between the ESI needle and the counter electrode. Charged droplets are formed from the tip of the Taylor cone, and these droplets evaporate as they move towards the entrance to the mass spectrometer to produce free, charged analyte molecules that can be analyzed for their mass-to-charge ratio.[85]

The charging of new surface as the droplets form and leave the tip requires a flow of charge from the power supply. The electrical circuit that sustains this current can be traced from the positive terminal of the power supply, to the solution via a metallic contact, through the gap that separates the capillary tip and the counter electrode, to ion neutralization at the counter electrode, and back to the negative power supply terminal (for negative ion ESI, the power supply is reversed). The current through each element of the series circuit must be the same. Thus, the current measured by the current meter shown in Figure 2.9 is a measure of the rate of the charge separation produced in the solution and leaving the capillary tip. The amount of charge on the droplets is, therefore, equal to the amount of charge separation. This charge is sometimes called the

UNIVERSITAT ROVIRA I VIRGILI
ASSEMBLY AND PROPERTIES OF POLYOXOMETALATES: A THEORETICAL POINT OF VIEW
Laia Vilà Nadal
ISBN.978-84-694-2170-3/DL:T. 1039-2011

excess charge[86] to differentiate it from the cations and anions in the droplet that are neutralized by counter-ions. It is important to distinguish between these excess and neutralized charges because the neutralized charges are not likely to result in gas-phase ions.

The formation of gas-phase ions from neutralized charge would require desolvation energies in excess of the Coulombic forces between the ions and their counterions. Consequently, the maximum rate of production of vapour phase ions is equal to the rate of charge separation, and the amount of vapor phase ions produced cannot exceed the amount of excess charge introduced into the droplets.

The continuous flow of charge from the metallic contact to the sample solution must occur via an electrochemical reaction at that contact.[87] The dominant reaction in positive ion ESI is oxidation, whereas in negative ion ESI it is reduction. The equivalents of electrochemical reactant consumed and electrochemical product produced by the electrochemical reaction are exactly equal to the amount of charge separation that occurs at the capillary tip.

The solvent plays a key role in ESI analysis. The ideal solvent composition for ESI analysis varies, depending on the application. If a charged analyte is to be studied by ESI-MS, then practically any moderately polar solvent can theoretically be used. The solvent provides a convenient method for producing a dilute solution of the analyte. It is preferable that the solvent has reasonable volatility, such that the drying gas can remove solvent from the charged droplets produced in the ESI process without recourse to excessively high temperatures that might cause sample decomposition. Solvents such as methanol, ethanol, acetonitrile and water are all commonly used, because of their moderate boiling points (<100 ºC) and polarities. In many cases, mixtures of water plus an organic solvent (often acetonitrile) are used. Such polar, protic solvents and mixtures thereof are

typically able to dissolve the miniscule quantities of most compounds –even sparingly soluble ones– so that MS analysis can be carried out.[88]

Nondestructive mass spectrometry of polyoxometalates has the potential to become a standard analysis technique for complex cluster systems since it provides vital complementary information of the cluster composition in solution which cannot be deduced from crystallographic studies.[70] The majority of electrospray instruments involve the implementation on quadrupole mass spectrometers, although some other analyzers are being implemented, like Fourier transform ion cyclotron resonance instruments.

From the very earliest days of the application of ESI-MS to inorganic systems, the utility of the technique for the characterisation of polyoxoanions was realised with the report of the ESI-MS spectrum of the heteropolymolybdate ion $[S_2Mo_{18}O_{62}]^{4-}$.[89]

Figure 2.10 is presented as an example of ESI-MS fragmentation experiment from $[W_6O_{19}]^{2-}$, these data has been extremely useful in the study of POMs assembly processes, as we will see in the following chapters. ESI-MS results were obtained on tetrabutylammonium salts of the cluster in acetonitrile solution. The cation-exchange process, *vide supra*, was used because the TBA^+ cations have a much higher mass than Na^+ or K^+ and give a larger separation between signals corresponding to differently charged or protonated cluster states. Exhaustive analysis of the ESI-MS data shows that the compounds can be unambiguously identified in both positive and negative ion modes.

UNIVERSITAT ROVIRA I VIRGILI
ASSEMBLY AND PROPERTIES OF POLYOXOMETALATES: A THEORETICAL POINT OF VIEW
Laia Vilà Nadal
ISBN.978-84-694-2170-3/DL:T. 1039-2011

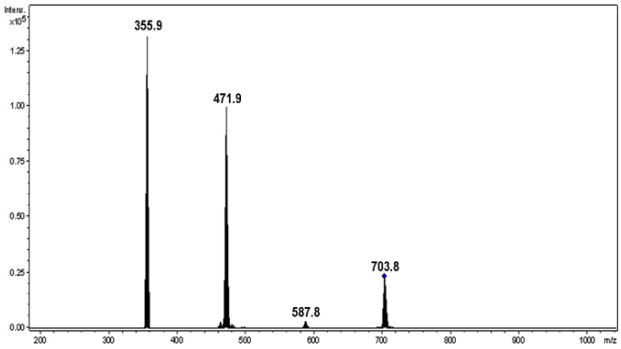

Figure 2.10. Mass spectral data showing the peaks associated with the species $[W_3O_{10}]^{2-}$ at 355.9 m/z, $[W_4O_{13}]^{2-}$ at 471.9 m/z, $[W_5O_{16}]^{2-}$ at 587.8 m/z, and $[W_6O_{19}]^{2-}$ at 703.8 m/z.

UNIVERSITAT ROVIRA I VIRGILI
ASSEMBLY AND PROPERTIES OF POLYOXOMETALATES: A THEORETICAL POINT OF VIEW
Laia Vilà Nadal
ISBN.978-84-694-2170-3/DL:T. 1039-2011

References and Notes

[1] a) P.A.M. Dirac, *Proc. Roy. Soc.* (London) **1929**, 123, 714. b) Italics added.

[2] G.P.F. Wood, Theoretical Investigations of Radical-Mediated Protein Oxidation. Ph. D. Thesis [Online], University of Sydney, School of Chemistry, June 2006. http://hdl.handle.net/2123/1413 (accessed Nov 3, 2010).

[3] Moores' Law is attributed to Gordon E. Moore and states that computing power increases in an exponential fashion. See: G.E. Moore, *Electronics*, **1965**, 38, 114.

[4] *L.* de Broglie, *Ann. Physik*, **1925**, 3, 25.

[5] E. Schrodinger, *Phys. Rev.*, **1926**, 28, 1049.

[6] M. Born, R. Oppenheimer, *Annalen der Physik*, **1927**, 84, 457.

[7] Chronon (θ_0), $\theta_0 = \frac{2}{3}\frac{ke^2}{m_0c^3} \simeq 6.266 \times 10^{-24}\ s$ is a hypothetical unit of time, taken as a ratio between the diameter of the electron and the velocity of light, equivalent to approximately 6.266×10^{-24} s.

[8] W. Koch, M.C. Holthausen, *A Chemist's Guide to Density Functional Theory*, Wiley-VCH, Weinheim, **2001**.

[9] a) A. Szabo, N.S. Ostlund, *Modern Quantum Chemistry*, McGraw- Hill: New York, **1989.** b) I.N. Levine, *Quantum Chemistry*, Prentice-Hall, Upper Saddle River, **2000**.

[10] P. Hohenberg, W. Kohn, *Phys. Rev.*, **1964,** 136, 864.

[11] F. Jensen, *Introduction to computational chemistry*, John Wiley&Sons: Wilshire, **2007**.

[12] W. Kohn, L.J. Sham, *Phys. Rev.* **1965**, 140, 1133.

[13] G. Te Velde, F.M. Bickelhaupt, E.J. Baerends, C. Fonseca Guerra, S.J.A. Van Gisbergen, J.G. Snijders, T. Ziegler, *J. Comput. Chem.* **2001**, *22*, 931.

[14] K. Capelle*, Brazilian J. Phys.*, **2006**, 36, 1318.

[15] A.D. Becke, *Phys. Rev.* **1988**, A38, 3098.

[16] C. Lee, W. Yang, R.G. Parr, *Phys. Rev. B*, **1998**, 37, 785.

[17] a)A.D. Becke, *J. Chem. Phys.*, **1993**, 98, 5648. b) P.J. Stephens, F.J. Delvin, C.F. Chabalowski, M.J. Frisch, *J. Phys. Chem.*, **1994**, 98, 11623

[18] a) A. Klamt, G.J. Schüürmann**,** *Chem. Soc.,Perkin Trans. 2.* **1993**, 799. b) J. Andzelm, C. Kölmel, A. Klamt, *J. Chem. Phys.* **1995**, *103*, 9312. c) A. Klamt, *J. Chem. Phys.* **1995**, *99*, 2224.

[19] C.C. Pye, T. Ziegler, *Theor. Chem. Acc.* **1999**, *101*, 396.

[20] A. Klamt*, Cosmo-RS From Quantum Chemistry to Fluid Phase Thermodynamics and Drug Design*, Elsevier: Amsterdam, **2005**.

[21] M. Cossi, B. Mennucci, *J. Comp. Chem*, **1996**, 1, 57.

UNIVERSITAT ROVIRA I VIRGILI
ASSEMBLY AND PROPERTIES OF POLYOXOMETALATES: A THEORETICAL POINT OF VIEW
Laia Vilà Nadal
ISBN.978-84-694-2170-3/DL:T. 1039-2011

[22] R. Car, M. Parrinello, *Phys. Rev. Lett.* **1985**, 55, 2471.

[23] a) A. Rodríguez-Fortea, L. Vilà-Nadal, J.M. Poblet, *Inorg Chem.*, **2008**, 17, 7745. b) L. Vilà-Nadal, A. Rodríguez-Fortea, L.K. Yan, E.F. Wilson, L. Cronin, J.M. Poblet, *Angew. Chem. Int. Ed.*, **2009**, 48, 5452.

[24] a) D.K. Remler, P.A. Madden, *Mol. Phys.*, **1990**, 70, 92. b) M.C. Payne, M.P. Teter, D.C. Allen, T.A. Arias, J.D. Joannopoulos, *Rev. Mod. Phys.* **1992**, 64, 1045. c) D. Marx, J. Hutter, *Forschungszentrum Jülich, NIC Series*, **2000**, 1, 301. d) J. Kohanoff, N. Gidopoulos, *Handbook of Molecular Physics and Quantum Chemistry*, John Wiley & Sons: Chichester, **2003**. e) J. Kohanoff, *Electronic Structure Calculations for Solids and Molecules*, Cambridge University Press: Cambridge, **2006**.

[25] B.J. Alder, T.E. Wainwright, *J. Chem. Phys.*, **1957**, 27, 1208.

[26] D. Marx, J. Hutter, *Ab initio Molecular Dynamics: Basic Theory and Advanced Methods*, Cambridge University Press; Cambridge, **2009.**

[27] a) C.G. Gray, K.E. Gubbins, *Theory of Molecular Fluids Vol. 1*, Claredon, Oxford, **1984**. b) A.J. Stone, *The Theory of Intramolecular Forces*, Claredon Press: Oxford, **1996** and **2002**.

[28] J.E. Lenard-Jones, *Proc. R. Soc. London*, *Ser. A* **1924**, 106, 463.

[29] R. Brooks, R.E. Bruccoleri, B.D. Olafson, D.J. States, S. Swamianathan, M. Karplus, *J. Comp. Chem.* **1983**, 4, 187.

[30] M.P. Allen, D.J. Tildesley, *Computer Simulation of Liquids*, Claredon, **1989**.

[31] E. Fermi, J. Pasta, S. Ulam, M. Tsignou, *Studies of nonlinear problems. I.* Technical Report # LA-1940 (20 pages and 9 figures), Los Alamos Scientific Laboratory of the University of California, May 1995.

[32] B.J. Alder, T.E. Wainwright, *J. Chem. Phys.* **1957**, 27, 1208.

[33] X. Li, J.M. Millam, H.B Schlegel, *J. Chem. Phys.* **2000**, 113, 10062.

[34] a) D.K. Remler, P.A. Madden, *Mol. Phys.* **1990**, 70, 921. b) J.S. Tse, *Ann. Rev. Phys. Chem.* **2002**, 53, 249.

[35] The Lagrangian, *L*, of a dynamical system is a function that summarizes the dynamics of the system. It is named after Joseph Louis Lagrange. The motion of small, but not too small, particles such as atoms and molecules is usually well described by Lagrangian mechanics, with the Lagrangian (*L*) defined as the kinetic energy (*T*) minus the potential energy (*V*), $L=T-V$.

[36] A. Laio, M. Parrinello, *Proc. Nat. Acad. Sci. USA.* **2002**, 99, 12562.

[37] A. Laio, F. L. Gervasio, J. Vande Vondele, M. Suplizi, U. Rothlisberger, *J. Phys. Chem. B* **2004**, 108, 7963.

[38] M. Alfonso, Study of the Reactivity of catalases by means of *ab initio* molecular dynamics. Ph. D. Thesis [Online], Universitat Autonoma de Barcelona, Parc Científic de Barcelona, December 2009. http://www.tdx.cat/TDX-0319110-135753 (accessed Dec 10, 2010).

UNIVERSITAT ROVIRA I VIRGILI
ASSEMBLY AND PROPERTIES OF POLYOXOMETALATES: A THEORETICAL POINT OF VIEW
Laia Vilà Nadal
ISBN.978-84-694-2170-3/DL:T. 1039-2011

[39] A. Laio, A. Rodríguez-Fortea, F. L. Gervasio, M. Ceccarelli, M. Parrinello, *J. Phys. Chem. B* **2005**, 109, 6714.

[40] X. Biaznés, A. Ardèvol, A. Planas, C. Rovira, A. Laio, M. Parrinello, *J. Am. Chem. Soc.* **2007**, 129, 10686.

[41] M. Iannuzzi, A. Laio, M. Parrinello, *Phys. Rev. Lett.* **2003**, 90, 238302.

[42] A. Laio, F. L. Gervasio, *Prep. Prog. Phys.* **2008**, 71, 126601

[43] H. Günther, *NMR spectroscopy, basic principles, concepts and applications in chemistry*, John Wiley&Sons: Chichester, **1996**.

[44] M.A. Nielsen, I.L. Chuang, *Quantum computation and quantum information*, Cambridge University Press: Cambridge, **2000**.

[45] W. Gerlach, O. Stern, *Z. Physik.* **1922**, 9, 353.

[46] A.K. Rajagopal, J. Callaway, *Phys. Rev. B.* **1973**, 7, 1912.

[47] J. Gauss, *Molecular Properties*, in J. Grotendorts (editor), *Modern methods and algorithms of quantum chemistry*, Vol. 3, NIC, John von Neuman Institute for Computing, Jülich, **2000**, 541.

[48] a) R. McWeeny, *Methods of molecular quantum mechanics*, Academic Press: London, **1992**. b) P.W. Atkins, R.S. Friedman, *Molecular Quantum Mechanics*, Oxford University Press: New York, **1997**.

[49] W. Kutzelnigg, U. Fleischer, M. Schindler, *NMR Basic Principles and Progress*, Vol. 23., Springer-Verlag: Berlin Heidelberg, **1990**.

[50] G. Schreckenbach, *Inorg. Chem.* **2002**, 41, 6560.

[51] G. Schreckenbach, T. Ziegler, *J. Phys. Chem.* **1995**, *99*, 606.

[52] G. Schreckenbach, T. Ziegler, *Theor. Chem. Acc.* **1998**, *99*, 71.

[53] Y. Ruiz-Morales, G. Schreckenbach, T. Ziegler, *J. Phys. Chem.* **1996**, *100*, 3359.

[54] Y. Ruiz-Morales, T. Ziegler, *J. Phys. Chem. A.* **1998**, *102*, 3970.

[55] M. Kaupp, O.L. Malkina, V.G. Malkin, P. Pyykkö, *Chem. Eur. J.* **1998**, *4*, 118.

[56] M. Bühl, M. Kaupp, V.G. Malkin, O.L. Malkina, *J. Comput. Chem.* **1999**, *20*, 91.

[57] a) ADF 2004.01. Department of Theoretical Chemistry. Vrije Universiteit. Amsterdam. E.J. Baerends, D.E. Ellis, P. Ros, *Chem. Phys.* **1973**, *2*, 41. b)L.L-Versluis, T. Ziegler, *J. Chem. Phys.* **1988**, *88*, 322. c) G. Te Velde, E.J. Baerends, *J. Comput. Phys.* **1992**, *99*, 84. d) C. Fonseca Guerra, J.G. Snijders, G. Te Velde, E.J. Baerends, *Theor. Chem. Acc.* **1998**, 99, 391.

[58] a) A.D. Becke, *J. Chem Phys.* **1986**, 84, 4524. b) A.D. Becke, *Phys. Rev. A.* **1988**, 38, 3098.

[59] S.H. Vosko, L. Wilk, M. Nusair, *Can. J. Phys.* **1980**, *58*, 1200.

[60] a) J.P. Perdew, *Phys. Rev. B.* **1986**, 33, 8822**.** b) J.P. Perdew**,** *Phys. Rev. B.* **1986**, 34, 7406.

UNIVERSITAT ROVIRA I VIRGILI
ASSEMBLY AND PROPERTIES OF POLYOXOMETALATES: A THEORETICAL POINT OF VIEW
Laia Vilà Nadal
ISBN.978-84-694-2170-3/DL:T. 1039-2011

[61] a) J.M. Poblet, X. López, C. Bo, *Chem. Soc. Rev.* **2003**, 32, 297. b) X. López, J.M. Maestre, C. Bo, J.M. Poblet, *J. Am. Chem. Soc.* **2001**, 123, 9571. c) X. López, J.A. Fernández, S. Romo, J.F. Paul, L. Kazansky, J.M. Poblet, *J. Com. Chem.* **2004**, 25, 1542.

[62] C. Lee, W. Yang, R.G. Parr, *Phys. Rev. A.* **1998**, 38, 3098.

[63] N. Troullier, J. L. Martins, *Phys. Rev. B.* **1991**, 43, 1993.

[64] S.G Louie, S. Froyen, M. L.Cohen, *Phys. Rev. B.* **1982**, 26, 1738.

[65] a) A.D. Becke, *Phys. Rev. A* **1988,** 38, 3098. b) C. Lee, W. Yang, R. Parr, *Phys. Rev. B.* **1988**, 37, 785.

[66] A. Kachmar, M. Bénard, M. M. Rohmer, M. Boero, C. Massobrio, *J. Phys. Chem. A* **2009**, 113, 9075.

[67] M. Filowitz, R.K.C Ho, W.G. Kemplerer, W. Shum, *Inorg. Chem.* **1979**, 18, 93.

[68] a) N.H. Hur, W.G. Klemperer, R.C. Wang, *Inorg. Synth.*, **1990**, 27, 77.

[69] E.O. North, *Inorg. Synth.* **1939**, 1, 129.

[70] C. Rocchiccioli-Deltcheff, M. Fournier, R. Franck, R., R. Thouvenot, *Inorg. Chem.* **1983**, 22, 207.

[71] C. Sanchez, J. Livage, J.P. Launay, M. Fournier, Y.J. Jeanin, *J. Am. Chem Soc.* **1982**, 104, 3194.

[72] H.N. Miras, D.-L. Long, P. Kögerler, L. Cronin*, Dalton Trans.* **2008**, 2, 214.

[73] D.K. Walanda, R.C. Burns, G.A. Lawrance, E.I. Von Nagy–Felsobuki, *Inorg. Chem. Commun*. **1999**, 10, 487.

[74] a) F. Sahureka, R.C. Burns, E.I. von Nagy-Felsobuki, *J. Am. Soc. Mass Spectrom.* **2001**, 10, 1136. b) C.A. Ohlin, E.M. Villa, J.C. Fettinger, W.H. Casey, *Angew. Chem. Int. Ed.* **2008**, 47, 1.

[75] a) D.K. Walanda, R.C. Burns, G.A. Lawrance, E.I. Von Nagy-Felsobuki, *Dalton Trans.* **1999**, 3, 311. b) E.C. Alyea, D. Craig, I. Dance, K. Fisher, G. Willett, M. Scudder, *Cryst. Eng. Comm.* **2005**, 7, 491.

[76] a) D.K. Walanda, R.C. Burns, G.A. Lawrance, E.I. Von Nagy-Felsobuki, *J. Cluster Sci.* **2000**, 1, 5. b) M. Bonchio, O. Bortolini, V. Conte, A. Sartorel, *Eur. J. Inorg. Chem.* **2003**, 4, 699. c) C. Boglio, G. Lenoble, C. Duhayon, B. Hasenknopf, R. Thouvenot, C. Zhang, R.C. Howell, B.P. Burton-Pye, L.C. Francesconi, E. Lacote, S. Thorimbert, M. Malacria, C. Afonso, J.C. Tabet, *Inorg. Chem.* **2006**, 3, 1389. d) C.R. Mayer, C. Roch-Marchal, H. Lavanant, R. Thouvenot, N. Sellier, J.C. Blais, F. Sécheresse, *Chem.–Eur. J.* **2004**, 21, 5517. e) C. Dablemont, A. Proust, R. Thouvenot, C. Afonso, F. Fournier, J.-C. Tabet, *Inorg. Chem.* **2004**, 43, 3514.

[77] F. Sahureka, R.C. Burns, E.I. von Nagy-Felsobuki, *Inorg. Chem. Commun.* **2002**, 5, 23.

[78] M.J. Deery, O.W. Howarth, K.R. Jennings, *Dalton Trans.* **1997**, 4783.

UNIVERSITAT ROVIRA I VIRGILI
ASSEMBLY AND PROPERTIES OF POLYOXOMETALATES: A THEORETICAL POINT OF VIEW
Laia Vilà Nadal
ISBN.978-84-694-2170-3/DL:T. 1039-2011

[79] D.L. Long, C. Streb, Y.F. Song, S. Mitchell, L. Cronin, *J. Am. Chem. Soc.* **2008**, 130, 1830.

[80] S.J. Gaskell, *J. Mass Spectr.* **1997**, 32, 677.

[81] D.C. Taflin, T.L. Ward, E.J. Davis, *Langmuir.* **1989**, 5, 376.

[82] P. Kebarle, M. Peschke, *Anal. Chem. Acta.* **1999**, 20070, 1.

[83] M. Dole, LL. Mack, R.L. Hines, R.C. Mobley, L.D. Ferguson, M.B. Alice, *J. Chem. Phys.* **1968**, 49, 2240.

[84] J.V. Iribarne, B.A. Thomson, J. Chem. Phys. **1976**, 64, 2287.

[85] N.B. Cech, C.G Enke, *Mass Spectr. Rev.* **2001**, 20, 362.

[86] Enke CG, *Anal Chem.* **1997**, 69, 4885.

[87] G.J. Van Berkel, *The electrolytic nature of electrospray ionization*, in R.B. Cole (editor), *Electrospray ionization mass spectrometry*. Wiley-New York: Wiley, **1997.**

[88] W. Henderson, J.S. McIndoe, *Mass Spectrometry of Inorganic, Coordination and Organometallic Compounds: Tools-Techniques-Tips,* John Wiley & Sons: Chichester, **2005**.

[89] R. Colton, J. C. Traeger, *Inorg. Chim. Acta.* **1992**, 201, 153.

UNIVERSITAT ROVIRA I VIRGILI
ASSEMBLY AND PROPERTIES OF POLYOXOMETALATES: A THEORETICAL POINT OF VIEW
Laia Vilà Nadal
ISBN.978-84-694-2170-3/DL:T. 1039-2011

Chapter 3
Formation Mechanisms of POTs with Low Nuclearities

UNIVERSITAT ROVIRA I VIRGILI
ASSEMBLY AND PROPERTIES OF POLYOXOMETALATES: A THEORETICAL POINT OF VIEW
Laia Vilà Nadal
ISBN.978-84-694-2170-3/DL:T. 1039-2011

"The process of formation of polyoxometalates de novo remains largely a mystery [...] we learn that the design of an unambiguous experiment directed towards the elucidation of mechanism may be hideously complicated."

M.T. Pope, A. Müller,
Polyoxometalates: from Platonic Solids to Anti-Retroviral Activity, 1994.

UNIVERSITAT ROVIRA I VIRGILI
ASSEMBLY AND PROPERTIES OF POLYOXOMETALATES: A THEORETICAL POINT OF VIEW
Laia Vilà Nadal
ISBN.978-84-694-2170-3/DL:T. 1039-2011

Chapter 3

Formation Mechanisms of POTs with Low Nuclearities

From an experimental point of view synthesis of classic polioxotungstates (POTs) does not represent a challenge. Synthetic routes to the most common structures are well known, mostly involving an acidification of alkaline aqueous solutions of simple oxoanions, the control of pH and temperature being also needed. Despite this synthetic knowledge few works were dedicated to analyze the formation mechanisms of POMs. The present chapter is devoted to shed a light on this issue. As a starting point we have analyzed the formation mechanism of the well known Lindqvist anion $[W_6O_{19}]^{2-}$*. Since* $[WO_4]^{2-}$ *is considered the main building block the aim of the initial part of the chapter is the study of hydration of hydrogentungstate anions. Then the different isomeric species that can be formed at successive steps of aggregation are analyzed. The formation of dinuclear and trinuclear species will be explained in more detail. Afterwards we will move on to higher nuclearity species that could lead to the Lindqvist anion. Finally, two formation mechanisms for this hexameric anion are proposed. Since the behavior of POTs in solution is complex to rationalize we have used complementary techniques, that is ESI-MS experiments, combined with computational approaches that include the effect of solvent in two different ways, either though a*

UNIVERSITAT ROVIRA I VIRGILI
ASSEMBLY AND PROPERTIES OF POLYOXOMETALATES: A THEORETICAL POINT OF VIEW
Laia Vilà Nadal
ISBN.978-84-694-2170-3/DL:T. 1039-2011

continuum model in standard DFT methods or as explicit molecules by means of Car–Parrinello molecular dynamics (MD) simulations. The main aspects regarding these techniques are discussed in Chapter 2.

3.1. Introduction

The aim of this brief introduction is to stress that the comprehension of POMs aggregation processes is not an easy task, and requires the contribution several disciplines. We know that the aqueous polytungstate equilibria are complex due to the large number of stable species observed. So, our study starts with an analysis of hydrogentungstate anions, because the knowing of the behaviour of the $[WO_4]^{2-}$ anion in solution is basic to understand the subsequent aggregation process. Later, we have progressed towards the elucidation of the formation mechanism of the Lindqvist anion $[W_6O_{19}]^{2-}$ through an exhaustive analysis of the possible intermediates.

3.2. Hydration of Mononuclear Species

Regarding their structural pattern, POMs can be described as an assemblage of metal-centered MO_n polyhedra. Having in mind several representative POM structures it is easy to notice that their fundamental block is an octahedral unit of MO_6. It was observed that the metal is not centered in the middle of the octahedral blocks, but it tends to be distorted towards one of the corners, see Figure 3.1. Not all the metals that are able to form a six-fold octahedral coordination can take part of MO_6 linkages. Indeed only certain values of the charge/radius ratio for the metals M^{n+} are found in the MO_6 units.

UNIVERSITAT ROVIRA I VIRGILI
ASSEMBLY AND PROPERTIES OF POLYOXOMETALATES: A THEORETICAL POINT OF VIEW
Laia Vilà Nadal
ISBN.978-84-694-2170-3/DL:T. 1039-2011

Figure 3.1. Ball-and-stick (left) and polyhedral (right) representation of the funtamental MO_6 unit. Colors for the atoms: O, red; W, grey.

POMs are formed in experimental conditions that allow linking of polyhedra: acidification of alkaline aqueous solutions of simple oxoanions. Discrete structures are formed as long as the system is not driven all the way to the oxide.[1] We will focus our study to polytungstate POMs, knowing that an analysis of aqueous polytungstate equilibria is complicated by the extreme number of stable isopolytungstates observed. In the formation of polyoxotungstates the tungstate anion, $[WO_4]^{2-}$, is considered the main building block. So the knowledge of the tungstate anion equilibria in solution is basic to understand the aggregation processes that occur in POMs. Moreover the nucleation is thought to be started when the $[WO_4]^{2-}$ anions are protonated, $[WO_3(OH)]^-$, and one W–O bond is therefore stretched in each tetrahedron.[2] Concerning the pK values, the second pK of $[WO_4]^{2-}$ is anomalousy low, similarly as occurs for the molybdate anion $[MoO_4]^{2-}$. An increase of the coordination number of the metal ion upon protonation was proposed to be the origin of such low pK values.[3]

Mononuclear and other larger cluster species in solution can also be identified using a combination of cation-exchange and electrospray-ionization mass spectrometry (ESI-MS), as recently shown by Cronin and co-workers for polyoxotungstates.[4] Speciation studies in vanadium inorganic and bioinorganic systems have been performed as well.[5-7] To the best of our knowledge, no theoretical studies have attempted to analyze the

hydration/dehydration equilibria of molybdate or tungstate anions in solution. Messaoudi et al. have focused on the dimerization mechanisms of molybdates in aqueous solutions at very acidic conditions.[8] They have also carried out an exhaustive work about the structure and stability of $[VO_2]^+$ in aqueous solutions.[9] Besides, Bühl and Parrinello have analyzed the hydration of $[VO_2(OH)_2]^-$ and $[VO_2(OH_2)_4]^+$ to elucidate the medium effects on ^{51}V NMR chemical shifts using Car–Parrinello MD simulations.[10]

In the following lines we present the study of the hydration equilibria of hydrogentungstate anion, $[WO_3(OH)]^-$, and its protonated counterparts $[WO_2(OH)_2]$ and $[WO(OH)_3]^+$. Afterwards, the formation mechanisms of POMs with low nuclearities are discussed. The five-coordinated complexes $[WO_3(OH)(H_2O)]^-$, $[WO_2(OH)_2(H_2O)]$ and $[WO(OH)_3(H_2O)]^+$ were obtained after the incorporation of a water molecule to $[WO_3(OH)]^-$, $[WO_2(OH)_2]$ and $[WO(OH)_3]^+$, respectively. The reaction energies, computed at DFT/COSMO level, for the possible isomers formed after intramolecular proton transfer are shown in Scheme 3.1.

UNIVERSITAT ROVIRA I VIRGILI
ASSEMBLY AND PROPERTIES OF POLYOXOMETALATES: A THEORETICAL POINT OF VIEW
Laia Vilà Nadal
ISBN.978-84-694-2170-3/DL:T. 1039-2011

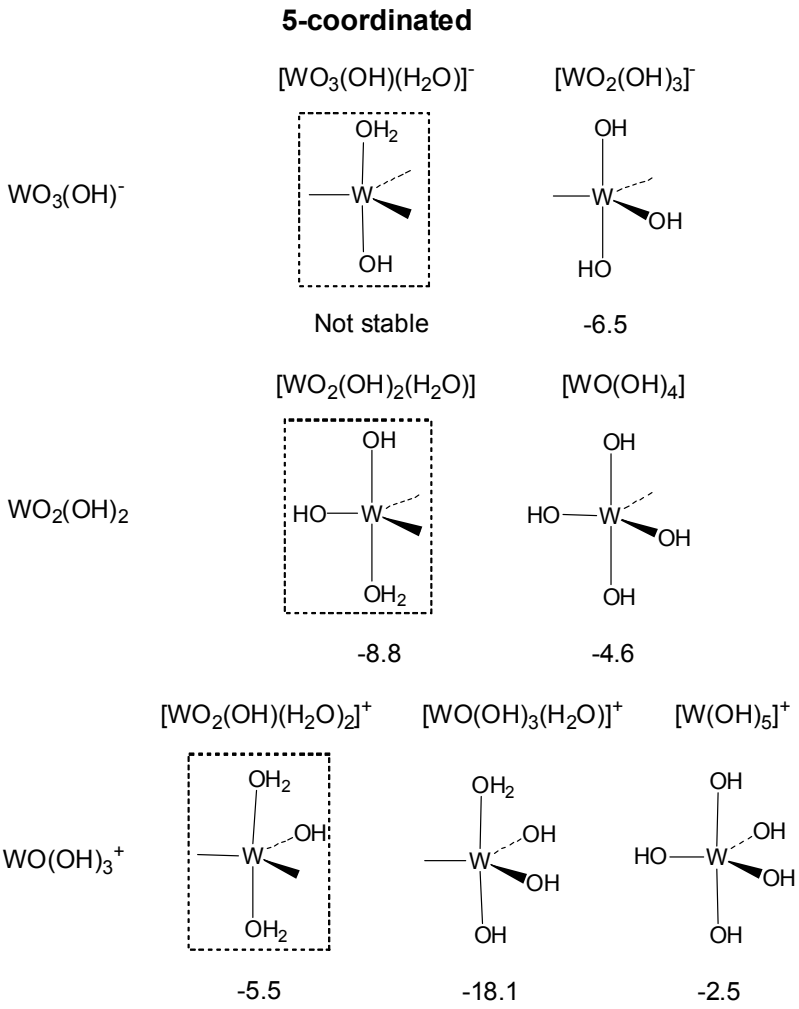

Scheme 3.1. Species with a 5-coordinated W(VI) ion obtained after the incorporation of a single water molecule to $[WO_3(OH)]^-$, $[WO_2(OH)_2]$ and $[WO(OH)_3]^+$. The hydration energies, $A + H_2O \rightarrow A{\cdot}H_2O$ ($A = [WO_3(OH)]^-$, $[WO_2(OH)_2]$ and $[WO(OH)_3]^+$), in kcal mol^{-1}, computed at BP86/COSMO level are also shown.

UNIVERSITAT ROVIRA I VIRGILI
ASSEMBLY AND PROPERTIES OF POLYOXOMETALATES: A THEORETICAL POINT OF VIEW
Laia Vilà Nadal
ISBN.978-84-694-2170-3/DL:T. 1039-2011

6-coordinated

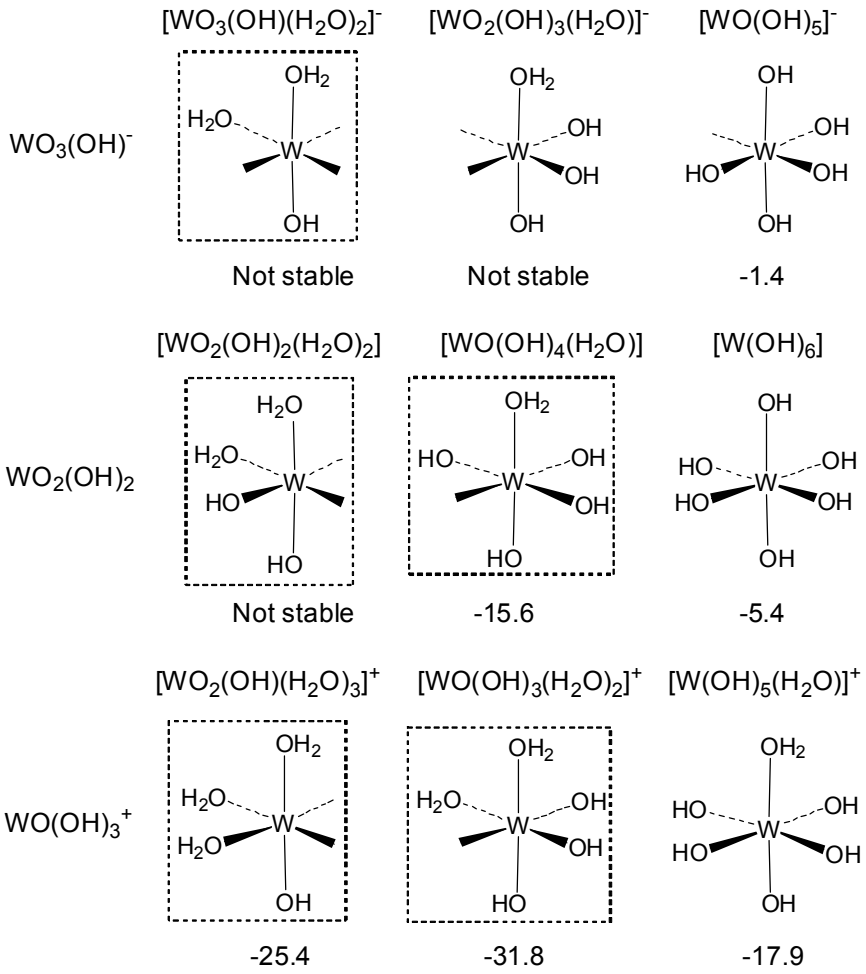

Scheme 3.2. Species with a 6-coordinated W(VI) ion obtained after the incorporation of two water molecules to $[WO_3(OH)]^-$, $[WO_2(OH)_2]$ and $[WO(OH)_3]^+$.The hydration energies, A + 2 H_2O → A·$(H_2O)_2$ (A = $[WO_3(OH)]^-$, $[WO_2(OH)_2]$ and $[WO(OH)_3]^+$), in kcal mol^{-1}, computed at BP86/COSMO level are also shown.

UNIVERSITAT ROVIRA I VIRGILI
ASSEMBLY AND PROPERTIES OF POLYOXOMETALATES: A THEORETICAL POINT OF VIEW
Laia Vilà Nadal
ISBN.978-84-694-2170-3/DL:T. 1039-2011

Two functionals (BP86, BLYP) and the solvation model with the SAS have been used. The species formed after the incorporation of two water molecules to $[WO_3(OH)]^-$, $[WO_2(OH)_2]$ and $[WO(OH)_3]^+$ are shown in Scheme 3.2. Depending on the relative position of the oxo, hydroxo and aqua ligands there are several geometric isomers, i.e. *cis*, *trans*, *mer*, *fac*. Only the value for the most stable is shown in Schemes 3.1 and 3.2.

Since the BLYP functional was used in the CPMD simulations, we have also used it at the DFT/COSMO level together with BP86. The reaction energies obtained with the BLYP functional are somewhat more exothermic than those obtained with BP86 (within 3 kcal mol^{-1}), but the qualitative trends are the same.

For the case of the hydrogentungstate anion, $[WO_3(OH)]^-$, complexes with aqua ligands directly attached to the W(VI) are not stable at any coordination number, i.e. the water molecules leave the coordination sphere of W. Complexes with hydroxo ligands, however, are more stable than reactants for the two coordination numbers five and six. The reaction is around 5 kcal mol^{-1} more exothermic when the coordination number of the W(VI) ion is five, for both BLYP and BP86 functionals.

For the neutral acid, $[WO_2(OH)_2]$, reaction energies are more exothermic than for the hydrogentungstate anion and coordination six favored. It is also noticeable that the six-coordinated complex with two aqua ligands is not stable at this level of computation.

Finally, for the most acidic species, $[WO(OH)_3]^+$, reaction energies are quite more exothermic for both coordination numbers five and six, specially for the second. All the complexes that contain aqua ligands are stable in this case.

This results indicate as a general trend that higher coordination numbers for the W(VI) ion are favored when the concentration of protons is increased, i.e. the pH is lowered, in aqueous solutions of tungstate anions. As the number of protons in the

UNIVERSITAT ROVIRA I VIRGILI
ASSEMBLY AND PROPERTIES OF POLYOXOMETALATES: A THEORETICAL POINT OF VIEW
Laia Vilà Nadal
ISBN.978-84-694-2170-3/DL:T. 1039-2011

complex increases, the W(VI) ion becomes more electrophilic and it is more effectively bound to nucleophilic aqua ligands.

When using continuous methods to simulate the solvent effects, knowing which solvent surface approach will provide the most reasonable description of the system is not a trivial task. In principle, one expects that the different types of surfaces will provide the same qualitative results. To check this effect, calculations using solvent accessible surface (SAS) and solvent excluding surface (SES) were performed. The results are shown in the following Tables 3.1 and 3.2.

As it is described in Chapter 2, the solvent surfaces are slightly different, SES being closer to the molecule than SAS. So it is not straightforward to compare energy values between these surfaces. What we have done is compare relative values and look for general tendencies.

Table 3.1. The hydration energies, $A + H_2O \rightarrow A{\bullet}H_2O$ ($A = [WO_3(OH)]^-$, $[WO_2(OH)_2]$ and $[WO(OH)_3]^+$), in kcal mol^{-1}, shown for the 5-coordinated species, computed at BP86/COSMO, with two kinds of molecular surfaces (SAS, SES).

	$[WO_2(OH)_3]^-$	$[WO_2(OH)_2(H_2O)]$	$[WO(OH)_4]$	$[WO_2(OH)(H_2O)_2]^+$	$[WO(OH)_3(H_2O)]^+$	$[W(OH)_5]^+$
SAS	−6.5	−8.8	−4.6	−5.5	−18.1	−2.5
SES	−1.2	−4.0	−0.8	−38.5	−1.2	−11.7
SAS/SES SP*	5.6	0.6	7.3	−1.2	−0.4	17.7

*The optimized geometry of BP86/SAS was recalculated as a single point (SP) using SES.

For the pentacoordinated species, when the geometry is optimized using the SAS and recalculated as a single point using SES (SAS/SES SP) the most stable species are two hydrated cations derived from protonated tungstic acid, similarly to what happens with SAS surface, see Table 3.1. Optimizations using the SES (SES) show that the most stable species is by far

UNIVERSITAT ROVIRA I VIRGILI
ASSEMBLY AND PROPERTIES OF POLYOXOMETALATES: A THEORETICAL POINT OF VIEW
Laia Vilà Nadal
ISBN.978-84-694-2170-3/DL:T. 1039-2011

$[WO_2(OH)(H_2O)_2]^+$, in contrast to the results obtained with SAS and SAS/SES SP levels.

Table 3.2. The hydration energies, A + 2 H_2O → A·$(H_2O)_2$ (A = $[WO_3(OH)]^-$, $[WO_2(OH)_2]$ and $[WO(OH)_3]^+$), in kcal mol^{-1}, shown for the 6-coordinated species, computed at BP86/COSMO, with two kinds of solvent surfaces (SAS, SES).

	$[WO(OH)_5]^-$	$[WO(OH)_4(H_2O)]$	$[WO(OH)_6]$	$[WO_2(OH)(H_2O)_3]^+$	$[WO(OH)_3(H_2O)_2]^+$	$[W(OH)_5(H_2O)]^+$
SAS	–1.4	–15.6	–5.4	–25.4	–31.8	–17.9
SES	12.6	4.0	15.7	–2.1	–0.4	9.9
SAS/SES SP*	14.8	6.0	17.1	–2.6	–1.6	11.4

*The optimized geometry of BP86/SAS was recalculated as a single point using SES.

In the case of the hexacoordinated species analogous results are observed, and $[WO_2(OH)(H_2O)_3]^+$, $[WO(OH)_3(H_2O)_2]^+$ are the most stable compounds regardless of the surface approximation used, see Table 3.2. Now there are no important differences when optimising and when doing a single-point calculation using the SES. When the structures are optimized using the SES some of the geometries are overestabilized for the case of several 5-coordinated species.

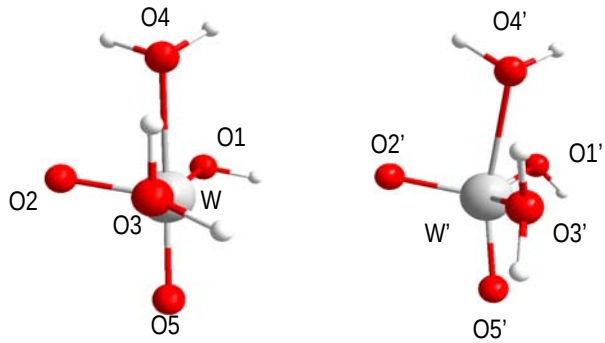

Figure 3.2. Ball-and-stick representation of the 5-coordinated $[WO_2(OH)(H_2O)_2]^+$ geometry. The first one is obtained after the optimization using SES, the second using SAS.

UNIVERSITAT ROVIRA I VIRGILI
ASSEMBLY AND PROPERTIES OF POLYOXOMETALATES: A THEORETICAL POINT OF VIEW
Laia Vilà Nadal
ISBN.978-84-694-2170-3/DL:T. 1039-2011

The root of the problem is the tendency of the SES to distort the structure in order to saturate the coordination of the W ion (hexacoordination). While the prove sphere rolls on the van der Waals surface it pushes the geometry to overstabilize distorted structures with the surface near the electrophilic center W(VI) ion. This distortion can be seen as solvent entering at the W coordination sphere. It becomes dramatic in the case of $[WO_2(OH)(H_2O)_2]^+$ after comparing the geometries, see Figure 3.2.

To illustrate this distortion some values for the angles of $[WO_2(OH)(H_2O)_2]^+$ optimized in both surfaces are presented in Table 3.3. These values show that in the SES optimization the geometry is distorted towards octahedral coordination, see for instance angle values for O1WO2 or O2WO3 that are near to 90º. For the case of SAS the angle values for O1'W'O2', O1'W'O3' and O2'W'O3' tend to 120º, showing a coordination more similar to a trigonal bipyramid. This problem does not appear in the hexacoordinated species. Therefore, one must be aware that unrealistic disorted structures are formed for tungstates with four- and five-coordinated W(VI) ions when optimized using the SES. Different alternatives are possible to circumvent this problem: optimization with the SAS, performing or not a single-point calculation with the SES; or introducing the solvent molecules explicitly.

In parallel with the static studies Car–Parrinello Molecular Dynamics (MD) simulations of a single hydrogentungstate anion with explicit water molecules have been also performed,[11] the results are presented in the following lines. We have analyzed the free energy changes that are consequence of the incorporation of water molecules to the coordination sphere of W(VI) ions at different pH conditions. Due to the large number of structural isomers involved in these equilibria (see Schemes 3.1 and 3.2), we have only considered those isomers highlighted in the schemes.

UNIVERSITAT ROVIRA I VIRGILI
ASSEMBLY AND PROPERTIES OF POLYOXOMETALATES: A THEORETICAL POINT OF VIEW
Laia Vilà Nadal
ISBN.978-84-694-2170-3/DL:T. 1039-2011

Table 3.3. Values for the selected angles in the optimized geometries of $[WO_2(OH)(H_2O)_2]^+$ using SES and SAS.

$[WO_2(OH)(H_2O)_2]^+$ SES	Angle (º)	$[WO_2(OH)(H_2O)_2]^+$ SAS	Angle (º)
O1WO2	97.70	O1'W'O2'	107.60
O1WO3	155.30	O1'W'O3'	131.80
O2WO3	95.30	O2'W'O3'	112.10
O4WO5	163.90	O4'W'O5'	157.30

To obtain the free-energy profile for the hydration/ dehydration equilibria of hydrogentugstate anion, equations 3.1 and 3.2:

$$WO_3(OH)^- + H_2O \rightleftarrows \left[WO_3(OH)(H_2O)\right]^- \quad (3.1)$$

$$\left[WO_3(OH)(H_2O)\right]^- + H_2O \rightleftarrows \left[WO_3(OH)(H_2O)_2\right]^- \quad (3.2)$$

we have performed several metadynamics simulations.[12] As shown in Figure 3.3, the four-coordinated tetrahedral $[WO_3(OH)]^-$ anion is somewhat more stable (3 kcal mol^{-1}) than the five-coordinated trigonal bipyramid structure. The free-energy barriers for the interconversion of the four- to the five-coordinated species and vice versa are far from being negligible (14 and 11 kcal mol^{-1}, respectively). Concerning the six-coordinated $[WO_3(OH)(H_2O)_2]^-$ anion, it is even more unstable than the the five-coordinated anion with a free-energy that is 10 kcal mol^{-1} higher than the lowest-energy tetrahedral species. Moreover, the barrier that has to be overcome to obtain it is as large as 17 kcal mol^{-1}. So, the hydrogentungstate anion in water solution keeps the tetrahedral coordination most of the time. The six-coordinated species with two extra aqua ligands will be observed very rarely, but the probability to find the five-coordinated complex is not so low.

UNIVERSITAT ROVIRA I VIRGILI
ASSEMBLY AND PROPERTIES OF POLYOXOMETALATES: A THEORETICAL POINT OF VIEW
Laia Vilà Nadal
ISBN.978-84-694-2170-3/DL:T. 1039-2011

To analyze the effect that acidification of the solution has on the incorporation of water molecules to the coordination sphere of W(VI) ion, we have studied the following equilibria, equations 3.3 and 3.4:[13]

$$WO_2(OH)_2 + H_2O \rightleftarrows \left[WO_2(OH)_2(H_2O)\right] \quad (3.3)$$

$$\left[WO_2(OH)_2(H_2O)\right] + H_2O \rightleftarrows \left[WO_2(OH)_2(H_2O)_2\right] \quad (3.4)$$

The computed free energy profile relative to $WO_2(OH)_2$ is depicted in Figure 3.4. Now, the relative stability of the different species is changed. The most stable compound is that with the six-coordinated W(VI) ion, $[WO_2(OH)_2(H_2O)_2]$, which is 4 and 9 kcal mol^{-1} more stable than the five- and four-coordinated species, respectively. Moreover, the barrier for the formation of the six-coordinated species (8 kcal mol^{-1}) is much lower than in the case of the hydrogentungstate anion (17 kcal mol^{-1}).

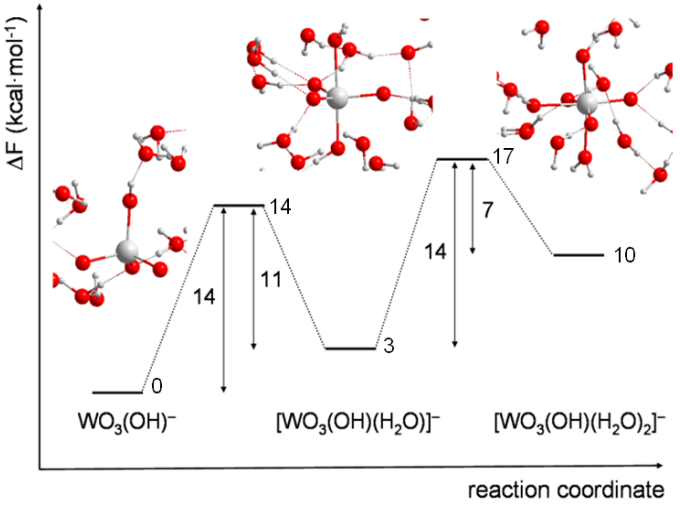

Figure 3.3. Free-energy profile (in kcal mol^{-1}) corresponding to the hydration/dehydration equilibria of hydrogentungstate anion, $[WO(OH)_3]^-$.

Once the tungstate is diprotonated, the W(VI) ion of the tungstic acid is more electrophilic than in the case of the

UNIVERSITAT ROVIRA I VIRGILI
ASSEMBLY AND PROPERTIES OF POLYOXOMETALATES: A THEORETICAL POINT OF VIEW
Laia Vilà Nadal
ISBN.978-84-694-2170-3/DL:T. 1039-2011

hydrogentungstate anion. As a result, the W(VI) ion is more easily attacked by the nucleophilic water molecules, thus decreasing the barrier for the formation of the aqua complexes. Therefore, a decrease of the pH of the aqueous solution involves an *expansion* of the coordination sphere of W(VI) ion, as supposed from the experimental results. It is also important to note that the most stable complex $[WO_2(OH)_2(H_2O)_2]$ calculated when doing Car–Parrinello metadynamics simulations is predicted to be not stable within the continuous COSMO model.

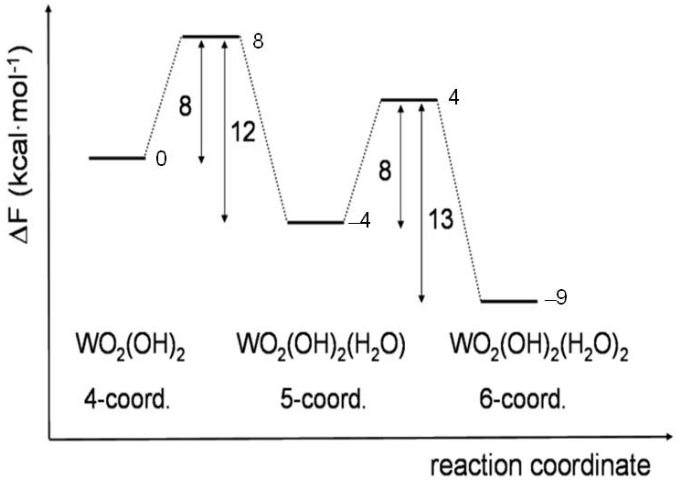

Figure 3.4. Free-energy profile (in kcal mol^{-1}) corresponding to the hydration/dehydration equilibria of tungstic acid, $[WO_2(OH)_2]$.

Finally, we have also examined the behavior of tungsten acid solutions at high acidic conditions looking at the fate of the six-coordinated structural isomers $[WO_2(OH)(H_2O)_3]^+$ and $[WO(OH)_3(H_2O)_2]^+$ (see Scheme 3.2). During the metadynamics[14] for $[WO_2(OH)(H_2O)_3]^+$ one proton is released from a water molecule coordinated to the W(VI) ion yielding the neutral tungstic acid $[WO_2(OH)_2(H_2O)_2]$ and a hydronium ion in the solution. The released proton recombines several times with the tungstic acid recovering the former $[WO_2(OH)(H_2O)_3]^+$

UNIVERSITAT ROVIRA I VIRGILI
ASSEMBLY AND PROPERTIES OF POLYOXOMETALATES: A THEORETICAL POINT OF VIEW
Laia Vilà Nadal
ISBN.978-84-694-2170-3/DL:T. 1039-2011

cation. The free-energy barrier from the six- to the five-coordinated cation is 13 kcal mol^{-1}, in good agreement with the results obtained for the tungstic acid. Since we have not accelerated the deprotonation/protonation equilibrium with any collective variable, we conclude that the barriers for proton transfers in such a system are low. Indeed, we have performed a standard Car–Parrinello MD simulation for 15 ps on the six-coordinated $[WO_2(OH)(H_2O)_3]^+$ cation and we have observed almost from the beginning the aforementioned proton transfers and the formation of tungstic acid $[WO_2(OH)_2(H_2O)_2]$ in solution. The W–O radial distribution function and its integration, which yields the W–O coordination number,[15] are displayed in Figure 3.5.

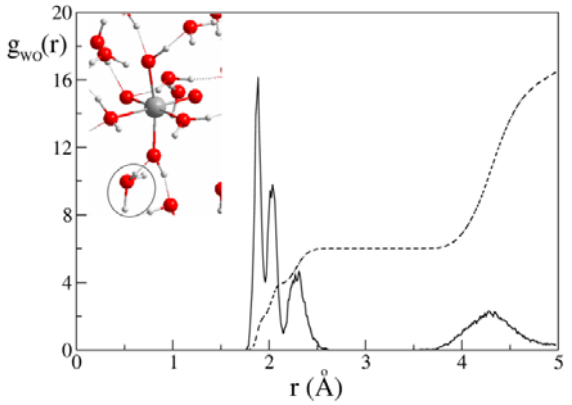

Figure 3.5. W–O radial distribution function (solid line) and its integration (broken line) computed for the 15 ps MD simulation starting from $[WO_2(OH)(H_2O)_3]^+$. The geometry of the six-coordinated species along with the nearest water molecules that solvate it is shown at the left top corner. The formed hydronium ion is highlighted.

The sharp spike below 2 Å that integrates two O atoms can be attributed to the oxo ligands. The spike at around 2 Å that integrates two more O atoms corresponds to the hydroxo ligands. Finally, the third spike between 2 and 2.5 Å, which integrates other two O atoms are due to the aqua ligands

UNIVERSITAT ROVIRA I VIRGILI
ASSEMBLY AND PROPERTIES OF POLYOXOMETALATES: A THEORETICAL POINT OF VIEW
Laia Vilà Nadal
ISBN.978-84-694-2170-3/DL:T. 1039-2011

coordinated to the W(VI) ion. At distances between 2.5 and 3.7 Å, the W–O coordination number shows a plateau associated with the presence of six O atoms in the coordination sphere of W(VI) ion. A shallow maximum appears between 4 and 4.5 Å that is ascribed to the first solvation sphere. This solvation sphere can be estimated to contain on average 10 water molecules.

A similar phenomenon occurs in the case of the structural isomer $[WO(OH)_3(H_2O)_2]^+$: at the beginning of a standard Car–Parrinello MD simulation one proton from an aqua ligand is released giving again an isomer of tungstic acid $[WO(OH)_4(H_2O)]$ and a hydronium ion in the solution. The simulation was extended up to 13 ps. During the first picosecond the hydronium ion recombines with tungstic acid recovering the former $[WO(OH)_3(H_2O)_2]^+$ cation. Afterwards, once the hydronium is released again, the isomer of tungstic acid $[WO(OH)_4(H_2O)]$ remains for around 7 ps. Then, the protonated cation $[WO(OH)_3(H_2O)_2]^+$ is recovered again and lasts up to the end of the simulation. The W–O radial distribution function and its integration are displayed in Figure 3.6.

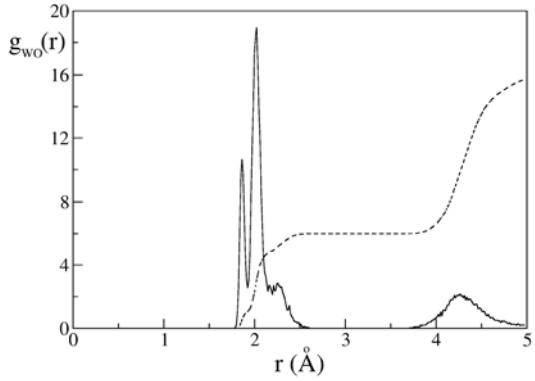

Figure 3.6. W–O radial distribution function (solid line) and its integration (broken line) computed for the 13 ps MD simulation starting from $[WO(OH)_3(H_2O)_2]^+$.

Two well separated spikes between 1.8 and 2.1 Å, which correspond to the oxo and hydroxo ligands, are now distinguished. The third spike, which is centred at 2.3 Å and corresponds to the aqua ligand, is not now so well defined. The three spikes integrate up to six O atoms, but the distribution pattern of ligands around W(VI) is different. Now there is only one oxo ligand. Regarding the distribution of hydroxo and aqua ligands around W(VI), the ratio of their averaged coordination numbers is approximately 3.5/1.5, consequence of the existence of both neutral tungstic acid $[WO(OH)_4(H_2O)]$ and the protonated cation $[WO(OH)_3(H_2O)_2]^+$ for similar periods during the simulation. The shallow maximum between 4 and 4.5 Å associated to the first solvation shell is also present. From the results of our simulations we infer that at high acidic conditions (i) proton transfers between protonated tungstic acid and the solvent molecules are likely events; and (ii) tungstic acid and its structural isomers have more probability to be found as neutral than as protonated. Much higher acidic conditions would have to be simulated to find protonated tungstic acid as the most likely species in solution.

Conclusions

We have studied the hydration/dehydration equilibria of hydrogentungstate anion, tungstic acid and protonated tungstic acid. The general conclusion regardless of the solvent surface used in the COSMO calcualtions is the following: a decrease of the pH involves an expansion of the coordination sphere of the W(VI). This has been also corroborated with Car–Parrinello molecular dynamics and metadynamics simulations, when the explicit water molecules were taken into account.[11]

Continuous solvation models have been shown to yield a good description of geometries and orbital energies of polyoxoanions in solution.[16] However, care must be taken before choosing the

solvent surface. Furthermore these methods are not able to predict some structures with low energy that are found when doing Car–Parrinello MD.[11]

This initial study provides a qualitative picture of the hydration equilibria of hydrogentungstate anion in acidic solutions, which is fundamental for further understanding of the nucleation processes that yield polyoxometalates.

UNIVERSITAT ROVIRA I VIRGILI
ASSEMBLY AND PROPERTIES OF POLYOXOMETALATES: A THEORETICAL POINT OF VIEW
Laia Vilà Nadal
ISBN.978-84-694-2170-3/DL:T. 1039-2011

3.3. Formation Mechanisms and Intermediate Structures

During the last decades extensive theoretical research about POMs has been done, but only few works were dedicated to analyze their formation mechanisms. In fact the aggregative processes involved in the formation of these molecules are still poorly understood. If we are to conceptualize the formation of polytungstates by acidification of monotungstate $[WO_4]^{2-}$, eqn. (3.5), a theoretical H^+/W ratio on an acidification scale between 0.0 and 2.0 can be assigned to the known isopolytungstates (IPAs). As shown in Fig. 3.7 all the characterized IPAs show H^+/W ratios higher than 1.[17] It is readily apparent the great number of characterized species, with different nuclearities, involved in these equilibria. It would be impossible to study all of them at this initial stage, so we have decided to study the formation mechanisms of the Lindqvist anion, $[W_6O_{19}]^{2-}$, since it is the IPA with the smallest structure.

$$x\left[WO_4\right]^{2-} + pH^+ \rightarrow \left[W_xO_y\left(OH\right)_z\right]^{n-} + \left(p-z\right)/2\,H_2O \qquad (3.5)$$

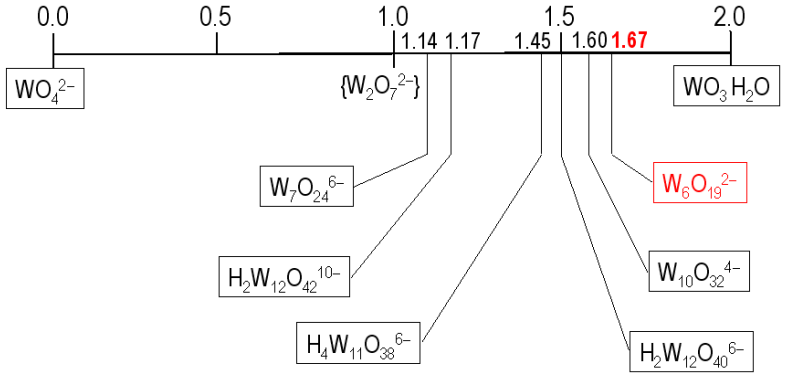

Figure 3.7. Schematic representation showing the stoichiometric amount of acid required to form polytungstate $[W_xO_y(OH)_z]^{n-}$, from $[WO_4]^{2-}$, according to equation (3.5). Structurally characterized species are in shaded boxes. In red the stoichiometry for the Lindqvist anion.

UNIVERSITAT ROVIRA I VIRGILI
ASSEMBLY AND PROPERTIES OF POLYOXOMETALATES: A THEORETICAL POINT OF VIEW
Laia Vilà Nadal
ISBN.978-84-694-2170-3/DL:T. 1039-2011

As stated above, for the time being, only a small number of previous studies have investigated the mechanism of formation of POMs with the main limitation being the development of a universal POM "lego" kit. Manipulating this "lego" kit carefully and correlating the synthetic conditions with the overall cluster architecture formed is a key aspect.[18] We have based our studies in two postulates proposed by Kepert[19] in the early sixties, and Tytko and Glemser in the seventies.[20] Kepert suggested that the formation of IPAs might involve the addition of WO_4 tetrahedra as shown in Fig. 3.8, whereby the first step would imply the addition of a $[WO_4]^{2-}$ unit, acting as a bidentate ligand, to a second WO_4 by expanding the coordination number of the latter metal ion to six. The nucleation is initiated as soon as the $[WO_4]^{2-}$ anions are protonated, then one W–O bond is stretched in each tetrahedron. Based on this addition process, Tytko and Glemser proposed elaborate mechanisms to explain the formation of IPAs and HPAs. Their mechanisms incorporate the fact that aggregation of monomers to yield large POMs requires the condensation of H_2O molecules at different reaction steps. See for example equation 3.6 for the formation of the Lindqvist anion where the condensation of 5 H_2O is necessary.

$$6\left[WO_3(OH)\right]^- + 4H^+ \rightarrow \left[W_6O_{19}\right]^{2-} + 5H_2O \qquad (3.6)$$

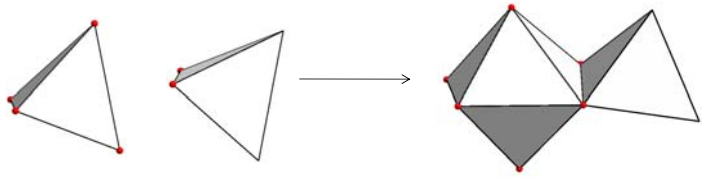

Figure 3.8. A representation of the aggregation process proposed by Kepert. The addition of $[WO_4]^{2-}$ tetrahedra drive the system to the expansion of the coordination sphere of W(VI).

The results obtained are presented as follows: first, we focus on the formation of dinuclear species. Afterwards the experimental ESI-MS results are presented. Then, we propose different

UNIVERSITAT ROVIRA I VIRGILI
ASSEMBLY AND PROPERTIES OF POLYOXOMETALATES: A THEORETICAL POINT OF VIEW
Laia Vilà Nadal
ISBN.978-84-694-2170-3/DL:T. 1039-2011

mechanisms consistent with the ESI-MS experiments. Finally we analyze the structural features and dynamic behavior of possible intermediates in the formation of the Lindqvist anion.

3.3.1. Dinuclear Species

The monoprotonated tungstate anion $[WO_3(OH)]^-$ is considered the building block in our construction scheme, because it is necessary to have one stretched W–O distance to form dinuclear species easily. In this first step two possible reactions are taken into account. The two stoichometric reactions are presented as follows:

$$2\left[WO_3(OH)\right]^- \rightarrow \left[W_2O_6(OH)_2\right]^{2-} \quad (3.7)$$

$$2\left[WO_3(OH)\right]^- \rightarrow \left[W_2O_7\right]^{2-} + H_2O \quad (3.8)$$

On one hand, reaction 3.7 yields the dimer $[W_2O_6(OH)_2]^{2-}$ due to a simple aggregation of two monomers. On the other hand, in reaction 3.8 the dimer $[W_2O_7]^{2-}$ is obtained after the aggregation followed by a water condensation process. Relative energies for dinuclear species with respect to the monomers, $[WO_3(OH)]^-$ computed at BP86/COSMO level are listed in Table 3.4. As we have done in previous studies two kinds of molecular surfaces that model the continuous solvent (SAS, SES) were taken into account.

The results for these surfaces are qualitatively equivalent. The most important difference corresponds to isomer 2 of $[W_2O_6(OH)_2]^{2-}$. Since calculations using the SES predict much better solvation energies than those with the SAS, we decide to adopt the SAS/SES SP methodology. The structures of the most representative geometries are displayed in Figure 3.9.

The lowest-energy minimum ($[W_2O_6(OH)_2]^{2-}$, structure 1), found at –12.5 and –7.5 kcal mol^{-1} with respect to the monomers for the SAS and SES solvent surfaces, respectively, corresponds to a

UNIVERSITAT ROVIRA I VIRGILI
ASSEMBLY AND PROPERTIES OF POLYOXOMETALATES: A THEORETICAL POINT OF VIEW
Laia Vilà Nadal
ISBN.978-84-694-2170-3/DL:T. 1039-2011

structure in which one W atom is four-coordinated and the other W is five-coordinated (a 5c-4c structure). This structure shows an intramolecular hydrogen bond (Figure 3.9 a).

Table 3.4. The reaction energies ΔE, in kcal mol^{-1}, for dinuclear species computed at BP86/COSMO, with two kinds of molecular surfaces that model the continuous solvent (SAS, SES).

Structure		ΔE SAS	ΔE SAS/SES SP*
$[W_2O_6(OH)_2]^{2-}$	**1**	−12.5	−7.5
	2	−10.0	+0.2
	3	+3.2	+10.2
$[W_2O_7]^{2-}$	**1**	−3.7	−4.4

*The optimized geometry of BP/SAS was recalculated as single point using SES.

The second most stable dimer (2) is the structure in which the two W atoms are five-coordinated (a 5c-5c structure) and the H atoms are located at terminal O atoms (Figure 3.9 b).

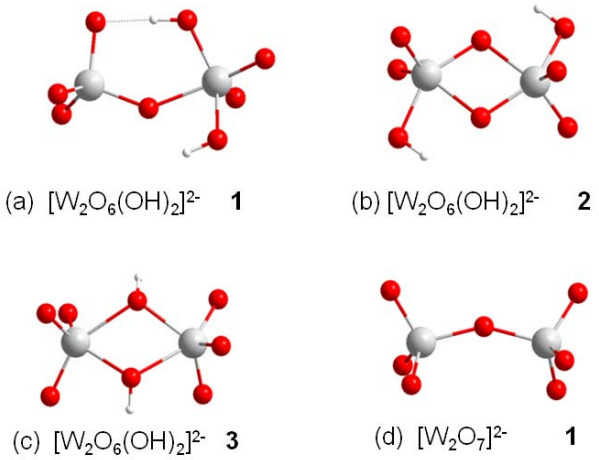

Figure 3.9. Optimized structures for the most representative dinuclear species.

Structure 2 has a relative energy of –10.0 kcal mol^{-1} when is optimized using the SAS molecular surface. This geometry is not

UNIVERSITAT ROVIRA I VIRGILI
ASSEMBLY AND PROPERTIES OF POLYOXOMETALATES: A THEORETICAL POINT OF VIEW
Laia Vilà Nadal
ISBN.978-84-694-2170-3/DL:T. 1039-2011

stabilized by intramolecular hydrogen bonds as occurs for structure 1. For SES, however, the energy difference between structures 1 and 2 is larger (almost 8 kcal mol^{-1}). When the dimer is surrounded by explicit solvent molecules, H_2O in our case, O and H atoms of the dimer are able to form H bonds with water molecules. Consequently the strength of intramolecular H bonds is reduced. The way in which the continuous models of solvation take into account this point would be a possible source of error that might be at the origin of this discrepancy. The quantitative estimation of this error is not simple and is out of the scope of this work.

Structure 3 consists of a 5c-5c framework with H atoms at the bridging positions (Figure 3.9 c). It is more than 10 kcal mol^{-1} less stable than structure 2 in both solvent surfaces. The only difference between both structures is the position of the H atoms (Fig. 3.9 b and c). Consequently, we can state that for dinuclear species with $[W_2O_6(OH)_2]^{2-}$ stoichiometry, terminal O atoms are more basic than those in the bridging positions. This fact is curious because large POMs behave in opposite way: the bridging positions are more basic.[21]

The reaction energy for the dehydration process was also computed, see equation 3.8. In this case the two solvation models drive us to similar results. An extra significant result is that dinuclear species proposed by Kepert, i.e. a 6c-4c structure, is not located as a minimum in the potential energy surface (PES). These structures are not found to be the first step in addition process at least when conventional geometry optimization methods are used. The geometry optimization attempts starting from a 6c-4c structure lead to 5c-5c structures.

Being aware of the fact that the stability of the structures with intramolecular H bonds can be overestimated due to the use of a continuum solvation model, Car–Parrinello MD simulations treating the solvent molecules explicitly at DFT level have been

UNIVERSITAT ROVIRA I VIRGILI
ASSEMBLY AND PROPERTIES OF POLYOXOMETALATES: A THEORETICAL POINT OF VIEW
Laia Vilà Nadal
ISBN.978-84-694-2170-3/DL:T. 1039-2011

also performed.[22] To accelerate the dynamics and to compute free energy barriers the metadynamics approach has also been used.[23] A description of this complementary work follows.

The system was formed by two $[WO_3(OH)]^-$ monomers and 27 H_2O molecules. To describe the formation of dinuclear species in solution three collective variables (CV) were used: the coordination number (CN) of each W atom with respect to the eight O atoms that belong to WO_4 groups, $C_{W1\text{-}O}$ and $C_{W2\text{-}O}$; and to account for the number of H atoms bonded to those O atoms bonded to W, a conditioned CN, $cC_{W\text{-}O\text{-}H}$ was used. The first two CN explore the phase space related to the formation of dinuclear species and the third CN accounts for the level of protonation/hydration of these species. In Figure 3.10 the evolution of the coordination numbers $C_{W1\text{-}O}$ and $C_{W2\text{-}O}$ along 11-ps metadynamics trajectory is depicted.[24]

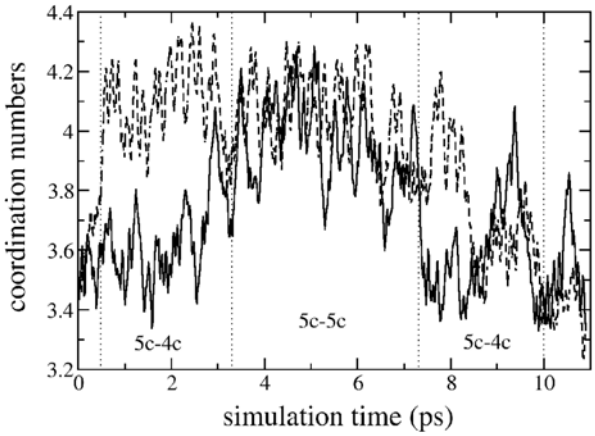

Figure 3.10. Evolution of the coordination numbers $C_{W1\text{-}O}$ and $C_{W2\text{-}O}$ along the trajectory of the metadynamics run. Vertical dotted lines separate the regions where different structures appear.

The first observed event is a H^+ transfer from one $[WO_3(OH)]^-$ monomer to the other indicating that H^+ transfer processes between monomers when they are close enough are highly

UNIVERSITAT ROVIRA I VIRGILI
ASSEMBLY AND PROPERTIES OF POLYOXOMETALATES: A THEORETICAL POINT OF VIEW
Laia Vilà Nadal
ISBN.978-84-694-2170-3/DL:T. 1039-2011

probable. At about 0.6 ps, dimerization takes place yielding a structure in which one W atom is four-coordinated and the other W is five-coordinated (a 5c-4c structure, see Fig. 3.10). Afterwards the formation of a 5c-5c structure that remains for around 3.5 ps is observed. One interesting structure with a H_2O molecule at the sixth coordination position of one of the W atoms is also seen. Finally recrossings to the 5c-4c structure and to the two monomers are observed.

The free energy surface (FES) explored by the metadynamics run can be evaluated directly through the added time-dependent potential. Such a method has been proved to be a reasonable approximation to the free energy barrier, $\Delta F^{\#}$.[25-33]The obtained free-energy profile is shown in Figure 3.11.

The process with the lowest barrier is the formation of the 5c-4c structure from the two $[WO_3(OH)]^-$ monomers, 7±3 kcal mol^{-1}. From the 5c-4c minimum two processes are showing similar probability (within the error), the system can escape to the 5c-5c structure or come back to form the monomers. All these barriers can be easily overcome at temperatures were IPAs are formed (ambient T or even higher). 5c-4c structure is around 9±3 kcal mol^{-1} more stable than the system formed by the two monomers and the water molecules. 5c-5c is almost degenerate with 5c-4c structure. An interesting point is that during the metadynamics we did not observe the 6c-4c structure proposed by Kepert.

UNIVERSITAT ROVIRA I VIRGILI
ASSEMBLY AND PROPERTIES OF POLYOXOMETALATES: A THEORETICAL POINT OF VIEW
Laia Vilà Nadal
ISBN.978-84-694-2170-3/DL:T. 1039-2011

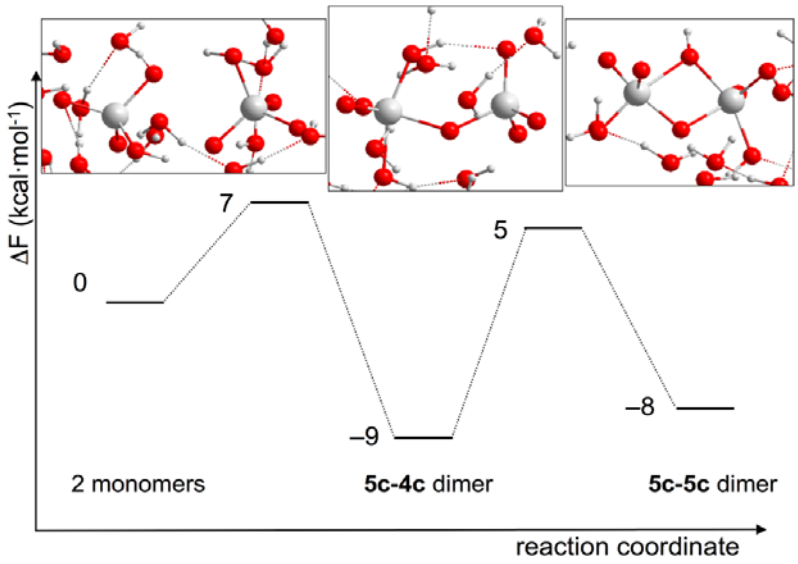

Figure 3.11. Free energy profile (in kcal·mol^{-1}) corresponding to the formation of dinuclear $[W_2O_6(OH)]^{2-}$ species.

The effect of the pH in the formation of dinuclear species was also analyzed performing simulations at low pH conditions with two $[WO_2(OH)_2]$ monomers surrounded by 27 H_2O molecules. In a standard Car–Parrinello MD the formation of a hydrated 5c-4c structure was already observed. So the dimerization process shows a low energy barrier and is highly probable. In this simulation Kepert structure is neither observed. The results obtained show that hydration gives extra stability to dimers and the lowest-energy species show hexacoordinated W ions. Figure 3.12 shows one of the most stable dinuclear species at low pH conditions.

Therefore we conclude that continuous solvation models are able to predict the species obtained when using Car–Parrinello MD. In the following stages SES surface (SAS/SES SP) will be used in order to calculate the reaction energies of the steps with different proposed mechanisms, because it is known that SES

UNIVERSITAT ROVIRA I VIRGILI
ASSEMBLY AND PROPERTIES OF POLYOXOMETALATES: A THEORETICAL POINT OF VIEW
Laia Vilà Nadal
ISBN.978-84-694-2170-3/DL:T. 1039-2011

reproduces much better experimental hydration energies in solution than in the SAS.[34]

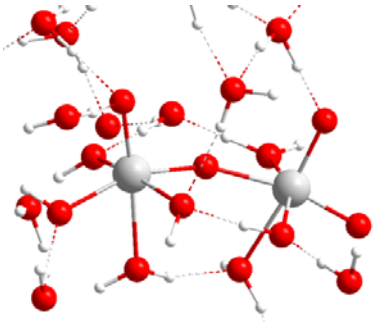

Figure 3.12. Optimized structure for one of the most stable dinuclear species in solution at low pH conditions. The two W atoms are hexacoordinated.

3.3.2. The Following Step in the Mechanism

To go one step further we increase the number of W atoms in the structures. The results obtained in the dinuclear species states that the first step will be the formation of $[W_2O_6(OH)_2]^{2-}$ after aggregation of two $[WO_3(OH)]^-$ monomers. Then three mechanisms are proposed for the following step (M1, M2, M3). The reaction energies in kcal mol^{-1} for each mechanism are listed in Table 3.5.

In the M1 mechanism, $[W_2O_6(OH)_2]^{2-}$ leads to $[W_2O_6(OH)]^-$ after the protonation and the subsequent water condensation. In the second mechanism, M2, $[W_2O_7]^{2-}$ is obtained after water condensation from $[W_2O_6(OH)_2]^{2-}$. Finally the third option, M3, would be the aggregation of $[WO_3(OH)]^-$ to $[W_2O_6(OH)_2]^{2-}$ and formation of a trinuclear species $[W_3O_9(OH)_3]^{3-}$. The structures obtained for each mechanism are shown in Figure 3.13.

The formation of $[W_3O_9(OH)_3]^{3-}$, in M3, is endothermic and therefore is less favourable than the formation of $[W_2O_6(OH)]^-$ in M1. M3 mechanism is also 8 kcal mol^{-1} more endothermic

UNIVERSITAT ROVIRA I VIRGILI
ASSEMBLY AND PROPERTIES OF POLYOXOMETALATES: A THEORETICAL POINT OF VIEW
Laia Vilà Nadal
ISBN.978-84-694-2170-3/DL:T. 1039-2011

than M2. So, we predict that the following step will pass through mechanisms M1 and M2, and not M3.

Table 3.5. Reaction energies in kcal mol^{-1}, computed at BP86/COSMO with SES.

Mechanism		ΔE
Step1	$[WO_3(OH)]^-_{(aq)} + [WO_3(OH)]^-_{(aq)} \rightarrow [W_2O_6(OH)_2]^{2-}_{(aq)}$	–7.5
M 1	1.2) $[W_2O_6(OH)_2]^{2-}_{(aq)} + H_3O^+_{(aq)} \rightarrow [W_2O_6(OH)]^-_{(aq)} + 2H_2O_{(aq)}$	–14.4
M 2	2.2) $[W_2O_6(OH)_2]^{2-}_{(aq)} \rightarrow [W_2O_7]^{2-}_{(aq)} + H_2O_{(aq)}$	+3.0
M 3	3.2) $[W_2O_6(OH)_2]^{2-}_{(aq)} + [WO_3(OH)]^-_{(aq)} \rightarrow [W_3O_9(OH)_3]^{3-}_{(aq)} + H_2O_{(aq)}$	+11.4

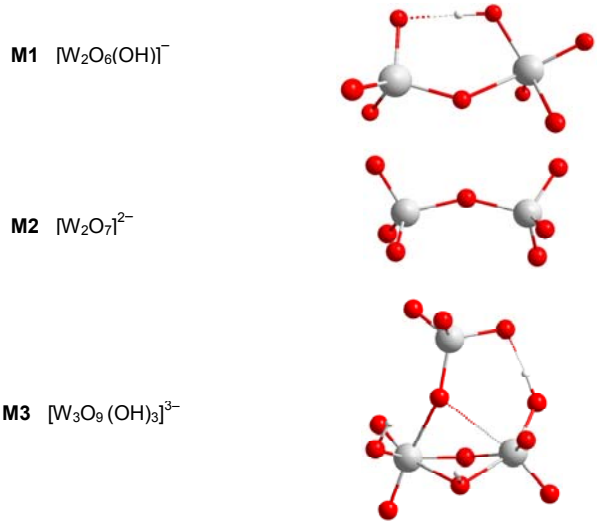

Figure 3.13. Most stable structures for the second step in the aggregation process. Structures for M1 and M2 are dinuclear; for M3 a trinuclear species is obtained.

3.3.3. ESI-MS Experiments

Since the ESI-MS experiments can provide fragmentation data, the correlation between these data and the mechanistic details could provide important information if the species observed in the fragmentation process can be related to those generated in the formation of the POM clusters. An example of an spectrum

UNIVERSITAT ROVIRA I VIRGILI
ASSEMBLY AND PROPERTIES OF POLYOXOMETALATES: A THEORETICAL POINT OF VIEW
Laia Vilà Nadal
ISBN.978-84-694-2170-3/DL:T. 1039-2011

for the Lindqvist anion with the subsequent assigned bands is presented in Figure 3.14.

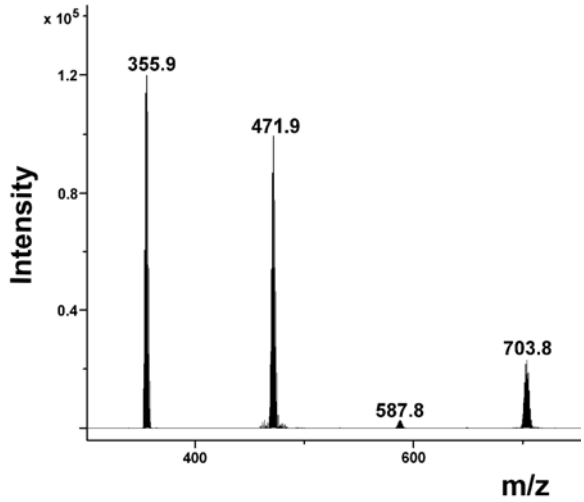

Figure 3.14. Mass spectral data recorded by collision-induced dissociation (CID) of the isolated $[W_6O_{19}]^{2-}$ peak at m/z 703.8. The peaks shown are associated with the species $[W_3O_{10}]^{2-}$ (355.9 m/z), $[W_4O_{13}]^{2-}$ (471.9 m/z), $[W_5O_{16}]^{2-}$ (587.8 m/z), and $[W_6O_{19}]^{2-}$ (703.8 m/z).

The peaks observed in the ESI-MS experiments of the Lindqvist anion are associated with the species $[WO_3(OH)]^-$, $[W_2O_7]^{2-}$, $[W_2O_6(OH)]^-$, $[W_3O_{10}]^{2-}$, $[W_3O_9(OH)]^-$, $[W_4O_{13}]^{2-}$, $[W_4O_{12}(OH)]^-$, $[W_5O_{16}]^{2-}$, $[W_6O_{19}]^{2-}$ and $[W_6O_{18}(OH)]^-$ (see Table 3.6). These results may suggest that the Lindqvist anion is formed by consecutive steps that incorporate one metal unit at each time. A formation mechanism based on the aggregation of two trinuclear species would not be fully compatible with these results. The presence of tetra- and pentanuclear stoichiometries in the ESI-MS spectra would not be easily explained if such a formation pathway were important. It is interesting to note that the stoichiometrys proposed in M3 $[W_3O_9(OH)_3]^{3-}$, which was not energetically favourable, is not detected.

UNIVERSITAT ROVIRA I VIRGILI
ASSEMBLY AND PROPERTIES OF POLYOXOMETALATES: A THEORETICAL POINT OF VIEW
Laia Vilà Nadal
ISBN.978-84-694-2170-3/DL:T. 1039-2011

Table 3.6. A summary of the peaks observed from the ESI-MS data collections, along with their associated species.

m/z	Peak Assignment
232.0	$[W^{V}O_3]^-$
247.9	$[WO_4H]^-$
463.9	$[W^{VI}W^{V}O_6]^-$
239.9	$[W_2O_7]^{2-}$
479.9	$[W_2O_7H]^-$
695.8	$[W^{VI}_2W^{V}O_9]^-$
355.9	$[W_3O_{10}]^{2-}$
712.8	$[W_3O_{10}H]^-$
471.9	$[W_4O_{13}]^{2-}$
944.8	$[W_4O_{13}H]^-$
587.8	$[W_5O_{16}]^{2-}$
703.8	$[W_6O_{19}]^{2-}$
1408.6	$[W_6O_{19}H]^-$
1649.9	$[((C_4H_9)_4N)W_6O_{19}]^-$

It should be noted that the isotope pattern match for the assigned peaks at 247.9 m/z and 479.9 m/z are not exact, being 1 m/z unit out from the predicted patterns for $[WO_3(OH)]^-$ and $[W_2O_7H]^-$ respectively. However, given the presence in these ESI-MS results of the anion series $[W_nO_{3n+1}H]^-$ for which n= 1 to 6, when assigning these species as $[WO_3(OH)]^-$ and $[W_2O_7H]^-$, along with the precedent in the literature for the observation of these species and anion series,[35-37] we believe these peak assignments to be correct.

In order to obtain the structures with the lowest energies that correspond to the detected stoichiometries we have carried out metadynamics calculations. In these cases the number of metals is the limiting factor, so the calculation with explicit waters is

UNIVERSITAT ROVIRA I VIRGILI
ASSEMBLY AND PROPERTIES OF POLYOXOMETALATES: A THEORETICAL POINT OF VIEW
Laia Vilà Nadal
ISBN.978-84-694-2170-3/DL:T. 1039-2011

unachievable for more than three metal units. To overcome this problem we have done metadynamics runs in the gas phase, and the geometries obtained were optimized using SAS at BP86/COSMO level for the solvent. Then single point calculations of the optimized geometries were done (SAS/SES SP methodology). In the following lines two postulated mechanisms that justify the clusters detected in the ESI-MS experiments will be discussed.

3.3.4. Proposed Mechanisms

Based on the stoichiometries detected in the ESI-MS experiments we propose two mechanisms for the formation of the Lindqvist anion, M1 and M2. Both mechanisms, presented in Table 3.7, are based on consecutive steps of nucleation and water condensation. Before discussing the two proposed mechanisms, we describe the relative energies and geometries for the lowest-energy tri-, tetra-, and pentanuclear species proposed in mechanisms M1 and M2.

The mechanisms proposed here, to be consistent with ESI-MS experiments, postulate that each protonation or/and water condensation processes occur after nucleation steps. No double protonation neither double nucleation is postulated at any step. As we have said previously, the mechanisms proposed in Table 3.7, incorporate the fact that aggregation of monomers to yield large POMs requires the condensation of H_2O molecules, at different reaction steps.

UNIVERSITAT ROVIRA I VIRGILI
ASSEMBLY AND PROPERTIES OF POLYOXOMETALATES: A THEORETICAL POINT OF VIEW
Laia Vilà Nadal
ISBN.978-84-694-2170-3/DL:T. 1039-2011

Table 3.7. Proposed mechanisms, M1 and M2 for the formation of the Lindqvist anion, $[W_6O_{19}]^{2-}$. The species detected in ESI-MS experiments are highlighted in bold.

Step	Mechanism	Reactions
1	1	$\mathbf{[WO_3(OH)]^-_{(aq)}}$ + $[WO_3(OH)]^-_{(aq)} \rightarrow [W_2O_6(OH)_2]^{2-}_{(aq)}$
	2	$\mathbf{[WO_3(OH)]^-_{(aq)}}$ + $[WO_3(OH)]^-_{(aq)} \rightarrow [W_2O_6(OH)_2]^{2-}_{(aq)}$
2	1	$[W_2O_6(OH)_2]^{2-}_{(aq)} + H_3O^+_{(aq)} \rightarrow \mathbf{[W_2O_6(OH)]^-_{(aq)}} + 2H_2O_{(aq)}$
	2	$[W_2O_6(OH)_2]^{2-}_{(aq)} \rightarrow \mathbf{[W_2O_7]^{2-}_{(aq)}} + H_2O_{(aq)}$
3	1	$[W_2O_6(OH)]^-_{(aq)} + [WO_3(OH)]^-_{(aq)} \rightarrow [W_3O_9(OH)_2]^{2-}_{(aq)}$
	2	$[W_2O_7]^{2-}_{(aq)} + [WO_3(OH)]^-_{(aq)} \rightarrow [W_3O_{10}(OH)]^{3-}_{(aq)}$
4	1	$[W_3O_9(OH)_2]^{2-}_{(aq)} + H_3O^+_{(aq)} \rightarrow \mathbf{[W_3O_9(OH)]^-_{(aq)}} + 2H_2O_{(aq)}$
	2	$[W_3O_{10}(OH)]^{3-}_{(aq)} + H_3O^+_{(aq)} \rightarrow \mathbf{[W_3O_{10}]^{2-}_{(aq)}} + 2H_2O_{(aq)}$
5	1	$[W_3O_9(OH)]^-_{(aq)} + [WO_3(OH)]^-_{(aq)} \rightarrow [W_4O_{12}(OH)_2]^{2-}_{(aq)}$
	2	$[W_3O_{10}]^{2-}_{(aq)} + [WO_3(OH)]^-_{(aq)} \rightarrow [W_4O_{13}(OH)]^{3-}_{(aq)}$
6	1	$[W_4O_{12}(OH)_2]^{2-}_{(aq)} + H_3O^+_{(aq)} \rightarrow \mathbf{[W_4O_{12}(OH)]^-_{(aq)}} + 2H_2O_{(aq)}$
	2	$[W_4O_{13}(OH)]^{3-}_{(aq)} + H_3O^+_{(aq)} \rightarrow \mathbf{[W_4O_{13}]^{2-}_{(aq)}} + 2H_2O_{(aq)}$
7	1	$[W_4O_{12}(OH)]^-_{(aq)} + [WO_3(OH)]^-_{(aq)} \rightarrow [W_5O_{15}(OH)_2]^{2-}_{(aq)}$
	2	$[W_4O_{13}]^{2-}_{(aq)} + [WO_3(OH)]^-_{(aq)} \rightarrow [W_5O_{16}(OH)]^{3-}_{(aq)}$
8	1	$[W_5O_{15}(OH)_2]^{2-}_{(aq)} + H_3O^+_{(aq)} \rightarrow [W_5O_{15}(OH)]^-_{(aq)} + 2H_2O_{(aq)}$
	2	$[W_5O_{16}(OH)]^{3-}_{(aq)} + H_3O^+_{(aq)} \rightarrow \mathbf{[W_5O_{16}]^{2-}_{(aq)}} + 2H_2O_{(aq)}$
9	1	$[W_5O_{15}(OH)]^-_{(aq)} + [WO_3(OH)]^-_{(aq)} \rightarrow [W_6O_{18}(OH)_2]^{2-}_{(aq)}$
	2	$[W_5O_{16}]^{2-}_{(aq)} + [WO_3(OH)]^-_{(aq)} \rightarrow [W_6O_{19}(OH)]^{3-}_{(aq)}$
10	1	$[W_6O_{18}(OH)_2]^{2-}_{(aq)} \rightarrow \mathbf{[W_6O_{19}]^{2-}_{(aq)}} + H_2O_{(aq)}$
	2	$[W_6O_{19}(OH)]^{3-}_{(aq)} + H_3O^+_{(aq)} \rightarrow \mathbf{[W_6O_{19}]^{2-}_{(aq)}} + 2H_2O_{(aq)}$

3.3.5. Trinuclear clusters

We present here the relative energies and geometries for some trinuclear species with the stoichiometries proposed in the formation mechanisms. The structures for representative trimers are shown in Figure 3.15. Both compact structures, $[W_3O_{10}(OH)]^{3-}$ and $[W_3O_{10}]^{2-}$, have a tri-coordinated O atom (μ_3-O). For $[W_3O_{10}(OH)]^{3-}$, the W_3O_3 central core (three W, two μ_2-O and the μ_3-O ligand) is planar. Interestingly $[W_3O_{10}]^{2-}$

UNIVERSITAT ROVIRA I VIRGILI
ASSEMBLY AND PROPERTIES OF POLYOXOMETALATES: A THEORETICAL POINT OF VIEW
Laia Vilà Nadal
ISBN.978-84-694-2170-3/DL:T. 1039-2011

presents the same structure as the one found recently by Müller and co-workers for a trinuclear cluster in the cavity of a Mo/W-storage protein.[38] This unit is also present as a constituent of the well-known $[W_{12}O_{40}H_2]^{6-}$ species.[39]

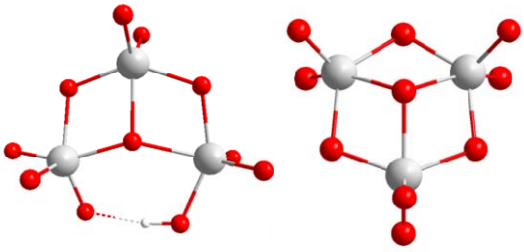

$[W_3O_{10}(OH)]^{3-}$ $[W_3O_{10}]^{2-}$

Figure 3.15. Optimized structures for the most representative compact trinuclear species.

The BP86/COSMO methodology predicts as the lowest-energy structure for the $[W_3O_{10}]^{2-}$ stoichiometry an open cluster in which the three W(VI) ions show tetrahedral coordination, that is, a chain of corner-sharing tetrahedra (10 and 16 kcal mol^{-1} lower in energy than the compact cluster in the gas phase and in the solvent, respectively). This open-chain isomer, however, does not keep in solution the three tetrahedral W(VI) ions. Standard Car–Parrinello MD simulations show that more compact clusters with expanded coordination spheres are rapidily formed. So, this open species might exist in the chamber of the mass spectrometrer but they are not likely intermediates in the formation of the Lindqvist anion. The structure for $[W_3O_{10}(OH)]^{3-}$ shown here is computed to be more stable (at least 8 kcal mol^{-1}) than other more open isomers with μ_2-O atoms (see Table 3.8 and Figure 3.16). It is remarkable that the planar W_3 structural motifs must confer high stability to the structure because they are also found in clusters with higher

UNIVERSITAT ROVIRA I VIRGILI
ASSEMBLY AND PROPERTIES OF POLYOXOMETALATES: A THEORETICAL POINT OF VIEW
Laia Vilà Nadal
ISBN.978-84-694-2170-3/DL:T. 1039-2011

nuclearities (vide infra). Thus, these planar W_3 motifs can be considered as structural building blocks.

Table 3.8. Relative energies (ΔE), in kcal mol^{-1}, for some representative trinuclear species at BP86/COSMO level.

Stoichiometry	Isomer	ΔE
$[W_3O_{10}(OH)]^{3-}$	**1**	0.0
	2	7.9
	3	10.0

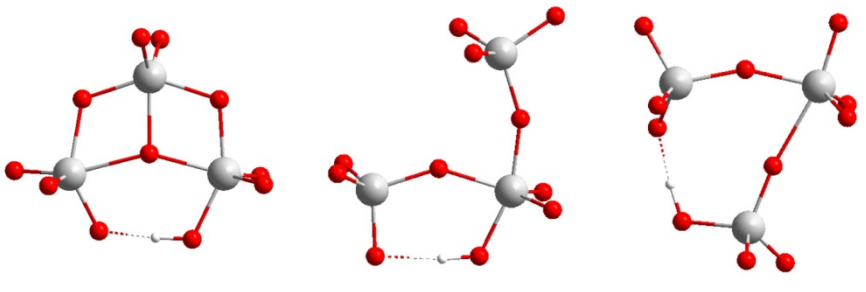

Figure 3.16. "Ball and stick" representation for the optimized structures of some representative trinuclear species with $[W_3O_{10}(OH)]^{3-}$ stoichiometry.

The formation and the stability of trinuclear clusters at acidic conditions were also analyzed by means of Car–Parrinello metadynamics, even though these simulations have an important computational cost. The system consists of one dimer $[W_2O_7]^{2-}$, one monomer $[WO_3(OH)]^-$, 57 H_2O and two H_3O^+. In this metadynamics run, we are more interested in visiting efficiently the phase space than in estimating the free energy barriers. Two CVs were chosen: a CN of the W atoms of the dimer with respect to the O atoms of the WO_4 group, C_{WdimO}, and a conditioned CN that counts for the number of W–O–W bonds formed by the W atom in the monomer with the W atoms in the dimer (see Chapter 2). Open trimers are formed firstly.

UNIVERSITAT ROVIRA I VIRGILI
ASSEMBLY AND PROPERTIES OF POLYOXOMETALATES: A THEORETICAL POINT OF VIEW
Laia Vilà Nadal
ISBN.978-84-694-2170-3/DL:T. 1039-2011

Furthermore, we observe that closed and not very tensioned trinuclear clusters are more stable than open structures (see Table 3.9). Two low-energy structures have been found to feature a three-fold coordinated O atom (μ_3-O), but a closed cluster with only two-fold coordinated O atoms (μ_2-O) is also very stable (Figure 3.17). The structure shown in Figure 3.17c is analogous to the lowest-energy structure found using the COSMO methodology to simulate the solvent (Figure 3.15, left).

Table 3.9. Relative energies (in kcal mol^{-1}) for different trinuclear species obtained from the annealing of structures observed in the metadynamics at low pH conditions (BLYP/PW level).

Structure	O coord[a]	Type	ΔE
5c+1w-5c-5c	2	closed	0
6c-6c-4c+1w	3	closed	1
5c+1w-5c-5c	3	closed	5
6c-5c+1w-4c	2	closed	6
5c-5c+1w-4c	2	open	11
5c-5c-5c	2	open	16
5c+1w-5c-4c	3	closed	17
6c-5c-5c	3	closed	19
4c-5c+1w-4c	2	open	20

[a] O atom with the highest coordination within the cluster.

In order to analyze the stability of $[W_3O_{10}]^{2-}$ in water, we have performed a standard Car–Parrinello molecular dynamics run for the system formed by $[W_3O_{10}]^{2-}$ and 58 H_2O. After approximately 5 ps of equilibration, a molecular dynamics of 20 ps was done. During the equilibration, a water molecule is already coordinated to one of the W ions (W1) occupying its sixth coordination position and yielding an octahedral

UNIVERSITAT ROVIRA I VIRGILI
ASSEMBLY AND PROPERTIES OF POLYOXOMETALATES: A THEORETICAL POINT OF VIEW
Laia Vilà Nadal
ISBN.978-84-694-2170-3/DL:T. 1039-2011

environment around it. After this process of coordination, the structure of the cluster is preserved. We will briefly describe here the most interesting events observed during the 20 ps dynamics.

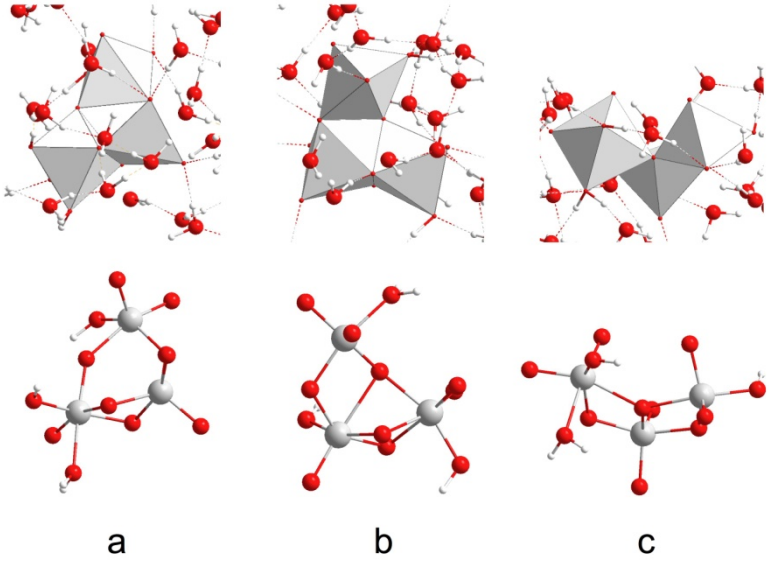

Figure 3.17. Polyhedral representation for the optimized structures of some representative trinuclear species $[W_3O_9(OH)_2]^{2-}$ in solution: a) μ_2-O **5c+1w-5c-5c** structure; b) μ_3-O **6c-6c-5c** structure; and c) μ_3-O **5c+1w-5c-5c** structure. "Ball and stick" representations without the surrounding water molecules are also displayed (down).

At the beginning, hydrolysis of the water ligand, i.e. formation of $[W_3O_{10}(OH)]^{3-}$ species, is observed. The released proton is transferred by means of two solvent molecules to an oxo ligand of the cluster, i.e. an intramolecular proton transfer mediated by the solvent molecules occur. So, at 3 ps the initial $[W_3O_{10}(H_2O)]^{2-}$ cluster has become $[W_3O_9(OH)_2]^{2-}$, with one W ion (W1) having four oxo and two hydroxo ligands and the other two keeping their original five oxo ligands (see Figure 3.18).

The structure of $[W_3O_9(OH)_2]^{2-}$ is then kept for four ps, the water molecules interacting with the O and H atoms of the cluster by means of hydrogen bonds.

UNIVERSITAT ROVIRA I VIRGILI
ASSEMBLY AND PROPERTIES OF POLYOXOMETALATES: A THEORETICAL POINT OF VIEW
Laia Vilà Nadal
ISBN.978-84-694-2170-3/DL:T. 1039-2011

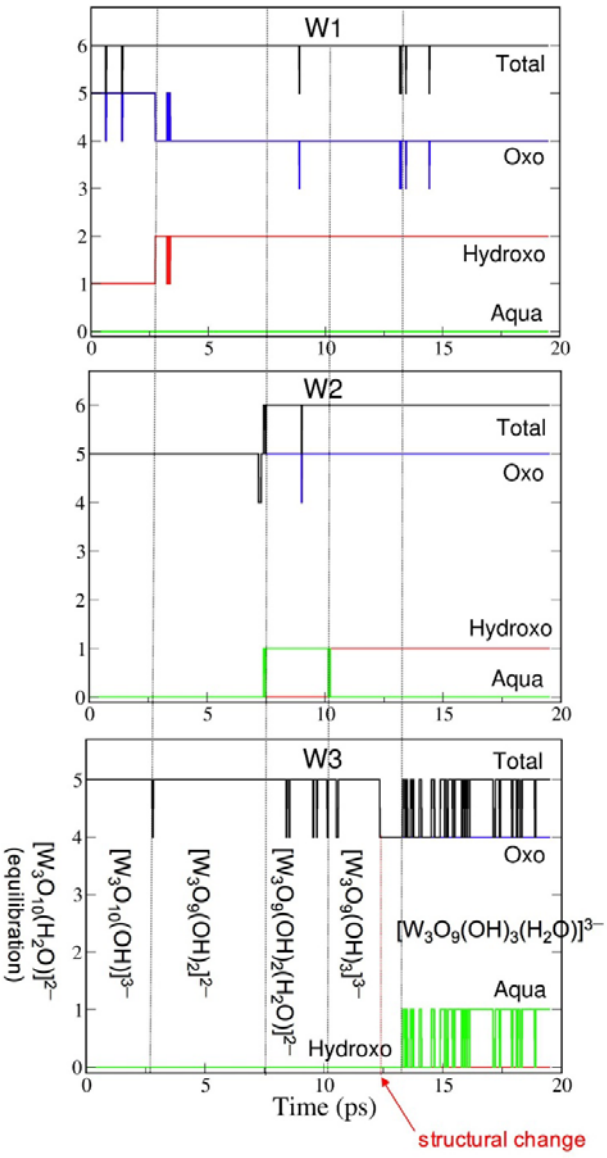

Figure 3.18. Number of oxo, hydroxo and aqua ligands as well as the total number of ligands for each of the W ions during the molecular dynamics simulation (W1, top; W2, middle; and W3, bottom). The species at each time interval are shown in the bottom plot.

UNIVERSITAT ROVIRA I VIRGILI
ASSEMBLY AND PROPERTIES OF POLYOXOMETALATES: A THEORETICAL POINT OF VIEW
Laia Vilà Nadal
ISBN.978-84-694-2170-3/DL:T. 1039-2011

At around 7.5 ps, coordination of a water molecule to one of the remaining five-coordinated W ions (W2) is observed. The cluster $[W_3O_9(OH)_2(H_2O)]^{2-}$, now with two six- and one five-coordinated W ions, preserves its original structure. At around 10 ps, the water molecule that is coordinated to one of the W ions (W2) is hydrolized, i.e., a proton is released to the solution forming a hydronium cation and a cluster of the type $[W_3O_9(OH)_3]^{3-}$. At 12.5 ps, the structure of the cluster undergoes a significant change: the bond between the five-coordinated W ion (W3) and the μ_3-O ligand is broken, leading to a μ_2-O ligand and a four-coordinated W ion (Figure 3.18, bottom). The new W_3 framework is very similar to the structure shown in Figure 3.17a. Only one ps later, another water molecule is attached to the four-coordinated W ion (W3) forming the cluster with stoichiometry $[W_3O_9(OH)_3(H_2O)]^{3-}$. This cluster, with two six- and one five-coordinated W ions keeps its structure up to the end of the simulation.

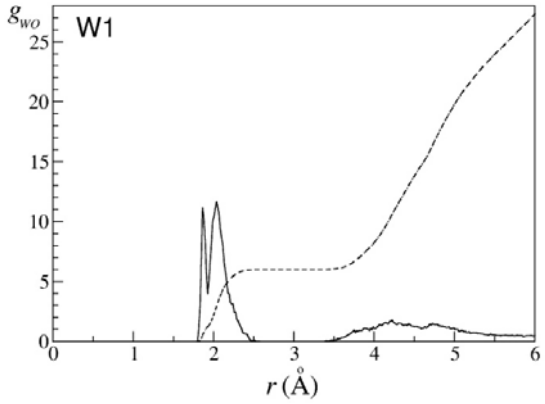

Figure 3.19. W−O radial distribution function, $g_{WO}(r)$, (solid line) and its integration, the coordination number (broken line), of W1 for 20 ps of MD simulation starting from $[W_3O_{10}(H_2O)]^{2-}$.

UNIVERSITAT ROVIRA I VIRGILI
ASSEMBLY AND PROPERTIES OF POLYOXOMETALATES: A THEORETICAL POINT OF VIEW
Laia Vilà Nadal
ISBN.978-84-694-2170-3/DL:T. 1039-2011

Figure 3.19 displays the W−O radial distribution function of one of the W ions that constitute the cluster, W1, along with its integration that yields the coordination number of W1 during the simulation. The sharp spike below 2 Å that integrates one O atom can be attributed to the terminal oxo ligands. The spike with the maximum around 2 Å and which is extended up to 2.5 Å integrates five O atoms. Two of these five O atoms correspond to hydroxo ligands (with bonds around 2 Å) and the other three O atoms are attributed to bridging oxo ligands, which feature longer W−O bond distances. At distances between 2.5 and 3.5 Å, the W1−O coordination number shows a plateau associated with the presence of six O atoms in the coordination sphere of the W1 ion. A shallow maximum appears at distances between 4 and 5 Å that is associated to the first solvation sphere and to the rest of O atoms that belong to the cluster, which most of them are found at distances between 4 and 5 Å. The W−O radial distribution functions for W2 and W3 are displayed in Figure 3.20.

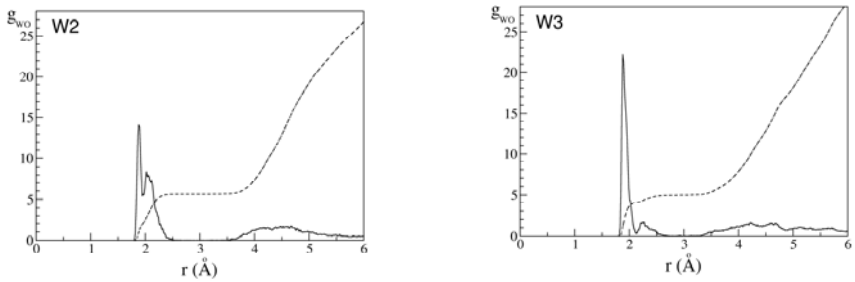

Figure 3.20. W−O radial distribution function, $g_{WO}(r)$, (solid line) and its integration, the coordination number (broken line), of W2 (left) and W3 (right) for 20 ps of MD simulation starting from $[W_3O_{10}(H_2O)]^{2-}$.

From the present simulation we can conclude that the W(VI) ions in the trinuclear $[W_3O_{10}]^{2-}$ cluster coordinate water molecules in order to have octahedral coordination spheres. These water molecules undergo hydrolysis processes yielding

UNIVERSITAT ROVIRA I VIRGILI
ASSEMBLY AND PROPERTIES OF POLYOXOMETALATES: A THEORETICAL POINT OF VIEW
Laia Vilà Nadal
ISBN.978-84-694-2170-3/DL:T. 1039-2011

hydroxo ligands through intramolecular proton transfers or releasing protons to the solution. So, in the presence of hydrogentungstate monomers, the nucleophilic O atoms of these anions would coordinate to W(VI) ions of the trinuclear cluster in order to saturate their coordination spheres yielding the tetranuclear species.

3.3.6. Further Steps to the Lindqvist Anion

Relative energies for tetranuclear ($[W_4O_{13}]^{2-}$, $[W_4O_{13}(OH)]^{3-}$) and pentanuclear ($[W_5O_{16}]^{2-}$, $[W_5O_{16}(OH)]^{3-}$) species with respect to their most stable isomer are listed in Table 3.10. The geometries for these species are displayed in Figures 3.21 and 3.22.

Table 3.10. Relative energies (in kcal mol^{-1}) for some representative $[W_xO_y(OH)_z]^{k-}$ tetra- (x=4, y=13, z=0 or 1) and pentanuclear (x=5, y=16, z=0 or 1) species. [a]Highest coordination of an O atom within the cluster.

Structure		O coord[a]	ΔE
$[W_4O_{13}]^{2-}$	**1**	4	0.0
	2	2	+7.6
$[W_4O_{13}(OH)]^{3-}$	**1**	3	0.0
	2	2	+0.2
	3	3	+2.7
	4	3	+4.6
$[W_5O_{16}]^{2-}$	**1**	3	0.0
	2	3	+3.3
	3	4	+3.2
$[W_5O_{16}(OH)]^{3-}$	**1**	3	0.0
	2	3	+5.7
	3	4	+6.1

UNIVERSITAT ROVIRA I VIRGILI
ASSEMBLY AND PROPERTIES OF POLYOXOMETALATES: A THEORETICAL POINT OF VIEW
Laia Vilà Nadal
ISBN.978-84-694-2170-3/DL:T. 1039-2011

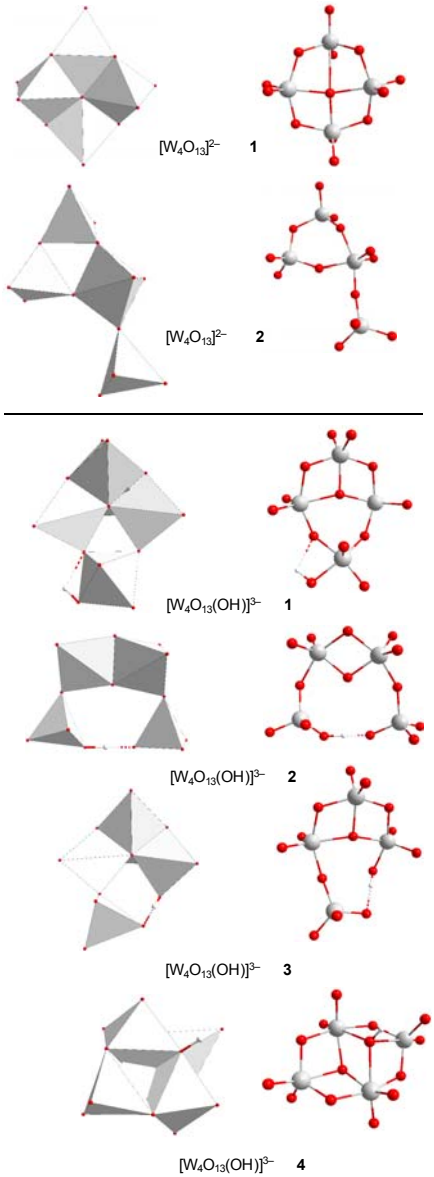

Figure 3.21. Polyhedral (left) and "ball and stick" (right) representations for the optimized structures of the most representative tetrenuclear species. For $[W_4O_{13}]^{2-}$ stoichiometry: structures 1 and 2 ; for $[W_4O_{13}(OH)]^{3-}$ stoichiometry: structures 1, 2, 3 and 4.

UNIVERSITAT ROVIRA I VIRGILI
ASSEMBLY AND PROPERTIES OF POLYOXOMETALATES: A THEORETICAL POINT OF VIEW
Laia Vilà Nadal
ISBN.978-84-694-2170-3/DL:T. 1039-2011

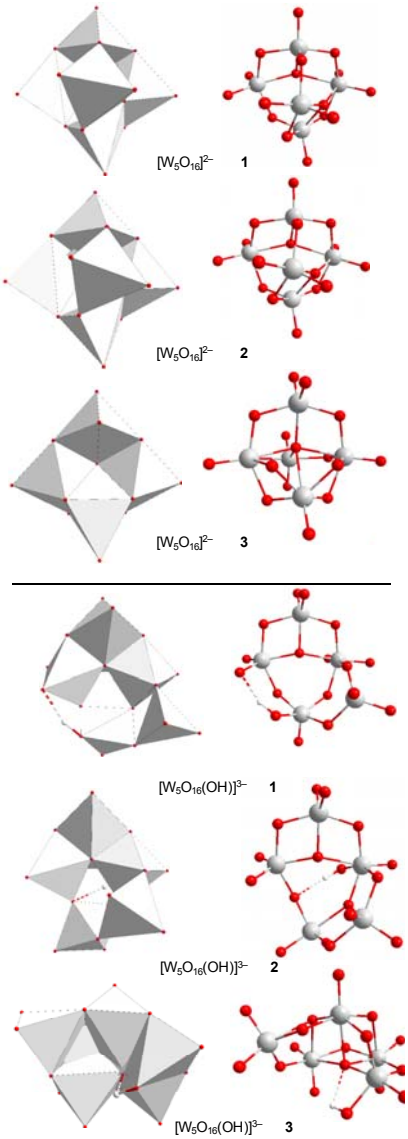

Figure 3.22. Polyhedral (left) and "ball and stick" (right) representations for the optimized structures of the most representative pentanuclear species. For $[W_5O_{16}]^{2-}$ stoichiometry: structures 1, 2 and 3 ; for $[W_5O_{16}(OH)]^{3-}$ stoichiometry: structures 1, 2, and 3.

UNIVERSITAT ROVIRA I VIRGILI
ASSEMBLY AND PROPERTIES OF POLYOXOMETALATES: A THEORETICAL POINT OF VIEW
Laia Vilà Nadal
ISBN.978-84-694-2170-3/DL:T. 1039-2011

The most stable structure that we have found for a $[W_4O_{13}]^{2-}$ stoichiometry, 1, corresponds to a compact cluster with a four-fold coordinated O atom. This structure is 7.6 kcal mol^{-1} more stable than structure 2. It means that the planar conformation of structure 1 and the μ_4-O atom confers stability to tetranuclear clusters. In the case of $[W_4O_{13}(OH)]^{3-}$ the most stable structure is again a planar tetramer, structure 1. This structure can also be seen as a trinuclear planar motif with an extra W atom attached to two W belonging to the trimer. Compared to structure 3, the extra W atom of structure 1 is attached to two oxygen atoms, this fact contributing to a major stabilization of the structure. Structure 4 is less stable than the others although it appears to be more compact. This can be explained due to the loss of the planar W_3 motif in this structure.

Regarding the $[W_5O_{16}]^{2-}$ stoichiometry three structures are found to be the most stable ones, two of them, 2 and 3, are quasi degenerate and somewhat more unstable than 1. The most stable structure presents a μ_3-O atom, and the planar W_3 motif is also found in it. Finally, for the case of $[W_5O_{16}(OH)]^{3-}$, again three structures are presented as the most representative ones. The planar motive W_3 is found in two of them: structures 1 and 2. Structure 3 is the less stable despite the coordination of a μ_4-O atom.

We have performed the same procedure in case of the hexanuclear species; the energy values are not presented here. Structures that are far from the Lindqvist anion show higher energies that those than are more similar. In Figure 3.23 one can observe an example of an hexanuclear $[W_6O_{19}(OH)]^{-}$ structure before evolving towards the Lindqvist anion $[W_6O_{19}]^{2-}$.

UNIVERSITAT ROVIRA I VIRGILI
ASSEMBLY AND PROPERTIES OF POLYOXOMETALATES: A THEORETICAL POINT OF VIEW
Laia Vilà Nadal
ISBN.978-84-694-2170-3/DL:T. 1039-2011

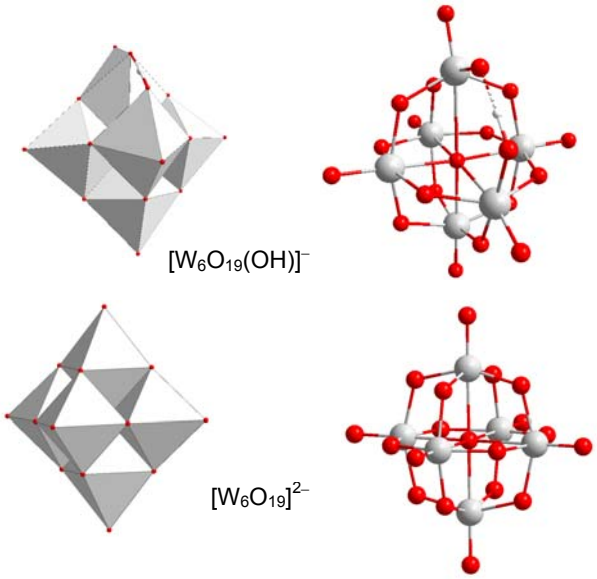

Figure 3.23. Polyhedral (left) and "ball and stick" (right) representations for the optimized structures for the stoichiometry $[W_6O_{19}(OH)]^-$ and the Lindqvist anion $[W_6O_{19}]^{2-}$.

3.3.7. Discussion About the Proposed Mechanisms

The mechanisms M1 and M2 are listed in tables 3.11 and 3.12, respectively. A search for the lowest-energy structure was performed for each proposed stoichiometry as previously described. The reaction energies (ΔE) for each step of the two mechanisms are computed using the most stable structure for each stoichiometry. For the $[W_3O_{10}]^{2-}$ stoichiometry, we have considered the energy of the compact structure.

After describing the most stable structures for the different stoichiometries, we now discuss the proposed mechanisms M1 an M2. As shown in equation (5) the formation of the Lindqvist anion from six $[WO_3(OH)]^-$ monomers requires four protonation steps and the condensation of five water molecules.

UNIVERSITAT ROVIRA I VIRGILI
ASSEMBLY AND PROPERTIES OF POLYOXOMETALATES: A THEORETICAL POINT OF VIEW
Laia Vilà Nadal
ISBN.978-84-694-2170-3/DL:T. 1039-2011

The dinuclear species predicted to be formed with stoichiometry $[W_2O_6(OH)_2]^{2-}$ should undergo protonation followed by a dehydration to $[W_2O_6(OH)]^-$ (in mechanism 1, step 2). This initial step is predicted to be somewhat exothermic. In the case of mechanism 2, the dinuclear species with $[W_2O_6(OH)_2]^{2-}$ stoichiometry that is predicted to be formed in the first step of aggregation should undergo dehydration to $[W_2O_7]^{2-}$ (M2, step 2).

Table 3.11. Proposed mechanism M1 for the formation of the Lindqvist anion, $[W_6O_{19}]^{2-}$. The species detected in ESI-MS experiments are highlighted in bold. Reaction energies, ΔE, in kcal mol^{-1}.

Mechanism 1		**ΔE**
1.1	$\mathbf{[WO_3(OH)]^-_{(aq)}} + [WO_3(OH)]^-_{(aq)} \rightarrow [W_2O_6(OH)_2]^{2-}_{(aq)}$	–7.4
1.2	$[W_2O_6(OH)_2]^{2-}_{(aq)} + H_3O^+_{(aq)} \rightarrow \mathbf{[W_2O_6(OH)]^-_{(aq)}} + 2H_2O_{(aq)}$	–14.4
1.3	$[W_2O_6(OH)]^-_{(aq)} + [WO_3(OH)]^-_{(aq)} \rightarrow [W_3O_9(OH)_2]^{2-}_{(aq)}$	–8.7
1.4	$[W_3O_9(OH)_2]^{2-}_{(aq)} + H_3O^+_{(aq)} \rightarrow \mathbf{[W_3O_9(OH)]^-_{(aq)}} + 2H_2O_{(aq)}$	+3.0
1.5	$[W_3O_9(OH)]^-_{(aq)} + [WO_3(OH)]^-_{(aq)} \rightarrow [W_4O_{12}(OH)_2]^{2-}_{(aq)}$	–18.8
1.6	$[W_4O_{12}(OH)_2]^{2-}_{(aq)} + H_3O^+_{(aq)} \rightarrow \mathbf{[W_4O_{12}(OH)]^-_{(aq)}} + 2H_2O_{(aq)}$	–17.2
1.7	$[W_4O_{12}(OH)]^-_{(aq)} + [WO_3(OH)]^-_{(aq)} \rightarrow [W_5O_{15}(OH)_2]^{2-}_{(aq)}$	+11.4
1.8	$[W_5O_{15}(OH)_2]^{2-}_{(aq)} + H_3O^+_{(aq)} \rightarrow [W_5O_{15}(OH)]^-_{(aq)} + 2H_2O_{(aq)}$	+2.8
1.9	$[W_5O_{15}(OH)]^-_{(aq)} + [WO_3(OH)]^-_{(aq)} \rightarrow [W_6O_{18}(OH)_2]^{2-}_{(aq)}$	–31.9
1.10	$[W_6O_{18}(OH)_2]^{2-}_{(aq)} \rightarrow \mathbf{[W_6O_{19}]^{2-}_{(aq)}} + H_2O_{(aq)}$	–15.7

In this case the process is slightly endothermic. Following the condensation step, an aggregation of $[WO_3(OH)]^-$ leads to the formation of the trimer. At our computational level, the formation of these species is somewhat exothermic within the two mechanisms M1 and M2.

The lowest-energy compact structures for tri-, tetra-, penta- and hexanuclear species with the same stoichiometries as those observed in the ESI-MS experiments are illustrated in Figure 3.24. The structures corresponding to stoichiometries derived

UNIVERSITAT ROVIRA I VIRGILI
ASSEMBLY AND PROPERTIES OF POLYOXOMETALATES: A THEORETICAL POINT OF VIEW
Laia Vilà Nadal
ISBN.978-84-694-2170-3/DL:T. 1039-2011

from mechanism M2 are almost identical to the ones shown in Fig. 3.15 with an extra H atom. This H atom can be attached in many different positions, the most stable being the corresponding to the most basic O atom. Since an analysis of the basicity of the different O atoms for all of these intermediate structures is out of the scope of the present work, this question will not be discussed here.

Table 3.12. Proposed mechanism M2 for the formation of the Lindqvist anion, $[W_6O_{19}]^{2-}$. The species detected in ESI-MS experiments are highlighted in bold. Reaction energies in kcal mol^{-1}.

Mechanism 2		**ΔE**
2.1	$\mathbf{[WO_3(OH)]^-}_{(aq)} + [WO_3(OH)]^-_{(aq)} \rightarrow [W_2O_6(OH)_2]^{2-}_{(aq)}$	–7.4
2.2	$[W_2O_6(OH)_2]^{2-}_{(aq)} \rightarrow \mathbf{[W_2O_7]^{2-}}_{(aq)} + H_2O_{(aq)}$	+5.1
2.3	$[W_2O_7]^{2-}_{(aq)} + [WO_3(OH)]^-_{(aq)} \rightarrow [W_3O_{10}(OH)]^{3-}_{(aq)}$	–5.8
2.4	$[W_3O_{10}(OH)]^{3-}_{(aq)} + H_3O^+_{(aq)} \rightarrow \mathbf{[W_3O_{10}]^{2-}}_{(aq)} + 2H_2O_{(aq)}$	+2.0
2.5	$[W_3O_{10}]^{2-}_{(aq)} + [WO_3(OH)]^-_{(aq)} \rightarrow [W_4O_{13}(OH)]^{3-}_{(aq)}$	–18.5
2.6	$[W_4O_{13}(OH)]^{3-}_{(aq)} + H_3O^+_{(aq)} \rightarrow \mathbf{[W_4O_{13}]^{2-}}_{(aq)} + 2H_2O_{(aq)}$	–14.9
2.7	$[W_4O_{13}]^{2-}_{(aq)} + [WO_3(OH)]^-_{(aq)} \rightarrow [W_5O_{16}(OH)]^{3-}_{(aq)}$	–2.5
2.8	$[W_5O_{16}(OH)]^{3-}_{(aq)} + H_3O^+_{(aq)} \rightarrow \mathbf{[W_5O_{16}]^{2-}}_{(aq)} + 2H_2O_{(aq)}$	+3.8
2.9	$[W_5O_{16}]^{2-}_{(aq)} + [WO_3(OH)]^-_{(aq)} \rightarrow [W_6O_{19}(OH)]^{3-}_{(aq)}$	–24.2
2.10	$[W_6O_{19}(OH)]^{3-}_{(aq)} + H_3O^+_{(aq)} \rightarrow \mathbf{[W_6O_{19}]^{2-}}_{(aq)} + 2H_2O_{(aq)}$	–34.7

For $[W_4O_{13}]^{2-}$, a compact structure with a μ_3-O atom, which could also be considered as μ_4-O because the distance between the central O atom and the fourth W atom is less than 3Å, is found to have the lowest energy among the structures that we have examined, as discussed previously. This structure already contains one of the two W_4O_4 rings of the Lindqvist anion. The formation of tetranuclear species is moderately exothermic whereas the formation of pentanuclear structures is predicted to be endothermic, especially through mechanism M1. Indeed, none of the pentanuclear species proposed in M1 are observed in the ESI-MS experiments.

UNIVERSITAT ROVIRA I VIRGILI
ASSEMBLY AND PROPERTIES OF POLYOXOMETALATES: A THEORETICAL POINT OF VIEW
Laia Vilà Nadal
ISBN.978-84-694-2170-3/DL:T. 1039-2011

For the only pentanuclear cluster observed, $[W_5O_{16}]^{2-}$, two structures with similar energy were found. Structure 1 (Fig. 3.24) features two μ_3-O atoms, each of them within a planar W_3 unit as in the tetranuclear cluster. These planar trinuclear motifs, also present in the Lindqvist anion and in the tetranuclear form, seems to confer stability to the cluster. Structure 2, which is only 3 kcal mol^{-1} more unstable than structure 1 and with a μ_5-O atom, shows a framework that fairly resembles that of the Lindqvist anion (see Fig. 3.24). Although structure 1 is slightly more stable than structure 2 the topology of the latter seems more favourable to lead to the hexametalate. The formation of the hexanuclear species are the most exothermic steps of those proposed, especially for mechanism M2.

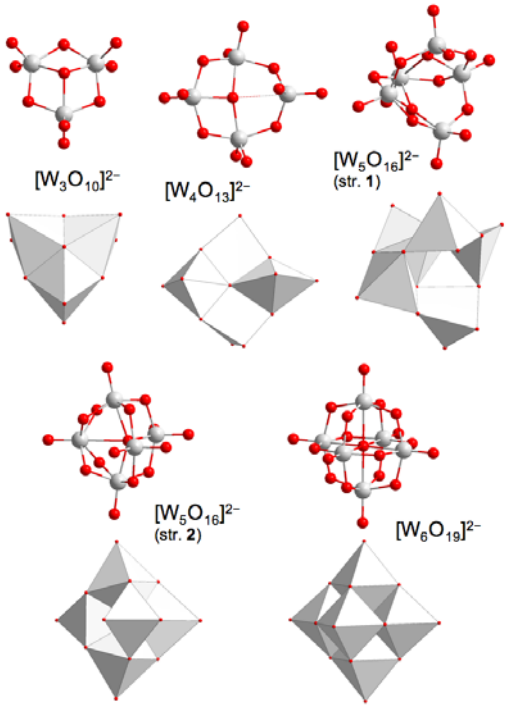

Figure 3.24. Polyhedral and "ball and stick" representations of the most-stable compact structures found at BP86/COSMO level for the stoichiometries observed in ESI-MS experiments.

UNIVERSITAT ROVIRA I VIRGILI
ASSEMBLY AND PROPERTIES OF POLYOXOMETALATES: A THEORETICAL POINT OF VIEW
Laia Vilà Nadal
ISBN.978-84-694-2170-3/DL:T. 1039-2011

3.4. Conclusions

In summary, the combined use of ESI-MS fragmentation experiments and complementary DFT calculations provide a deeper insight about the formation mechanisms of POMs with low nuclearities, in particular for the Lindqvist anion, $[W_6O_{19}]^{2-}$. The first step, i.e. the formation of dinuclear species, is shown to be attainable at ambient temperature for medium and low pH conditions.

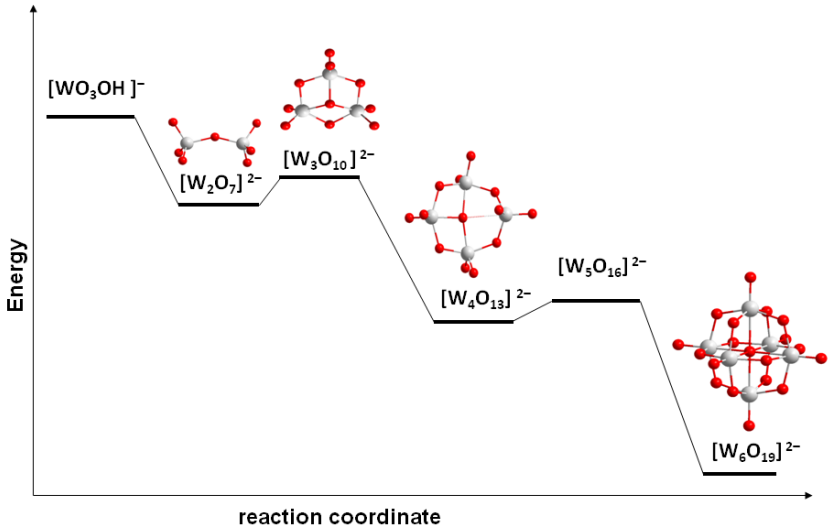

Figure 3.25. Schematic representation of the energetic profile for mechanism M2 based on successive aggregation steps of hydrogentungstate anion as the "building block", followed by protonation and water condensation.

The dinuclear structure proposed by Kepert is not found to be stable. Other structures in which the W atoms are four- or five-fold coordinated are predicted to be the most stable by DFT methods. Once the dinuclear species have been formed, successive steps of protonation and water condensation followed by aggregation are postulated (mechanisms M1 and M2) to justify the clusters detected in the ESI-MS experiments. An

energetic cascade profile is predicted for both mechanisms, represented in Figure 3.25, with the last steps being the most exothermic. So, the Lindqvist anion is formed by consecutive steps that incorporate one metal unit at each time. For the most-stable tetra- and pentanuclear intermediate clusters, planar W_3 building blocks that confer them high stability can be identified. The complementarity between theory and experiment provides important clues about the formation steps of the Lindqvist anion.

UNIVERSITAT ROVIRA I VIRGILI
ASSEMBLY AND PROPERTIES OF POLYOXOMETALATES: A THEORETICAL POINT OF VIEW
Laia Vilà Nadal
ISBN.978-84-694-2170-3/DL:T. 1039-2011

References and Notes

[1] D.L. Long, E. Burkholder, L. Cronin, *Chem. Soc. Rev.* **2007**, 36, 105.

[2] M.T. Pope, *in Heteropoly and Isopoly Oxometalates*. Springer-Verlag: Berlin, **1983**.

[3] J.J. Cruywagen, J. B. B. Heyns, *Polyhedron* **2000,** 19, 907

[4] D. L. Long, C. Streb, Y. F. Song, S. Mitchell, L. Cronin, *J. Am. Chem. Soc.* **2008,** 130, 1830.

[5] I. Andersson, A. Gorzsas, C. Kerezsi, I. Toth, L. Pettersson, *Dalton Trans.* **2005**, 3658.

[6] A. G. Baro, I. Andersson, L. Pettersson, A. Gorzsas, *Dalton Trans.* **2008**, 1095.

[7] Pettersson, L.; Andersson, I.; Gorzsas, A. *Coord. Chem. Rev.* **2003,** 237, 77.

[8] S. Messaoudi, E. Furet, R. Gautier, E. Le Fur, J. Y. Pivan, *Phys. Chem. Chem. Phys.* **2004,** 6, 2083.

[9] A. Sadoc, S. Messaoudi, E. Furet, R. Gautier, E. Le Fur, L. Le Polles, J. Y. Pivan, *Inorg. Chem.* **2007,** 46, 4835.

[10] M. Buhl, M. Parrinello, *Chem. Eur. J.* **2001,** 7, 4487.

[11] A. Rodríguez-Fortea, L. Vilà-Nadal, J.M. Poblet, *Inorg. Chem.*, 2008, 17, 7745.

[12] In all of the metadynamics runs that we have performed we have chosen as collective variable (CV) the distance between the W(VI) ion and the O atom of a nearby water molecule. The cell box that contains one $[WO_3(OH)]^-$ or $[WO_2(OH)_2]$ or $[WO_2(OH)(H_2O)]^+$ and 29 H_2O molecules (a = b = c = 9.959 Å) is repeated periodically in space by the standard periodic boundary conditions. We have done one simulation for each of the following processes:

(i) $[WO_3(OH)]^- + H_2O \rightarrow [WO_3(OH)(H_2O)]^-$

The parameters used in this run are: k = 0.2 a.u., M = 10 a.m.u. The height of the hills (W) is 0.31 kcal mol^{-1}, their perpendicular width ($\Delta s^{\perp}$) 0.1, and the deposition rate (Δt) 0.0144 ps. The estimated error (ε) in the computation of the free-energy is 1 kcal mol^{-1}. The total simulation time (t_{total}) was 9 ps.

(ii) $[WO_3(OH)(H_2O)]^- \rightarrow [WO_3(OH)]^- + H_2O$

k = 0.2 a.u., M = 10 a.m.u., W = 0.19 kcal mol^{-1}, $\Delta s^{\perp}$ = 0.1 a.u., Δt = 0.0144 ps, ε= 1 kcal mol^{-1}, t_{total} = 19 ps.

(iii) $[WO_3(OH)(H_2O)]^- + H_2O \rightarrow [WO_3(OH)(H_2O)_2]^-$

Same parameters as for (i), except t_{total} = 11.5 ps.

(iv) $[WO_3(OH)(H_2O)_2]^- \rightarrow [WO_3(OH)(H_2O)]^- + H_2O$

Same parameters as for (ii), except t_{total} = 5 ps.

[13] Different metadynamics runs were performed with the same CV as in the previous simulations. One for each of the following processes:

(i) $[WO_2(OH)_2] + H_2O \rightarrow [WO_2(OH)_2(H_2O)]$

Same parameters as for the previous metadynamics, except W = 0.19 kcal mol^{-1} and t_{total} = 25 ps.

(ii) $[WO_2(OH)_2(H_2O)] \rightarrow [WO_2(OH)_2] + H_2O$

Same parameters as for (i), except t_{total} = 17 ps.

(iii) $[WO_2(OH)_2(H_2O)] + H_2O \rightarrow [WO_2(OH)_2(H_2O)_2]$

Same parameters as for (i), except t_{total} = 9 ps.

(iv) $[WO_2(OH)_2(H_2O)_2] \rightarrow [WO_2(OH)_2(H_2O)] + H_2O$

Same parameters as for (i), except W = 0.25 kcal mol^{-1} and t_{total} = 6 ps.

[14] Same parameters as for the previous metadynamics, except W = 0.19 kcal mol^{-1} and ttotal = 5 ps

[15] M. Buhl, M. Parrinello, *Chem. Eur. J.*, **2001**, 7, 4487.

[16] a) J.M. Poblet, X. López, C. Bo, *Chem. Soc. Rev.*, **2003**, 32, 297; b) X. López, J.M. Maestre, C. Bo, J.M. Poblet, *J. Am. Chem. Soc.*, **2001**, 123, 9571; c) X. López, J.A. Fernández, S. Romo, J.F. Paul, L. Kazansky, J.M. Poblet, *J. Com. Chem.,* **2004**, 25, 1542

[17] R.J. Errington, M.D. Kerlogue, D.G. Richards, *J. Chem. Soc. Chem. Comun.*, **1993**, 649.

[18] (a) D.L. Long, P. Kögerler, L.J. Farrugia, L. Cronin, *Angew. Chem.,Int. Ed.*, **2003**, 42, 4180. (b) L. Cronin, C. Beugholt, E. Krickemeyer, M. Schmidtmann, H. Bögge, P. Kögerler, T.K.K. Luong, A. Müller, *Angew. Chem., Int. Ed.*, **2002**, 41, 2805. (c) K. Wassermann, M.H. Dickman, M.T. Pope, *Angew. Chem., Int. Ed. Engl.*, **1997**, 36, 1445.

[19] D.L. Kepert, *Inorg. Chem.*, **1969,** 7, 1556.

[20] K.H. Tytko, O. Glemser, *Adv. Inorg. Chem. Radiochem.*, **1976**, 19, 239.

[21] J.A. Fernández, X. López, J.M. Poblet, *J. Mol. Cat. A:Chem.* **2007**, 262, 236.

[22] L. Vilà-Nadal, A. Rodríguez-Fortea, L.K. Yan, E.F. Wilson, L. Cronin, J.M. Poblet, *Angew. Chem. Int. Ed.*, **2009**, 48, 5452.

[23] a) M. Iannuzzi, A. Laio, M. Parrinello, *Phys. Rev. Lett.* **2003,** 90, 238302. b) A. Laio, M. Parrinello, *Proc. Natl. Acad. Sci. U.S.A.* **2002,** 99, 12562. c) A. Laio, A. Rodriguez-Fortea, F. Gervasio, M. Ceccarelli, M. Parrinello, *J. Phys. Chem. B* **2005,** 109, 6714.

[24] In the following, the parameters for the different metadynamics (MTD) runs performed through this work are presented:

1) To describe the formation of dinuclear species, $[W_2O_6(OH)_2]^{2-}$, in solution we have used three CV: the CN of each W atom with respect to the eight O atoms that belong to WO_4 groups, $C_{W1\text{-}O}$ and $C_{W2\text{-}O}$, and a conditioned CN, $cC_{W\text{-}O\text{-}H}$, that counts the number of H atoms bonded to those O atoms bonded to W (MTD1). The parameters used in this run are: $k_1 = k_2 = k_3 = 1.0$ a.u., $M_1 = M_2 = M_3 = 100$ a.m.u. The height of the hills (W) is 1.00 kcal·mol^{-1}, their perpendicular width ($\Delta s^{\perp}$)

UNIVERSITAT ROVIRA I VIRGILI
ASSEMBLY AND PROPERTIES OF POLYOXOMETALATES: A THEORETICAL POINT OF VIEW
Laia Vilà Nadal
ISBN.978-84-694-2170-3/DL:T. 1039-2011

0.06, and the deposition rate (Δt) 0.0144 ps. The estimated error (ε) in the computation of the free-energy is 3 kcal·mol^{-1}. The total simulation time (t_{total}) was 11 ps.

2) We have also performed additional metadynamics runs using other sets of CV. Considering a set of two CV, the CN of each W atom with respect to all the O atoms, we treat on an equal footing O atoms from WO_4 groups and from H_2O molecules. The parameters corresponding to this run (MTD2) are: $k_1 = k_2 = 1.0$ a.u., $M_1 = M_2 = 15$ a.m.u., W = 1.26 kcal·mol^{-1}, $\Delta s^{\perp} = 0.06$, and $\Delta t = 0.0101$ ps. The total simulation time (t_{total}) was 10 ps. In good agreement with previous results, dimerization is more probable than hydration for $[WO_3(OH)]^-$ monomers. When a third CV, the $cC_{W\text{-}O\text{-}H}$, is added the main features of the previous metadynamics runs are retrieved.

3) To describe the formation of dinuclear species, $[W_2O_7(OH)]^{3-}$, in solution we have used two CV: the CN of each W atom with respect to the eight O atoms that belong to WO_4 groups, $C_{W1\text{-}O}$ and $C_{W2\text{-}O}$ (MTD3-1). The parameters used in this run are: $k_1 = k_2 = 1.0$ a.u., $M_1 = M_2 = 15$ a.m.u., W = 0.75 kcal·mol^{-1}, $\Delta s^{\perp} = 0.05$, $\Delta t = 0.0115$ ps, $\varepsilon = 1$ kcal·mol^{-1}, $t_{total} = 3.5$ ps. Since the $[W_2O_7(OH)]^{3-}$ dimer has been formed in a standard Car–Parrinello MD, we have performed another MTD run (MTD3-2) to avaluate the formation barrier from the $[WO_3(OH)]^-$ and $[WO_4]^{2-}$ monomers. The parameters used in this run are: $k_1 = k_2 = 1.0$ a.u., $M_1 = M_2 = 15$ a.m.u., W = 0.31 kcal·mol^{-1}, $\Delta s^{\perp} = 0.03$, $\Delta t = 0.0072$ ps, $\varepsilon = 1$ kcal·mol^{-1}, $t_{total} = 1$ ps.

4) We have done a metadynamics run (MTD4) with a set of three CV: the two CN $C_{W1\text{-}O}$ and $C_{W2\text{-}O}$, where O are all the oxygen atoms, and the conditioned CN $cC_{W\text{-}O\text{-}H}$ to account for the level of protonation of O atoms attached to W. The parameters used in this run are: $k_1 = k_2 = 1.5$ a.u., $M_1 = M_2 = 20$ a.m.u., W = 0.94 kcal·mol^{-1}, $\Delta s^{\perp} = 0.08$, $\Delta t = 0.0130$ ps, $\varepsilon = 2$ kcal·mol^{-1}, $t_{total} = 15$ ps.

To conclude this section of the SI, we describe the strategy followed in the search of the lowest-energy structure for each of the stoichiometries proposed in mechanisms M1 and M2. First, we have performed a metadynamics run in the gas phase in order to explore the configurational space for each of the stoichiometries. In these MTD runs, we have used CNs $C_{Wi\text{-}O}$ as CVs. So as to explore the most interesting regions of the configurational space, i.e. the more compact structures, constraining potentials on the CVs have been introduced. Afterwards, the most characteristic structures observed during the MTD are optimized at BP86/COSMO(SAS) level and finally a single-point calculation using the SES is performed.

[25] A. Rodríguez-Fortea, L. Vilà-Nadal, J. M. Poblet, *Inorg. Chem.* **2008**, 47, 7745.

[26] X. Biarnes, A. Ardèvol, A. Planas, C. Rovira, A. Laio, M. Parrinello, *J. Am. Chem. Soc.* **2007**, 129, 10686.

[27] J. Blumberger, B. Ensing, M. L. Klein, *Angew. Chem. Int. Ed.* **2006**, 45, 2893.

UNIVERSITAT ROVIRA I VIRGILI
ASSEMBLY AND PROPERTIES OF POLYOXOMETALATES: A THEORETICAL POINT OF VIEW
Laia Vilà Nadal
ISBN.978-84-694-2170-3/DL:T. 1039-2011

[28] B. Ensing, M. De Vivo, Z. W. Liu, P. Moore, M. L. Klein, *Acc. Chem. Res.* **2006**, 39, 73.

[29] B. Ensing, M. L. Klein, *Proc. Natl. Acad. Sci. U.S.A.* **2005**, 102, 6755.

[30] A. Rodríguez-Fortea, M. Iannuzzi, *J. Phys. Chem. C*, **2008**, 112, 19642.

[31] A. Rodríguez-Fortea, M. Iannuzzi, M. Parrinello, *J. Phys. Chem. B* **2006**, 110, 3477.

[32] A. Rodríguez-Fortea, M. Iannuzzi, M. Parrinello, *J. Phys. Chem. C* **2007**, 111, 2251.

[33] A. Stirling, M. Iannuzzi, M. Parrinello, F. Molnar, V. Bernhart, G. A. Luinstra, *Organometallics* **2005**, 24, 2533.

[34] C.C. Pye, T. Ziegler, *Theor. Chem. Acc.*, **1999**, 101, 396.

[35] a) R. Colton, J. C. Traeger, *Inorg. Chim. Acta* **1992**, *2*, 153. b) J. L. Tuoi, E. Muller, *Rapid Commun. Mass Spectrom.* **1994**, *9*, 692. c) T. Lau, J. Wang, R. Guevremont, K. Siu, *J. Chem. Soc. Chem. Commun.* **1995**, *8*, 2. d) M. J. Deery, O. W. Howarth, K. R. Jennings, *J. Chem. Soc. Dalton Trans.* **1997**, *24*, 4783.

[36] a) D. K. Walanda, R. C. Burns, G. A. Lawrance, E. I. von Nagy-Felsobuki, *J. Chem. Soc. Dalton Trans.* **1999**, *3*, 311. b) D. K. Walanda, R. C. Burns, G. A. Lawrance, E. I. von Nagy-Felsobuki, *Inorg. Chem. Commun.* **1999**, *10*, 487. c) D. K. Walanda, R. C. Burns, G. A. Lawrance, E. I. von Nagy-Felsobuki, *J. Cluster Sci.*, **2000**, *1*, 5. d) F. Sahureka, R. C. Burns, E. I. von Nagy-Felsobuki, *J. Am. Soc. Mass Spectrom.* **2001**, *10*, 1136. e) F. Sahureka, R. C. Burns, E. I. von Nagy-Felsobuki, *Inorg. Chem. Comm*, **2002**, 5, 23.

[37] C. Boglio, G. Lenoble, C. Duhayon, B. Hasenknopf, R. Thouvenot, C. Zhang, R. C. Howell, B. P. Burton-Pye, L. C. Francesconi, E. Lacote,S. Thorimbert, M. Malacria, C. Afonso, J. C. Tabet, *Inorg. Chem.* **2006**, *3*, 1389.

[38] J. Schemberg, K. Schneider, U. Demmer, E. Warkentin, A. Müller, U. Ermler, *Angew. Chem. Int. Ed.* **2007**, 46, 2408.

[39] M. T. Pope, A. Muller, *Angew. Chem. Int. Ed. Engl.* **1991**, *30*, 34.

UNIVERSITAT ROVIRA I VIRGILI
ASSEMBLY AND PROPERTIES OF POLYOXOMETALATES: A THEORETICAL POINT OF VIEW
Laia Vilà Nadal
ISBN.978-84-694-2170-3/DL:T. 1039-2011

Chapter 4

Formation Mechanisms of Polyoxomolybdates with Low Nuclearities

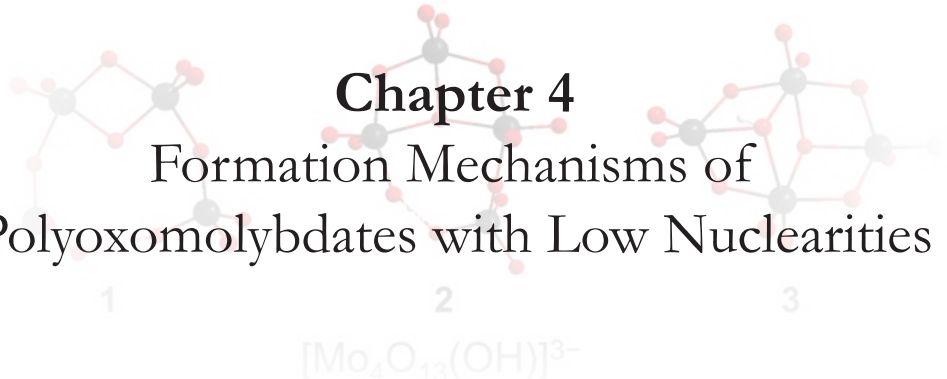

UNIVERSITAT ROVIRA I VIRGILI
ASSEMBLY AND PROPERTIES OF POLYOXOMETALATES: A THEORETICAL POINT OF VIEW
Laia Vilà Nadal
ISBN.978-84-694-2170-3/DL:T. 1039-2011

"Natural science does not simply describe and explain Nature, it is part of the nature and ourselves; it describes nature as exposed to our method of questioning."

W. Heisenberg,
Physics and Philosophy, 1959.

UNIVERSITAT ROVIRA I VIRGILI
ASSEMBLY AND PROPERTIES OF POLYOXOMETALATES: A THEORETICAL POINT OF VIEW
Laia Vilà Nadal
ISBN.978-84-694-2170-3/DL:T. 1039-2011

Chapter 4

Formation Mechanisms of Polyoxomolybdates with Low Nuclearities

In Chapter 3 we have proposed mechanisms for the nucleation of the Lindqvist anion $[W_6O_{19}]^{2-}$. Theoretical predictions combined with electrospray ionization mass spectrometry (ESI-MS) experiments have revealed to be a powerful tool to understand such nucleation process. The present Chapter, among other points, is devoted to the formation mechanisms of $[Mo_6O_{19}]^{2-}$ as a continuation of previous works devised to shed light on the formation of iso- and heteroPOMs with low nuclearities. Here we have also performed ESI-MS experiments on the cluster in combination with an exhaustive theoretical screening of intermediates. After a short introduction, the Chapter evolves towards the understanding of the hydratation-dehydratation equilibria of molybdenum monomeric structures $[MoO_3(OH)]^-$, $[MoO_2(OH)_2]$ and the formation of dinuclear clusters, i. e. $[Mo_2O_6(OH)_2]^{2-}$, $[Mo_2O_7]^{2-}$. This has been done by means of Car–Parrinello molecular dynamics. Then after presenting the ESI-MS results we discuss the following steps in the mechanism from trinuclear species to the Lindqvist anion. The Chapter finishes with the most general conclusions for the formation of $[Mo_6O_{19}]^{2-}$.

4.1. Introduction

As we have said in the previous lines, the present chapter covers the formation mechanisms of $[Mo_6O_{19}]^{2-}$. To achieve this goal, as the case of $[W_6O_{19}]^{2-}$, we have performed ESI-MS experiments on $((C_4H_9)_4N)_2Mo_6O_{19}$[1] combined with complementary computational techniques that deal with the solvent effects in different manner. The Lindqvist structure, which is the IPA with the lowest nuclearity, consists of a compact assemblage of edge sharing octahedra, leading to an overall octahedral cluster with full O_h symmetry. Molybdenum and tungsten behave similarly in *nature*. In the environment, Mo and W are mainly present in their anionic forms, molybdate (MoO_4^{2-}) and tungstate (WO_4^{2-}), and their protonated and polymerised species. Both elements belong to the same group of the periodic table so similar reactivity is expected. Actually when trioxides of molybdenum and tungsten are dissolved in aqueous alkali, the resulting solutions contain tetrahedral MO_4^{2-} ions and simple molybdates and tungstates can be crystallized from them. If these solutions are made strongly acid, precipitates of yellow ($MoO_3 \cdot 2H_2O$) or white color ($WO_3 \cdot 2H_2O$) are obtained. At pHs between these extremes polymerisation occurs and polyoxometalates can be obtained.[2] It is readily apparent the great number of characterized species, with different nuclearities, involved in these equilibria. The main limitation in the development of a universal polyoxometalate "lego" kit lies with the great sensitivity between synthetic conditions (pH, solvent, temperature, countercations) and the overall cluster architecture formed.[3] We herein analyze the formation-fragmentation mechanisms of the Lindqvist anion, $[Mo_6O_{19}]^{2-}$, focusing on the structures of the possible intermediate species. Before doing so, a study of the hydration of the monomeric building blocks $[MoO_3(OH)]^-$ at different pH conditions is also presented. Mononuclear six-coordinated molybdenum species such as

UNIVERSITAT ROVIRA I VIRGILI
ASSEMBLY AND PROPERTIES OF POLYOXOMETALATES: A THEORETICAL POINT OF VIEW
Laia Vilà Nadal
ISBN.978-84-694-2170-3/DL:T. 1039-2011

$[MoO_3(H_2O)_3]$ or $[MoO_2(OH)(H_2O)_3]^+$ have been detected at molybdate concentrations lower than 10^{-4} M and low pH values.[4] Such an expansion of the coordination sphere of Mo upon protonation was proposed to be at the origin of the low $pK_{a,2}$ value of $[MoO_4]^{2-}$. The present analysis will show how the coordination number of the Mo atoms changes at different pH conditions.

4.2. Hydration of $[MoO_3(OH)]^-$ and $[MoO_2(OH)_2]$

We have studied the hydration-dihydration equilibria of hydrogenmolybdate anion, $[MoO_3(OH)]^-$, and molybdic acid, $[MoO_2(OH)_2]$, including explicit solvent (water) molecules using Car-Parrinello MD and metadynamics simulations.[5] First of all, the stability of $[MoO_3(OH)]^-$ and the corresponding mono-, $[MoO_3(OH)(H_2O)]^-$, and di-hydrated species, $[MoO_3(OH)(H_2O)_2]^-$, is analyzed. The non-hydrated tetrahedral anion is seen to be stable during the simulations in good agreement with experiments. However, the five-coordinated mono-hydrated and the six-coordinated di-hydrated species are not found to be stable, i.e. the water molecules that were initially bound to the Mo^{VI} ion are rapidly released during standard Car-Parrinello MD simulations, specially the five-coordinated species, which lasts for less than 1 ps. So, the hydrogenmolybdate anion keeps the tetrahedral coordination most of the time.

The effect of the acidification of the solution on the hydration equilibria is also considered. To do so, we have analyzed the free-energy changes for the following equilibrium reactions (eqs 4.1 and 4.2),

$$\left[MoO_2\left(OH\right)_2\right] + H_2O \rightleftharpoons \left[MoO_2(OH)_2\left(H_2O\right)\right] \qquad (4.1)$$

UNIVERSITAT ROVIRA I VIRGILI
ASSEMBLY AND PROPERTIES OF POLYOXOMETALATES: A THEORETICAL POINT OF VIEW
Laia Vilà Nadal
ISBN.978-84-694-2170-3/DL:T. 1039-2011

$$\left[MoO_2(OH)_2(H_2O)\right] + H_2O \rightleftharpoons \left[MoO_2(OH)_2(H_2O)_2\right] \quad (4.2)$$

Molybdic acid is the predominant species when the pH of the solution is somewhat lower than $pK_{a,1}$. The computed free-energy profile, depicted in Figure 4.1, is obtained averaging the results of several metadynamics simulations (see Annex A). The compound with the six-coordinated Mo^{VI} ion shows the lowest free energy, 9 and 6 kcal mol^{-1} lower than for the five- and four-coordinated species, respectively, in contrast with the results observed at higher pH conditions with the hydrogenmolybdate anion.

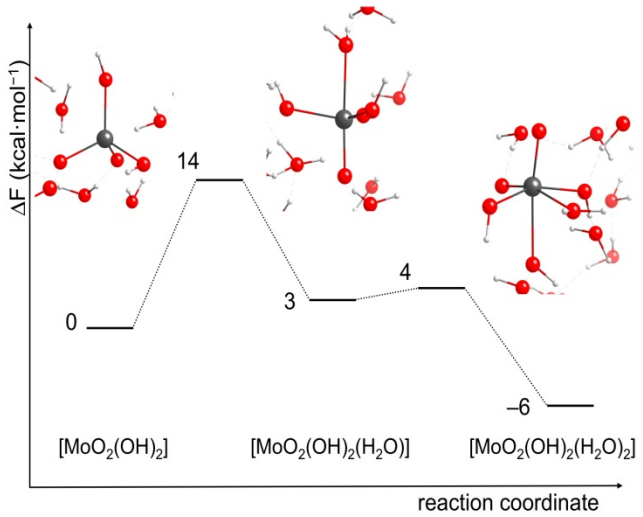

Figure 4.1. Free-energy profile (in kcal·mol^{-1}) corresponding to the hydration-dehydration equilibria of molybdic acid along with the ball-and-stick representation of the four-, $[MoO_2(OH)_2]$, five-, $[MoO_2(OH)_2(H_2O)]$, and six-coordinated, $[MoO_2(OH)_2(H_2O)_2]$, species.

Although the free-energy barrier for the formation of the six-coordinated species from the five-coordinated one is very small (1 kcal mol^{-1}), the barrier for the formation of the latter is far from being negligible. However, we have to consider these 14 kcal mol^{-1} as an upper limit for the barrier because during the

UNIVERSITAT ROVIRA I VIRGILI
ASSEMBLY AND PROPERTIES OF POLYOXOMETALATES: A THEORETICAL POINT OF VIEW
Laia Vilà Nadal
ISBN.978-84-694-2170-3/DL:T. 1039-2011

metadynamics simulation corresponding to this process (eq 4.1), deprotonation of the molybdic acid is observed previous to hydration. These results can be easily rationalized from a qualitative point of view: the Mo^{VI} ion is more electrophilic in the molybdic acid than in the hydrogenmolybdate anion and, therefore, it is more easily attacked and stabilized by the nucleophilic water molecules. So, similarly to what is observed for mononuclear tungstate species,[6] a decrease of the pH of the aqueous solution involves an expansion of the coordination sphere of the Mo^{VI} ion, as proposed from the experimental results. We have also examined the stability at low pH conditions ($pH < pK_{a,1}$) of two structural isomers of six-coordinated molybdic acid, $[MoO_2(OH)_2(H_2O)_2]$ and $[MoO_3(H_2O)_3]$. From standard Car-Parrinello MD simulations, we have observed that the two structural isomers are stable during 28 ps, i.e. both of them remain as six-coordinated species (see below and Annex A). The Mo−O radial distribution function for $[MoO_3(H_2O)_3]$ and its integration, which yields the Mo−O coordination number, are displayed in Figure 4.2.

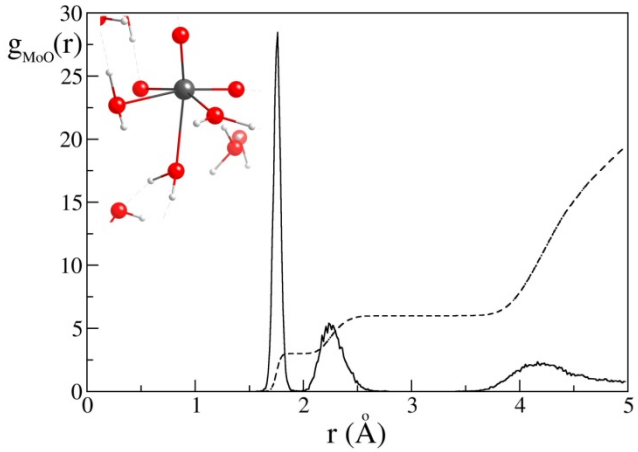

Figure 4.2. Mo−O radial distribution function (solid line) and its integration (broken line) for the 28 ps MD simulation starting from $[MoO_3(H_2O)_3]$. The ball-and-stick representation of the hydrated monomer is shown at the top left corner.

The sharp spike below 2 Å, which integrates three O atoms, is attributed to the oxo ligands. The spike between 2 and 2.6 Å, which integrates three other O atoms, is due to the aqua ligands coordinated to the Mo^{VI} ion. At distances between 2.6 and 3.7 Å, the Mo−O coordination number shows a plateau associated with the presence of six O atoms in the coordination sphere of the Mo^{VI} ion. The shallow maximum that appears at around 4 Å and that does not fall to zero above 4.5 Å is associated to the first solvation shell of $[MoO_3(H_2O)_3]$ and the exchange of water molecules between this shell and the bulk solvent. So, the structural isomers derived from hydrated molybdic acid with Mo^{VI} ions featuring expanded coordination spheres are shown to be stable at low molybdate concentrations and low pH conditions.

4.3. Formation of Dinuclear Clusters

Car-Parrinello MD simulations were also performed to study the first step of the growth mechanism at medium pH conditions, i.e. the formation of dinuclear $[Mo_2O_6(OH)_2]^{2-}$ species from the $[MoO_3(OH)]^-$ building blocks. The metadynamics approach was used to accelerate the dynamics and to compute the free-energy profile. The system was formed by 2 $[MoO_3(OH)]^-$ monomers and 27 H_2O molecules. To describe the formation of dinuclear species several metadynamics runs were done, all of them using as collective variables (CV) the coordination number (CN) of each Mo atom with respect to the eight O atoms from the MoO_4 groups, C_{Mo1-O} and C_{Mo2-O}. Several common events are observed in the different simulations. First, formation of a dinuclear species in which one Mo^{VI} ion is five-coordinated and the other is four-coordinated (a **5c-4c** structure, see Figure 4.3) is observed. After some ps, a recrossing to reactants takes place, i.e. the dimolybdate is broken yielding the two original

UNIVERSITAT ROVIRA I VIRGILI
ASSEMBLY AND PROPERTIES OF POLYOXOMETALATES: A THEORETICAL POINT OF VIEW
Laia Vilà Nadal
ISBN.978-84-694-2170-3/DL:T. 1039-2011

hydrogenmolybdate anions. Afterwards, the **5c-4c** structure is formed and broken again for a while and finally the **5c-5c** structure is obtained (see Figure 4.3). During the simulation H^+-transfers between (i) the monomers; (ii) the solvent molecules; and (iii) the molybdates and the solvent molecules are also frequent. Thus, these events, which have not been accelerated by the metadynamics, must have small free-energy barriers, i.e. they are highly likely. Two other points are also interesting to mention here. The first is that, in contrast to dinuclear tungstates, no expansion of the coordination sphere of the Mo^{VI} ions is observed at this pH due to coordination of the solvent water molecules, in good agreement with the previous results on hydrogenmolybdate anions. The second is that the **6c-4c** structure proposed by Kepert for the first aggregation step was not observed in these simulations. So, this type of dimer, if it exists, must have a higher formation barrier than the **5c-4c** and **5c-5c** structures.

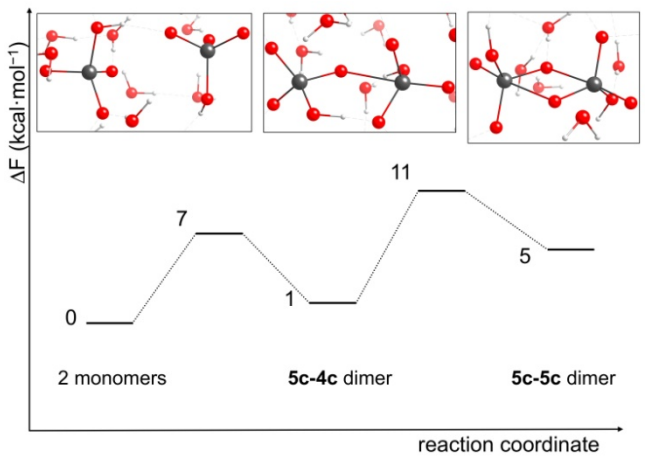

Figure 4.3. Free-energy profile (in kcal·mol^{-1}) corresponding to the formation of dinuclear $[Mo_2O_6(OH)_2]^{2-}$ species along with the ball-and-stick representation of the three observed minima: the 2 monomers, the **5c-4c** dimer and **5c-5c** dimer.

UNIVERSITAT ROVIRA I VIRGILI
ASSEMBLY AND PROPERTIES OF POLYOXOMETALATES: A THEORETICAL POINT OF VIEW
Laia Vilà Nadal
ISBN.978-84-694-2170-3/DL:T. 1039-2011

The free-energy profile (Figure 4.3) shows that formation of the **5c-4c** structure requires surpassing a barrier of only 7 ± 1 kcal mol^{-1}. The barrier for breaking the **5c-4c** dimer is smaller than that for the formation of the **5c-5c** structure (6 vs 10 kcal mol^{-1}). All these barriers are, however, easily overcome at the temperature at which POMs are formed. Regarding to the relative free energies of the minima, the formation of the **5c-5c** structure is clearly endergonic (5 kcal mol^{-1}), whereas the **5c-4c** structure shows a free-energy similar to that of the two monomers (1 kcal mol^{-1}).

Reaction energies for dinuclear species with respect to the two hydrogenmolybdate anions (eq 4.3) using the COSMO methodology to account for the solvation effects are listed in Table 4.1.

$$2\left[MoO_3(OH)\right]^- \rightleftharpoons \left[Mo_2O_6(OH)_2\right]^{2-} \quad (4.3)$$

$$2\left[MoO_3(OH)\right]^- \rightleftharpoons \left[Mo_2O_7\right]^{2-} + H_2O \quad (4.4)$$

The lowest-energy minimum for the $[Mo_2O_6(OH)_2]^{2-}$ stoichiometry corresponds to the **5c-4c** structure, which is at least 7 kcal mol^{-1} more stable than the other **5c-5c** dimers. The formation of these dimers are predicted to be endothermic in all cases. The difference between the two **5c-5c** structures is that in **1** the H atoms are located at the terminal O atoms, whereas in **2** they are located at the bridge O atoms. The lower energy of **1** with respect to **2** indicates that terminal O atoms are more basic than those in bridging positions. This result is similar to that found for ditungstates,[7] but it is in contrast to the behavior observed for large POMs in which the bridging positions are those with the highest basicities.[8] The formation of the dehydrated dimer, $[Mo_2O_7]^{2-}$, with a **4c-4c** structure (see Eq 4.4 and Annex A), is somewhat exothermic (−2.2 kcal mol^{-1}). It is interesting to point out that the **6c-4c** structure proposed by Kepert is not found as a minimum in the potential energy surface

UNIVERSITAT ROVIRA I VIRGILI
ASSEMBLY AND PROPERTIES OF POLYOXOMETALATES: A THEORETICAL POINT OF VIEW
Laia Vilà Nadal
ISBN.978-84-694-2170-3/DL:T. 1039-2011

(PES) of $[Mo_2O_6(OH)_2]^{2-}$. All the geometry optimization attempts starting from a **6c-4c** structure lead to **5c-5c** structures.

Table 4.1. Reaction energies (kcal mol^{-1}) for di- and trinuclear[a)] Mo species with respect to two monomers using the COSMO methodology. The values for M = Cr and W are also provided for comparison.[b)]

Stoichiometry	Structure	Cr	Mo	W
$[M_2O_6(OH)_2]^{2-}$	**5c-4c**	+17.0	+0.4	–7.4
	5c-5c (1)	dissociation	+7.4	+0.2
	5c-5c (2)	dissociation	+11.4	+10.2
$[M_2O_7]^{2-}$	**4c-4c**	–2.7	–2.2	–5.3
$[M_3O_{10}(OH)]^{3-}$	**1**[c)]	+33.4	+7.8	–3.7

a) For $[M_3O_{10}(OH)]^{3-}$, reaction energy with respect to $[M_2O_7]^{2-}$ and $[MO_3(OH)]^-$. b) The values for M = W are from ref. 7. c) See Figure 4.5.

We would also like to mention here the case of chromates. It is experimentally well known that the behavior of Cr is very different from that of W or Mo. Inorganic chemistry textbooks teach that yellow solutions of chromate anions, $[CrO_4]^{2-}$, become orange when the pH of the solution is lowered due to the formation of stable dichromate anions, $Cr_2O_7^{2-}$, according to process (eq. 4.5).[2] In general, no further nucleation is observed at low pH in contrast to the behavior found for tungstates or molybdates.

$$2\left[CrO_4\right]^{2-} + 2H_3O^+ \rightarrow \left[Cr_2O_7\right]^{2-} + 3H_2O \qquad (4.5)$$

The reaction energies for the three structural isomers of $[Cr_2O_6(OH)_2]^{2-}$ and for the lowest-energy structure of $[Cr_3O_{10}(OH)]^{3-}$ are displayed in Table 1. The formation of the dehydrated dichromate anion, $[Cr_2O_7]^{2-}$, is much more favourable (20 kcal mol^{-1}) than the formation of the $[Cr_2O_6(OH)_2]^{2-}$ dimer indicating the preference of Cr(VI) ions

UNIVERSITAT ROVIRA I VIRGILI
ASSEMBLY AND PROPERTIES OF POLYOXOMETALATES: A THEORETICAL POINT OF VIEW
Laia Vilà Nadal
ISBN.978-84-694-2170-3/DL:T. 1039-2011

for tetrahedral coordination. Moreover, only the **5c-4c** structure is stable for $[Cr_2O_6(OH)_2]^{2-}$ stoichiometry whereas the **5c-5c** ones dissociate in their monomers. The formation of the trinuclear species $[Cr_3O_{10}(OH)]^{3-}$, predicted to be an highly endothermic process, can explain the fact that polyoxochromates with higher nuclearities are much less abundant than polyoxotungstates and molybdates.

4.4. From Trinuclear Species to the Lindqvist Anion: Combining Theory and ESI-MS Results

On the basis of consecutive steps of nucleation and water condensation, mechanisms for the formation of the Lindqvist anion, $[Mo_6O_{19}]^{2-}$, consistent with the ESI-MS experiments are put forward (Table 4.2). The peaks observed in the ESI-MS experiments (Annex A and Figure 4.4) are associated with the species $[Mo_2O_7]^{2-}$, $[Mo_3O_{10}]^{2-}$, $[Mo_4O_{13}]^{2-}$, $[Mo_5O_{16}]^{2-}$ and $[Mo_6O_{19}]^{2-}$.

The observed set of peaks belong to the previously observed group of species with the general formula $[Mo_mO_{3m+1}]^{2-}$ and in agreement with the studies of Walanda, von Nagi-Felsobuki *et al.*[9] and Llusar, Vicent et. al.[10] In this case we did not detect any species of the protonated set with the general formula $[HMo_mO_{3m+1}]^{-}$ since their formation depends greatly upon the solvent composition (aqueous and protic acidified media) and application of harsher ionization conditions (high collision energy values).[11,12] Consequently, the use of acetonitrile solution and application of mild ionization condition during the course of our fragmentation experiments led only to the formation of the non-protonated set, $[Mo_mO_{3m+1}]^{2-}$, of species in the gas phase.

UNIVERSITAT ROVIRA I VIRGILI
ASSEMBLY AND PROPERTIES OF POLYOXOMETALATES: A THEORETICAL POINT OF VIEW
Laia Vilà Nadal
ISBN.978-84-694-2170-3/DL:T. 1039-2011

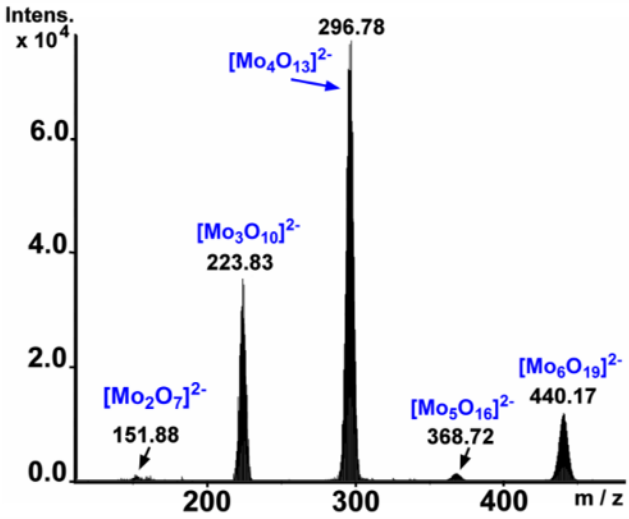

Figure 4.4. Mass spectral data recorded by collision induced dissociation (CID) of the isolated $[Mo_6O_{19}]^{2-}$ peak at m/z 440.17 (see the Annex A for more details). The fragment peaks shown are associated with the species $[Mo_2O_7]^{2-}$ (*m/z* 151.88), $[Mo_3O_{10}]^{2-}$ (*m/z* 223.83), $[Mo_4O_{13}]^{2-}$ (*m/z* 296.78) and $[Mo_5O_{16}]^{2-}$ (*m/z* 368.72).

Table 4.2. Proposed mechanism (M1) for the formation of the Lindqvist anion $[Mo_6O_{19}]^{2-}$.[a)] The species detected in the ESI-MS experiments are highlighted in bold.

1) $[MoO_3(OH)]^-_{(aq)} + [MoO_3(OH)]^-_{(aq)} \rightarrow [Mo_2O_6(OH)_2]^{2-}_{(aq)}$	+0.4
2) $[Mo_2O_6(OH)_2]^{2-}_{(aq)} \rightarrow \mathbf{[Mo_2O_7]^{2-}_{(aq)}} + H_2O_{(aq)}$	−2.7
3) $[Mo_2O_7]^{2-}_{(aq)} + [MoO_3(OH)]^-_{(aq)} \rightarrow [Mo_3O_{10}(OH)]^{3-}_{(aq)}$	+7.8
4) $[Mo_3O_{10}(OH)]^{3-}_{(aq)} + H_3O^+_{(aq)} \rightarrow \mathbf{[Mo_3O_{10}]^{2-}_{(aq)}} + 2\ H_2O_{(aq)}$	−11.0
5) $[Mo_3O_{10}]^{2-}_{(aq)} + [MoO_3(OH)]^-_{(aq)} \rightarrow [Mo_4O_{13}(OH)]^{3-}_{(aq)}$	−10.7
6) $[Mo_4O_{13}(OH)]^{3-}_{(aq)} + H_3O^+_{(aq)} \rightarrow \mathbf{[Mo_4O_{13}]^{2-}_{(aq)}} + 2\ H_2O_{(aq)}$	−20.6
7) $[Mo_4O_{13}]^{2-}_{(aq)} + [MoO_3(OH)]^-_{(aq)} \rightarrow [Mo_5O_{16}(OH)]^{3-}_{(aq)}$	+9.3
8) $[Mo_5O_{16}(OH)]^{3-}_{(aq)} + H_3O^+_{(aq)} \rightarrow \mathbf{[Mo_5O_{16}]^{2-}_{(aq)}} + 2\ H_2O_{(aq)}$	−2.2
9) $[Mo_5O_{16}]^{2-}_{(aq)} + [MoO_3(OH)]^-_{(aq)} \rightarrow [Mo_6O_{19}(OH)]^{3-}_{(aq)}$	−6.2
10) $[Mo_6O_{19}(OH)]^{3-}_{(aq)} + H_3O^+_{(aq)} \rightarrow \mathbf{[Mo_6O_{19}]^{2-}_{(aq)}} + 2\ H_2O_{(aq)}$	−31.8

a) Reaction energies are in kcal mol^{-1}

UNIVERSITAT ROVIRA I VIRGILI
ASSEMBLY AND PROPERTIES OF POLYOXOMETALATES: A THEORETICAL POINT OF VIEW
Laia Vilà Nadal
ISBN.978-84-694-2170-3/DL:T. 1039-2011

Even though the peaks for the $[Mo_nO_{3n}(OH)]^-$ stoichiometries (n = 2 to 6) were not observed in the mass spectra, we have also proposed a mechanism that involves such species in analogy with previous studies in isopolytungstates (see Annex A for the alternative mechanism, M2).[11] For each of the stoichiometries observed in the ESI-MS spectra, a search for the lowest-energy structure in solution was carried out using the COSMO methodology. Geometry optimizations in the gas phase were also done for some clusters.

The dinuclear species with $[Mo_2O_6(OH)_2]^{2-}$ stochiometry, which are formed in the first step of nucleation, should undergo dehydration to $[Mo_2O_7]^{2-}$ to be consistent with the ESI-MS results. Relative energies and geometries for representative structural isomers of $[Mo_3O_{10}]^{2-}$ and $[Mo_3O_{10}(OH)]^{3-}$ are presented in Table 4.3 and Figure 4.5. The structures corresponding to stoichiometries derived from the alternative mechanism, which differ only in one H^+, are very similar to the ones shown here (see Annex A). The lowest-energy structure that we found for the $[Mo_3O_{10}]^{2-}$ stoichiometry, isomer 1, corresponds to an open cluster in which the three Mo^{VI} ions show tetrahedral coordination, i.e. a chain of corner-sharing tetrahedra (Figure 4.5). This type of structures were proposed by Walanda *et al.* as intermediates for an open-chain addition polymerization mechanism that might explain the formation of isopolymolybdates in the charged droplets formed in the ESI-MS experiments.[8] An open-chain cluster with two five- and one four-coordinated Mo^{VI} ions (isomer **2**) and one close-compact structure with a central tri-coordinated O atom, μ_3-O, (isomer **3**) show much larger energies. The trinuclear open-chain isomer **1** is also much more stable than the compact isomer **3** in the gas phase (19 kcal mol^{-1}).

UNIVERSITAT ROVIRA I VIRGILI
ASSEMBLY AND PROPERTIES OF POLYOXOMETALATES: A THEORETICAL POINT OF VIEW
Laia Vilà Nadal
ISBN.978-84-694-2170-3/DL:T. 1039-2011

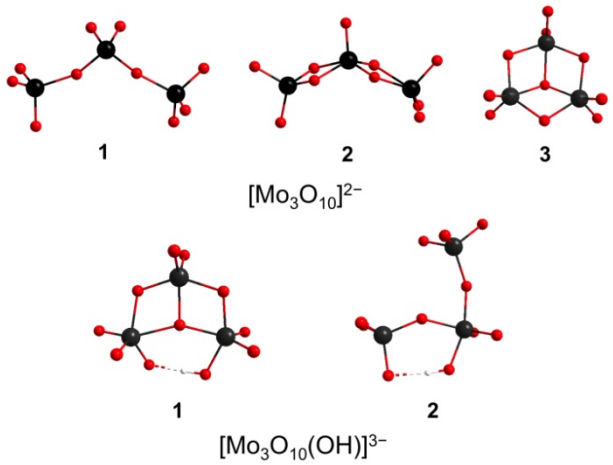

Figure 4.5. Ball-and-stick representations for the optimized structures of the most representative trinuclear species with $[Mo_3O_{10}]^{2-}$ (isomers **1**, **2** and **3**) and $[Mo_3O_{10}(OH)]^{3-}$ (isomers **1** and **2**) stoichiometries.

Table 4.3. Relative energies (ΔE, kcal mol^{-1}) for the optimized structures (COSMO methodology) of some representative $[Mo_xO_y(OH)_z]^{k-}$ tri- (x = 3, y = 10, z = 0 or 1, k = 2 or 1), tetra- (x = 4, y = 13, z = 0 or 1, k = 2 or 1) and pentanuclear (x = 5, y = 16, z = 0 or 1, k = 2 or 1) species.

Stoichiometry	Isomer	O coordination [a)]	ΔE
$[Mo_3O_{10}]^{2-}$	**1**	2	0.0
	2	2	15.4
	3	3	19.4
$[Mo_3O_{10}(OH)]^{3-}$	**1**	3	0.0
	2	2	0.5
$[Mo_4O_{13}]^{2-}$	**1**	3	0.0
	2	4	3.9
$[Mo_4O_{13}(OH)]^{3-}$	**1**	2	0.0
	2	3	1.1
	3	3	5.5
$[Mo_5O_{16}]^{2-}$	**1**	3	0.0
	2	5	1.0
$[Mo_5O_{16}(OH)]^{3-}$	**1**	3	0.0
	2	4	3.4

a) Highest coordination of an O atom within the cluster.

UNIVERSITAT ROVIRA I VIRGILI
ASSEMBLY AND PROPERTIES OF POLYOXOMETALATES: A THEORETICAL POINT OF VIEW
Laia Vilà Nadal
ISBN.978-84-694-2170-3/DL:T. 1039-2011

But, does this open-chain isomer **1** keep in solution the three tetrahedral Mo^{VI} ions without coordination of nucleophilic solvent (water) molecules? So as to answer this question, a 13-ps standard Car-Parrinello MD simulation for the system formed by one open-chain $[Mo_3O_{10}]^{2-}$ cluster and 58 H_2O molecules was performed, even though the high computational resources required. An analysis of the trajectory as well as the Mo−O radial distribution function for each of the Mo^{VI} ions show that some H_2O molecules interact with the Mo^{VI} ions, especially with the central one. In fact, an expansion to octahedral coordination takes place for this central Mo^{VI} ion. The terminal Mo^{VI}, which retain their initial tetrahedral coordination, remain singly bonded to the central octahedron maintaining the original open structure. It is interesting to point out that the central Mo^{VI} ion is predicted to be the most electrophilic among the three metal ions. So, the most electrophilic Mo^{VI} ions from the structures predicted without taking into account explicitly the solvent molecules (COSMO methodology) might expand their coordination sphere due to the water molecules or the nucleophilic solvent. Regarding the $[Mo_3O_{10}(OH)]^{3-}$ stoichiometry, a compact and planar μ_3-O trinuclear cluster show slightly lower energies than the open ones (Table 4.3). This structure was also found to have the lowest energy for the trinuclear $[W_3O_{10}(OH)]^{3-}$ isopolytungstates.[6]

UNIVERSITAT ROVIRA I VIRGILI
ASSEMBLY AND PROPERTIES OF POLYOXOMETALATES: A THEORETICAL POINT OF VIEW
Laia Vilà Nadal
ISBN.978-84-694-2170-3/DL:T. 1039-2011

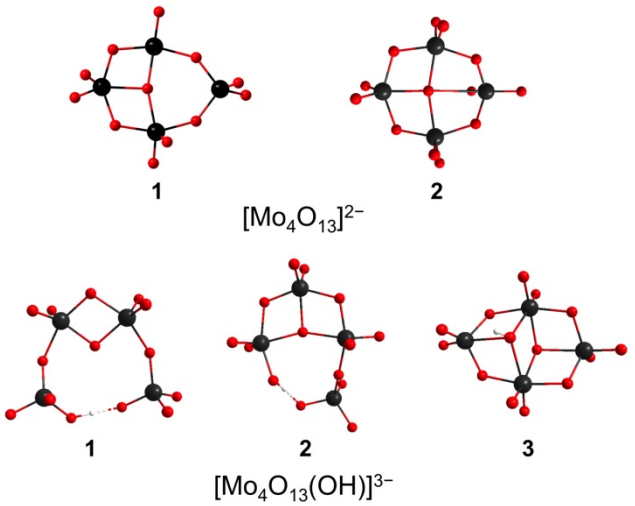

Figure 4.6. Ball-and-stick representations for the optimized structures of the most representative tetranuclear species with $[Mo_4O_{13}]^{2-}$ (isomers **1** and **2**) and $[Mo_4O_{13}(OH)]^{3-}$ (isomers **1**, **2** and **3**) stoichiometries.

The lowest-energy structure that we found for $[Mo_4O_{13}]^{2-}$ stoichiometry, **1**, corresponds to a compact cluster where a trinuclear planar motif with a three-fold coordinated O atom (μ_3-O) can be identified (see Table 4.3 and Figure 4.6). A similar compact structure with a μ_4-O atom, **2**, shows a somewhat higher energy (3.9 kcal mol^{-1}). The open-chain linear cluster with four corner-sharing tetrahedral Mo^{VI} ions (see Annex A) lays only 1.3 kcal mol^{-1} higher in energy than **1** (5.4 kcal mol^{-1} in the gas phase). Although we have not performed Car-Parrinello MD simulations to analyze the behaviour of such species in solution due to their high computational cost, we can state that some of the four Mo^{VI} ions will expand their coordination sphere in solution as observed for the trinuclear linear cluster.

For $[Mo_4O_{13}(OH)]^{3-}$, the lowest-energy structure among those that we have computed, **1**, resembles that of a 5c-5c dimer with two extra corner-shared tetrahedral MoO_4 units (Figure 4.6). A

structure with the abovementioned planar trinuclear motif with an extra corner-shared monomer, **2**, is almost quasidegenerate with **1** (1.1 kcal mol^{-1}). Structure **3**, with two μ_3-O atoms, is more compact and symmetric than the others, but it appears to have a higher energy than them (5 kcal mol^{-1}, Table 4.3).

Regarding the $[Mo_5O_{16}]^{2-}$ stoichiometry, two compact structures are found to have very similar energies (Table 4.3, Figure 4.7). Structure **2**, with a μ_5-O atom, shows a framework that is rather similar to that of the Lindqvist anion. An analogous structure was also proposed for the case of isopolytungstates. Interestingly, the open-chain linear structures with five corner-shared tetrahedra are predicted to have much lower energies than these compact clusters **1** and **2** (around 10 and 30 kcal mol^{-1} in gas-phase and water solution, respectively). Although the COSMO methodology overstabilizes such type of structures with respect to compact clusters (*vide infra*), it is probable that they are more stable than compact structures in solution. If this were the case, some of their Mo^{VI} ions would expand their coordination sphere up to six. However, it is not likely that the formation mechanism of the compact hexanuclear anion would pass through such pentanuclear open-chain linear structures. So, these species might exist in the chamber of the spectrometer when doing the ESI-MS experiments, but they are not probable intermediates in the formation of the Lindqvist anion. The structures with the lowest energies for $[Mo_5O_{16}(OH)]^{3-}$ are depicted in Figure 4.7. Similarly to the previous case, the most compact structure **2** with a μ_4-O atom show a somewhat higher energy than structure **1**, which shows a stabilizing planar trinuclear motif (3.4 kcal mol^{-1}, Table 4.3).

UNIVERSITAT ROVIRA I VIRGILI
ASSEMBLY AND PROPERTIES OF POLYOXOMETALATES: A THEORETICAL POINT OF VIEW
Laia Vilà Nadal
ISBN.978-84-694-2170-3/DL:T. 1039-2011

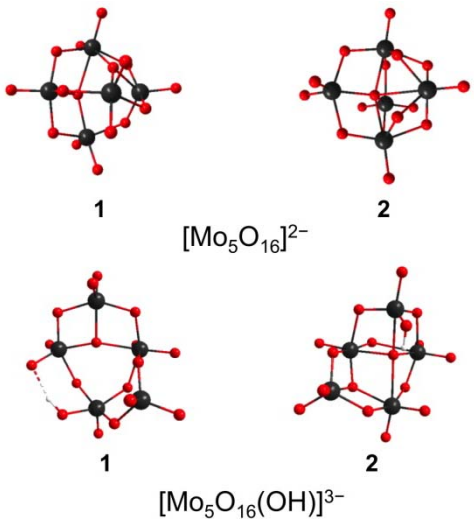

Figure 4.7. Ball-and-stick representations for the optimized structures of the most representative pentanuclear species with $[Mo_5O_{16}]^{2-}$ (isomers **1** and **2**) and $[Mo_5O_{16}(OH)]^{3-}$ (isomers **1** and **2**) stoichiometries.

Finally, the same analysis was performed for hexanuclear species. According to the results obtained for isopolytungstates,[6] only compact structures that resemble that of the Lindqvist anion are analyzed here. In Figure 4.8 one can observe a $[Mo_6O_{19}(OH)]^{3-}$ structure which will lead to the Lindqvist anion after a protonation and a dehydration. It is important to note that the open-chain $[Mo_6O_{19}]^{2-}$ structure with six corner-shared tetrahedra shows a much higher energy than the Lindqvist structure in the gas phase (around 30 kcal mol^{-1}), but it is predicted to have an even lower energy (−2.1 kcal mol^{-1}) when the solvent is taken into account. As detailed in the experimental section, the $[Mo_6O_{19}]^{2-}$ anion is usually prepared in non-aqueous media (DMF), but it was originally obtained by precipitation from acidified aqueous molybdate solution.[12] So, it is clear that the COSMO methodology that we are using here is overestabilizing those linear compounds with corner-sharing

UNIVERSITAT ROVIRA I VIRGILI
ASSEMBLY AND PROPERTIES OF POLYOXOMETALATES: A THEORETICAL POINT OF VIEW
Laia Vilà Nadal
ISBN.978-84-694-2170-3/DL:T. 1039-2011

Mo^{VI} tetrahedra with respect to compact edge-sharing Mo^{VI} octahedra. This overestabilization is, however, minimized when comparing structures whose Mo^{VI} ions feature similar coordination spheres. The origin of this overstabilization is now under study. We would like to remark here that for the $[Mo_6O_{19}]^{2-}$ stochiometry, the compact Lindqvist structure shows a much lower energy than the open-chain linear isomer in the gas phase in contrast to the idea of Walanda *et al.* who stated that close-packed clusters are generally associated with larger-sized highly negative charged aggregates in the ESI-MS experiments.

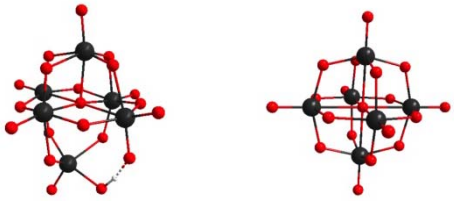

Figure 4.8. Ball-and-stick representations for the optimized structures corresponding to $[Mo_6O_{19}(OH)]^{3-}$ stoichiometry and the Lindqvist anion $[Mo_6O_{19}]^{2-}$.

4.5. The mechanism

As stated previously, Table 4.2 shows our mechanistic proposal for the formation of the $[Mo_6O_{19}]^{2-}$ anion, based on the peaks observed in the ESI-MS experiments. An additional mechanism is also proposed with protonated intermediates as it was done for the formation of isopolytungstates (M2, see Annex A). From a themodynamic point of view, the reaction energy for the formation of the Lindqvist molybdate from the tetrahedral monomers is not as exothermic as that for the corresponding tungstate (by 30 kcal mol^{-1}). This result is in agreement with the fact that the Lindqvist molybdate can be fragmented more easily than the tungstate in the ESI-MS experiments. Due to the

UNIVERSITAT ROVIRA I VIRGILI
ASSEMBLY AND PROPERTIES OF POLYOXOMETALATES: A THEORETICAL POINT OF VIEW
Laia Vilà Nadal
ISBN.978-84-694-2170-3/DL:T. 1039-2011

abovementioned shortcomings of the continuous model (COSMO) in predicting correctly the relative energies of the open-chain linear structures, we have not considered any of them in the computation of the reaction energies for the different steps of the mechanism. As for the Lindqvist tungstate, an energetic cascade profile is predicted for both mechanisms with the last step being the most exothermic. The formations of trinuclear $[Mo_3O_{10}(OH)]^{3-}$ and pentanuclear $[Mo_5O_{16}(OH)]^{3-}$ clusters are somewhat endothermic, but are largely compensated by the considerable exothermic process that are the formation of tetramers and hexamers.

4.6. Conclusions

Using Car-Parrinello molecular dynamics to analyze the hydration-dehydration equilibrium processes in the hydrogenmolybdate anion and the molybdic acid, we have confirmed that increasing the acidity of the aqueous solution involves an expansion of the coordination sphere of the Mo^{VI} ion from four to six, in agreement with experiment. Both Car-Parrinello simulations, with explicit solvent molecules, and standard static DFT calculations with continuous models of solvation predict the formation of dinuclear species different from that proposed by Kepert many years ago, as observed for the polyoxotungstates. Formation of dinuclear molybdates is predicted to be less favorable than tungstates. We have also found that although dichromate is a very stable species in acidic solutions, the formation of compact and closed structures with higher nuclearities is importantly endothermic in good agreement with the low number of polyoxochromates known so far. With the help of ESI-MS experiments, we postulate mechanisms with energy-cascade profiles for the formation of the $[Mo_6O_{19}]^{2-}$ Lindqvist anion based on consecutive aggregations of

UNIVERSITAT ROVIRA I VIRGILI
ASSEMBLY AND PROPERTIES OF POLYOXOMETALATES: A THEORETICAL POINT OF VIEW
Laia Vilà Nadal
ISBN.978-84-694-2170-3/DL:T. 1039-2011

hydrogenmolybdate anions followed by protonation and water condensation steps, confirming the results already observed for the isopolytungstates. So, it is proposed that the $[Mo_6O_{19}]^{2-}$ anion is also formed by the aggregation of one Mo unit at a time. Although planar Mo_3 building blocks are also found for the lowest-energy intermediate tetra- and pentanuclear species, significant differences in comparison with the isopolytungstates are detected. In general, open-chain linear structures are more favored in the case of the isopolymolybdates. The inclusion of the solvent effects with a continuous model provides a correct *qualitative* description of these phenomena, but several shortcomings prevent this methodology to be used for quantitative predictions. The coordination sphere of the Mo^{VI} ions in polynuclear clusters might be expanded due to the interaction with the water molecules. Therefore, the inclusion of discrete solvent molecules is advisable whenever is possible. After the initial work devised to elucidate the aggregation mechanisms in isopolytungstates combining theoretical calculations and ESI-MS experiments this is a new step in the rationalization of such complex processes that are involved in the formation of molecular oxide nanostructures.

References and Notes

[1] M. Filowitz, R.K.C. Ho, W.G. Klemperer, W. Shum, *Inorg. Chem.*, **1979**, 18, 93.

[2] N.N. Greenwood, A. Earnshaw, *Chemistry of the elements,* Elsevier, Oxford, **2006**.

[3] (a) D.L. Long, P. Kögerler, L.J. Farrugia L. Cronin L., *Angew. Chem. Int. Ed.*, **2003**, 42, 4180. (b) L. Cronin, C. Beugholt, E. Krickemeyer, M. Schmidtmann, H. Bögge, P. Kögerler, T.K.K. Luong, A. Müller, *Angew. Chem. Int. Ed.*, **2002**, 41, 2805. (c) K. Wassermann, M.H. Dickman, M.T. Pope, *Angew. Chem. Int. Ed. Engl.*, **1997**, 36, 1445.

[4] J.J. Cruywagen, J.B.B. Heyns, *Polyhedron*, **2000**, 19, 907.

[5] The cell box that contains: (i) one $[MoO_3(OH)]^-$ and 29 H_2O molecules (a = b = c = 9.959 Å); (ii) two $[MoO_3(OH)]^-$ and 27 H_2O molecules (a = b = c = 9.959 Å); or (iii) three $[MoO_3(OH)]^-$ and 58 H_2O molecules (a = b = c = 12.580 Å) is repeated periodically in space by the standard periodic boundary conditions.

[6] A. Rodríguez-Fortea, L. Vilà-Nadal, J.M. Poblet, *Inorg. Chem.* **2008**, 17, 7745.

[7] L. Vilà-Nadal, A. Rodríguez-Fortea, J.M. Poblet, *Eur. J. Inorg. Chem.* **2009**, 5125.

[8] J.A. Fernandez, X. Lopez, J.M. Poblet, *J. Mol. Catal. A* **2007**, 262, 236.

[9] D.K. Walanda, R.C. Burns, G.A. Lawrence, E.I. Von Nagy-Felsobuki, J. *Chem. Soc. Dalton Trans.* **1999**, 311.

[10] R. Llusar, I. Sorribes, C. Vicent, J. *Clust. Sci.* **2009**, 20, 177.

[11] L. Vilà-Nadal, A. Rodríguez-Fortea, L.K. Yan, E.F. Wilson, L. Cronin, J.M. Poblet, *Angew. Chem. Int. Ed.* **2009**, 48, 5452.

[12] J. Fluchs, K.F. Jahr, *Z. Naturfrosch.* **1968**, 23b, 1380.

UNIVERSITAT ROVIRA I VIRGILI
ASSEMBLY AND PROPERTIES OF POLYOXOMETALATES: A THEORETICAL POINT OF VIEW
Laia Vilà Nadal
ISBN.978-84-694-2170-3/DL:T. 1039-2011

UNIVERSITAT ROVIRA I VIRGILI
ASSEMBLY AND PROPERTIES OF POLYOXOMETALATES: A THEORETICAL POINT OF VIEW
Laia Vilà Nadal
ISBN.978-84-694-2170-3/DL:T. 1039-2011

Chapter 5
Formation Mechanisms of HeteroPOMs with Low Nuclearities

UNIVERSITAT ROVIRA I VIRGILI
ASSEMBLY AND PROPERTIES OF POLYOXOMETALATES: A THEORETICAL POINT OF VIEW
Laia Vilà Nadal
ISBN.978-84-694-2170-3/DL:T. 1039-2011

"The only way of finding the limits to the possible is by going beyond them into the impossible."

A. C. Clarke,
The Lost Worlds of 2001, 1972.

UNIVERSITAT ROVIRA I VIRGILI
ASSEMBLY AND PROPERTIES OF POLYOXOMETALATES: A THEORETICAL POINT OF VIEW
Laia Vilà Nadal
ISBN.978-84-694-2170-3/DL:T. 1039-2011

Chapter 5

Formation Mechanisms of HeteroPOMs with Low Nuclearities

In this Chapter we have analized the first nucleation steps in the formation of the $[XM_{12}O_{40}]^{n-}$ Keggin polyoxometalates (POMs) (where addenda metal atom M = W or Mo, and the heteroatom X = P or As). Again complimentary combination of Density Functional Theory (DFT) methodology and Electrospray Ionization-Mass Spectrometry (ESI-MS) was decisive. We postulate the formation of isodinuclear species (e.g. $[M_2O_7]^{2-}$), which undergoes successive steps of protonation and water condensation and leads to the constituent parts required for subsequent aggregation to the assembly of higher nuclearity heteropolyanions. Importantly, the results of both DFT modelling and ESI-MS both suggest that the heteroanion, $[XO_2(OH)_2]^-$, is not incorporated into the polyanion in the first steps of nucleation and nucleation therefore proceeds firstly via isodinuclear fragments. Once the heterotrimer, $[XM_2O_9]^-$, is formed the heteroanion is inserted and acts as a template for the formation of the plenary Keggin heteropolyanion. The structure and stability of calculated structures of the numerous postulated intermediates in the first steps of the formation of the Keggin polyoxometalates have been analysed and discussed in detail and, furthermore, these results have been corroborated by experimental mass spectrometric analysis on both single crystals and reaction solutions of

the same Keggin clusters. This Chapter both complements and expands previous work and provides new key information towards the rationalization of the complex processes involved in the formation of complex molecular metal-oxide clusters.

5.1. Introduction

The ultimate aim of nanoscience is the control and understanding of assembly at small scale. In this respect, it is worth pointing out that 'bulk' metal-oxides have been responsible for the revolution in materials science that provides many of the substrates for electronic devices.[1] Today the bottom-up approach has revealed a key route for the preparation of a whole range of systems from cages[2] to metal organic frameworks[3] and the formation of macrocycles[4] from comparatively simple small molecule building blocks.

The formation of heteropolyoxoanions from the hydrogenmetalate anion, $[MO_3(OH)]^-$ (M= W, Mo), and the heteroanion, $[XO_2(OH)_2]^-$ (X= P, As), which are abundant species under the conditions for synthesis of POMs, requires several steps of protonation and water condensation. In particular, up to 10 protonations and 12 water condensations are stoichiometrically needed to obtain the Keggin anion, $[XM_{12}O_{40}]^{3-}$. Similarly to our recent work regarding the formation mechanisms of the Lindqvist anion, (see Chapter 3) we also postulate here that once the dinuclear species are formed, consecutive steps of protonation and water condensation followed by aggregation occur to justify the clusters observed in the ESI-MS experiments.

In acidic media, protonation of $[MO_4]^{n-}$ leads to modification of the coordination geometry of the metal, for example $[MO_{6-y}(OH)_y]^{m-}$, and yields a polyoxometalate via a polycondensation

UNIVERSITAT ROVIRA I VIRGILI
ASSEMBLY AND PROPERTIES OF POLYOXOMETALATES: A THEORETICAL POINT OF VIEW
Laia Vilà Nadal
ISBN.978-84-694-2170-3/DL:T. 1039-2011

reaction. The acidification of an aqueous solution of the $[MO_4]^{n-}$ starting material results in an expansion of the metal coordination shell from 4 to 6, i.e. from a tetrahedral (T_d) to an octahedral (O_h) oxygen coordination environment. This consequently enables protonation of the terminal oxygens and facilitates condensation reactions between individual $[MO_6]$ fragments thereby resulting in the self-assembly of larger structures in solution. Typically, heteropolyanions result from the acidic polycondensation of $[MO_x]$ fragments around a central heteroelement, which behaves as a template to the forming structure. Thus, the symmetry and geometry of the resulting polyanion depends strongly on the coordination geometry of the heteroanions. For example under general POM reaction conditions, B tends to be trigonal; whereas Si, Ge, and P adopt a tetrahedral geometry; and transition metals such as Mo, W, Co and Ni prefer to be octahedral. Furthermore, syntheses are complicated further still as the products are often dependent on the ratio of M:X in solution.

The formation of the 12 metal-centered Keggin anion, $[XM_{12}O_{40}]^{n-}$, can be considered to be a fundamental case of the self-assembly process involved in POM chemistry (see Figure 2). This polyoxoanion structure is comprised of a tetrahedral template around which corner- and edge-sharing $[MO_6]$ octahedra bind. As such, the Keggin heteropolyanion can be dissected into distinctive principal building units: four trinuclear $[M_3O_{13}]$ triads –which are assembled from three edge-sharing $[MO_6]$ octahedra– arranged around a central XO_4 heteroanion template so that the central μ_3-oxygen ligand of each $[M_3O_{13}]$ fragment links to the central heteroatom X (where X = P, As, S etc) (Figure 5.1). The resultant cluster anion is a dodecanuclear metal-oxide anion with tetrahedral symmetry where each metal centre occupies the corner of a truncated tetrahedron. Baker and Figgis[5] postulated the existence of five isomers for the metal-oxide core of the Keggin anion, $[XM_{12}O_{40}]^{n-}$ arising from the

UNIVERSITAT ROVIRA I VIRGILI
ASSEMBLY AND PROPERTIES OF POLYOXOMETALATES: A THEORETICAL POINT OF VIEW
Laia Vilà Nadal
ISBN.978-84-694-2170-3/DL:T. 1039-2011

rotation of $[M_3O_{13}]$ triads. The corresponding energy scale is commensurate with the experimental findings showing that as the number of rotated triads increases, so too does the energy of the metal-oxide core, resulting in the order $\alpha < \beta < \gamma < \delta < \varepsilon$. In addition, the molecular formula remains the same in all cases; but the redox properties do not. A combination of experimental[6,7], and theoretical[8,9] data prove that the redox properties vary from isomer to isomer;[10] however, fully oxidized Keggin anions prefer to adopt the α arrangement[11], a result which has been further verified by theoretical evidence.[12]

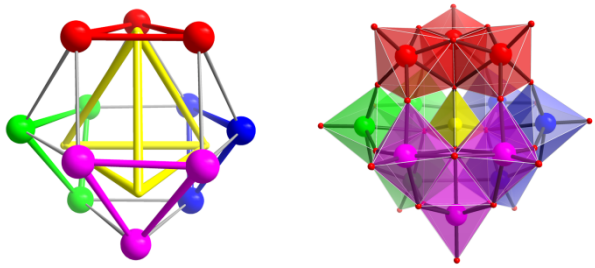

Figure 5.1. Rationalisation of the 12 metal-centered Keggin heteropolyoxoanion structure, $[\alpha\text{-}XM_{12}O_{40}]^{n-}$. The anion is composed of four independent $[M_3O_{13}]$ triads (red, green, magenta, blue) interconnected by threefold nodes only. The structure exhibits idealised tetrahedral (T_d) symmetry as indicated by the inscribed tetrahedron (yellow) which is introduced by the central templating anion $[XO_4]^{n-}$.

In order to develop our understanding of the nucleation processes involved in Keggin formation, a series of Keggin type polyoxotmetalate anions were transferred to the gas phase via electrospray ionization (ESI), and the fragmentation products of these anions examined by collision-induced dissociation (CID). Fragmentation provides insight into the favoured decomposition pathways of gas-phase clusters and, in combination with ESI-MS studies of their assembly, might also provide broader understanding of the intermediates relevant to their formation.

In this chapter we expand on our previous observations concerning the nucleation mechanisms of small polyoxoanions

and provide an insight into the formation of larger heteropolyoxometalates, $[XM_yO_z]^{q-}$; specifically the 12-metal-centered Keggin anions. The combination of experiment and theory serves as a powerful tool for rationalizing the nucleation mechanisms of this class of compounds.

5.2. Inital steps in the Keggin anion formation

As we have done for the Lindqvist anion[13] we also postulate here that once the dinuclear species are formed, consecutive steps of protonation and water condensation followed by aggregation occur to justify the clusters observed in the ESI-MS experiments. Two different dinuclear species are now viable: either the isodimer, $[M_2O_6(OH)_2]^{2-}$, occuring in the first formation step of the Lindqvist anion; or the heterodimer, $[MXO_5(OH)_3]^{2-}$. Standard DFT studies at BP86/TZP level taking into account the effect of the solvent in a continuous manner (COSMO methodology)[14] along with the results obtained from the ESI-MS experiments point to the formation of the iso- instead of the heterodimer. Formation of the isodimer is energetically more feasible than the formation of the heterodimer according to the reaction energies (see Table 5.1 and Figure 5.2). The values shown in Table 5.1 correspond to the following reactions:

$$2\left[MO_3(OH)\right]^- \rightarrow \left[M_2O_6(OH)_2\right]^{2-} \quad (5.1)$$

$$2\left[MO_3(OH)\right]^- \rightarrow \left[M_2O_7\right]^{2-} + H_2O \quad (5.2)$$

$$2\left[MO_3(OH)\right]^- + H_3O^+ \rightarrow \left[M_2O_6\left(OH\right)\right]^- + 2H_2O \quad (5.3)$$

$$\left[MO_3(OH)\right]^- + \left[XO_2\left(OH\right)_2\right]^- \rightarrow \left[XMO_5(OH)_3\right]^{2-} \quad (5.4)$$

$$\left[MO_3(OH)\right]^- + \left[XO_2\left(OH\right)_2\right]^- \rightarrow \left[XMO_6(OH)\right]^- + H_2O \quad (5.5)$$

$$\left[MO_3(OH)\right]^- + \left[XO_2\left(OH\right)_2\right]^- + H_3O^+ \rightarrow \left[XMO_5\left(OH\right)_2\right]^- + 2H_2O \quad (5.6)$$

UNIVERSITAT ROVIRA I VIRGILI
ASSEMBLY AND PROPERTIES OF POLYOXOMETALATES: A THEORETICAL POINT OF VIEW
Laia Vilà Nadal
ISBN.978-84-694-2170-3/DL:T. 1039-2011

The simple aggregation of two monomeric building blocks is much more favoured for the iso-, $[M_2O_6(OH)_2]^{2-}$, than for the heterodimer, $[MXO_5(OH)_3]^{2-}$, regardless of the metal M and the heteroatom X (see Table 5.1). The reaction for the ditungstate is moderately exothermic (−7.4 kcal mol^{-1}) whereas for the dimolybdate it is slightly endothermic (+0.4 kcal mol^{-1}). They are both, however, more exothermic (less endothermic) than those for the heterodimers, especially when the metal is tungsten (more than 8 kcal mol^{-1}).

Table 5.1. Reaction energies (in kcal mol^{-1}) for dinuclear species with respect to the monomers. Detected stoichiometries in ESI-MS are $[W_2O_7]^{2-}$, $[Mo_2O_7]^{2-}$ and $[W_2O_6(OH)]^-$ highlighted in boldface type.

Structure			ΔE (kcal mol^{-1})			
			M=W		M=Mo	
			X=P	X=As	X=P	X=As
$[M_2O_6(OH)_2]^{2-}$	**1**	a	–7.5		+0.4	
	2	b	+0.2		+7.4	
	3	c	+10.2		+11.4	
$[M_2O_7]^{2-}$	**1**	d	–4.4		–2.2	
	2	e	–3.3		–2.1	
$[M_2O_6(OH)]^-$	**1**	f	–21.9		–17.9	
$[XMO_5(OH)_3]^{2-}$	**1**	g	+2.4	+1.3	+4.2	+3.7
	2	h	+12.6	+13.2	+15.7	+14.0
	3	i	+3.0	+3.2	+5.5	+8.4
	4	j	+27.3	+10.3	+30.2	+12.9
$[XMO_6(OH)]^{2-}$	**1**	k	+0.8	+2.5	+1.6	+1.76
	2	l	+2.2	+0.6	+1.7	+0.92
	3	m	+1.5	–0.3	+1.5	+0.16
$[XMO_5(OH)_2]^-$	**1**	n	–18.6	–22.2	–17.2	–21.4

UNIVERSITAT ROVIRA I VIRGILI
ASSEMBLY AND PROPERTIES OF POLYOXOMETALATES: A THEORETICAL POINT OF VIEW
Laia Vilà Nadal
ISBN.978-84-694-2170-3/DL:T. 1039-2011

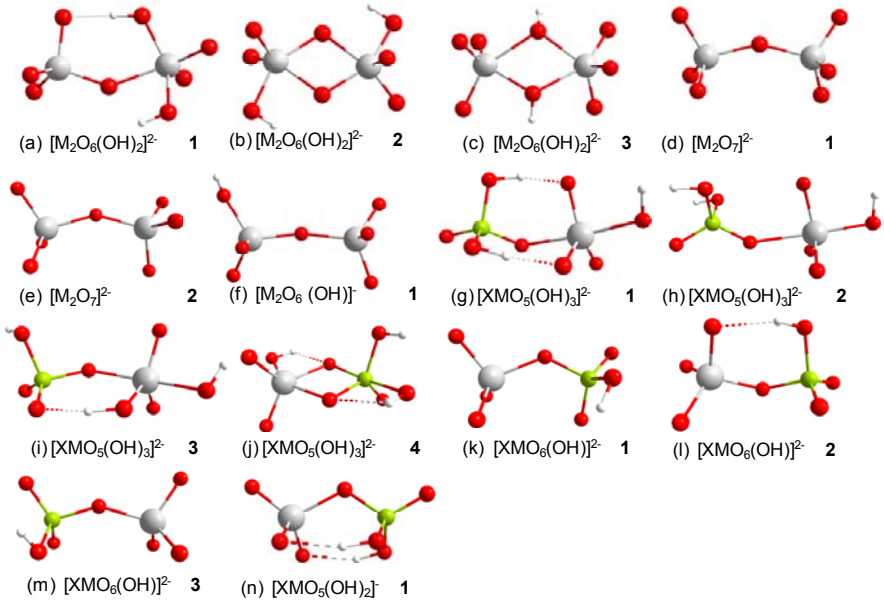

Figure 5.2. Ball-and-stick representations of optimized structures for the most representative dinuclear species (red spheres are oxygens, grey spheres are metal centres, green spheres are the heteroatoms and white spheres are hydrogen atoms).

Once the initial step is established we have to discuss the following steps on the mechanisms, see Table 5.2. The second step, corresponding to water condensation preceded (mechanism H-M2) or not (H-M1) by protonation, is somewhat more favoured for the heterodimers (compare Tables 5.1 and 5.2). This notwithstanding, the formation of the dehydrated isodimers is still more favoured than those of the heterodimers in most of the cases. The reaction energy for the formation of the ditungstate without protonation is more exothermic than those for the phospho and the arsenotungstate (−5.3 vs. +0.8 and −0.3 kcal mol^{-1}, respectively, see Tables 5.1 and 5.2). The differences are smaller for the case of molybdates, the isodimer being still

UNIVERSITAT ROVIRA I VIRGILI
ASSEMBLY AND PROPERTIES OF POLYOXOMETALATES: A THEORETICAL POINT OF VIEW
Laia Vilà Nadal
ISBN.978-84-694-2170-3/DL:T. 1039-2011

slightly favoured with respect to the formation of the phospho and arsenomolybdate (−2.3 vs. +1.5 and +0.1 kcal mol^{-1}). Regarding to mechanism H-M2, the isodimers are favoured with respect to the phosphometalates (−21.8 vs. −18.6 kcal mol^{-1} for M = W; and −17.9 vs. −17.2 kcal mol^{-1} for M = Mo), but the arsenometalates are competitive with the isodimers (compare Tables 5.1 and 5.2), especially in the case of molybdates. Therefore, in most of the cases analyzed here the heteroanion is predicted to be incorporated in later steps of the aggregation process.

The lowest-energy structures for $[XMO_5(OH)_3]^{2-}$ (H-M1 and H-M2), $[XMO_6(OH)]^{2-}$ (H-M1) and $[XMO_5(OH)_2]^{-}$ (H-M2) stoichiometries are depicted in Figure 5.3. Other structures together with their relative energies are shown in Figure 5.2 and Table 5.1). For all of them, the M atom is five-coordinated and the X atom is four-coordinated (what we call **5c-4c** structures). **5c-5c** structures show much higher energies, especially for the case in which X = P, due to the preference of the heteroatom to remain with a tetrahedral environment (see Table 5.1).

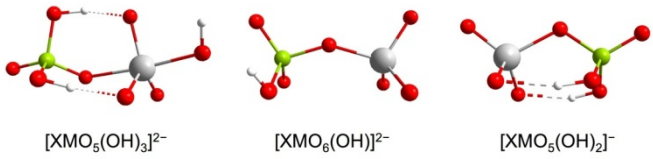

Figure 5.3. Lowest-energy structures at BP86/COSMO level for heterodimers with $[XMO_5(OH)_3]^{2-}$ (H-M1 and H-M2), $[XMO_6(OH)]^{2-}$ (H-M3) and $[XMO_6(OH)_2]^{2-}$ (H-M4) stoichiometries.

UNIVERSITAT ROVIRA I VIRGILI
ASSEMBLY AND PROPERTIES OF POLYOXOMETALATES: A THEORETICAL POINT OF VIEW
Laia Vilà Nadal
ISBN.978-84-694-2170-3/DL:T. 1039-2011

Table 5.2. Proposed mechanisms for the formation of the heterodimer (H-M1 and H-M2) and for the formation of heteropolyanions with higher nuclearities (up to the tetramer, H-M3 and H-M4). [a]The species detected in ESI-MS experiments are highlighted in bold.

Mechanism H-M1	W-P	W-As	Mo-P	Mo-As
1) **$[MO_3(OH)]^-_{(aq)}$** + $[XO_2(OH)_2]^-_{(aq)} \rightarrow [XMO_5(OH)_3]^{2-}_{(aq)}$	+2.4	+1.3	+4.2	+3.7
2) $[XMO_5(OH)_3]^{2-}_{(aq)} \rightarrow [XMO_6(OH)]^{2-}_{(aq)} + H_2O_{(aq)}$	–1.6	–1.6	–2.7	–3.6
Mechanism H-M2	W-P	W-As	Mo-P	Mo-As
1) **$[MO_3(OH)]^-_{(aq)}$** + $[XO_2(OH)_2]^-_{(aq)} \rightarrow [XMO_5(OH)_3]^{2-}_{(aq)}$	+2.4	+1.3	+4.2	+3.7
2) $[XMO_5(OH)_3]^{2-}_{(aq)} + H_3O^+_{(aq)} \rightarrow [XMO_5(OH)_2]^-_{(aq)} + H_2O_{(aq)}$	–21.0	–23.5	–21.4	–25.2
Mechanism H-M3	W-P	W-As	Mo-P	Mo-As
1) **$[MO_3(OH)]^-_{(aq)}$** + $[MO_3(OH)]^-_{(aq)} \rightarrow$ **$[M_2O_6(OH)_2]^{2-}_{(aq)}$**	–7.4	–7.4	+0.4	+0.4
2) **$[M_2O_6(OH)_2]^{2-}_{(aq)}$** $\rightarrow [M_2O_7]^{2-}_{(aq)} + H_2O_{(aq)}$	+2.1	+2.1	–2.7	–2.7
3) $[M_2O_7]^{2-}_{(aq)} + [XO_2(OH)_2]^-_{(aq)} \rightarrow [XM_2O_9(OH)_2]^{3-}_{(aq)}$	+1.3	+2.2	–0.5	–0.8
4) $[XM_2O_9(OH)_2]^{3-}_{(aq)} + H_3O^+_{(aq)} \rightarrow [XM_2O_9(OH)]^{2-}_{(aq)} + 2H_2O_{(aq)}$	–18.4	–20.5	–20.1	–19.9
5) $[XM_2O_9(OH)]^{2-}_{(aq)} + H_3O^+_{(aq)} \rightarrow$ **$[XM_2O_9]^-_{(aq)}$** $+ 2H_2O_{(aq)}$	+4.5	–1.2	–0.9	–4.7
6) **$[XM_2O_9]^-_{(aq)}$** + $[MO_3(OH)]^-_{(aq)} \rightarrow [XM_3O_{12}(OH)]^{2-}_{(aq)}$	–31.6	–25.1		
7) $[XM_3O_{12}(OH)]^{2-}_{(aq)} + H_3O^+_{(aq)} \rightarrow$ **$[XM_3O_{12}]^-_{(aq)}$** $+ 2H_2O_{(aq)}$	+1.0	–2.8		
Mechanism H-M4	W-P	W-As	Mo-P	Mo-As
1) **$[MO_3(OH)]^-_{(aq)}$** + $[MO_3(OH)]^-_{(aq)} \rightarrow$ **$[M_2O_6(OH)_2]^{2-}_{(aq)}$**	–7.4	–7.4	+0.4	+0.4
2) **$[M_2O_6(OH)_2]^{2-}_{(aq)}$** $+ H_3O^+_{(aq)} \rightarrow [M_2O_6(OH)]^-_{(aq)} + 2H_2O_{(aq)}$	–14.4	–14.4	–18.3	–18.3
3) $[M_2O_6(OH)]^-_{(aq)} + [XO_2(OH)_2]^-_{(aq)} \rightarrow [XM_2O_8(OH)_3]^{2-}_{(aq)}$	–16.9	–6.6	–7.4	–5.4
4) $[XM_2O_8(OH)_3]^{2-}_{(aq)} + H_3O^+_{(aq)} \rightarrow$ **$[XM_2O_8(OH)_2]^-_{(aq)}$** $+ 2H_2O_{(aq)}$	+1.8	–7.0	–11.4	–10.9
5) **$[XM_2O_8(OH)_2]^-_{(aq)}$** + $[MO_3(OH)]^-_{(aq)} \rightarrow [XM_3O_{11}(OH)_3]^{2-}_{(aq)}$	–20.2	–18.4		
6) $[XM_3O_{11}(OH)_3]^{2-}_{(aq)} + H_3O^+_{(aq)} \rightarrow$**$[XM_3O_{11}(OH)_2]^-_{(aq)}$** $+ 2H_2O_{(aq)}$	+6.7	+10.2		

[a] Reaction energies are in kcal mol^{-1}.

We have also analyzed the formation of these heterodimers by means of Car–Parrinello molecular dynamics simulations in combination with the metadynamics approach, which is used to accelerate the dynamics and to compute free-energy barriers.[15] This methodology has been shown to be valid in previous studies as for example the formation mechanisms of the Lindqvist anion $[W_6O_{19}]^{2-}$.[16] The studied system was formed by

one $[WO_3(OH)]^-$ monomer, one $[PO_2(OH)_2]^-$ heteroanion and 27 H_2O molecules. To describe the formation of heterodinuclear species in solution we used as a single collective variable (CV) the coordination number of the W atom with respect to the eight O atoms that belong to the WO_4 and PO_4 groups, C_{W-O} (see Annex B for details about the parameters of the metadynamics). The evolution of the coordination number C_{W-O} along the 26-ps metadynamics trajectory is shown in Figure 5.4. A qualitative description of the events observed in this metadynamics follows. We observe the formation of the $[XMO_5(OH)_3]^{2-}$ heterodimer at the very beginning (0.2 ps) indicating that it is a likely event with a small barrier (around 1 kcal mol^{-1} according to our predictions). At 3.6 ps, an intramolecular H^+ transfer from the O atom of the phosphate group to the O atom of the tungstate takes place making the W ion more electrophilic. As a consequence, at 5.2 ps a H_2O molecule is bonded to the W atom becoming now a six-coordinated ion. This **5c+1w-4c** structure (see Figure 5.4, **w** stands for coordinated water molecule) lasts for 13 ps and then the hydrated heterodimer is broken into the constituent monomers, i.e. the heteroanion and the hydrated $[WO_3(OH)]^-$ monomer. The stability of the hydrated heterodimer with respect to the monomers in terms of free energy is predicted to be around 15 kcal mol^{-1}. Additional metadynamics runs with the use of other collective variables (W···O distances, where the O atom belongs to the heteroanion, see Annex B) were also performed and the same conclusions were retrieved.

UNIVERSITAT ROVIRA I VIRGILI
ASSEMBLY AND PROPERTIES OF POLYOXOMETALATES: A THEORETICAL POINT OF VIEW
Laia Vilà Nadal
ISBN.978-84-694-2170-3/DL:T. 1039-2011

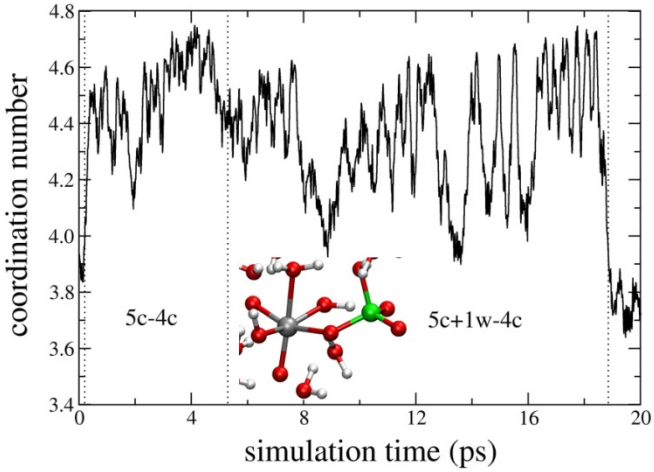

Figure 5.4. Evolution of the coordination number C_{W-O} along the trajectory of the metadynamics run for the system formed by one $[WO_3(OH)]^-$ monomer, one $[PO_2(OH)_2]^-$ heteroanion and 27 H_2O molecules.

5.3. ESI-MS results

In order to investigate the initial steps of the assembly processes that yield the Keggin polyoxoanions $[XM_{12}O_{40}]^{3-}$ (X = P, As; M = W, Mo), the reaction solutions of these clusters were transferred to the gas phase by ESI and their subsequent nucleation studied. An important point, a common feature of ESI, is the observation of charge reduction during the electrospray process.[17] This has been attributed to the instability of highly charged clusters due to the Coulombic repulsion in the bare clusters following desolvation.[18] This charge reduction has two common manifestations: (i) ion association of discrete gas-phase ion clusters comprised of multiply charged polyoxoanions and multiple available counterions and (ii) protonation of oxo ligands of the cluster to form hydroxo ligands, often followed by a loss of water from the cluster framework. Importantly, the latter process results in the formal removal of O^{2-} from the

UNIVERSITAT ROVIRA I VIRGILI
ASSEMBLY AND PROPERTIES OF POLYOXOMETALATES: A THEORETICAL POINT OF VIEW
Laia Vilà Nadal
ISBN.978-84-694-2170-3/DL:T. 1039-2011

polyoxoanion cluster. Established experimental procedures were followed to synthesize the series of Keggin anions.[19] At the point where crystallization or precipitation was due to begin, the prepared solutions were analyzed by ESI-MS. Interestingly, the assigned peaks correspond to monomers and isodinuclear species, as for example: $[MO_3(OH)]^-$, $Na[MO_4]^-$, $Na[M_2O_7]^-$ and other species with different numbers of solvent molecules (water and acetonitrile, see Figures 6 and 7 in Annex B for a more detailed description). In addition for Mo-based Keggin anions, species such as $[Mo_2O_6(OH)]^-$ or $A[Mo_2O_6(OH)_2]^-$ (A: countercation), which were already postulated to be formed,[8] were also detected (see Figure 5.5).

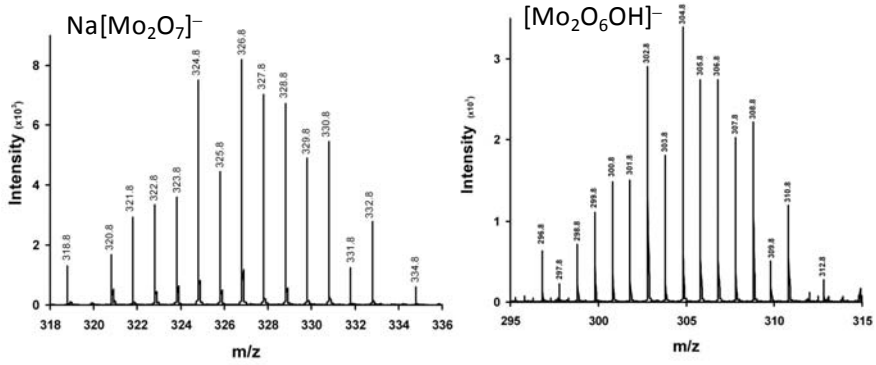

Figure 5.5. Left: isodimeric fragment $Na[Mo_2O_7]^-$ (*m/z* 326.8) observed in the assembly solution of $[(n\text{-}C_4H_9)_4N]_3PMo_{12}O_{40}$ in the Mass Spectrometer. Right: Protonated isodimeric fragment $[Mo_2O_6(OH)]^-$ (*m/z* 304.8) observed in the assembly solution of $[(n\text{-}C_4H_9)_4N]_3PMo_{12}O_{40}$ in the Mass Spectrometer.

These experiments confirm the theoretical predictions: the heterodimers should form easily as a consequence of their small barrier of formation, but they are not observed because they are less stable than the isodinuclear species. Since the arsenometalates are predicted to be competitive with the isodimers through mechanism H-M2, an apparent contradiction

UNIVERSITAT ROVIRA I VIRGILI
ASSEMBLY AND PROPERTIES OF POLYOXOMETALATES: A THEORETICAL POINT OF VIEW
Laia Vilà Nadal
ISBN.978-84-694-2170-3/DL:T. 1039-2011

seems to appear. However, the assembly experiments have been performed at mildly acidic conditions (pH around 5), so mechanism H-M1, which predicts the formation of the isodimer, might be favoured with respect to H-M2. With the combined experimental and theoretical results obtained so far, we suggest that the isodimers are preferentially formed with respect to heterodimers in the conditions at which heteropolyanions are synthesized.

At this point, the following question arises: will the heteroanion incorporate in the next step of the reaction or will the isotrimer be formed? Fragmentation studies on the same range of well-defined Keggin anions, transferred to the gas phase by ESI, were performed and provide us with important information relating to intermediates in their formation. In order to study the fragmentation of these anions, tetrabutylammonium salts ([(n-$C_4H_9)_4N]^+$ = TBA^+) of these anions were prepared. The cation exchange process was used firstly because TBA^+ cations have a much higher mass than Na^+ or K^+ and give a large separation between signals corresponding to differently charged or protonated cluster states. Secondly, the TBA^+ cations have a lower affinity than Na^+ or K^+ for the cluster anions and solvent molecules and consequently, the use of acetonitrile can prevent clusters from decomposing, aggregating, or converting into other species in the gas phase. Before fragmentation, the major ions observed in the gas phase are $[XM_{12}O_{40}]^{3-}$ and ((n-$C_4H_9)_4N)[XM_{12}O_{40}]^{2-}$ (see Figure 5.6).

UNIVERSITAT ROVIRA I VIRGILI
ASSEMBLY AND PROPERTIES OF POLYOXOMETALATES: A THEORETICAL POINT OF VIEW
Laia Vilà Nadal
ISBN.978-84-694-2170-3/DL:T. 1039-2011

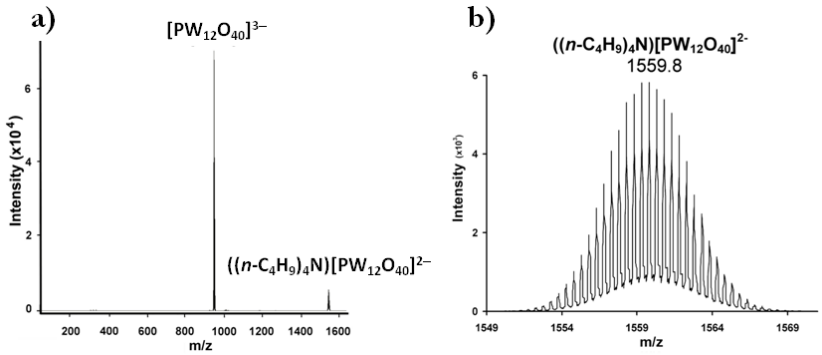

Figure 5.6. Electrospray Ionisation Mass Spectrometry of $[(n\text{-}C_4H_9)_4N]_3PW_{12}O_{40}$ showing the major ions observed in the gas phase are $[XM_{12}O_{40}]^{3-}$ and $((n\text{-}C_4H_9)_4N)[XM_{12}O_{40}]^{2-}$.

Fragmentation of these species leads to a range of anions in solution (see Figure 5.7), the most intense of which being $[M_6O_{19}]^{2-}$. Upon increasing the collision energy the resulting collision induced dissociation (CID) of the parent Keggin anions produce low mass fragments assigned to $[M_xO_{3x+1}]^{2-}$ (x=3-8), including heterotrimeric and tetrameric fragments such as $[PW_2O_9]^-$ and $[PW_2O_8(OH)_2]^-$ (see Figure 5.7) as well as species such as $((n\text{-}C_4H_9)_4N)[Mo_8O_{25}]^-$ and $((n\text{-}C_4H_9)_4N)[Mo_7O_{22}]^-$. It is possible that the latter fragments in particular are the result of neutral losses of MoO_3 or Mo_2O_6 from parent ions, for example $((n\text{-}C_4H_9)_4N)[Mo_8O_{25}]^-$ to $((n\text{-}C_4H_9)_4N)[Mo_7O_{22}]^-$ and $((n\text{-}C_4H_9)_4N)[Mo_6O_{19}]^-$ (see Figure 3 in Annex B), although the trend in increasing collision energy indicated the progressive fragmentation of parent Keggin anions. Table 5.3 lists the m/z peak assignments common to all assembly and fragmentation ESI-MS experiments in this study, clearly showing the trend of the assembly into isodimeric species and fragmentation down to isotrimeric species and heterotetrameric moieties.

UNIVERSITAT ROVIRA I VIRGILI
ASSEMBLY AND PROPERTIES OF POLYOXOMETALATES: A THEORETICAL POINT OF VIEW
Laia Vilà Nadal
ISBN.978-84-694-2170-3/DL:T. 1039-2011

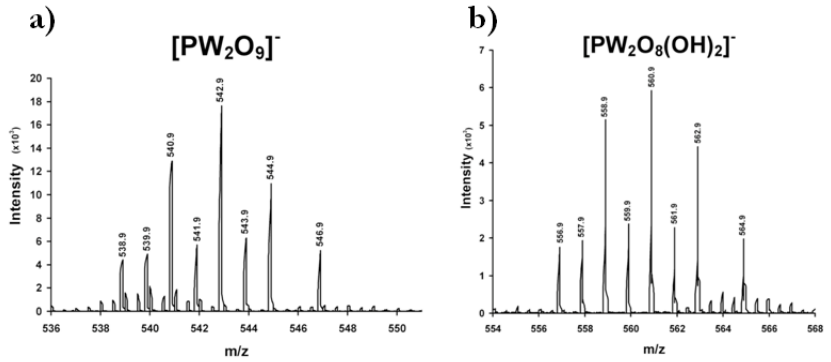

Figure 5.7. Electrospray Ionisation Mass Spectrometry of $[(n\text{-}C_4H_9)_4N]_3PW_{12}O_{40}$ showing that upon increasing the collision energy the parent Keggin anions produce low mass heterotrimeric fragments such as $[PW_2O_9]^-$ (m/z 542.9) and $[PW_2O_8(OH)_2]^-$ (m/z 560.9).

Table 5.3. List of m/z peak assignments common to the assembly and fragmentation of all four Keggin polyoxoanions $[XM_{12}O_{40}]^{3-}$ (X = P, As; M = W, Mo).

Common *m/z* peak assignments	
Assembly[a]	**Fragmentation**
$Na[MO_4]^-$	$[M_3O_{10}]^{2-}$
$[MO_3(OH)]^-$	$[M_4O_{13}]^{2-}$
$Na[M_2O_7]^-$	$[XM_3O_{12}]^-$
$[M_2O_6(OH)_2]^{2-}$	$[XM_4O_{15}]^-$
	$[M_5O_{16}]^{2-}$
	$[M_6O_{19}]^{2-}$
	$[M_7O_{22}]^{2-}$
	$[M_8O_{25}]^{2-}$
	$[XM_{12}O_{40}]^{3-}$
	$((n\text{-}C_4H_9)_4N)[XM_{12}O_{40}]^{2-}$
	$((n\text{-}C_4H_9)_4N)_2[XM_{12}O_{40}]^{1-}$

[a] Refer to the experimental section for reaction conditions followed.

UNIVERSITAT ROVIRA I VIRGILI
ASSEMBLY AND PROPERTIES OF POLYOXOMETALATES: A THEORETICAL POINT OF VIEW
Laia Vilà Nadal
ISBN.978-84-694-2170-3/DL:T. 1039-2011

5.4. Discussion about the Mechanisms: Trinuclear and Tetranuclear Species

Mechanisms H-M3 and H-M4 are proposed according to the peak assignments in ESI-MS fragmentation experiments of Keggin anions. Reaction energies from mechanisms H-M3 (steps 3-5) and H-M4 (steps 3-4) show that heterotrimers are more favoured than their iso- counterparts (see Table 5.2). Formation of $[XM_2O_9]^-$ from the isodimers is more exothermic than formation of $[M_3O_{10}]^{2-}$ (mechanism H-M3): −12.6 (X = P) and −19.5 (X = As) vs −1.7 kcal mol^{-1} for tungstates and −21.5 (X = P) and −25.5 (X = As) vs −3.2 kcal mol^{-1} for molybdates. Similar results are obtained from the comparison between $[XM_2O_8(OH)_2]^{2-}$ and $[M_3O_9(OH)]^-$ (mechanism H-M4): −15.1 (X = P) and −13.6 (X = As) vs −5.7 kcal mol^{-1} for tungstates and −18.8 (X = P) and −16.3 (X = As) vs −8.4 kcal mol^{-1} for molybdates. The lowest-energy structures for $[XM_2O_9(OH)_2]^{3-}$ (H-M3), $[XM_2O_9(OH)]^{2-}$ (H-M3), $[XM_2O_9]^-$ (H-M3), $[XM_2O_8(OH)_3]^{2-}$ (H-M4), and $[XM_2O_8(OH)_2]^-$ (H-M4) stoichiometries are depicted in Figure 5.8.

UNIVERSITAT ROVIRA I VIRGILI
ASSEMBLY AND PROPERTIES OF POLYOXOMETALATES: A THEORETICAL POINT OF VIEW
Laia Vilà Nadal
ISBN.978-84-694-2170-3/DL:T. 1039-2011

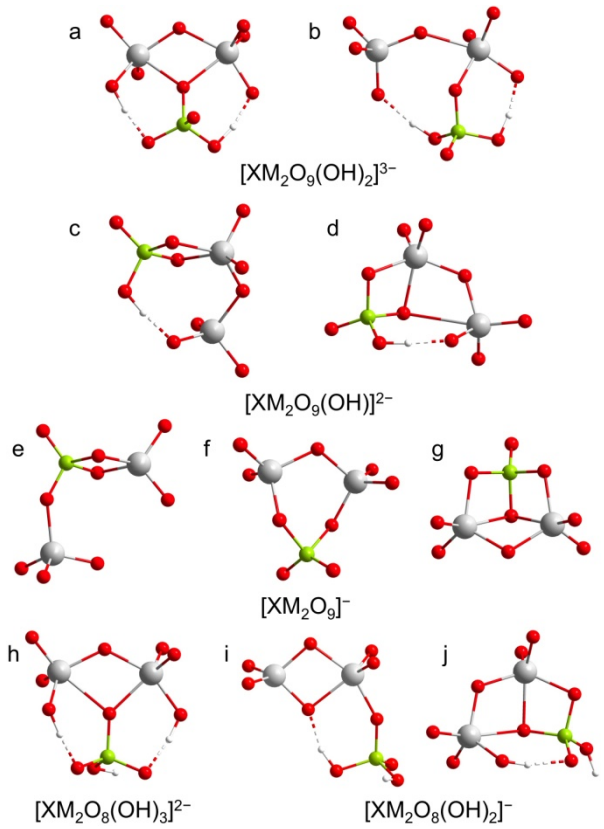

Figure 5.8. Lowest-energy structures at BP86/COSMO level for heterotrimers with $[XM_2O_9(OH)_2]^{3-}$ (H-M3), $[XM_2O_9(OH)]^{2-}$ (H-M3), $[XM_2O_9]^-$ (H-M3), $[XM_2O_8(OH)_3]^{2-}$ (H-M4), and $[XM_2O_8(OH)_2]^-$ (H-M4) stoichiometries.

We have analyzed a significant number of structures for each of these stoichiometries. In particular, sixteen for $[XM_2O_9(OH)_2]^{3-}$ (H-M3), six for $[XM_2O_9(OH)]^{2-}$ (H-M3), $[XM_2O_9]^-$ (H-M3) and $[XM_2O_8(OH)_2]^-$ (H-M4), and five for $[XM_2O_8(OH)_3]^{2-}$ (H-M4). The starting structures have been generated by chemical intuition and with the help of the metadynamics technique. All these structures along with their relative energies are shown in Figures 2-6 and Tables 2-4 (Annex B). For $[XW_2O_9(OH)2]^{3-}$ (H-M3), the

UNIVERSITAT ROVIRA I VIRGILI
ASSEMBLY AND PROPERTIES OF POLYOXOMETALATES: A THEORETICAL POINT OF VIEW
Laia Vilà Nadal
ISBN.978-84-694-2170-3/DL:T. 1039-2011

lowest-energy structures feature a μ_3-O bridging atom see Figure 5.8. None of the other structures show any μ_3-O bridging atom, i.e. they are not so compact, except one with a five-coordinated As atom which is 9.8 kcal mol^{-1} more unstable. The only structure in which the P atom is five-coordinated is very unstable compared to the other (almost 30 kcal mol^{-1} with respect to the lowest energy). For M = Mo, a similar structure with somewhat lower energy is found, but now with μ_2-O bridging atoms as a consequence of the lengthening of one of the Mo···O distances (see Figure 5.8, b). The compact structures with the μ_3-O atom are only 1 (X = P) and 3 kcal mol^{-1} (X = As) higher in energy. Open structures feature much higher energies (more than 8 kcal mol^{-1} relative to the minimum). Similar conclusions are drawn for the structures with stoichiometry $[XM_2O_8(OH)_3]^{2-}$ (H-M4), which only differs in an extra H^+ from the stoichiometry previously analyzed. Now, the lowest-energy structure is that with the μ_3-O atom for both M = W and Mo (see Figure 5.8, h). The structure with the five-coordinated X atom is by far the most unstable for X = P, but not so unstable for X = As due to its higher ability to expand the coordination sphere. For $[XM_2O_9(OH)]^{2-}$ (H-M3), the most stable structure for all the four possible species (M = W, Mo and X = P, As) shows the heteroanion coordinated to the metal in a bidentate fashion, but without presence of any μ_3-O atom (see Figure 5.8, c). A structure in which the heteroanion also acts as a bidentate ligand but with a μ_3-O atom is only about 1 (M = Mo) and 3 kcal mol^{-1} (M = W) higher in energy (Figure 5.8, d). For $[XM_2O_8(OH)_2]^-$ (H-M4), with an extra H^+ with respect to the previous stoichiometry, the lowest-energy structure for all the species, except for M = W and X = As, shows now the heteroanion coordinated to the metal in a monodentate fashion without any μ_3-O atom (Figure 5.8, i). For $[AsW_2O_8(OH)_2]^-$ a most compact structure with a μ_3-O atom is predicted to be the most stable one (Figure 5.8, j). For the other three species, this last structure

UNIVERSITAT ROVIRA I VIRGILI
ASSEMBLY AND PROPERTIES OF POLYOXOMETALATES: A THEORETICAL POINT OF VIEW
Laia Vilà Nadal
ISBN.978-84-694-2170-3/DL:T. 1039-2011

is only less than 3 kcal mol^{-1} less stable than the minimum. Finally, for $[XM_2O_9]^-$ (H-M3), compact and closed structures are by far much more stable than open and linear ones. The most stable structures show the heteroanion acting as a tri- or bidentate ligand yielding fairly compact structures which can be open or closed as a ring (Figure 5.8, e and f). A structure with a μ_3-O atom and the heteroanion acting as a tridentate ligand shows somewhat higher energies, which range between 3 and 6 kcal mol^{-1} depending on the species in consideration (Figure 5.8, j).

Car–Parrinello simulations in combination with the metadynamics approach have been also performed to analyze the formation of the heterotrimers. The system was built up by one $[W_2O_6(OH)]^-$ dimer, one $[PO_2(OH)_2]^-$ heteroanion and 58 H_2O molecules. The coordination number of the W ions with respect to the O atoms of the phosphate was selected as collective variable. Standard Car–Parrinello simulations previous to the metadynamics already show that the heterotrimer is formed when the nucleophilic O atom of the $[PO_2(OH)_2]^-$ heteroanion attacks to one of the W^{VI} ions of the $[W_2O_6(OH)]^-$ dimer. As a consequence, the barrier for this process will be small. Hydration of the dimer was previously observed as well. So, the W^{VI} ions want to expand their coordination sphere so as to get to pseudo-octahedral environment. A 30-ps metadynamics run (see Annex B for details) shows that attack of the OH group of the heteroanion to the electrophilic W^{VI} ion of the dihydrated $[W_2O_6(OH)]^-$ dimer (**4c+1w-4c+1w**) is not so effective (i.e. fast) as that of the oxo group in good agreement with its lower nucleophilicity. After 6.5 ps, the heterotrimer is formed (see Figure 5.9). The estimation of the free-energy barrier for this process is 13 kcal mol^{-1}. At this point, one of the W^{VI} ions shows a coordination number of six and the other a coordination number of five. The P atom remains as four coordinated during

the whole trajectory. A new hydration is observed at 9 ps, the second W^{VI} ion becoming six-coordinated as well (see structure on the upper left corner in Figure 5.9). Intramolecular H-bonds are effective involving (i) H atoms of the coordinated H_2O molecules and the O atoms coordinated to the other W^{VI} ion; or (ii) OH groups of W^{VI} and the O atoms of the heteroanion. This very-stable species lasts for more than 13 ps. At 22.5 ps, a structure with the heteroanion acting as a bidentate ligand is observed enlarging the coordination of one of the W^{VI} ions up to seven (see structure on the down right corner in Figure 5.9). This structure lasts for around 1 ps. Afterwards, the previous so-stable structure is formed again until the bond with the PO_4 groups is broken and the hydrated dimer regenerated (at around 30 ps). The barrier for the breaking of this W−O(P) bond is predicted to be of 29 kcal mol^{-1}. From a metadynamics run on the system built up by one $[W_2O_6(OH)]^-$ dimer, one $[WO_3(OH)]^-$ monomer and 58 H_2O molecules we have also analyzed the formation and stability of the isotrimer. We predict an almost negligible formation barrier and a stability comparable to the heterotrimer, albeit somewhat lower (around 2 kcal mol^{-1}) in good agreement with experiments.

UNIVERSITAT ROVIRA I VIRGILI
ASSEMBLY AND PROPERTIES OF POLYOXOMETALATES: A THEORETICAL POINT OF VIEW
Laia Vilà Nadal
ISBN.978-84-694-2170-3/DL:T. 1039-2011

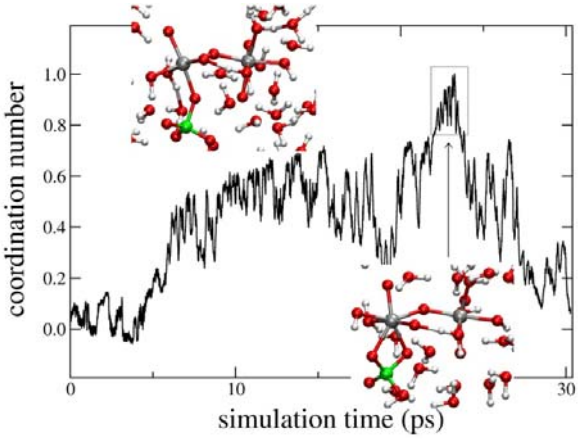

Figure 5.9. Evolution of the coordination number $C_{W-O(P)}$ along the trajectory of the metadynamics run for the system formed by one $[W_2O_6(OH)]^-$ dimer, one $[PO_2(OH)_2]^-$ heteroanion and 58 H_2O molecules.

Once the heterotrimers are formed, aggregation of a new $[WO_3(OH)]^-$ monomer is postulated by mechanisms H-M3 and H-M4. The formed species, $[XM_3O_{12}(OH)]^{2-}$ and $[XM_3O_{11}(OH)_3]^{2-}$, would lead to the observed ESI-MS stoichometries $[XM_3O_{12}]^-$ and $[XM_3O_{11}(OH)_2]^-$, respectively, after one step of protonation and water condensation (see H-M3 and H-M4). Now we have only analyzed the case M = W. As for lower nuclearity stages, we have performed an exhaustive study considering a large number of structures for each of these stoichiometries. In particular, nine for $[XW_3O_{12}(OH)]^{2-}$ (H-M3), thirteen for $[XW_3O_{12}]^-$ (H-M3), twelve for $[XW_3O_{11}(OH)_3]^{2-}$ (H-M4), and thirteen for $[XW_3O_{11}(OH)_2]^-$ (H-M4). As in the previous case, the initial structures have been generated by chemical intuition and with the help of the metadynamics technique. All these structures along with their relative energies are shown in Annex B: Figures 15-18 and Tables 6-19. For $[XW_3O_{12}(OH)]^{2-}$ (H-M3), the lowest-energy structure shows a μ_3-O bridging atom within a planar W_3 motif (see Figure 10, a), which has been shown to be very stable.[12] This structure, in

UNIVERSITAT ROVIRA I VIRGILI
ASSEMBLY AND PROPERTIES OF POLYOXOMETALATES: A THEORETICAL POINT OF VIEW
Laia Vilà Nadal
ISBN.978-84-694-2170-3/DL:T. 1039-2011

which the heteroanion is acting as a bidentate ligand, is by far the most stable among those that we have computed (more than 10 kcal mol^{-1} for X = P). Different positions and orientations of the H atom on the two terminal O atoms of the heteroanion yield to almost-degenerate structures (see Figure 17 and Table 8 in the Annex B). For $[XW_3O_{12}]^-$ (H-M3), the lowest-energy structure presents a μ_4-O bridging atom with the heteroanion acting as a tridentate ligand (see Figure 5.10, b).

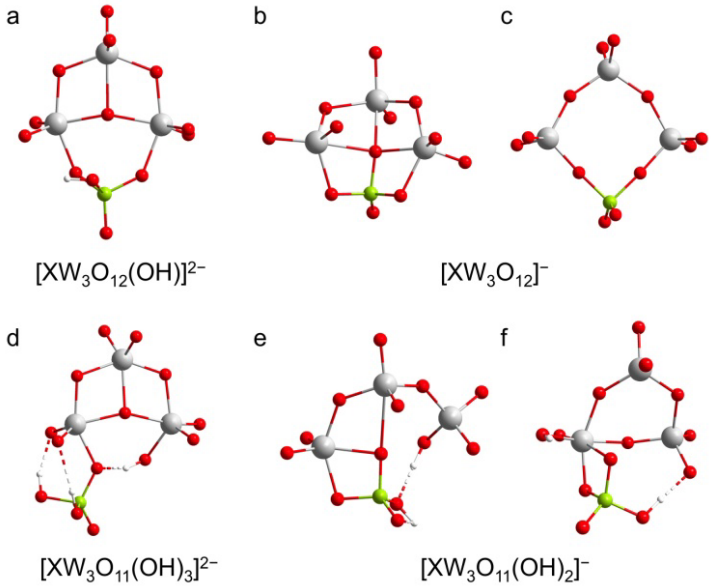

Figure 5.10. Lowest-energy structures at BP86/COSMO level for heterotetramers with $[XW_3O_{12}(OH)]^{2-}$ (H-M3), $[XW_3O_{12}]^-$ (H-M3), $[XW_3O_{11}(OH)_3]^{2-}$ (H-M4), and $[XW_3O_{11}(OH)_2]^-$ (H-M4) stoichiometries.

Another closed cyclic structure that is not so compact as the previous one (see Figure 5.10, c) shows somewhat higher energies (around 5 kcal mol^{-1} for both X = P and As). Other more tensioned compact structures are at least 10 kcal mol^{-1} higher in energy. The linear structures are even more unstable

UNIVERSITAT ROVIRA I VIRGILI
ASSEMBLY AND PROPERTIES OF POLYOXOMETALATES: A THEORETICAL POINT OF VIEW
Laia Vilà Nadal
ISBN.978-84-694-2170-3/DL:T. 1039-2011

(see Annex B, Table 9 and Figure 18). Regarding to $[XW_3O_{11}(OH)_3]^{2-}$ (H-M4), the lowest-energy structure for both X = P and As also shows a μ_3-O bridging atom within a planar W_3 motif (see Figure 5.10, d). The heteroanion is acting as a monodentate ligand forming hydrogen bonds with the W_3 motif. This structure is by far the most stable among all those that we have computed (around 13 and 20 kcal mol^{-1} for X = P and As, respectively). Finally, for $[XW_3O_{11}(OH)_2]^-$ (H-M4) the two most-stable structures are also depicted in Figure 5.10 (e and f). These two structures show an energy difference of around 4 kcal mol^{-1} for X = P, but they are quasidegenerate for X = As. In both of them, the heteroanion is acting as a bidentate ligand. The most important difference is that the most stable structure presents a μ_3-O bridging atom involving the heteroanion (Figure 5.10, e). Other symmetric and compact structures are found within less than 10 kcal mol^{-1} compared to the most-stable one (see structure 4 in Annex B Figure 16). As a general trend, the heteroatom is tetracoordinated in all the structures with the lowest energies among the different stoichiometries that we have analyzed here.

Aggregation of another $[MO_3(OH)]^-$ monomer to the $[XM_3O_{12}]^-$ species (H-M3), followed by protonation and dehydration, would justify the ESI peak corresponding to $[XM_4O_{15}]^-$. Similar steps would follow to finally lead, after a total of 10 protonations and 12 dehydrations, to the Keggin anion. Peaks corresponding to higher nuclearities in the $[XM_xO_{3x+3}]^-$ series (x = 5 and 6) have been detected in previous ESI-MS experiments.[20] These species, not observed here, might have been fragmented at our experimental settings. To conclude, we would like to point out that the heteropolynuclear species formed in the early steps of the nucleation process, which we have analyzed in detail here, might develop not only to the Keggin anion, but also to other heteroPOMs such as the Dawson, $[P_2W_{18}O_{62}]^{6-}$, or the Preyssler,

UNIVERSITAT ROVIRA I VIRGILI
ASSEMBLY AND PROPERTIES OF POLYOXOMETALATES: A THEORETICAL POINT OF VIEW
Laia Vilà Nadal
ISBN.978-84-694-2170-3/DL:T. 1039-2011

$[NaP_5W_{30}O_{110}]^{14-}$, depending on the particular experimental reaction conditions, i.e. temperature, solvent, pH, counterions, etc. (Figure 5.11). In fact, the peak corresponding to $[XM_3O_{12}]^-$ has been detected in ESI-MS experiments on the Dawson anion as well as in some of its lacunary derivatives.[19]

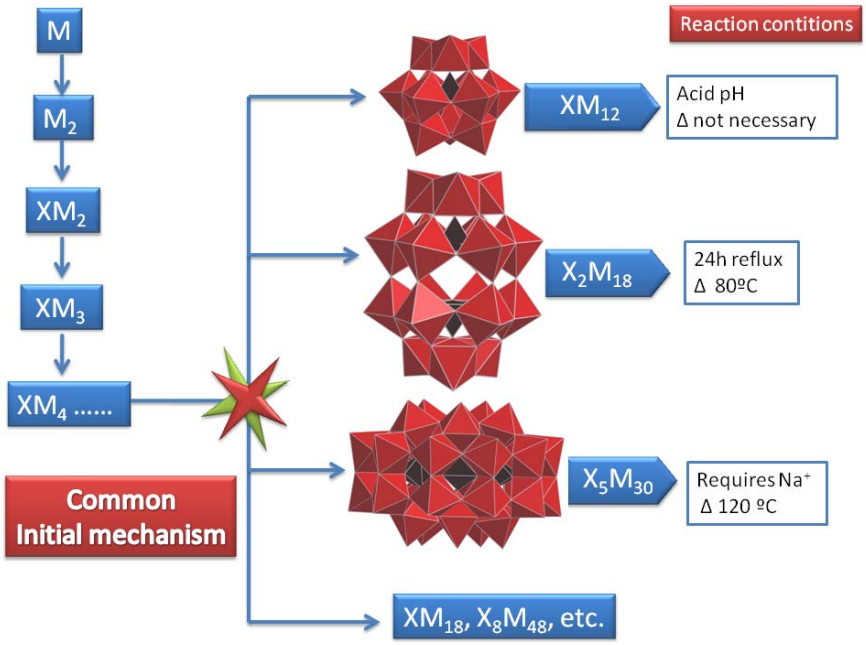

Figure 5.11. Schematic representation of the formation mechanisms of heteropolyanions sharing common initial steps: the Keggin $[PW_{12}O_{40}]^{3-}$, Dawson $[P_2W_{18}O_{62}]^{6-}$, and Preyssler $[NaP_5W_{30}O_{110}]^{14-}$ anions.

5.5. Conclusions

We have studied the first steps of nucleation of the Keggin anions using the complimentary combination of DFT methodologies with ESI-MS assembly and fragmentation experiments and have proposed plausible mechanisms for their

UNIVERSITAT ROVIRA I VIRGILI
ASSEMBLY AND PROPERTIES OF POLYOXOMETALATES: A THEORETICAL POINT OF VIEW
Laia Vilà Nadal
ISBN.978-84-694-2170-3/DL:T. 1039-2011

formation. As previously described for the Lindqvist anion,[12a] we postulate that once the dinuclear species have been formed, successive steps of protonation and water condensation with subsequent aggregation occur to justify the clusters observed in the ESI-MS experiments. We propose that the heteroanion, $[XO_2(OH)]^{2-}$, is not incorporated to the polyanion in the first step of the nucleation, i.e. forming a heterodimer, but in a later step. Once the heterotrimer is formed, the heteroanion acts as a template for the formation of the Keggin anion. The structure and stability of different possible intermediates in the first steps of the formation of the Keggin anion according to our proposed mechanisms have been analyzed in detail. In general, no significant differences are found when changing the metal atom (W or Mo) or the heteroatom (P or As), except that arsenometalate heterodimers might be competitive with isodimers at low pH conditions. Small differences among the lowest-energy structures are also detected. Compact geometries with a four-coordinated heteroatom are among the most stable structures for the different stoichiometries studied. Car–Parrinello simulations show that the coordination sphere of W^{VI} ions might be expanded up to six-coordination with water molecules, as observed in the isopolyanions. The barriers for the first nucleation steps are predicted to be low. In summary, the present study on the nucleation mechanisms of heteropolyanions, which complements the previous work on the Lindqvist anion, is a new step towards the rationalization of the complex processes that take place in the formation of such a family of molecular oxides.

UNIVERSITAT ROVIRA I VIRGILI
ASSEMBLY AND PROPERTIES OF POLYOXOMETALATES: A THEORETICAL POINT OF VIEW
Laia Vilà Nadal
ISBN.978-84-694-2170-3/DL:T. 1039-2011

References and Notes

[1] D.L. Long, R. Tsunashima, L. Cronin, *Angew. Chem. Int. Ed.*, **2010**, 49, 1736.

[2] a) S. Sato, J. Iida, K. Suzuki, M. Kawano, T. Ozeki, M. Fujita, *Science*, **2006**, 313, 1273. b) P. Mal, B. Breiner, K. Rissanen, J.K. Nitschke, *Science*, **2009**, 324, 1697. c) P.N.W. Baxter, in *Comprehensive Supramolecular Chemistry*, Vol. 9, J.L Atwood, J.E.D. Davies, D.D. MacNicol, F. Vögtle, Eds. (Pergamon/Elsevier,New York, **1996**), 165.

[3] a) H.K. Chae, D.Y. Siberio-Pérez, J. Kim, Y. Go, M. Eddaoudi, A.J. Matzger, M. O'Keeffe, O.M. Yaghi, *Nature*, **2004**, 427, 523. b) R. Matsuda, R. Kitaura, S. Kitagawa, Y. Kubota, R.V. Belosludov, T.C. Kobayashi, H. Sakamoto, T. Chiba, M. Takata, Y. Kawazoe, Y. Mita, *Nature*, **2005**, 436, 238.

[4] B.J. Holliday, C.A. Mirkin, *Angew. Chem. Int. Ed.*, **2001**, 40, 2022.

[5] L.C.W. Baker, J.S. Figgis, *J. Am. Chem. Soc.,* **1970**, 92, 3794.

[6] L. Lisnard, A. Dolbecq, P. Mialane, J. Marrot, F. Sécheresse, Inorg. *Chim. Acta*, **2004**, 357, 845.

[7] T. McGlone, C. Streb, D.-L. Long, L. Cronin, *Chem.-Asian. J.*, **2009**, 4, 1612.

[8] H.N. Miras, J. Yan, D.L. Long, L. Cronin, *Angew. Chem. Int. Ed.*, **2008**, 47, 8420.

[9] M.T. Pope, A. Müller, *Angew. Chem. Int. Ed.*, **1991**, 30, 34.

[10] a) C. Baffert, J.F. Boas, A.M. Bond, P. Kögerler, D.L. Long, J.R. Pilbrow, L. Cronin, *Chem. Eur. J.*, **2006**, 12, 8472. b) I.M. Mbomekall, X. López, J.M. Poblet, F Sécheresse, B. Keita, L. Nadjo, *Inorg. Chem.*, **2010**, 49, 7001.

[11] L.C.W. Baker, V.E.S. Baker, G.A. Candela, A.H. Kahan, S.H. Wasfi, *J. Chem. Phys.*, **1972**, 56, 4917.

[12] X. López, J.M. Poblet, *Inorg. Chem.*, **2004**, 43, 6863.

[13] a) L. Vilà-Nadal, A. Rodríguez-Fortea, L.K. Yan, E.F. Wilson, L. Cronin, J.M. Poblet, *Angew. Chem. Int. Ed.*, **2009**, 48, 1. b) L. Vilà-Nadal, A. Rodríguez-Fortea, J.M. Poblet, *Eur. J. Inorg. Chem.* **2009**, 5125.

[14] X. López, J.A. Fernández, S. Romo, J.F. Paul, L. Kazansky, J.M. Poblet, *J. Comp. Chem.*, **2004**, 12, 1542.

[15] a) M. Iannuzzi, A. Laio, M. Parrinello, *Phys. Rev. Lett.* **2003**, 90, 238302. b) A. Laio, M. Parrinello, *Proc. Natl. Acad. Sci. U.S.A.* **2002**, 99, 12562. c) A. Laio, A. Rodriguez-Fortea, F.L.Gervasio, M. Ceccarelli, M. Parrinello, *J. Phys. Chem. B* **2005**, 109, 6714.

[16] a) A. Rodríguez-Fortea, L. Vilà-Nadal, J.M. Poblet, *Inorg. Chem.* **2008**, 47, 7745. b) X. Biarnes, A. Ardèvol, A. Planas, C. Rovira, A. Laio, M. Parrinello, *J. Am. Chem. Soc.* **2007**, 129, 10686. c) J. Blumberger, B. Ensing, M.L. Klein, *Angew. Chem. Int. Ed.* **2006**, 45, 2893. d) A. Rodríguez-Fortea, M. Iannuzzi, *J. Phys. Chem. C* **2008**, 112, 19642. e) A. Rodríguez-Fortea, M. Iannuzzi, M. Parrinello, *J. Phys. Chem. C* **2007**, 111, 2251. f) A. Rodríguez-Fortea, M. Iannuzzi M. Parrinello, *J. Phys. Chem. B* **2006**, 110, 3477. g) A. Stirling, M. Iannuzzi, M. Parrinello, F. Molnar, V. Bernhart, G. A. Luinstra, *Organometallics* **2005**, 24, 2533.

UNIVERSITAT ROVIRA I VIRGILI
ASSEMBLY AND PROPERTIES OF POLYOXOMETALATES: A THEORETICAL POINT OF VIEW
Laia Vilà Nadal
ISBN.978-84-694-2170-3/DL:T. 1039-2011

[17] M.T. Ma, T. Waters, K. Beyer, R. Palamarczuk, P.J.S. Richardt, R.A. J. O'Hair, A. G. Wedd, *Inorg. Chem.*, **2009**, 48, 598.

[18] a) T. Waters, X. Huang, X.B. Wang, H.K. Woo, R.A.J. O'Hair, A.G. Wedd, L.S. Wang, *J. Phys. Chem. A*, **2006**, 110, 10737. b) H.J. Zhai, X. Huang, T. Waters, X.B. Wang, R.A.J O'Hair, A.G. Wedd, L.S.Wang, *J. Phys. Chem. A*, **2005**, 109, 10512. c) L.S Wang, X.B. Wang, *J. Phys. Chem. A*, **2000**, 104, 1978.

[19] a) C. Rocchiccioli-Deltcheff, M. Fournier, R. Franck, R. Thouvenot, *Inorg. Chem.* **1983**, 22, 207. b) E.O. North, *Inorg. Synth.* **1939**, 1, 132. c) C. Sanchez, J. Livage, J. P. Launay, M. Fournier, Y. Jeanin, *J. Am. Chem Soc.* **1982**, 104, 3194.

[20] a) M.T. Ma, T. Waters, K. Beyer, R. Palamarczuk, P.J.S. Richardt, R.A. J. O'Hair, A.G. Wedd, *Inorg. Chem.* **2009**, 48, 598. b) C. Boglio, G. Lenoble, C. Duhayon, B. Hasenknopf, R. Thouvenot, C. Zhang, R.C. Howell, B.P. Burton-Pye, L.C. Francesconi, E. Lacôte, S. Thorimbert, M. Malacria, C. Afonso, J.C. Tabet, *Inorg. Chem.* **2006**, 45, 1389.

UNIVERSITAT ROVIRA I VIRGILI
ASSEMBLY AND PROPERTIES OF POLYOXOMETALATES: A THEORETICAL POINT OF VIEW
Laia Vilà Nadal
ISBN.978-84-694-2170-3/DL:T. 1039-2011

UNIVERSITAT ROVIRA I VIRGILI
ASSEMBLY AND PROPERTIES OF POLYOXOMETALATES: A THEORETICAL POINT OF VIEW
Laia Vilà Nadal
ISBN.978-84-694-2170-3/DL:T. 1039-2011

Chapter 6

Isomerism of the Wells–Dawson Anion: α, β, γ and α*, β*, γ*

UNIVERSITAT ROVIRA I VIRGILI
ASSEMBLY AND PROPERTIES OF POLYOXOMETALATES: A THEORETICAL POINT OF VIEW
Laia Vilà Nadal
ISBN.978-84-694-2170-3/DL:T. 1039-2011

"Science is always wrong. It never solves a problem without creating ten more."

G. Bernard Shaw,
Timeline Book of Science, 1995.

UNIVERSITAT ROVIRA I VIRGILI
ASSEMBLY AND PROPERTIES OF POLYOXOMETALATES: A THEORETICAL POINT OF VIEW
Laia Vilà Nadal
ISBN.978-84-694-2170-3/DL:T. 1039-2011

Chapter 6

Isomerism of the Wells–Dawson Anion: α, β, γ and α^*, β^*, γ^*

From the structural point of view, POMs are highly ordered clusters with an additional richness arising from the existence of various isomeric forms in some cases, notably in the common $[XM_{12}O_{40}]^{q-}$ *Keggin and* $[X_2M_{18}O_{62}]^{q-}$ *Wells–Dawson (WD) structures. Isomerism in POMs has been largely studied and their properties deeply analyzed experimentally and computationally, although some basic points are still not completely clear. The main interest on isomerism is related to the possibility of tuning some properties with controlled geometrical changes, such as the different location of a given atom (positional isomerism) or a rotation of a fragment of the molecule (rotational isomerism). In a different way from the previous chapters, mainly based in the assembly of POMs, here we have focused our efforts in understanding the rotational isomerism of the Wells–Dawson anion. Its structure is larger than that of the Keggin anion with a general formula of* $[X_2M_{18}O_{62}]^{n-}$ *and six isomers have been predicted (a, β, γ,* α^*, β^*, γ^**). The initial part of the chapter is devoted to explain the geometric differences between the isomers, later we will analyze their stability studying different heteroanions (X=P, As, S,…) when the metal M=W. Afterwards we discuss the stability of these new classes of Dawson-like clusters* $\{W_{18}X\}$.

UNIVERSITAT ROVIRA I VIRGILI
ASSEMBLY AND PROPERTIES OF POLYOXOMETALATES: A THEORETICAL POINT OF VIEW
Laia Vilà Nadal
ISBN.978-84-694-2170-3/DL:T. 1039-2011

6.1. Introduction

As we have described in previous chapters, the Keggin structure has twelve equivalent metal centers in its α form presenting a T_d symmetry. In the middle 40's A. F. Wells[1] postulated the structure for the α–$[P_2W_{18}O_{62}]^{6-}$ anion. Afterwards in 1953, B. Dawson reported the first (low-resolution) X-ray experiment for the same anion.[2] More accurate results to determine the structure were later performed by Strandberg[3] and D'Amour.[4] The compound is nowadays generally formulated as $[X_2M_{18}O_{62}]^{n-}$. At variance to the fully regular Keggin anion, the eighteen metal centers are not fully equivalent. Hence it is established that $[X_2M_{18}O_{62}]^{n-}$ structure is formed by two M_3 rings, located at the polar regions, are also called *caps*, (see red and blue octahedra in Figure 6.1) and two M_6 rings are located at the equatorial region, forming the *belt* (green and purple octahedra in Fig. 6.1).

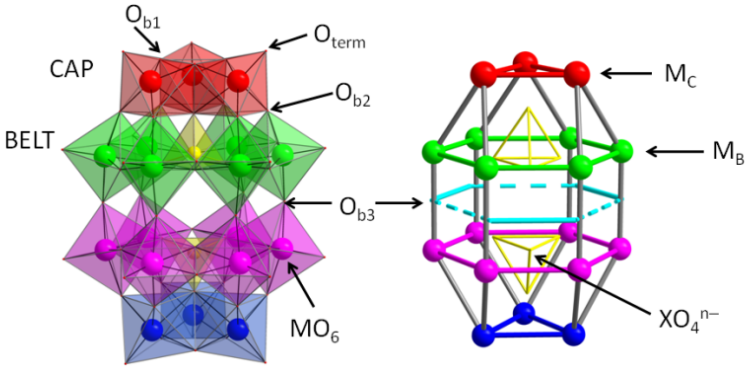

Figure 6.1. Left: polyhedral representation of the α–$X_2W_{18}O_{62}^{n-}$ Wells–Dawson anion. Right: rationalization of the 18-metal centered α–Wells–Dawson structure. Two identical fragments or hemispheres are easily identifiable, each composed of one $[M_3O_6]$ triad (red and blue, named CAP) and one $[M_6O_{18}]$ equatorial belt with six WO_6 octahedra (green and purple, named BELT). $[M_6O_{18}]$ units are interconnected by six oxygens in turquoise, a solid line represents the short $O_{b3}\cdots O_{b3}$ distance around 3Å, whereas a dashed line represents a larger distance about 4.2 Å. In both cases XO_4^{n-} units are represented as yellow octahedra. Relevant positions are labelled for further discussion.

UNIVERSITAT ROVIRA I VIRGILI
ASSEMBLY AND PROPERTIES OF POLYOXOMETALATES: A THEORETICAL POINT OF VIEW
Laia Vilà Nadal
ISBN.978-84-694-2170-3/DL:T. 1039-2011

Each of the equatorial octahedra is connected to a polar octahedron by a single corner and it shares one edge with a neighbour of the same belt and a corner to the other belt. Two XO_4^{n-} units are encapsulated inside the formally neutral $M_{18}O_{54}$ cage,[5] containing the greater part of the negative charge of the POM. The structural characterisation of the WD anion is compatible with a D_{3h} point group of symmetry. From the information provided here concerning the nature of the assembly of the octahedra in the WD framework, not only a geometrical distinction but a chemical one can be made for the two different regions of the structure. All over this chapter, we have often used a short-hand notation, in which the formula of the anion is represented without oxygen atoms and charge; for example α–As_2W_{18} represents the α–$[As_2W_{18}O_{62}]^{6-}$ anion. The WD derivative may be seen as a derivative of the Keggin structure as follows. The removal of three neighbouring corner-sharing octahedra in, say, α–PW_{12}, produces a lacunary structure, formulated as Aα-PW_9, which is ready to join another equivalent moiety to produce the α–P_2W_{18} assembly (Figure 6.2).

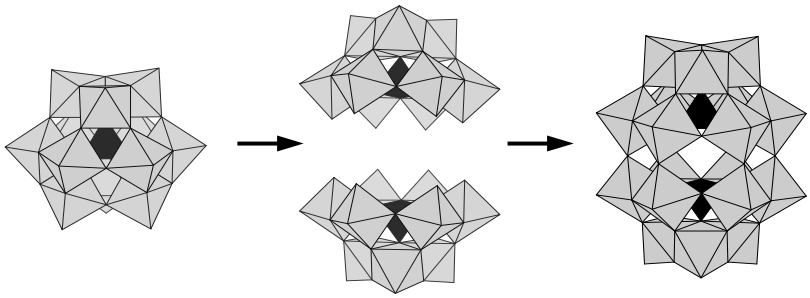

Figure 6.2. Build-up process from the α-Keggin to the A-α-Wells-Dawson structure. Gray octahedra are MO_6 units (M = W, Mo), and black tetrahedra are XO_4 anions.

Dawson structure derive from the phosphotungstate and molybdate anions, $[P_2M_{18}O_{62}]^{6-}$ (P_2M_{18}, M = W, Mo).

UNIVERSITAT ROVIRA I VIRGILI
ASSEMBLY AND PROPERTIES OF POLYOXOMETALATES: A THEORETICAL POINT OF VIEW
Laia Vilà Nadal
ISBN.978-84-694-2170-3/DL:T. 1039-2011

Compounds containing As or S instead of P have also been reported (Table 6.1 for further detail and references). The electronic structure of the Dawson anion is such that the first unoccupied molecular orbital (LUMO) is delocalized over the equatorial region.[6] On the other hand, the first virtual orbital located on the cap region has been computed to be at 0.85 eV from the lowest energy one.[7] Multiple metal substitutions can be carried out on the original structure.

6.2. Wells–Dawson isomerism

Six isomers for the $[X_2M_{18}O_{62}]^{6-}$ anion ($X=As^V$, P^V; $M=Mo^{VI}$, W^{VI}) were postulated in the 1970 by Baker and Figgis, depicted in Fig. 6.3 and named α, β, γ and α*, β*, γ*. The α–$[X_2M_{18}O_{62}]^{6-}$ anion is built up from two A-α-XM_9O_{34} half units joined by six common oxygen atoms, the structure belonging to D_{3h} point group.[8]

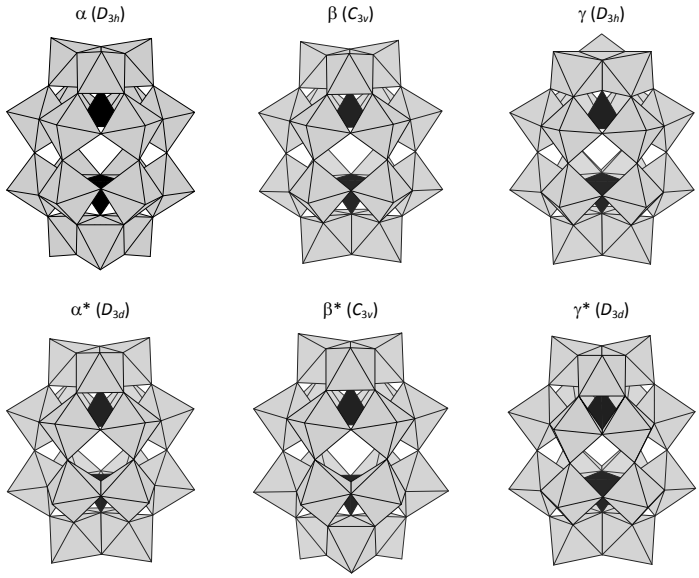

Figure 6.3. The six rotational isomers of the Dawson structure. Top: α, β, γ. Bottom: α*, β*, γ*.

UNIVERSITAT ROVIRA I VIRGILI
ASSEMBLY AND PROPERTIES OF POLYOXOMETALATES: A THEORETICAL POINT OF VIEW
Laia Vilà Nadal
ISBN.978-84-694-2170-3/DL:T. 1039-2011

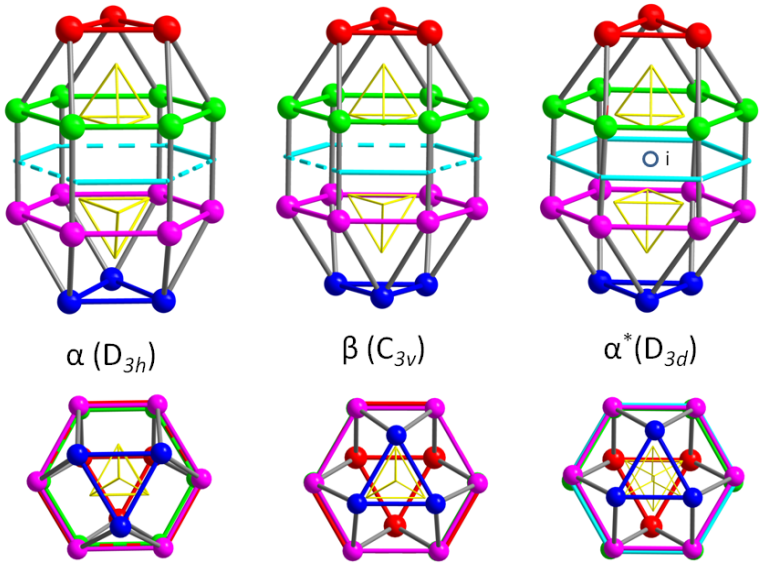

Figure 6.4. Top: rationalisation of the 18 metal-centered α, β and α* Wells–Dawson structures. Bottom: vision along the C_3 axis. In the α isomer both CAP (red and blue) triads appear eclipsed along the C_3. On the contrary, the CAP triads appear staggered in the β and α* isomers. This is due to a π/3 rotation of the blue CAP in the α isomer that leads to the β anion. Another rotation of the red CAP in the β isomer will derive in the γ isomer, not depicted here. The short–long alternation in the distances between the oxygens that interconnect both BELT units, depicted in turquoise, is maintained in the α, β and γ isomers. If both CAP-BELT, A-α-XM_9O_{34} subunits are related through an inversion center "i", depicted in the figure, we obtain the α* isomer with a D_{3d} symmetry. In this case the distance alternation between central oxygens (turquoise) disappears. The same happens with β* and γ*, since the oxygens are related through the improper axis S_6. Like β and γ isomers, a π/3 rotation of the blue CAP in the α* isomer will lead to the β* and the rotation of both CAP (blue and red) to γ*. Note from the bottom figures, vision along the C_3 axis, that XO_4^{n-} yellow octahedral appear eclipsed in α, β, consequently in γ isomers, whereas are staggered in α* and subsequently in β*, γ*.

The β anion, see Fig. 6.4, derives from α isomer by a formal rotation by π/3 of a polar (cap) M_3O_{13} group: the symmetry is lowered to C_{3v}. The formal rotation by π/3 of the second polar M_3O_{13} group restores the symmetry plane and the point group D_{3h} for the γ isomer. In all these anions the hexagonal belts of both XM_9 moieties are symmetry related through the equatorial

UNIVERSITAT ROVIRA I VIRGILI
ASSEMBLY AND PROPERTIES OF POLYOXOMETALATES: A THEORETICAL POINT OF VIEW
Laia Vilà Nadal
ISBN.978-84-694-2170-3/DL:T. 1039-2011

horizontal plane and their twelve tungsten atoms appear eclipsed along the direction of the C_3.

If the two A-α-XM_9O_{34} subunits are related through an inversion center, as postulated by Wells[9] in 1945 for $P_2W_{18}O_{62}$, the resulting anion named α^* would belong to the D_{3d} point group. Rotation of one or both polar (cap) M_3O_{13} group of this α^* anion would generate the two remaining isomers, β^* (C_{3v}) and γ^* (D_{3d}) respectively. In this case the hexagonal belts of both XM_9 moieties are symmetry related through the inversion center. As depicted in Table 6.1, only α, β, γ and γ^* isomers have been detected and solved by X-ray.[10]

Table 6.1. Experimentally detected Dawson $[X_2M_{18}O_{62}]^{q-}$ isomers.

Isomer	M=Mo	M=W	Ref.
α	P, As, S	P, As	11, 12
β		P, As	13
γ		P, As	14
α^*			
β^*			
γ^*		As, S	15

UNIVERSITAT ROVIRA I VIRGILI
ASSEMBLY AND PROPERTIES OF POLYOXOMETALATES: A THEORETICAL POINT OF VIEW
Laia Vilà Nadal
ISBN.978-84-694-2170-3/DL:T. 1039-2011

6.3. Dawson cluster $\{W_{18}X_2\}$

In a previous study DFT calculations were used to analyze the relative stability of the α and β isomers of the Wells−Dawson (WD) heteropolyanions.[7] Here, we have extended that previous work towards γ and α*, β*, γ* isomers. Geometry optimizations performed on the six isomers of WD anion with the heteroatoms As, P, S led to structures listed in Table 6.4. All the isomers were computed under each correspondent symmetry constraints. For instance, α isomer of As_2W_{18} was computed under the constraints of D_{3h} symmetry group, whereas for the corresponding β isomer the symmetry of the molecule is C_{3v}, etc.

The reader will notice from Table 6.4 that the geometrical differences between isomers of the same formula are very small. Distances between O_{term}–M_c, O_{b1}–M_c and O_{b2}–M_c are maintained through all the isomers. The distance between $O_{b3}\cdots O_{b3}$ reproduces the short-long alternation in α, β, γ isomers. As it is discussed above these alternation disappears for isomers α* and γ*. Due to the presence of the heteroatom angle, M_c–O_{b1}–M_c is contracted, see the difference of 15º between α–W_{18} box and α–As_2W_{18}. On the contrary the variations for the angle M_b–O_{b3}–M_b are smaller, 5º when comparing W_{18} box.

Structural differences among isomers of the same formula are not significant, see Table 6.4, with differences ≤ 10º for angles and < 0.8 Å for distances.

Table 6.4. Computed angles (in deg) and interatomic distances (in Å) for series of fully oxidized α, β, γ, α*, β*, γ* Wells-Dawson anions.[a] We have computed $[W_{18}O_{54}]$ box without heteroatom and $[XW_{18}O_{54}]^{q-}$ (X=As, P, S).[b]

	Isomer and Symmetry		$M_c–O_{term}$	$M_c–O_{b1}$	$M_c–O_{b2}$	$O_{b3}\cdots O_{b3}$	$M_c–O_{b1}–M_c$	$M_b–O_{b3}–M_b$
α	W_{18}	D_{3h}	1.73	1.93	1.93	3.04–3.70	134.60	162.92
β	W_{18}	C_{3v}	1.73	1.94	1.92	3.90–3.92	119.12–119.60 [c]	162.45
γ	W_{18}	D_{3h}	1.73	1.93	1.93	3.04–3.71	134.55	162.90
α*	W_{18}	D_{3d}	1.74	1.94	1.92	3.76	122.49	170.75
β*	W_{18}	C_{3v}	1.73	1.92	1.92	3.09–3.66	137.72–134.47	163.16
γ*	W_{18}	D_{3d}	1.73	1.94	1.92	3.76	122.37	170.45
α	As_2W_{18}	D_{3h}	1.73	1.95	1.92	3.28–4.36	122.70	161.54
β	As_2W_{18}	C_{3v}	1.73	1.95	1.92	3.41–4.24	122.16–122.76	164.71
γ	As_2W_{18}	D_{3h}	1.73	1.95	1.93	3.54–4.06	123.94	168.41
α*	As_2W_{18}	D_{3d}	1.74	1.95	1.92	3.89	121.84	164.24
β*	As_2W_{18}	C_{3v}	1.73	1.95	1.92	3.68–4.01	123.78–121.48	165.30
γ*	As_2W_{18}	D_{3d}	1.73	1.95	1.92	3.82	124.78	168.46
α	P_2W_{18}	D_{3h}	1.73	1.95	1.92	3.09–4.28	124.18	163.14
β	P_2W_{18}	C_{3v}	1.73	1.95	1.92	3.25–4.17	123.71–124.06	167.24
γ	P_2W_{18}	D_{3h}	1.73	1.94	1.92	3.45–3.93	125.12	173.70
α*	P_2W_{18}	D_{3d}	1.73	1.94	1.92	3.74	123.08	171.21
β*	P_2W_{18}	C_{3v}	1.73	1.94	1.92	3.45–3.92	126.87–123.55	169.80
γ*	P_2W_{18}	D_{3d}	1.73	1.94	1.90	3.65	126.07	176.38
α	S_2W_{18}	D_{3h}	1.72	1.94	1.92	3.17–4.24	129.22	164.61
β	S_2W_{18}	C_{3v}	1.72	1.94	1.92	3.36–4.08	128.40–129.20	170.78
γ	S_2W_{18}	D_{3h}	1.72	1.94	1.92	3.59–3.85	129.91	176.25
α*	S_2W_{18}	D_{3d}	1.72	1.94	1.92	3.77	128.00	173.78
β*	S_2W_{18}	C_{3v}	1.72	1.94	1.92	3.52–3.95	128.12–131.22	171.10
γ*	S_2W_{18}	D_{3d}	1.72	1.94	1.92	3.72	130.51	176.86

[a] See Figure 6.1 for the notation of the metal and oxygen sites. [b] Geometry optimized BP86/SES. [c] Values for angle $M_c–O_{b1}–M_c$ in β and β* isomers appear duplicated due to non symmetric caps.

UNIVERSITAT ROVIRA I VIRGILI
ASSEMBLY AND PROPERTIES OF POLYOXOMETALATES: A THEORETICAL POINT OF VIEW
Laia Vilà Nadal
ISBN.978-84-694-2170-3/DL:T. 1039-2011

We will now discuss the structural properties and stability of α, β, γ and α*, β*, γ* isomers of the $[As_2W_{18}O_{62}]^{6-}$ anion. The results in Table 6.2 are relative to the most stable isomer in gas phase and also including the effect of the solvent through a continuum model. In both cases we have obtained the same stability trend being γ* the most stable isomer and α* the less stable. These results are consistent with the experimental observed species: γ* isomer has been detected while isomers α* and β* have not.

Table 6.2. Relative energies in kcal mol^{-1} with respect to the most stable $[As_2W_{18}O_{62}]^{6-}$ isomer.

Isomer	Symmetry	Solvent	Gas phase
α	D_{3h}	1.1	3.5
β	C_{3v}	2.4	3.9
γ	D_{3h}	0.6	1.2
α*	D_{3d}	16.5	17.5
β*	C_{3v}	6.5	6.9
γ*	D_{3d}	0.0	0.0

We have also studied how stability of the isomer can be modulated by the presence of different heteroatoms. As a first step, we have evaluated the relative stability of the isomers considering only the $[W_{18}O_{54}]$ box without the internal anions $[(XO_4)_2]^{q-}$. As shown in Table 6.3, there are two groups with different stability order: isomers α, γ, β* and around 3 kcal mol^{-1} less stable we have isomers β, α* and γ*.

Table 6.3. Relative energies in kcal mol^{-1} with respect to the most stable isomer for $[W_{18}O_{54}(XO_4)_2]^{q-}$ where X= As, P and S, compared to $[W_{18}O_{54}]$ box.

Isomer	Symmetry	[a] $[W_{18}O_{54}]$	[b] $[W_{18}O_{54}(AsO_4)_2]^{6-}$	[b] $[W_{18}O_{54}(PO_4)_2]^{6-}$	[b] $[W_{18}O_{54}(SO_4)_2]^{4-}$
α	D_{3h}	0.3	1.1	0.0	0.0
β	C_{3v}	3.3	2.4	5.2	3.6
γ	D_{3h}	0.0	0.6	5.4	3.7
α*	D_{3d}	3.3	16.5	22.1	16.7
β*	C_{3v}	0.1	6.5	12.6	7.0
γ*	D_{3d}	3.3	0.0	7.5	1.9

[a] Geometry optimized BP86, in gas phase. [b] Geometry optimized BP86/SES

UNIVERSITAT ROVIRA I VIRGILI
ASSEMBLY AND PROPERTIES OF POLYOXOMETALATES: A THEORETICAL POINT OF VIEW
Laia Vilà Nadal
ISBN.978-84-694-2170-3/DL:T. 1039-2011

The relative stability of the polyoxometalate isomers is significantly altered after encapsulating the two $[XO_4]$ anions. When X= As, $[As_2W_{18}O_{62}]^{6-}$, the relative energy of the four isomers γ^*, γ, α and β was found to differ in less than 2.5 kcal mol^{-1}. Indeed, these four isomers have been characterized experimentally (see Table 6.1). Isomer β^* appears at 6.5 kcal mol^{-1} above isomer γ^*, which is the lowest-energy anion.

For $[P_2W_{18}O_{62}]^{6-}$ the results are slightly different: here the most stable isomer comes to be α, that differs around 5 kcal mol^{-1} from isomers β and γ. In this case the stability order $\alpha>\beta>\gamma$, again agrees with the experimentally obtained isomers. Finally, for the case with X=S, we have found that the stability order is $\alpha>\gamma^*>\beta>\gamma$. In fact, γ^* is the only isomer experimentally resolved for the Dawson tetranion $[S_2W_{18}O_{62}]^{4-}$. Knowing that isomers α and γ^* have a difference of only 1.9 kcal mol^{-1}, we can expect a thermodynamically favorable synthesis of α–$[S_2W_{18}O_{62}]^{4-}$. A graphical representation of the relative energies of the isomers is given in Figure 6.5.

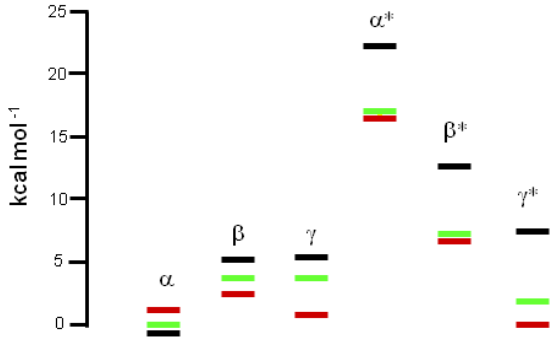

Figure 6.5. Graphical representation of relative energies with respect to the most stable isomer for $[W_{18}O_{54}(XO_4)_2]^{q-}$ where X= As (red), P (black) and S (green).

As a final point, we have also compared the HOMO–LUMO gaps for several isomers, as shown in Figure 6.6 for the case of

UNIVERSITAT ROVIRA I VIRGILI
ASSEMBLY AND PROPERTIES OF POLYOXOMETALATES: A THEORETICAL POINT OF VIEW
Laia Vilà Nadal
ISBN.978-84-694-2170-3/DL:T. 1039-2011

$[As_2W_{18}O_{62}]^{6-}$. As it is common for totally oxidized POMs, the HOMO orbitals correspond to oxygen atoms and LUMO orbitals correspond to metal atoms. When X=As the HOMO–LUMO gap is around 2.2 eV for all isomers, the same trend was observed when X = P and S, the results are not presented here. (see Annex D for more details)

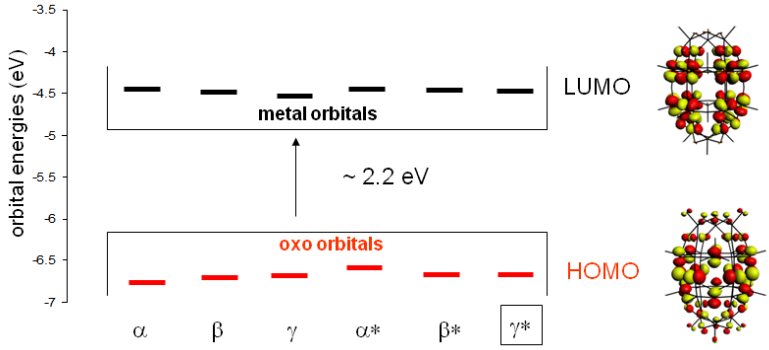

Figure 6.6. Graphical representation of HOMO and LUMO orbital energies for the six isomers α, β, γ, α*, β*, γ* when X=As, $[As_2W_{18}O_{62}]^{6-}$. As an example, we have also depicted 3D orbitals for isomer γ* (D_{3d}): HOMO (orbital of symmetry A_{2u}, mainly composed of p-oxygen orbitals delocalized over oxygen bridge, belt and terminal atoms) and LUMO (orbital of A_{1u} symmetry, mainly composed of d-metal orbitals delocalized over the metal belt atoms).

6.4. Dawson-like clusters $\{W_{18}X\}$

Conventionally, redox-inactive anions, such as SO_4^{2-} and PO_4^{3-}, are often used as templating anions in the formation of many POM clusters. A strategy to create new functional POMs involves the encapsulation of redox-active templates instead. By utilizing sulfite, selenite, tellurite, and periodate anions as templates, several new types of redox-active heteropolyoxometalates have been isolated. The POM cluster $[M_{18}O_{54}(SO_3)_2]^{3-}$ (M=W, Mo), which contains two embedded

UNIVERSITAT ROVIRA I VIRGILI
ASSEMBLY AND PROPERTIES OF POLYOXOMETALATES: A THEORETICAL POINT OF VIEW
Laia Vilà Nadal
ISBN.978-84-694-2170-3/DL:T. 1039-2011

redox-active sulfite templates, can be activated by a metallic surface and can reversibly interconvert between two electronic states.[16] Both templates can be replaced by a single template located in the centre of the cluster to give a Dawson-like $\{W_{18}X\}$ POM.[17] The first member of this family to be discovered was actually an isopolyanion $\{W_{19}\}$ with a Dawson-type cage; the nineteenth tungsten is located at the centre of the cluster instead of the two tetrahedral heteroatoms that are usually found inside conventional Dawson clusters.[18] Structural analysis of the cluster shows that the nineteenth tungsten could be replaced by other elements, such as Pt^{IV}, Sb^{V}, Te^{VI}, or I^{VII}. The POMs β^*-$[H_3W_{18}O_{56}(IO_6)]^{6-}$ embedded with high-valent iodine[19] and γ^*-$[H_3W_{18}O_{56}(TeO_6)]^{7-}$ that captures the tellurate anion TeO_6^{6-} were discovered thereafter (Figure 6.7).[20]

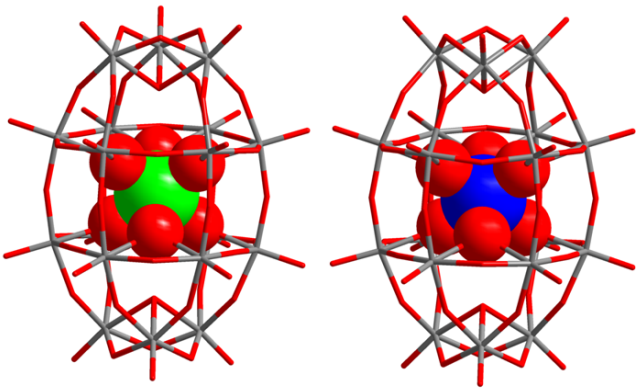

Figure 6.7. Structures of the new Dawson-like $\{W_{18}X\}$ POM type, the $\{W_{18}\}$ cages are shown as sticks and the central $\{XO_6\}$ group is represented as space filling model. Left: γ^*–$[W_{18}O_{56}(XO_6)]^{10-}$ X=W^{VI} and Te^{VI}. Right: β^*–$[W_{18}O_{56}(IO_6)]^{9-}$ being the first example of β^* isomer.

It is worth mentioning, that the presence of the $[IO_6]$ unit inside the $\{W_{18}\}$ cage is able to stabilize the β^* cage, which was found rather high in energy in conventional Dawson anions. The fully analysis of isomerism in these Dawson-like anion is much more complex because of the presence of protons. Redox properties and their influence in the isomer stability is also an interesting

UNIVERSITAT ROVIRA I VIRGILI
ASSEMBLY AND PROPERTIES OF POLYOXOMETALATES: A THEORETICAL POINT OF VIEW
Laia Vilà Nadal
ISBN.978-84-694-2170-3/DL:T. 1039-2011

property that should be understood from experiments and theory. In the following lines we will study these isomers and understand their preferences for certain conformations. For simplicity reasons we have not included protons in {W_{18}} cage, consequently the charge of the anions has increased, i.e. instead of $[H_3W_{18}O_{56}(IO_6)]^{6-}$ we have studied $[W_{18}O_{56}(IO_6)]^{9-}$.

Table 6.4 shows the relative energies with respect to the most stable isomer for the $[W_{18}O_{56}(XO_6)]^{q-}$ Dawson type isomers. The same trend as box $[W_{18}O_{54}]$ is observed for the box $[W_{18}O_{56}]^{4-}$, being the isomers α, γ and β* the most stable ones. We can divide the results for $[W_{18}O_{56}(XO_6)]^{q-}$ when X= W, Te and I in two groups being α*, β* and γ* the most stable (more than 10 kcal mol^{-1} compared to α, β and γ isomers). The main geometrical differences between the isomers have been shown in Figure 6.4. Here we would like to highlight for $[W_{18}O_{56}(XO_6)]^{q-}$ that the internal oxygens are eclipsed in isomers α, β, γ and staggered in α*, β*, γ*. We have depicted these differences in Figure 6.8. This geometrical difference follows the same trend as the relative energies, so it can give us a clue to explain the stability of these isomers. Finally, Table 6.5 shows the HOMO–LUMO (H–L) gaps and the X–O_{inner} distances for the fully optimizations of the six isomers $[W_{18}O_{56}(XO_6)]^{q-}$ when X= W, Te and I.

Table 6.4. Relative energies in kcal mol^{-1} with respect to the most stable isomer for $[W_{18}O_{56}(XO_6)]^{q-}$ where X= W, Te and I, compared to $[W_{18}O_{56}]^{4-}$ box.

Isomer	Symmetry	[a]$[W_{18}O_{56}]^{4-}$	[b]$[W_{18}O_{56}(WO_6)]^{10-}$	[b]$[W_{18}O_{56}(TeO_6)]^{10-}$	[b]$[W_{18}O_{56}(IO_6)]^{9-}$
α	D_{3h}	0.0	9.1	13.3	26.2
β	C_{3v}	1.9	13.0	18.0	24.7
γ	D_{3h}	0.0	16.1	21.3	19.7
α*	D_{3d}	1.9	7.0	4.6	5.0
β*	C_{3v}	0.0	0.0	0.0	1.5
γ*	D_{3d}	1.0	0.1	1.5	0.0

[a] Geometry optimized BP86, gas phase. [b] Geometry optimized BP86/SES

UNIVERSITAT ROVIRA I VIRGILI
ASSEMBLY AND PROPERTIES OF POLYOXOMETALATES: A THEORETICAL POINT OF VIEW
Laia Vilà Nadal
ISBN.978-84-694-2170-3/DL:T. 1039-2011

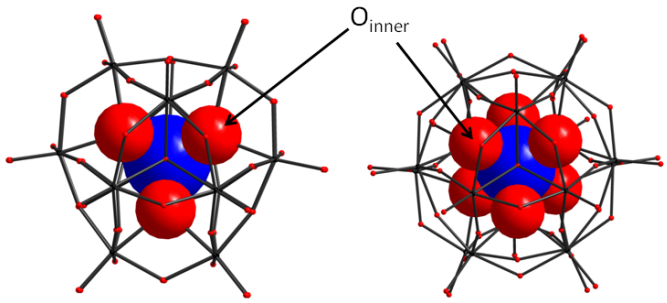

Figure 6.8. Dawson-like structures $\{W_{18}X\}$ POM type, the $\{W_{18}\}$ cages are shown as sticks and the central $\{XO_6\}$ group is represented as space filling model, X: blue sphere; O: red sphere. Left: for the α isomer the inner oxygen atoms appear eclipsed; the same happens for the β and γ isomers. Right: for the α^* isomer the inner oxygen atoms appear staggered as they are for β^* and γ^* isomers.

Table 6.5. HOMO–LUMO gaps and the $X–O_{inner}$ distance for the six isomers $[W_{18}O_{56}(XO_6)]^{q-}$ where X= W, Te, and I.

Isomer	Symmetry	HOMO–LUMO gap (eV)			Distance $X–O_{inner}$ (Å)		
		X=W	X=Te	X=I	X=W	X=Te	X=I
α	D_{3h}	1.3	0.8	0.2	2.00	2.14	2.13
β	C_{3v}	1.2	0.8	0.1	2.19–2.18	2.14–2.13	2.14–2.13
γ	D_{3h}	1.2	0.8	0.1	2.29	2.14	2.19
α^*	D_{3d}	1.7	1.7	1.1	1.99	2.10	2.08
β^*	C_{3v}	1.9	1.7	1.0	1.85–2.17	2.09–2.11	2.08–2.07
γ^*	D_{3d}	1.9	1.6	1.0	1.99	2.10	2.07

The results suggest that the preferred conformations for $[W_{18}O_{56}(XO_6)]^{q-}$ are α^* , β^* and γ^*. On one hand, H–L gaps are considerably larger for these isomers compared to α, β and γ isomers: ~0.9 eV in the case of X=Te, I and slightly smaller (~0.6 eV) in the case of X=W. On the other hand, we have also found geometrical differences in the $X–O_{inner}$ distances: they are much larger (~0.05 Å, X=I) in the α, β, γ isomers than in α^*, β^*, γ^*. Figure 6.9 aims to summarize these observations in an effort to rationalize the results. We have taken as example the $[W_{18}O_{56}(IO_6)]^{9-}$ anion.

UNIVERSITAT ROVIRA I VIRGILI
ASSEMBLY AND PROPERTIES OF POLYOXOMETALATES: A THEORETICAL POINT OF VIEW
Laia Vilà Nadal
ISBN.978-84-694-2170-3/DL:T. 1039-2011

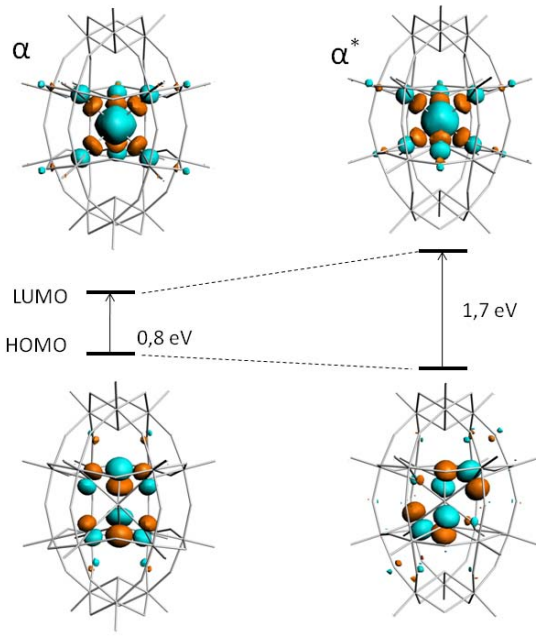

Figure 6.9. Graphical representation of the HOMO–LUMO Gap, in eV, for α (D_{3h}) and α* (D_{3d}) isomers of $[W_{18}O_{56}(IO_6)]^{9-}$. 3D representations for the HOMO (orbital delocalized over the inner oxygen atoms) and the LUMO (orbital delocalized over the I atom an the inner oxygen atoms).

The most stable isomer in Fig. 6.9 is α*, where the inner oxygen atoms are staggered. HOMO in α* isomer is more stable than HOMO in α, whereas the opposite situation happens for LUMOs, being the α LUMO more stable than α*. Let's start explaining the relative stabilization for α* HOMO orbital. Due to the eclipsed disposition of inner O atoms in the α isomer, the antibonding interactions in the HOMO of the α isomer are more important than in the HOMO of α*, where these interactions are minimized thanks to the staggered disposition of inner O atoms. Let us now explain the destabilization for α* LUMO orbital. The key parameter here is the distance between central atom and inner oxygen atoms. As we have said previously this distance is slightly smaller for α* isomer: so, the antibonding X–O

UNIVERSITAT ROVIRA I VIRGILI
ASSEMBLY AND PROPERTIES OF POLYOXOMETALATES: A THEORETICAL POINT OF VIEW
Laia Vilà Nadal
ISBN.978-84-694-2170-3/DL:T. 1039-2011

interactions in the LUMO are much more effective than those in the LUMO of the α isomers, thus becoming more destabilizend than α^* LUMO.

6.5. Conclusions

The analysis of isomerism in polyoxometalates is not an easy task. As we have seen for the case $\{W_{18}X_2\}$, it is not straightforward to predict which isomer is the most stable in each case. Small structural and electronic differences between isomers of the same type have been found. The new Dawson-like $\{W_{18}X\}$ family represents a challenge for theoretical analysis due to its high charge and redox properties. Our results suggest that if the central atom adopts an octahedral disposition, $\{W_{18}X\}$, α, β and γ isomers will not be found, in fact only β^* and γ^* have been synthesised. For $\{W_{18}X\}$ the differences in stability between α^*, β^* and γ^* are small (around 5 kcal mol^{-1}), probably given by small geometrical or electronic variations. Further study is needed to understand these differences but we can predict the thermodynamically favourable formation of α^*–$W_{18}X$ isomers. In conclusion, the study of the rotational isomers in Wells–Dawson structure is a delicate task and to fully understand it a much deeper analysis is needed.

UNIVERSITAT ROVIRA I VIRGILI
ASSEMBLY AND PROPERTIES OF POLYOXOMETALATES: A THEORETICAL POINT OF VIEW
Laia Vilà Nadal
ISBN.978-84-694-2170-3/DL:T. 1039-2011

References and Notes

[1] A. F. Wells, *Structural Inorganic Chemistry*. Clarendon Press. Oxford, U. K., **1945**.

[2] B. Dawson, *Acta Crystallogr.*, Sect. B. **1953**, 6, 113.

[3] R. Strandberg, *Acta Chem. Scand.*, Ser. A. **1975**, 29, 350.

[4] H. D'Amour, *Acta Cryst.*, Sect C. **1976**, 32, 729.

[5] V.W. Day, W.G. Klemperer, *Science*. **1985**, 228, 533.

[6] X. Lopez, C. Bo, J.M Poblet, *Inorg. Chem.*, **2003**, 42, 2634.

[7] a) López, X.; Bo, C.; Poblet, J. M. J. Am. Chem. Soc. **2002**, 124, 12574. b) Keita, B.; Levy, B.; Nadjo, L.; Contant, R. New. J. Chem. **2002**, 26, 1314.

[8] G. Herve, A. Tézé , *Inorg. Chem.*, **1977**, 6, 2115.

[9] A.F. Wells, *Structural Inorganic Chemistry*, Oxford University Press, Oxford, **1945**, 344.

[10] M.T. Pope, *Comprehensive Coordination Chemistry II*, Elsevier, **2003**.

[11] S. Himeno, T. Hori, A. Saito, *Bull. Chem. Soc. Jpn*., **1989**, 62, 2184.

[12] T. Hori, O. Tamada, S. Himeno, *J. Chem. Soc. Dalton. Trans*., **1989**, 1491.

[13] a) R.I. Maksimovskaya, G.M. Maksimov, *Russ. J. Inorg. Chem.*, **1995**, 40, 1319. b) R.I. Maksimovskaya, G.M. Maksimov, *Russ. J. Inorg. Chem.*, **1995**, 40, 1313.

[14] R. Contant, R. Thouvenot, *Inorg. Chem. Acta*, **1993**, 212, 41.

[15] a) R. Acerte, C. Hammer, L.C. Baker, *Inorg. Chem.*, **1984**, 23, 1478. b) H. Neubert, J. Fuchs, *Z. Naturforsch.* B: *Chem. Sci.*, **1987**, 42, 951. c) P.J.S Richardt, R.W. Gable, A.M. Bond, A.G. Wedd, *Inorg. Chem.*, **2001**, 40, 703.

[16] a) C. Fleming, D.L. Long, N. McMillan, J. Johnston, N. Bovet, V. Dhanak, N. Gadegaard, P. Kögerler, L. Cronin, M. Kadodwala, *Nat. Nanotechnol.*, **2008**, 3, 229. b) N. Fay, A.M. Bond, C. Baffert, J.F. Boas, J.R. Pilbrow, D.L. Long, L. Cronin, *Inorg. Chem.*, **2007**, 46, 3502.

[17] D.L. Long, Y.F. Song, E. F Wilson, P. Kögerler, S. X. Guo, A. M. Bond, J. S. J. Hargreaves, L. Cronin, *Angew. Chem. Int. Ed.*, **2008**, 47, 4384.

[18] D.L. Long, P. Kögerler, A.D.C. Parenty, J. Fielden, L. Cronin, *Angew. Chem. Int. Ed.*, **2006**, 45, 4798.

[19] D.L. Long, Y.F. Song, E.F. Wilson, P. Kögerler, S.X. Guo, A.M. Bond, J.S.J. Hargreaves, L. Cronin, *Angew. Chem. Int. Ed.*, **2008**, 47, 4384.

[20] J. Yan, D.L. Long, E.F. Wilson, L. Cronin, *Angew. Chem. Int. Ed.* **2009**, 48, 4376.

UNIVERSITAT ROVIRA I VIRGILI
ASSEMBLY AND PROPERTIES OF POLYOXOMETALATES: A THEORETICAL POINT OF VIEW
Laia Vilà Nadal
ISBN.978-84-694-2170-3/DL:T. 1039-2011

UNIVERSITAT ROVIRA I VIRGILI
ASSEMBLY AND PROPERTIES OF POLYOXOMETALATES: A THEORETICAL POINT OF VIEW
Laia Vilà Nadal
ISBN.978-84-694-2170-3/DL:T. 1039-2011

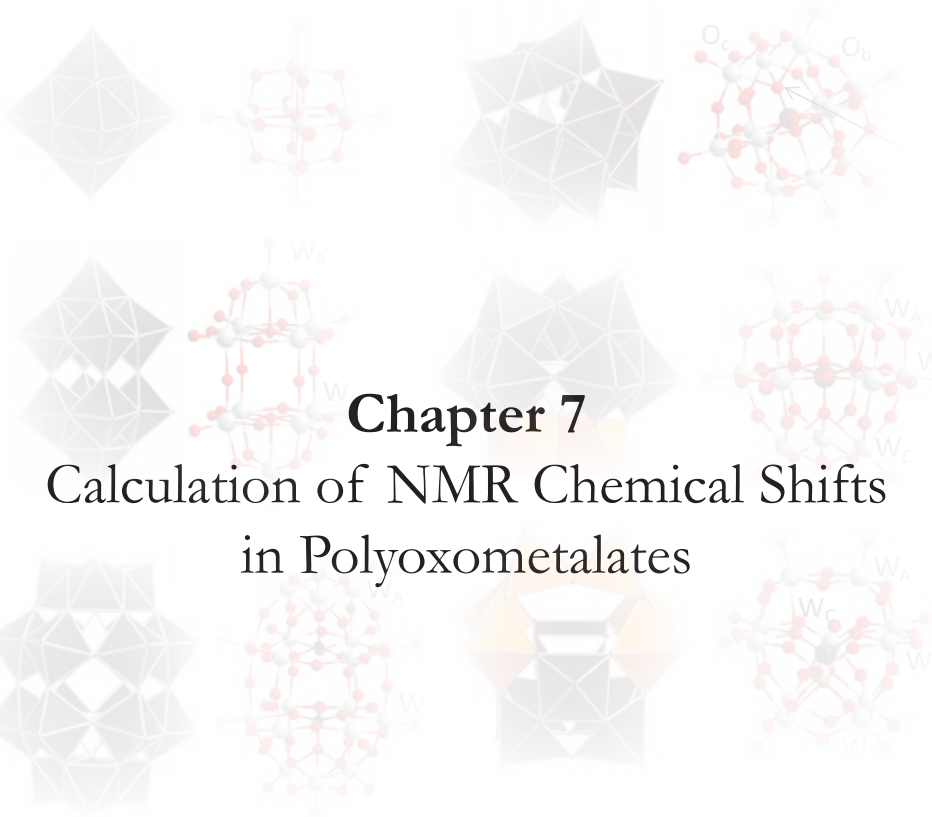

Chapter 7
Calculation of NMR Chemical Shifts in Polyoxometalates

UNIVERSITAT ROVIRA I VIRGILI
ASSEMBLY AND PROPERTIES OF POLYOXOMETALATES: A THEORETICAL POINT OF VIEW
Laia Vilà Nadal
ISBN.978-84-694-2170-3/DL:T. 1039-2011

"An experiment is a question which science poses to Nature, and a measurement is the recording of Nature's answer."

M. Planck,
Scientific Autobiography and Other Papers, 1949.

UNIVERSITAT ROVIRA I VIRGILI
ASSEMBLY AND PROPERTIES OF POLYOXOMETALATES: A THEORETICAL POINT OF VIEW
Laia Vilà Nadal
ISBN.978-84-694-2170-3/DL:T. 1039-2011

Chapter 7

Calculation of NMR Chemical Shifts in Polyoxometalates

Nuclear magnetic resonance (NMR) is a powerful method for characterizing POMs, both in solution and in solid state. Hence the prediction of NMR shielding in POMs has been a classical subject of study in the recent years. The present chapter aims to show recent DFT calculations carried out to study ^{183}W NMR chemical shifts in the family of the Keggin anions with formula α–$[XW_{12}O_{40}]^{q-}$, where X = B, Al, Si, P, Ga, Ge, As, Zn, in the β– and γ– $[SiW_{12}O_{40}]^{4-}$ geometric isomers, in the derivative Dawson anion $[P_2W_{18}O_{62}]^{6-}$, in the most symmetrical Lindqvist $[W_6O_{19}]^{2-}$ anion and its derivative $[W_{10}O_{32}]^{4-}$. The main aspects about the calculation of NMR parameters are described in Chapter 2. The present chapter is organized as follows: starting with a brief description about the relevance of NMR ^{183}W signals, along with the introduction of relevant nomenclature and structures. Afterwards we will focus in the chemical shifts of α–Keggin anions. Using very large basis sets of QZ4P quality and taking into account the COSMO procedure to model the aqueous and organic solution good geometries were found for the polyoxoanions. From these optimal geometries the ^{183}W NMR chemical shifts were computed with the more standard basis sets of TZP quality and including spin-orbit corrections within the ZORA approximation to

UNIVERSITAT ROVIRA I VIRGILI
ASSEMBLY AND PROPERTIES OF POLYOXOMETALATES: A THEORETICAL POINT OF VIEW
Laia Vilà Nadal
ISBN.978-84-694-2170-3/DL:T. 1039-2011

describe the relativistic effects of the internal electrons. With this strategy the mean absolute error between experimental and theoretical values was found to be less than 10 ppm, which is similar to the experimental error. We also discuss how the geometry of the polyoxoanion influences on the shielding.

7.1. Introduction

Polyoxometalates or POMs, as described in previous chapters, are constituted by early transition metals and oxo ligands forming distorted MO_6 octahedra, which can be combined by corners, edges and sometimes by faces.[1-2] POMs have general formula $[X_xM_mO_y]^{q-}$, where typically M is W^{6+}, Mo^{6+} or V^{5+}, and X or heteroatom is often a main group element but it can also be a transition metal.[1]

NMR analysis of the ^{183}W nucleus has revealed as the principal tool for the characterization of POMs in solution. It provides direct information on the tungsten environment in these rather complex frameworks. When studying coordination chemistry, including NMR, ESR, optical, vibrational and other properties of metal complexes, computational approaches have usually met with great challenges.[3] One of the best examples is the theoretical characterization of ^{183}W NMR chemical shifts in POMs. First, DFT calculations for tungsten chemical shifts were carried out for small and rather simple molecules such as $[WO_{4-x}S_x]^{2-}$, $W(CO)_6$, WF_6 and WCl_6,[4-5] for which an almost linear correlation between experimental and theoretical values was found. The first attempts to calculate NMR chemical shifts for large POMs were not so successful due to large systematic error arising from the use of basis sets with effective core potentials (ECP).[6] Afterwards, due to improvements in the calculation approach some qualitative linear correlation between calculated and experimental shifts for a large number of POMs with

UNIVERSITAT ROVIRA I VIRGILI
ASSEMBLY AND PROPERTIES OF POLYOXOMETALATES: A THEORETICAL POINT OF VIEW
Laia Vilà Nadal
ISBN.978-84-694-2170-3/DL:T. 1039-2011

different structures and their reduced species was reported,[7] but again their results were far to be quantitatively acceptable.[8] Incorporating spin-orbit (SO) corrections at ZORA approximation and including the solvent effects in the calculations Bagno and co-workers[9-10] have reported the most precise ^{183}W NMR chemical shifts to date, reaching an average mean error of 35 ppm in a series of POMs.[9] Given that the experimental error for ^{183}W NMR chemical shifts in this family of compounds is estimated to be less than 10 ppm, we should conclude that the disagreement between experimental and theoretical values is still excessive for quantitative purposes. In contrast, experimental coupling constants $^{2}J_{ww}$ have revealed easier to estimate and rationalize from computational methods.[10]

Our group has contributed research, which demonstrates that standard DFT methods can be useful to rationalize chemical properties of POMs. Using classical functionals such as BP86 and Slater basis sets of TZP (or similar) quality the computed geometries for these nanoscale molecular oxygen–metal clusters[11] are good enough to reproduce and rationalize vibrational[12] and electronic[13] spectra as well as electrochemical properties,[14] reactivity[15-16] or even some magnetic properties.[17] Typically, the largest discrepancies between experimental and theoretical geometries are associated with terminal M=O bonds, which are about 0.05 Å longer in average. Since NMR chemical shifts are sensitive to very minor geometry changes, optimal geometries are necessary to reproduce accurately the experimental values. Here we will demonstrate how the enhancement in the quality of the computed geometry significantly reduces the error between experimental and theoretical ^{183}W NMR chemical shifts. As we will show later, accurate experimental structures from X-ray or neutron diffraction measurements are not appropriate to compute NMR properties such as the ^{183}W NMR chemical shifts. With this purpose, ^{183}W chemical shifts were computed using highly

UNIVERSITAT ROVIRA I VIRGILI
ASSEMBLY AND PROPERTIES OF POLYOXOMETALATES: A THEORETICAL POINT OF VIEW
Laia Vilà Nadal
ISBN.978-84-694-2170-3/DL:T. 1039-2011

symmetrical (T_d) Keggin anions with formula α–$[XW_{12}O_{40}]^{q-}$, where X = B, Al, Si, P, Ga, Ge, As and Zn. The Keggin anion displays a single resonance associated with the twelve equivalent tungsten ions. In this anion, each W atom is bound to one terminal oxygen atom (O_d), one internal tetrahedral oxygen atom (O_a) and four bridging oxygen atoms, two edge (O_b) and two (O_c) corner-shared, see Figure 7.1.

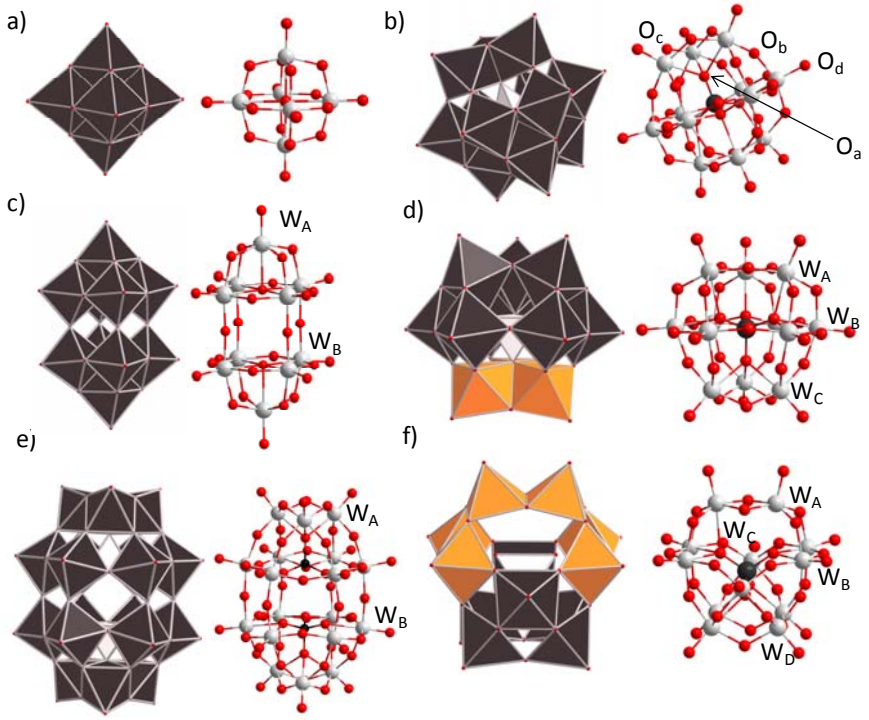

Figure 7.1. Polyhedra and ball-and-stick representation for several polyoxotungstates. $[W_6O_{19}]^{2-}$ (a), α–$[XW_{12}O_{40}]^{q-}$ (b), $[W_{10}O_{32}]^{4-}$ (c), β–$[SiW_{12}O_{40}]^{4-}$ (d), $[P_2W_{18}O_{62}]^{6-}$ (e), and γ–$[SiW_{12}O_{40}]^{4-}$ (f). Colors for the atoms (O: red, W: grey, X: black). The α–$[XW_{12}O_{40}]^{q-}$ isomer is characterized by an assembly of four edge-sharing triads W_3.Octahedra highlighted in orange show 60º-rotation of 1 and 2 triads, leading to β and γ $[XW_{12}O_{40}]^{q-}$ isomers respectively.

Along the chapter we use symbols B1//B1, B1+SO//B1, B1//B2, etc. All the NMR calculations were performed with a

UNIVERSITAT ROVIRA I VIRGILI
ASSEMBLY AND PROPERTIES OF POLYOXOMETALATES: A THEORETICAL POINT OF VIEW
Laia Vilà Nadal
ISBN.978-84-694-2170-3/DL:T. 1039-2011

Slater–TZP–quality basis set to describe the valence electrons. This basis set is called B1. Geometries were also optimized with an all electron basis set of QZ4P quality, called B2 in this chapter.

In the B2 basis the internal electrons are described by three Slater functions. For example, B1//B1 means that NMR chemical shifts were computed with basis set B1 with the geometry optimized with the same basis set. Similarly, B1 + SO // B2 + COSMO means that the NMR calculations were determined with basis B1 including spin-orbit (SO) corrections for the geometry optimized with basis B2 in solution. All chemical shifts were referred to $[WO_4]^{2-}$ computed at the corresponding level (B1//B1, B1+SO//B1,…), except for values in tables 7.2 and 7.3 in which the experimental geometry was used.

The geometry for the α–Keggin anion was optimised at several computational levels in order to check the relevance of the optimized structure in the calculation of the tungsten NMR chemical shifts. Once determined the best approach, it is used to calculate chemical shifts for the less symmetrical anions, such as: β–$[SiW_{12}O_{40}]^{4-}$ (C_{3v}), γ–$[SiW_{12}O_{40}]^{4-}$ (C_{2v}) revealing three and four resonance lines, respectively; α– $[P_2W_{18}O_{62}]^{6-}$ (D_{3h}) known as the Dawson anion with two NMR lines; $[W_{10}O_{32}]^{4-}$ (D_{4h}) with two quite separated NMR resonances; and finally the highly symmetrical Lindqvist anion $[W_6O_{19}]^{2-}$ (O_h) with a unique resonance signal that appears at more positive values (see Figure 1). Furthermore, we will analyse the influence of the solvent on the tungsten chemical shifts. Along this study, we have often used a short-hand notation, in which the formula of the anion is represented without oxygens and charge; for example α-SiW_{12}, represents the α–$[SiW_{12}O_{40}]^{4-}$ anion, or W_6 the Lindqvist anion $[W_6O_{19}]^{2-}$.

UNIVERSITAT ROVIRA I VIRGILI
ASSEMBLY AND PROPERTIES OF POLYOXOMETALATES: A THEORETICAL POINT OF VIEW
Laia Vilà Nadal
ISBN.978-84-694-2170-3/DL:T. 1039-2011

7.2. ^{183}W NMR Chemical Shifts in α–Keggin Anions

Chemical shifts were computed for a series of anions with formula $[XW_{12}O_{40}]^{q-}$, where X is B, Al, Ga, Si, Ge, P, As and Zn. The computed values relative to $[WO_4]^{2-}$ are given in Table 7.1. Whereas all the NMR chemical shifts were computed with a standard basis set of TZP quality with frozen cores (B1, see above), the geometry of the anion was optimized at different levels of accuracy. In the first series of calculations the optimal structures and the chemical shifts were obtained with the same basis set, fifth column in Table 7.1 (B1//B1). Because of the T_d symmetry of the α–Keggin anions all tungsten atoms are identical (Figure 7.1) and give a single line in the range of –65 to –131 ppm. At the B1//B1 level, the computed chemical shifts exhibit a significant absolute deviation with respect to the experimental values that extends from 5 up to 67.1 ppm with a mean absolute error (MAE) of 37.7 ppm. When the spin-orbit (SO) correction is included in the calculations of the NMR chemical shifts using the same geometry (B1+SO//B1) the MAE significantly decreases from 37.7 to 19.6 ppm, in line with previous theoretical characterizations reported by several authors.[4,5,9]

The geometries of the α–Keggin anions were recomputed with the very large all-electron basis set of QZ4P quality (B2). The simple use of the B2 geometry is not enough. At B1//B2 level the MAE is very large, 65.2 ppm. Again the incorporation of the SO term is very important reducing the deviation up to 22.2, however it is not better than the value reached at the B1+SO//B1 level. In previous studies, we have shown that the X-ray structures of POMs are always better reproduced if the geometries are optimized in solution rather than in the gas phase; this improvement depends perceptibly on the charge and size of the anion.[18]

UNIVERSITAT ROVIRA I VIRGILI
ASSEMBLY AND PROPERTIES OF POLYOXOMETALATES: A THEORETICAL POINT OF VIEW
Laia Vilà Nadal
ISBN.978-84-694-2170-3/DL:T. 1039-2011

Table 7.1. Observed and computed chemical shifts for α–$[XW_{12}O_{40}]^{n-}$ Keggin anions.[a]

X	n-	$\delta_{X,exp}$[b]	Ref	B1 // B1	B1+SO // B1	B1 // B2	B1+SO // B2	B1 // B2+COSMO	B1+SO // B2+COSMO	B1+ SO+ COSMO // B2+COSMO
B^{III}	–5	–131	19	–166	–122.3	–197.5	–155.7	–186.7	–144.8	–134.1
Al^{III}	–5	–113	20	–132.1	–92	–166.6	–128.2	–160.1	–121.6	–109.7
Ga^{III}	–5	–89	21	–83.9	–43.8	–147.5	–109.5	–139.8	–102.1	–90.6
Si^{IV}	–4	–104	30	–157.1	–107.9	–177.9	–130.1	–163.5	–115.3	–110.1
Ge^{IV}	–4	–82	30	–127	–79.8	–147.5	–103.3	–136.6	–91.9	–88.0
P^{V}	–3	–99	30	–171.3	–118.8	–184.1	–132.3	–166.3	–113.9	–114.1
As^{V}	–3	–65	22	–132.1	–83.1	–147.2	–98.6	–131.7	–82.6	–82.9[d]
Zn^{II}	–6	–95.8	30	–100.9	–58.3	–134.1	–93	–132.6	–92.8	–74.7
MAE[c]				37.7	19.6	65.5	22.2	54.8	11.5	9.3

[a] Chemical shifts relative $[WO_4]^{2-}$ in ppm. [b] Experimental values measured in water except for X=As that was determined in DMF. For this series the COSMO calculations were performed using water as solvent. [c] Mean absolute error: $MAE = \sum|\delta_{cal,i} - \delta_{exp,i}|/N$ [d] The computed value for X = As in DMF is -87.6 ppm.

Using these ideas Bagno and co-workers demonstrated that computed ^{183}W NMR chemical shifts in solution are, in general, much better than those computed in the gas phase.[9] Consequently, when the solvent is incorporated during the calculations the results improve significantly. Using the geometries optimized with basis set B2 the MAE decreases up to 11.5 ppm (B1+SO//B2+COSMO) and up to 9.3 ppm if the COSMO correction is also considered in the NMR calculations (B1+SO+COSMO//B2+COSMO). It is worth noting that it has not been necessary to improve the basis set during the NMR

UNIVERSITAT ROVIRA I VIRGILI
ASSEMBLY AND PROPERTIES OF POLYOXOMETALATES: A THEORETICAL POINT OF VIEW
Laia Vilà Nadal
ISBN.978-84-694-2170-3/DL:T. 1039-2011

calculations to obtain good estimates for the tungsten NMR chemical shifts in α–Keggin anions. The reader can notice from the values of the most right column in Table 7.1 that the deviation between the experimental and computed values is even lower than 5 ppm for four of the eight compounds. We want also to emphasize that in our study all the chemical shifts are referred to $[WO_4]^{2-}$, being not necessary to use as reference a POM such as the Linqvist anion $[W_6O_{19}]^{2-}$ in order to reduce the value of the MAE.

At this point we could ask why do not use experimental structures obtained from X-ray or neutron diffraction to compute the ^{183}W chemical shifts. NMR experiments are usually performed in solution and the structure of a given POM in solution is somewhat different from that in the solid state. Packing effects in the crystalline phase may cause noticeable changes in the geometrical parameters when compared with the structure in solution. Moreover, NMR experiments detect symmetrical structures with averaged geometrical parameters. In fact, the computed ^{183}W chemical shifts for a non symmetrical experimental X-ray structure of the α-Keggin SiW_{12} anion (refcode in the Cambridge Structural Database: KIDWIE, R=0.0497)[23] deviate significantly from the experimental value. If the reference $[WO_4]^{2-}$ is computed at B1+SO+COSMO //B2+COSMO level, the twelve signals expand in a range larger than 130 ppm (from –156 to –288 ppm) with an average value of –220 ppm (see Table 7.2). We have observed a similar deviation if the signals are referred to experimental structures of $[WO_4]^{2-}$ (ref. code in CSD: HUKYER),[24] see Table 7.3. These values are very far from the experimental and from the value computed with the best optimized geometry (–110 ppm).

UNIVERSITAT ROVIRA I VIRGILI
ASSEMBLY AND PROPERTIES OF POLYOXOMETALATES: A THEORETICAL POINT OF VIEW
Laia Vilà Nadal
ISBN.978-84-694-2170-3/DL:T. 1039-2011

Table 7.2. Calculated ^{183}W chemical shieldings for α–$[SiW_{12}O_{40}]^{4-}$ at B1+SO+COSMO//Exp. level. $[WO_4]^{2-}$ used as a reference is computed at B1+SO+COSMO// B2+COSMO level.

	σ_p	σ_d	σ_{so}	σ_{total}	δ_{cal}	δ_{exp}	$\lvert\delta_{exp}-\delta_{cal}\rvert$
$[WO_4]^{2-}$	–6944.9	9661.9	–175.8	2541.1	0	0	0
W1	–6665.7	9655.5	–206.5	2783.2	–242.1	–104	138.3
W2	–6618.1	9655.3	–207.6	2829.5	–288.4	–104	184.6
W3	–6698.7	9655.7	–210.1	2746.9	–205.8	–104	102.0
W4	–6698.6	9655.6	–209.4	2747.6	–206.5	–104	102.7
W5	–6718.1	9655.8	–208.5	2729.2	–188.1	–104	84.3
W6	–6691.3	9655.9	–208.8	2755.8	–214.7	–104	110.9
W7	–6700.3	9655.8	–212.0	2743.5	–202.3	–104	98.5
W8	–6720.0	9655.3	–210.0	2725.3	–184.2	–104	80.4
W9	–6748.9	9655.9	–209.4	2697.6	–156.4	–104	52.6
W10	–6650.9	9655.5	–210.6	2793.9	–252.8	–104	149.0
W11	–6674.5	9655.5	–209.4	2771.6	–230.5	–104	126.7
W12	–6633.9	9655.6	–208.2	2813,4	–272.3	–104	168.5
				$\overline{X}_{(\delta_{cal})}$	-220.3	$\overline{X}_{(\delta_{cal})-\delta_{exp}}$	116.5

Table 7.3. Calculated ^{183}W chemical shieldings for α–$[SiW_{12}O_{40}]^{4-}$ at B1+SO+COSMO//Exp. level. $[WO_4]^{2-}$ used as a reference is computed at B1+SO+COSMO// Exp. level.

	σ_p	σ_d	σ_{so}	σ_{total}	δ_{cal}	δ_{exp}	$\lvert\delta_{exp}-\delta_{cal}\rvert$
$[WO_4]^{2-}$	–6761.4	9661.3	–170.2	2729.7	0	0	0
W1	–6665.7	9655.5	–206.5	2783.2	–53.6	–104	–50.2
W2	–6618.1	9655.3	–207.6	2829.5	–99.9	–104	–3.9
W3	–6698.7	9655.7	–210.1	2746.9	–17.2	–104	–86.6
W4	–6698.6	9655.6	–209.4	2747.6	–17.9	–104	–85.9
W5	–6718.1	9655.8	–208.5	2729.2	0.5	–104	–104.3
W6	–6691.3	9655.9	–208.8	2755.8	–26.1	–104	–77.7
W7	–6700.3	9655.8	–212.0	2743.5	–13.8	–104	–90.0
W8	–6720.0	9655.3	–210.0	2725.3	4.4	–104	–108.2
W9	–6748.9	9655.9	–209.4	2697.6	32.1	–104	–135.9
W10	–6650.9	9655.5	–210.6	2793.9	–64.3	–104	–39.5
W11	–6674.5	9655.5	–209.4	2771.6	–41.9	–104	–61.9
W12	–6633.9	9655.6	–208.2	2813.4	–83.8	–104	–20.0
				$\overline{X}_{(\delta_{cal})}$	-31.8	$\overline{X}_{(\delta_{cal})-\delta_{exp}}$	72.0

UNIVERSITAT ROVIRA I VIRGILI
ASSEMBLY AND PROPERTIES OF POLYOXOMETALATES: A THEORETICAL POINT OF VIEW
Laia Vilà Nadal
ISBN.978-84-694-2170-3/DL:T. 1039-2011

To sum up, the observed ^{183}W NMR chemical shifts for α-Keggin POMs can be well reproduced if the chemical shifts are computed with a middle-sized basis set of TZP quality, including the SO corrections and the effect of the solvent and using a high precise geometry obtained with a large basis set of QZ4P quality in aqueous solution. Established a procedure to compute reasonable tungsten NMR chemical shifts for POMs, we have applied it to the less symmetrical β– and γ–SiW_{12} Keggin anions, to the more complex α–P_2W_{18} Dawson anion, and to the isopolyanions W_6 and W_{10}. Beforehand, we will analyse the effect of the solvent on the chemical shifts.

7.3. Solvent Dependence of the Chemical Shift

From the experimental data it is known that for any anion all the resonance lines undergo positive shift in solvents with lower dielectric constants. To verify if our procedure is able to reproduce this behaviour we have recomputed the ^{183}W NMR chemical shift for α-SiW_{12} in *N,N*-dimethylformamide (DMF). The experimental signal shifts from -104.0 ppm in water to –92.1 ppm in DMF (Table 7.4), trend that it is very well reproduced theoretically: the re-optimization of the α–SiW_{12} structure in the organic media results in a slightly increase of the W-O bond distances within the WO_6 octahedra giving the expected positive shift from –110.1 ppm in water to -101.0 ppm in DMF (Table 7.4).

The two most right columns in Table 7.1 clearly show that the incorporation of the solvents effects during the calculation of the tungsten NMR chemical shift can significantly modify the computed values. The effect of the solution is obviously more important for the most charged anions. Hence, for $Zn^{II}W_{12}$ the solvent correction is about 20 ppm whereas for the less charged anions $P^{V}W_{12}$ and $As^{V}W_{12}$ is almost negligible. The relevance of

the solvent effects was already pointed out by Bagno and co-workers.[9] From experiments, however, the comparison is not between water and the gas phase, but between water and organic solvents, frequently DMF or acetonitrile.[1] In general, the transfer of a POM from water to DMF results in deshielding of about 5–10 ppm. For α–SiW_{12} the observed deshielding is 12 ppm, behavior well reproduced from calculations (Table 7.4). It is worth noting that the value of δ does not change appreciably if using the geometry optimized in water the chemical shift is recomputed in DMF. However, re-optimization of the α-SiW_{12} anion in the organic solvent resulted in slight enlargement of the WO_6 octahedra. A small increase in the W–O distances should shift the resonance line to more positive values, as we will show later. Indeed, the chemical shift computed in DMF using the optimal geometry in the organic solvent was –101.0 ppm, 9.1 ppm more positive than in water.

Therefore, the deshielding due to the organic solvent is not related to a repolarization of the charge density, as it happens when we compare the two most right columns in Table 7.1, but to a slight increase of the W–O bonds (0.011Å for six W–O bonds). This must not surprise to the reader since DMF is an organic solvent with a high dielectric constant of 37. For less polar organic solvents the direct electronic effect could be more important.

UNIVERSITAT ROVIRA I VIRGILI
ASSEMBLY AND PROPERTIES OF POLYOXOMETALATES: A THEORETICAL POINT OF VIEW
Laia Vilà Nadal
ISBN.978-84-694-2170-3/DL:T. 1039-2011

Table 7.4. Observed and computed chemical shifts for several polyoxoanions.

Anion	Solvent	Atom	Shift		Ref.
			calculated	experimental	
α–$[SiW_{12}O_{40}]^{4-}$	H_2O		–110.1	–104.0	36
	DMF		–101.0	–92.1	25
β–$[SiW_{12}O_{40}]^{4-}$	H_2O	W_A	–133.3	–129.8	26
		W_B	–111.9	–114.5	
		W_C	–103.0	–110.0	
β–$[SiW_{12}O_{40}]^{4-}$	DMF	W_A	–130.9	–120.5	41
		W_B	–109.5	–104.0	
		W_C	–102.6	–103.5	
γ–$[SiW_{12}O_{40}]^{4-}$	DMF	W_A	–154.7	–160.1	27
		W_B	–108.1	–104.7	
		W_C	–126.6	–116.8	
		W_D	–135.8	–127.4	
$[P_2W_{18}O_{62}]^{6-}$	H_2O	W_A	–126.0	–128.1	36
		W_B	–170.0	–173.8	
$[W_{10}O_{32}]^{4-}$	DMF	W_A	–171.4	–166.0	28
		W_B	–8.6	–23	
$[W_6O_{19}]^{2-}$	DMF		+65.1	+58.9	35

UNIVERSITAT ROVIRA I VIRGILI
ASSEMBLY AND PROPERTIES OF POLYOXOMETALATES: A THEORETICAL POINT OF VIEW
Laia Vilà Nadal
ISBN.978-84-694-2170-3/DL:T. 1039-2011

7.4. ^{183}W NMR Chemical Shifts in POMs with Lower Symmetries

Lowering symmetry in β–SiW_{12}, due to rotation of a W_3O_{13} triplet (W_C) by 60º, results in splitting a single line into three lines with intensity ratio 1:2:1 and in more negative shift of all lines. The lowest shift with respect to the α–parent anion is for W_A. Computed chemical shifts are in good coincidence with the experimental ones, deviations for the three signals being lower than 7 ppm in water and slightly higher in DMF. Indeed, again we have observed the expected positive trend for all three lines when the solvent has a lower dielectric constant (Table 7.4). The rotation of two triads in the α–Keggin anion leads to the γ–isomer, which displays four resonance lines (2:1:2:1), going from –104.7 to –160.1 ppm for the silicon derivative in DMF.[43] W_A, with a particular environment resonates at a rather negative shift. The sequence of the shifts is adequately represented by calculations with small deviations (less than 10 ppm) with respect to the experimental values. Even for the large Dawson anion, P_2W_{18} we have been capable of optimizing the geometry of the anion with the B2 basis set in solution. With this QZ4P basis set the whole number of atomic functions was 6448. Despite the complexity of the molecule the calculated shifts were found to be very close to the observed ones for both the cap (W_A) and the belt (W_B) tungsten atoms. The computed shifts of –126.0 (W_A) and –170.0 ppm (W_B) almost coincide with the observed values of –128.1 and –173.8 ppm, respectively. The cap triplet resembles one of the four constituting triplets in Keggin anions and therefore the chemical shift is rather close, but slightly more negative relative to the chemical shift for PW_{12}. The belt W atoms are in different oxygen environment – three corner-sharing oxygen atoms – giving rise to a more negative shift with respect to the cap W atoms. The smallest highly symmetrical W_6, unstable in water, gives a single line in DMF. This anion was

UNIVERSITAT ROVIRA I VIRGILI
ASSEMBLY AND PROPERTIES OF POLYOXOMETALATES: A THEORETICAL POINT OF VIEW
Laia Vilà Nadal
ISBN.978-84-694-2170-3/DL:T. 1039-2011

chosen because it exhibits a ^{183}W NMR signal at a rather positive value, +58.9 ppm. Again, we can observe that the procedure delineated in this work is able to reproduce rather well the tungsten NMR chemical shifts in POMs. The resonance was computed to be +65.1 ppm only 6.2 ppm more positive than the experimental resonance. Built from two fragments of the Lindqvist anion, the decatungstate $[W_{10}O_{32}]^{4-}$ results in two types of tungsten atoms; W_A and W_B giving rise to quite separated resonances with a large negative shift for W_A. The computed values were also found very close to the experimental ones, with deviations of 5.4 and 14.4 ppm.

It is worth noting that in overall, the MAE for all the 24 signals studied in this work is about 7 ppm (a satisfactory deviation) and that all signals expand from +65.1 ppm to –170.1 ppm, very close to the experimental range of +58.9 to –173.8 ppm. In Figure 7.2, a plot of the calculated (at the B1+SO+COSMO//B2+COSMO level) versus the experimental ^{183}W chemical shifts is presented for all the studied anions, showing almost unity slope with small deviations from a straight line except for ZnW_{12} and AsW_{12}.

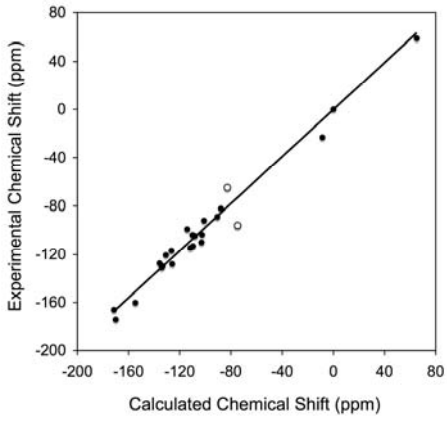

Figure 7.2. Plot between experimental and calculated ^{183}W chemical shifts for α-$[XW_{12}O_{40}]^{n-}$ where X= B, Al, Si, P, Ga, Ge, As, β– and γ–$[SiW_{12}O_{40}]^{4-}$, $[P_2W_{18}O_{62}]^{6-}$, $[W_{10}O_{32}]^{4-}$ and $[W_6O_{19}]^{2-}$. The largest deviations occur for $[ZnW_{12}O_{40}]^{6-}$ and $[AsW_{12}O_{40}]^{3-}$ (empty circles).

UNIVERSITAT ROVIRA I VIRGILI
ASSEMBLY AND PROPERTIES OF POLYOXOMETALATES: A THEORETICAL POINT OF VIEW
Laia Vilà Nadal
ISBN.978-84-694-2170-3/DL:T. 1039-2011

We could think that for the latter the deviation is in part due to the fact that the experimental value has been measured in an organic solvent, whereas all the COSMO calculations in Table 7.1 were performed in water. However, the value computed for AsW_{12} using DMF as solvent (–87.6 ppm) deviates even more from experiment (–65 ppm). This counterintuitive result can be understood by the changes in some of the W–O–W angles (β) in the AsW_{12} framework once it is optimized in DMF (vide infra). The case of ZnW_{12} is rather puzzling; from all the anions studied in this work it is the only representative having a transition metal as a heteroatom supporting the largest negative charge (6–). At present, we do not have a clear explanation on the origin of the observed deviation.

7.5. Geometries

As stated above basis set B1 has been extensively used in the theoretical calculation of polyoxometalates, giving typical discrepancies of 0.05 Å in the terminal bond lengths $W–O_d$.[11] The improvement is perceptible if a large basis set of QZ4P quality is used in combination with the incorporation of the external effects of the solution. Figure 7.3 compares the four distinct experimental W–O and X–O distances with the corresponding optimized values at the B2+COSMO level for the eight studied α-Keggin anions. The plot shows that the computed values correlate rather well with the experimental ones. It must be remarked, however, that all computed bond lengths are slightly larger than for expected trend with unity slope. This fact may reflect some relaxation of the structure when passing from the crystalline phase into solution.

As an example, Table 7.5 shows how the structural parameters for α–$[GaW_{12}O_{40}]^{5-}$ change with different approaches (data for all anions are given in Table 1 in the Annex D). The use of a

UNIVERSITAT ROVIRA I VIRGILI
ASSEMBLY AND PROPERTIES OF POLYOXOMETALATES: A THEORETICAL POINT OF VIEW
Laia Vilà Nadal
ISBN.978-84-694-2170-3/DL:T. 1039-2011

larger basis set as well as the incorporation of the solvent effects contract slightly the geometry obtained at B1 level. For the X–O_a bond length the largest discrepancy with basis set B1 (gas phase) was found for X = Ga, which is about 0.1 Å larger than the experimental value.

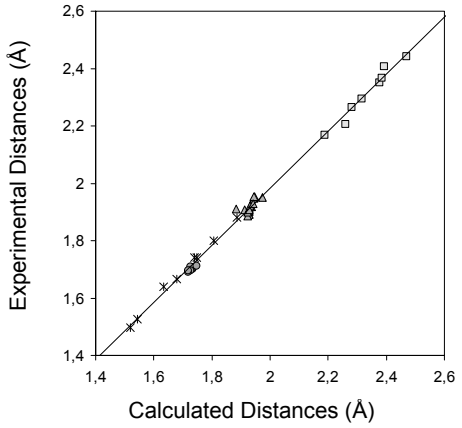

Figure 7.3. Comparison of computed and experimental W–O_d (circles), W–$O_{b,c}$ (triangles), W–O_a (squares) and X–O_a (stars) distances for $[XW_{12}O_{40}]^{n-}$ with X= B, Al, Ga, Si, Ge, P, As, Zn.

Table 7.5. Selected experimental and calculated bond distances (in Å), calculated charge q on W and shielding σ for α–$[GaW_{12}O_{40}]^{5-}$ anion.

	B1[a)]	B2[a)]	B2+COSMO[a)]	Exp.	Ref.
d_{X-Oa}[b)]	1.905	1.810	1.807	1.799	38
d_{X-Oa}[b)]	2.228	2.263	2.259	2.205	
d_{X-Oa}[b)]	1.7571	1.743	1.734	1.707	
q[c)]	2.298	2.360	2.378		
σ	2509.5	2611.5	2641.3		
ΣR_{W-O6}[d)]	11.803	11.762	11.743	11.630	
ΣR_{W-O5}[d)]	10.052	10.019	10.009		

[a] B1 means geometry optimized with a TZP basis set; B2 with a QZ4P basis set and B2 + COSMO means that the geometry was computed with the QZ4P basis set in aqueous solution. [b] For labels see Figure 1. [c] Atomic charges for W computed with the multipole derived charge method (MDC-q). [d] Sum of the six and five W–O bond lengths

UNIVERSITAT ROVIRA I VIRGILI
ASSEMBLY AND PROPERTIES OF POLYOXOMETALATES: A THEORETICAL POINT OF VIEW
Laia Vilà Nadal
ISBN.978-84-694-2170-3/DL:T. 1039-2011

If we take into account the solvent effects and the larger B2 basis set is used, the Ga–O_a distance decreases up to 1.807 Å, with a very small expansion with respect to the X-ray distance (1.799 Å). The terminal W–O_d and the W–O_a bond lengths feature larger expansions in solution (the real value of the bond distances in solution will be in between the B2+COSMO distances and the solid state values). Table 7.6, which contains the mean average deviation for the distinct distances of the α-Keggin anions when compared to the experimental values, shows that the larger expansion occurs for W–O_d bond lengths with a mean value for the eight anions studied of 0.027 Å at the B2+COSMO level.

Table 7.6. The mean average deviation of bond lengths for α–$[XW_{12}O_{40}]^{n-}$.

Optimization level	X–O_a	W–O_a	W–O_b	W–O_c	W–O_d
B2+COSMO	0.009	0.022	0.024	0.006	0.027

7.6. Dependence on the Structural Parameters

Let us now discuss how the geometry of the cluster influences on the shielding. Unfortunately, the complete rationalization of the ^{183}W NMR chemical shifts in POMs is not a trivial task. In this section, we will provide some qualitative ideas that will help to understand what factors may have influence in the final value of δ. As well known, ^{183}W NMR chemical shifts are rather sensitive to even minor structural changes. Hence, for example, for the simple tetrahedral anion $[WO_4]^{2-}$ the change in 0.008 Å in the W–O bond modifies in about 10 ppm the total shielding computed for the W atom. In larger systems the values of δ also depend on the O–W–O and W–O–W angles. Chemical shifts in

the highly symmetric α-Keggin anion mainly depend on three structural parameters: the four tungsten-bridging oxygen (O_b and O_c) bond lengths, the W–O_c–W (α) angles and the O_a–W–O_d (β) angles. We can see in Figure 7.4 that an increase in the W–O bond distance results in a deshielding, whereas an increase of the β angle (Figure 7.5) is accompanied by a clear increase of the shielding. The dependence of the chemical shift with the α angle is more scattered see Figure 7.6. The shieldings are the sum of three contributions, the diamagnetic and paramagnetic terms and the term corresponding to the spin-orbit correction (see Annex D, Tables 4-6). The diamagnetic contribution is determined mainly by the inner shells of the nucleus in question and therefore it is almost constant (~9656 ppm at the present level of calculation). The spin-orbit term, see Chapter 2 for more detail, varies in a small range of 15 ppm, going for α–$[XW_{12}O_{40}]^{q-}$ from ~ –205 ppm (q=5–), to ~ –215 ppm (q=3–). Therefore any change in the chemical shift is mainly determined by the paramagnetic shielding, whose principal contribution u_{ai} can be expressed as

$$u_{ai} \propto -\frac{1}{2(\varepsilon_i^0 - \varepsilon_a^0)} \left\langle \Psi_a \left| \hat{M}_\mu \right| \Psi_i \right\rangle \qquad (7.1)$$

where ε^o_i and ε^o_a are the orbital energies of the occupied and unoccupied MOs and the integral represents the first-order magnetic coupling between the occupied and unoccupied orbitals.

In general, a contraction of the WO_6 polyhedron induces a larger interaction between the d orbitals of the metal and the corresponding orbitals of the oxo ligands. Consequently, the gap between the occupied and unoccupied orbitals increases with a contraction of the W–O distances and therefore u_{ai} becomes less negative giving larger negative values of δ. The β angle reflects the interaction along the pseudo C_4 axis. Indeed, the energy of

UNIVERSITAT ROVIRA I VIRGILI
ASSEMBLY AND PROPERTIES OF POLYOXOMETALATES: A THEORETICAL POINT OF VIEW
Laia Vilà Nadal
ISBN.978-84-694-2170-3/DL:T. 1039-2011

the antibonding W–d_z^2–O orbitals is rather sensitive to the β angle. Hence, an increase of β destabilizes this orbital that in turn gives larger negative values of δ (Figure 7.5).

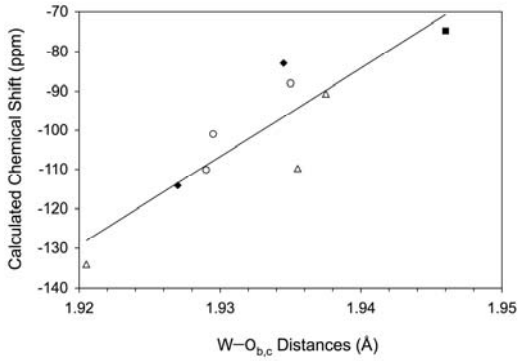

Figure 7.4. Plot between the mean W–$O_{b,c}$ distance and calculated chemical shifts δ ppm for α–$[XW_{12}O_{40}]^{q-}$, with X = P, As (diamond), Si, Ge (circle), B, Al, Ga (triangle) and Zn (square). The values for $[SiW_{12}O_{40}]^{4-}$ in DMF are also included. The line is only given to show a trend.

Several years ago, Kazansky found that the number of corner-sharing connections between MO_6 octahedra markedly shifts the resonance lines to more negative values.[29] For instance, the observed resonance line for $[W_6O_{19}]^{2-}$, which shows only edge-sharing links, shifts negatively from positive value (+58.9 ppm) to –23 ppm for the belt W atom in $[W_{10}O_{32}]^{4-}$ with one corner-sharing oxygen, and to around –100 (±40) ppm in the Keggin anions with two corner-sharing oxygens for each W atom.

UNIVERSITAT ROVIRA I VIRGILI
ASSEMBLY AND PROPERTIES OF POLYOXOMETALATES: A THEORETICAL POINT OF VIEW
Laia Vilà Nadal
ISBN.978-84-694-2170-3/DL:T. 1039-2011

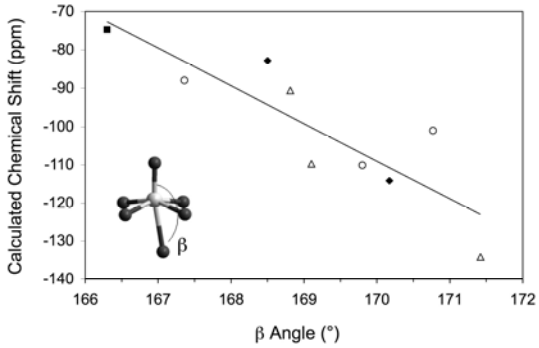

Figure 7.5. Plot between the calculated chemical shift and the O_a–W–O_d (β) angle for the α–$[XW_{12}O_{40}]^{q-}$ Keggin anions with X = P, As (diamond); Si, Si (DMF), Ge (circle); B, Al, Ga (triangle) and Zn (square).

The belt tungsten atoms in the α-Dawson anion, $[P_2W_{18}O_{62}]^{6-}$, which have three corner-sharing oxygen atoms, display a more negative shift at –173 ppm, and finally, a resonance line at –288 ppm is observed in a Preyssler anion $[NaP_5W_{30}O_{110}]^{14-}$ for the axial or polar tungsten atoms with four corner-sharing links.[30] The main structural difference between corner- and edge-sharing connections concerns to the equatorial W–O–W oxygen angles, which noticeably increase from ~118 degrees in the less shielded Lindqvist (W_6) anion, passing by 149-153 degrees in the W_{12}-based framework, to more than 160 degrees in the belt W site in the Dawson anion and the axial or polar tungsten site in the Preyssler anion, with the particularity that for the latter anion each axial tungsten atom has four corner-sharing interactions with two angles about 162º and two about 155º. The values in Annex D Table 1 and Figures 3 and 4 clearly show that the chemical shift in polyoxotungstates correlates with the average equatorial W–O–W angle.

UNIVERSITAT ROVIRA I VIRGILI
ASSEMBLY AND PROPERTIES OF POLYOXOMETALATES: A THEORETICAL POINT OF VIEW
Laia Vilà Nadal
ISBN.978-84-694-2170-3/DL:T. 1039-2011

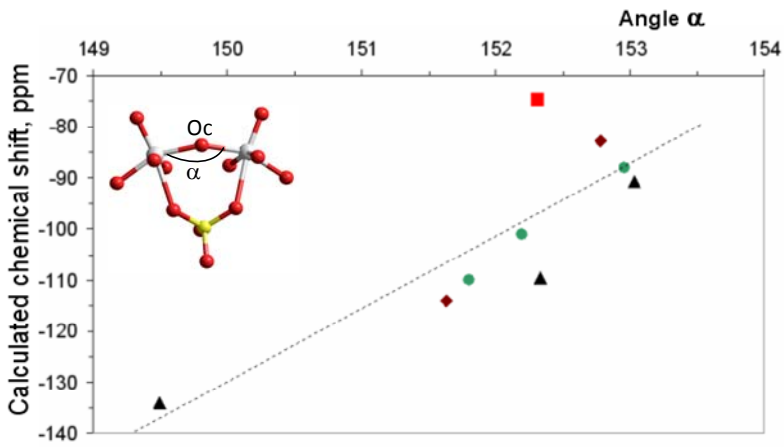

Figure 7.6. Plot between the calculated chemical shifts and the angle (α) angle W–O_c–W at corner sharing oxygen atom for α–$XW_{12}O_{40}^{q-}$ (X: ◆ for P, As; ●: for Si, Si (DMF), Ge; ▲: B, Al, Ga; ■: Zn)

In addition to the influence of the geometrical parameters on the computed chemical shift, we should not forget the possible effect of the electronic component given by the inner heteroatom X. In order to split the electronic from geometric effects we have recomputed some chemical shifts at a frozen geometry. Taking the structure of the $[AlW_{12}O_{40}]^{5-}$ anion the chemical shift for X = Ga and Ge were recomputed without relaxing the structure. As shown in Table 7.7, the substitution of Al^{3+} by Ga^{3+} reduces the shielding from 2660 ppm to 2651 ppm. However when the central ion is Ge^{4+} the shielding falls up to 2601 ppm. After geometry relaxation the sigma values are 2641 and 2631 ppm, respectively. This clearly shows that in combination with the structural factors there are also electronic factors that affect to the final value of δ. The W atomic charges are not able to rationalize themselves this behaviour. Nevertheless, analysis of the energy levels ε^o_a of the virtual MO for Ga and especially for Ge gives some clues to understand the values of the chemical shifts.

UNIVERSITAT ROVIRA I VIRGILI
ASSEMBLY AND PROPERTIES OF POLYOXOMETALATES: A THEORETICAL POINT OF VIEW
Laia Vilà Nadal
ISBN.978-84-694-2170-3/DL:T. 1039-2011

Table 7.7. Computed shielding, X-O_d bond lengths, charges on W for the Keggin anions with the optimal $[AlW_{12}O_{40}]^{5-}$ geometry (X=Al, Ga and Ge).

	Geometry of $[AlW_{12}O_{40}]^{5-}$			Optimized geometry	
X	Al^{5-}	Ga^{5-}	Ge^{4-}	Ga^{5-}	Ge^{4-}
σ[a]	2660	2651	2601	2641	2631
X–O_a	1.748	1.748	1.748	1.807	1.740
q[c]	2.366	2.378	2.342	2.378	2.372
ΣW–O[b]	9.487	9.487	9.487	9.538	9.583

[a] Shielding in ppm. [b] Sum of all bond distances of the octahedron excluding W–O_a. [c] Atomic charges for W computed with the multipole derived charge method (MDC–q).

Namely, those MOs that are composed of W–d_{z2} orbitals are slightly stabilized when passing from Al to Ga and Ge in the non-relaxed structure, the other MOs almost remaining completely unchanged. Then the decreased energy level separation, explains the largest values, in magnitude, for the paramagnetic shielding u_{ai} when going from AlW_{12} (–6411 ppm) to GeW_{12} (–6507 ppm) for the anions computed in the same AlW_{12} geometry. Therefore we may assume that some scatter observed in the plots shown in Figures 7.6, 7.7 and 7.8 may be due to the electronic effect of the central heteroatom.

7.7. Conclusions

Since the preliminary studies on small molecules the theoretical determination of ^{183}W NMR chemical shifts in polyoxtungstates has found serious difficulties. In this chapter, we have shown

UNIVERSITAT ROVIRA I VIRGILI
ASSEMBLY AND PROPERTIES OF POLYOXOMETALATES: A THEORETICAL POINT OF VIEW
Laia Vilà Nadal
ISBN.978-84-694-2170-3/DL:T. 1039-2011

that the calculation of these chemical shifts requires a preliminary computational effort to determine very good geometries for the POM. We have used the highly symmetric α–Keggin anion ($[XW_{12}O_{40}]^{q-}$, X belonging to groups 12–15) to find a strategy to compute precise chemical shifts. DFT geometry optimizations with standard basis set of TZP quality in POMs provide structures that are not suitable to reproduce accurately the experimental ^{183}W NMR signals. The geometry optimization using all electron basis sets of QZ4P quality contracts slightly the distorted WO_6 octahedra found at TZP level, significantly improving the computed chemical shifts. As shown previously, the inclusion of spin–orbit corrections is also fundamental to obtain accurate shieldings for tungsten NMR chemical shifts. For a series of eight Keggin anions a mean absolute error of 9.8 ppm was reached when the chemical shifts were computed using a frozen-core TZP basis set with geometries optimized in solution with an all-electron QZ4P basis In overall, when the chemical shift is measured in an organic solvent there is a slight expansion of the WO_6, which shifts the signal ca. 5–10 ppm to more positive values.

The mean average error (MAE) for a total of 24 ^{183}W NMR signals computed for a series of POMs was 7.3 ppm, a value which is within the estimated experimental error. Despite these encouraging results we have to state that the routine determination of NMR chemical shifts in polyoxotungstates is still far to be accomplished. The computational effort to obtain very precise geometries is still prohibitive in less symmetric anions, especially in frameworks containing WO_6 with two W=O terminal bonds or in larger systems.

Atomic charges on W atoms do not affect chemical shifts in a direct way. Only the occupied–virtual transitions, which are determined by the geometry of anion, are the principal contributions in the variation of the paramagnetic shielding with small corrections in the SO term. Along with the W–O distances

the O–W–O and W–O–W angles may play an important role as well.

Certainly at present, it seems rather unachievable, for example, to theoretically assign all 17 lines in the ^{183}W NMR spectra of the chiral polyoxoanion α_1–$[P_2W_{17}O_{61}]^{10-}$ with the spread of the shifts from –100 to –230 ppm as it was done by a special approach by Thouvenot et al.,[31] but the calculation and analysis of the ^{183}W NMR chemical shift for still unexplored anions like recently synthesized $[SW_{12}O_{40}]^{2-}$ is affordable and valuable.[32]

UNIVERSITAT ROVIRA I VIRGILI
ASSEMBLY AND PROPERTIES OF POLYOXOMETALATES: A THEORETICAL POINT OF VIEW
Laia Vilà Nadal
ISBN.978-84-694-2170-3/DL:T. 1039-2011

References and Notes

[1] M. T. Pope, *Heteropoly and Isopoly Oxometalates*. Springer-Verlag, Berlin, **1983**.

[2] D. L. Long, E. Burkholder, L Cronin, *Chem. Soc. Rev.* **2007**, 36, 105.

[3] J. Autschbach, *Coord. Chem. Rev.* **2007**, 251, 1796.

[4] A. Rodríguez-Fortea, P. Alemany, T. Ziegler, *J. Phys. Chem.* **1999**, 103A, 8288.

[5] M. Hada, H. Kaneko, H. Nakatsuji, *Chem. Phys. Lett.* **1996**, 261, 7.

[6] A. Bagno, M. Bonchio, *Chem. Phys. Lett.* **2000**, 317, 123.

[7] J. Gracia, J.M. Poblet, J. Autschbach, L.P. Kazansky, *Eur. J.Inorg. Chem.* **2006**, 1139.

[8] J. Gracia, J.M. Poblet, J.A. Fernandez, J. Autschbach, L.P. Kazansky, *Ibid*, **2006**, 1149.

[9] A. Bagno, M. Bonchio, J. Autschbach, *Chem. Eur. J.* **2006**, 12, 8460.

[10] A. Bagno, M. Bonchio, *Angew. Chem. Int. Ed.* **2005**, 44, 2023.

[11] J.M. Poblet, X. López, C. Bo, *Chem. Soc. Rev.* **2003**, *32*, 297.

[12] A.J. Bridgeman, *Chem. Eur. J.* **2006**, *12*, 2094.

[13] J.M. Maestre, X. López, C. Bo, J.M. Poblet, C. Daul, *Inorg. Chem.* **2002**, *41*, 1883.

[14] J.A. Fernández, X. López, C. Bo, C. de Graaf, E.J. Baerends, J.M. Poblet, *J. Am. Chem. Soc.* **2007**, 129, 12244.

[15] D. Quiñonero, Y. Wang, K. Morokuma, L.A. Khavrutskii, B. Botar, Y.V. Geletii, C.L. Hill, D.G. Musaev, *J. Phys. Chem. B* **2006**, *110*, 170.

[16] D. Kumar, E. Derat, A.M. Khenkin, R. Neumann, S. Shaik, *J. Am. Chem. Soc.* **2005**, 127, 17712.

[17] H. Duclusaud, S.A. Borshch, *J. Am. Chem. Soc.* **2001**, 123, 2825.

[18] X. López, J.A. Fernández, S. Romo, J. F. Paul, L. Kazansky, J.M Poblet, *J. Comput. Chem.* **2004**, 25, 1542.

[19] R. Acerete, C.F. Hammer, L.C.W. Baker, *J. Am. Chem. Soc.* **1982**, 104, 5384.

[20] I.A. Weinstock, J.J. Cowan, E.M.G. Barbuzzi, H. Zeng, C.L Hill, *J.Am. Chem. Soc.* **1999**, 121, 4608.

[21] K.M. Sundaram, W.A. Neiwert, C. L. Hill, I.A. Weinstock *Inorg. Chem.* **2006**, 45, 958.

[22] R. Thouvenot, M. Fournier, R. Frank, Rocchicchioli-Deltcheff. *Inorg. Chem.* **1984**, 23, 598.

[23] J. Liu, Y. Li, E. Wang, D. Xiao, L. Fan, Z. Zhang, Y. Wang, *J. Mol. Struct.*, **2007**, 837, 237.

[24] W. Bi, D. Sun, R. Cao, J. Chen, M. Hong, *Acta Crystallogr.*, **2002**, 58, 611.

[25] O.A. Gansow, R.K.C. Ho, W.G. Klemperer, *J.Organomet.Chem.* **1980**, 187, C27.

[26] J. Lefebvre, F. Chauveau, P. Doppelt, C. Brevard, *J.Am.Chem. Soc.* **1981**, 103, 4589.

[27] A. Teze, J. Canny, L. Gurban, R. Thouvenot, G. Herve, *Inorg.Chem.* **1996**, 35, 1001.

[28] D.C. Duncan, C.L. Hill, *Inorg. Chem.* **1996**, 35, 5828.

[29] L. P. Kazansky, *Chem.Phys.Lett.* **1994,** 223, 289.

[30] M.H. Alizadeh, S.P. Harmalker, Y. Jeannin, J. Martin-Frére, M.T. Pope, *J. Am. Chem. Soc.* **1985**, 107, 2662.

[31] G. Lenoble, B. Hasenknopf, R. Thouvenot*, J.Am. Chem. Soc.* **2006**, 128, 5735.

[32] S. Himeno, M. Takamoto, M. Hoshiba, A. Higuchi, M. Hashimoto, *Bull. Chem.Soc. Japan*. **2004**, 77, 519.

UNIVERSITAT ROVIRA I VIRGILI
ASSEMBLY AND PROPERTIES OF POLYOXOMETALATES: A THEORETICAL POINT OF VIEW
Laia Vilà Nadal
ISBN.978-84-694-2170-3/DL:T. 1039-2011

Chapter 8
Concluding remarks

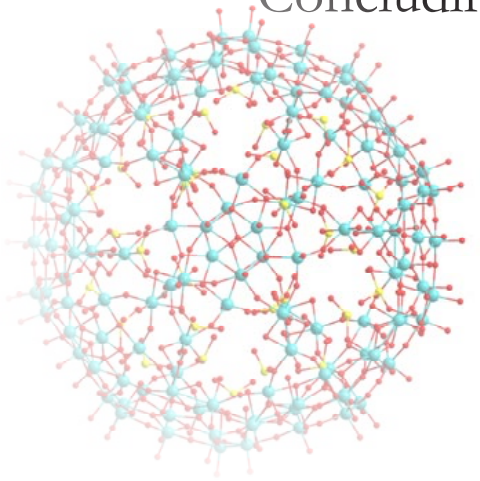

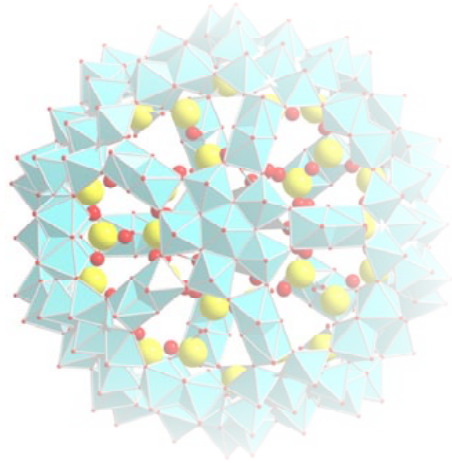

UNIVERSITAT ROVIRA I VIRGILI
ASSEMBLY AND PROPERTIES OF POLYOXOMETALATES: A THEORETICAL POINT OF VIEW
Laia Vilà Nadal
ISBN.978-84-694-2170-3/DL:T. 1039-2011

"One never notices what has been done; one can only see what remains to be done…"

M. Curie,
in a letter to her brother. March 18, 1894.

UNIVERSITAT ROVIRA I VIRGILI
ASSEMBLY AND PROPERTIES OF POLYOXOMETALATES: A THEORETICAL POINT OF VIEW
Laia Vilà Nadal
ISBN.978-84-694-2170-3/DL:T. 1039-2011

Chapter 8

Concluding remarks

In the present thesis we have studied formation mechanisms, isomerism and NMR shielding of POMs. This chapter aims to add a global overview of the work and conclusions that have already been presented thorough this thesis.

- Combining DFT approaches and ESI-MS experiments self-assembly mechanisms of POMs were studied. This procedure allowed us to obtain information about the assembly process of POMs architectures, as summarized in Figure 8.1. So, the complementarity between theory and experiment provides key clues about the formation steps of the POM assembly process.
- Car–Parrinello molecular dynamics analysis of the hydration-dehydration equilibrium processes in the hydrogentungstate anion, tungstic acid, hydrogenmolybdate anion and molybdic acid demonstrated that a decrease of the pH involves an expansion of the coordination sphere of W^{VI} and Mo^{VI}.
- Both Car–Parrinello simulations, with explicit solvent molecules, and standard static DFT calculations with continuous models of solvation predict the formation of dinuclear species different from that proposed by Kepert by both polyoxotungstates and molybdates.

UNIVERSITAT ROVIRA I VIRGILI
ASSEMBLY AND PROPERTIES OF POLYOXOMETALATES: A THEORETICAL POINT OF VIEW
Laia Vilà Nadal
ISBN.978-84-694-2170-3/DL:T. 1039-2011

- Formation of dinuclear molybdates is less favorable than tungstates.
- We postulate mechanisms with energy-cascade profiles for the formation of the Lindqvist $[M_6O_{19}]^{2-}$ (M=W and Mo) and Keggin $[XM_{12}O_{40}]^{3-}$ (M=W, Mo and X=P and As) anions, based on consecutive steps of $[MO_2(OH)]^-$ aggregation followed by protonation and water condensation steps to justify the clusters detected in the ESI-MS experiments.

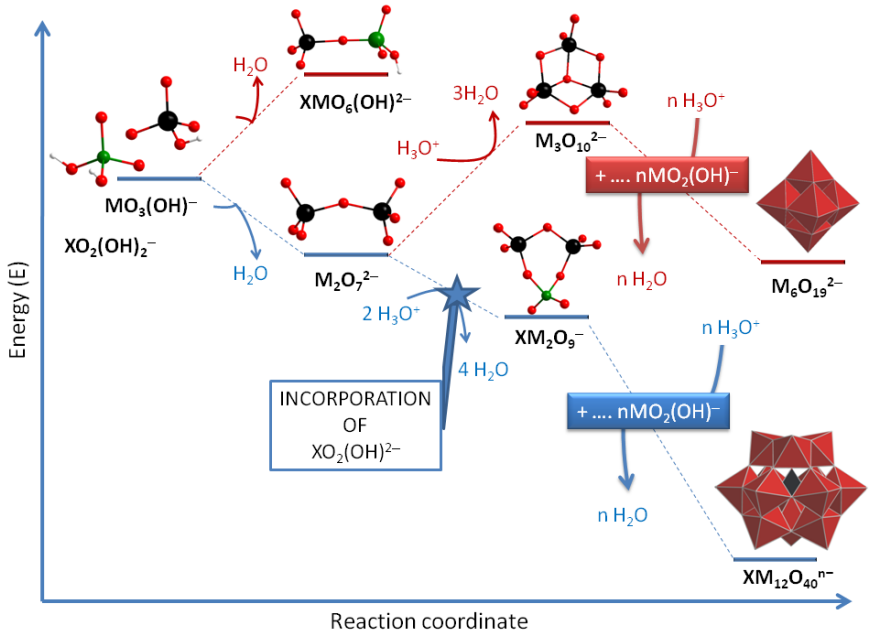

Figure 8.1. Schematic representation of the formation mechanisms for the Lindqvist $[M_6O_{19}]^{2-}$ (M=W and Mo) and Keggin $[XM_{12}O_{40}]^{3-}$ (M=W, Mo and X=P and As) anions.

- The Lindqvist anion $[M_6O_{19}]^{2-}$ (M=W and Mo) is formed by consecutive steps that incorporate one metal unit each time.

UNIVERSITAT ROVIRA I VIRGILI
ASSEMBLY AND PROPERTIES OF POLYOXOMETALATES: A THEORETICAL POINT OF VIEW
Laia Vilà Nadal
ISBN.978-84-694-2170-3/DL:T. 1039-2011

- For the formation of the Keggin anion $[XM_{12}O_{40}]^{3-}$ (M=W, Mo and X=P and As), the heteroanion $[XO_2(OH)]^{2-}$, is not incorporated to the polyanion in the first step of the nucleation, i.e. forming a heterodimer, but in a later step. Once the heterotrimer is formed, the heteroanion acts as a template for the formation of the Keggin anion.
- In the formation of the Keggin anion $[XM_{12}O_{40}]^{3-}$ (M=W, Mo and X=P and As), we have not found significant differences when changing the metal atom (W or Mo) or the heteroatom (P or As), except that arsenometalate heterodimers might be competitive with isodimers at low pH conditions.
- Understanding the isomerism in POMs is a complicated task. For the case of the Wells–Dawson anion $\{W_{18}X_2\}$, it is not simple to predict which isomer is the most stable in each case. We have also studied the new Dawson-like $\{W_{18}X\}$ family. Our results suggest that if the central atom adopts an octahedral disposition, $\{W_{18}X\}$, α, β and γ isomers will not be found, in fact only β^* and γ^* have been synthesised.
- We have also worked to determine ^{183}W NMR chemical shifts in polyoxtungstates. As showed in Fig. 8.2 good agreement between experimental and theoretical data has been reached.

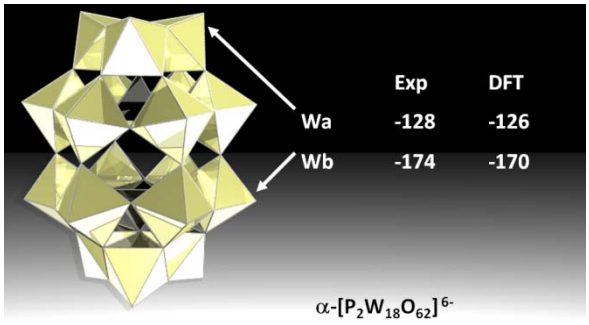

Figure 8.2. Schematic representation of the calculated and experimental chemical shifts for the Wells–Dawson α-$[P_2W_{18}O_{62}]^{6-}$ anion.

- DFT geometry optimizations with standard basis set of TZP quality in POMs provide structures that are not suitable to reproduce accurately the experimental ^{183}W NMR signals. The geometry optimization using all electron basis sets of QZ4P quality contracts slightly the distorted WO_6 octahedra found at TZP level, significantly improving the computed chemical shifts.

UNIVERSITAT ROVIRA I VIRGILI
ASSEMBLY AND PROPERTIES OF POLYOXOMETALATES: A THEORETICAL POINT OF VIEW
Laia Vilà Nadal
ISBN.978-84-694-2170-3/DL:T. 1039-2011

Publications

UNIVERSITAT ROVIRA I VIRGILI
ASSEMBLY AND PROPERTIES OF POLYOXOMETALATES: A THEORETICAL POINT OF VIEW
Laia Vilà Nadal
ISBN.978-84-694-2170-3/DL:T. 1039-2011

UNIVERSITAT ROVIRA I VIRGILI
ASSEMBLY AND PROPERTIES OF POLYOXOMETALATES: A THEORETICAL POINT OF VIEW
Laia Vilà Nadal
ISBN.978-84-694-2170-3/DL:T. 1039-2011

- Hydration of Hydrogentungstate Anions at Different pH Conditions. Rodríguez-Fortea A., Vilà-Nadal L., Poblet J.M., *Inorganic Chemistry*, **2008**, 47, 7745-7750.
- Nucleation Mechanisms of Molecular Oxides: A Study of the Assembly-Dissassembly of $W_6O_{19}^{2-}$ Using Theory and Mass Spectrometry. Vilà-Nadal L., Rodríguez-Fortea A., Yan L., Wilson E., Cronin L., Poblet J.M., *Angewandte Chemie-International Edition*, **2009**, 48, 5452-5456.
- Theoretical Analysis of the Possible Intermediates in the Formation of $[W_6O_{19}]^{2-}$. Vilà-Nadal L., Rodríguez-Fortea A., Poblet J.M., *European Journal of Inorganic Chemistry*, **2009**, 34, 5125-5133. (Contribution to composite cover picture)
- Towards the Accurate Calculation of ^{183}W NMR Chemical Shifts in Polyoxometalates. Vilà-Nadal L., Sarasa J.P., Rodríguez-Fortea A., Igual J., Kazansky L.P., Poblet J.M., *Chemistry-An Asian Journal*, **2010**, 5, 97-104.
- Titanium Containing Polyoxometalates Including the Capture of {Ti=O} in a Unique Coordination Environment. McGlone T., Miras H.N., Vilà-Nadal L., Long D.L., Poblet J.M, Cronin L., *Dalton Transactions,* **2010**, 39, 11599-11604.
- Theoretical View on the Origin and Implications of Structural Distorsions in Polyoxometalates. López X., Vilà-Nadal L., Aparicio X., Poblet J.M., *Physics Procedia*, , 8, 94-103.
- Structural and Electronic Features of Wells-Dawson Polyoxometalates. Vilà-Nadal L., Romo S., López X., Poblet J.M., *NATO Science Series*, (accepted).
- Nucleation Mechanisms of Heteropolyoxometalates: A Combined Theoretical and Mass Spectrometry Study. Vilà-Nadal L., Rodríguez-Fortea A., Mitchell S., Miras H.N., Poblet J.M., Cronin L., *submitted for publication.*
- Aggregation mechanisms of Molecular Oxides: the Formation of $[Mo_6O_{19}]^{2-}$. Vilà-Nadal L., Rodríguez-Fortea A., Cronin L., Poblet J.M., *in preparation*.
- Isomerism in Dawson polyoxometalate structure (α, β, γ, α*, β*, γ*). Vilà-Nadal L., Rodríguez-Fortea A., Poblet J.M., *in preparation*.

UNIVERSITAT ROVIRA I VIRGILI
ASSEMBLY AND PROPERTIES OF POLYOXOMETALATES: A THEORETICAL POINT OF VIEW
Laia Vilà Nadal
ISBN.978-84-694-2170-3/DL:T. 1039-2011

UNIVERSITAT ROVIRA I VIRGILI
ASSEMBLY AND PROPERTIES OF POLYOXOMETALATES: A THEORETICAL POINT OF VIEW
Laia Vilà Nadal
ISBN.978-84-694-2170-3/DL:T. 1039-2011

1

2

$[Mo_4O_{13}]^{2-}$

Annex A
(chapter 4)

1

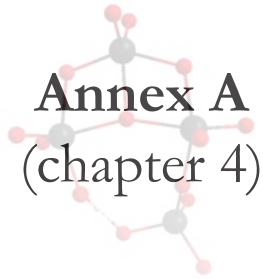

2

3

$[Mo_4O_{13}(OH)]^{3-}$

UNIVERSITAT ROVIRA I VIRGILI
ASSEMBLY AND PROPERTIES OF POLYOXOMETALATES: A THEORETICAL POINT OF VIEW
Laia Vilà Nadal
ISBN.978-84-694-2170-3/DL:T. 1039-2011

UNIVERSITAT ROVIRA I VIRGILI
ASSEMBLY AND PROPERTIES OF POLYOXOMETALATES: A THEORETICAL POINT OF VIEW
Laia Vilà Nadal
ISBN.978-84-694-2170-3/DL:T. 1039-2011

1) **ESI-MS Solution Preparations**

$((n\text{-}C_4H_9)_4N)_2Mo_6O_{19}$ Stock Solution: Into 5mL MeCN was dissolved 0.01g of $((n\text{-}C_4H_9)_4N)_2Mo_6O_{19}$.
MS Dilution: An aliquot of 20μL of $((n\text{-}C_4H_9)_4N)_2Mo_6O_{19}$ Stock Solution was made up to 4mL with MeCN.

2) ESI-MS Experimental and Analyses

All MS data was collected using a Q-trap, time-of-flight MS (MicrOTOF-Q MS) instrument equipped with an electrospray (ESI) source supplied by Bruker Daltonics Ltd. The detector was a time-of-flight, micro-channel plate detector and all data was processed using the Bruker Daltonics Data Analysis 4.0 software, whilst simulated isotope patterns were investigated using Bruker Isotope Pattern software and Molecular Weight Calculator 6.45. The following parameters were consistent for all ESI-MS scans given below. The calibration solution used was Agilent ES tuning mix solution, Recorder No. G2421A, enabling calibration between approximately 100 m/z and 3000 m/z. This solution was diluted 60:1 with acetonitrile. Samples were introduced into the MS *via* direct injection at 180 μL/h. The electrospray source was used with the drying nitrogen gas temperature at approx +180 ºC. The ion polarity for all MS scans recorded was negative, with the end plate offset at -500 V, funnel 1RF at 300 Vpp, funnel 2 RF at 400 Vpp, and hexapole RF at 400 Vpp. The collision cell was filled with argon collision gas. Other MS parameters, and CID (also referred to as MS/MS(MRM), i.e. MS/MS multiple reaction monitoring) parameters, which are set to specific values for each scan, are given in the following table. All theoretical peak assignments were determined via comparison of the experimentally determined isotopic patterns for each peak, with simulated isotopic patterns.

UNIVERSITAT ROVIRA I VIRGILI
ASSEMBLY AND PROPERTIES OF POLYOXOMETALATES: A THEORETICAL POINT OF VIEW
Laia Vilà Nadal
ISBN.978-84-694-2170-3/DL:T. 1039-2011

Table 1. MS parameters set to specific values for each scan are presented.

MS Parameter	***Data Collection***				
	Run A	**Run B**	**Run C**	**Run D**	**Run E**
Mass Range / m/z	50-3000	50-1500	50-1000	50-2000	50-3000
Capillary / V	4500	4500	4500	4000	3500
Collision Energy / eV	-10	-10	-10	-10	-10
Collision Cell RF / Vpp	500	500	500	500	500
Transfer time / µs	110	110	110	110	110
Pre-pulse Storage Time / µs	10	10	10	10	10
Summation	5000	5000	5000	5000	10000
Time of Acquisition / min	1	1	1	1	1
Active focus	OFF	OFF	ON	ON	ON
Collision cell **MS/MS(MRM) parameters**	OFF	ON	ON	ON	ON
Peak selected / m/z	-	440.2	440.2	440.2	440.2
Isolation width / m/z	-	20	20	20	20
Collision Energy / eV	-	2	12	16	20

5) ESI-MS Results Summary

Table 2. A summary of the peaks observed from the ESI-MS data collections, along with their associated species are shown.

m/z	Peak Assignment
151.9	$[Mo_2O_7]^{2-}$
223.8	$[Mo_3O_{10}]^{2-}$
296.8	$[Mo_4O_{13}]^{2-}$
368.2	$[Mo_5O_{16}]^{2-}$
440.2	$[Mo_6O_{19}]^{2-}$

6) ESI-MS Spectra

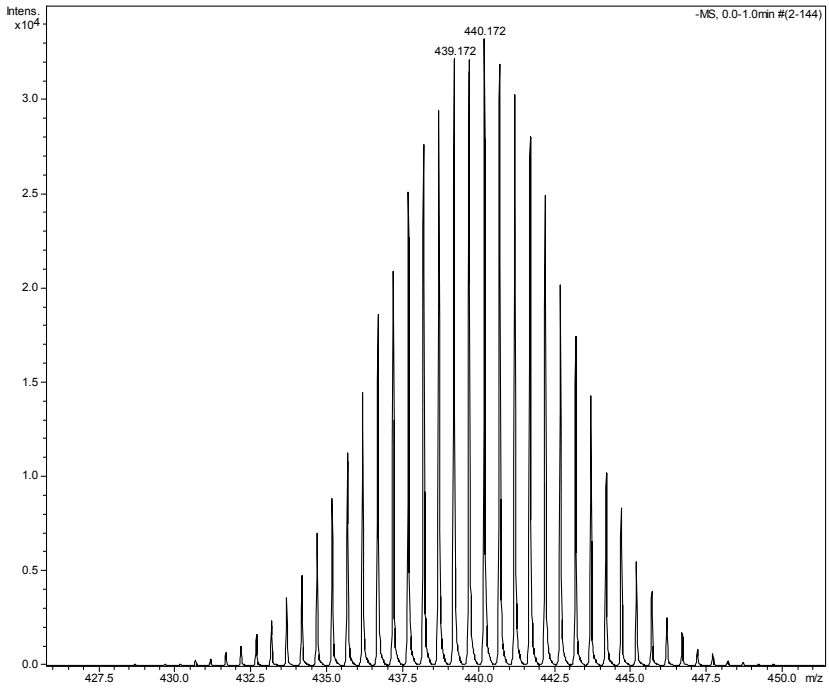

Figure 1 Mass spectral data from Run A showing the peak associated with the $[Mo_6O_{19}]^{2-}$ species at 440.17 m/z.

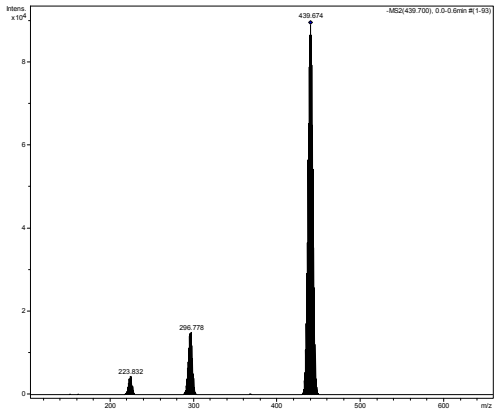

Figure 2 Mass spectral data from Run B showing the peak associated with the species $[Mo_6O_{19}]^{2-}$ at 440.17, $[Mo_4O_{13}]^{2-}$ at 296.77 and $[Mo_3O_{10}]^{2-}$ at 223.88 m/z respectively.

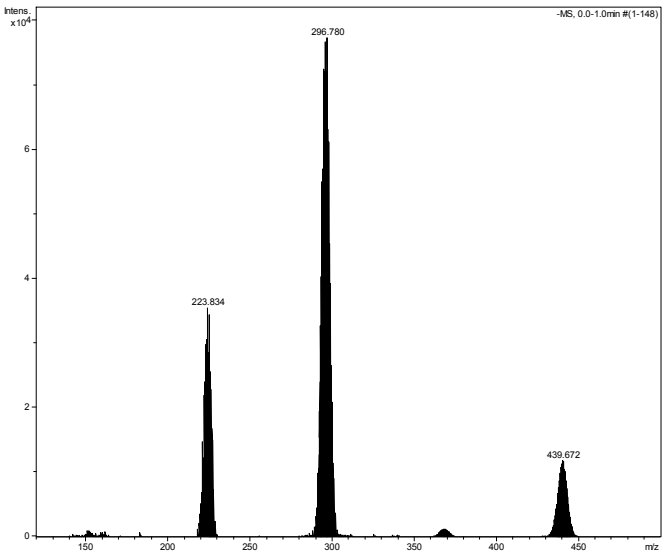

Figure 3 Mass spectral data from Run E showing the peak associated with the species $[Mo_6O_{19}]^{2-}$ at 440.17, $[Mo_5O_{16}]^{2-}$ at 368.72, $[Mo_4O_{13}]^{2-}$ at 296.77, $[Mo_3O_{10}]^{2-}$ at 223.88 and $[Mo_2O_7]^{2-}$ at 151.88 m/z respectively.

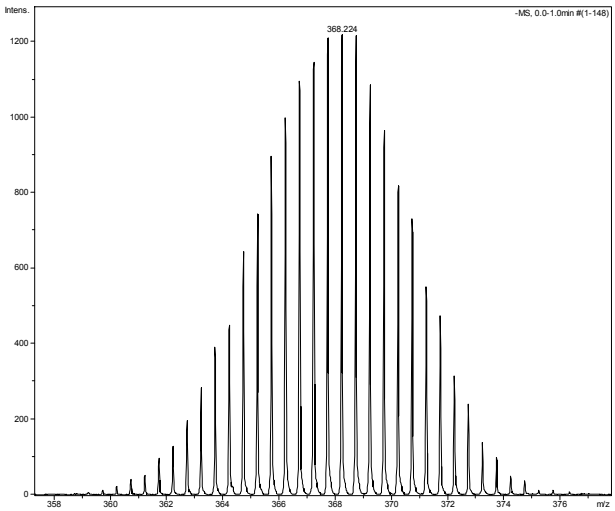

Figure 4 Mass spectral data from Run E showing the expanded envelope associated with the $[Mo_5O_{16}]^{2-}$ species at 368.22 m/z.

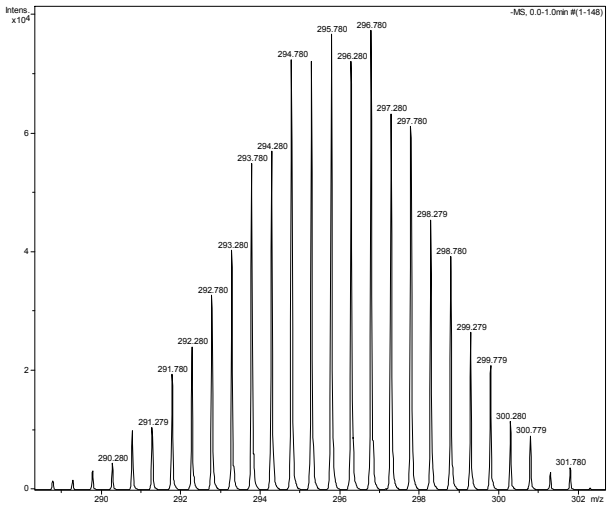

Figure 5 Mass spectral data from Run E showing the expanded envelope associated with the $[Mo_4O_{13}]^{2-}$ species at 296.78 m/z.

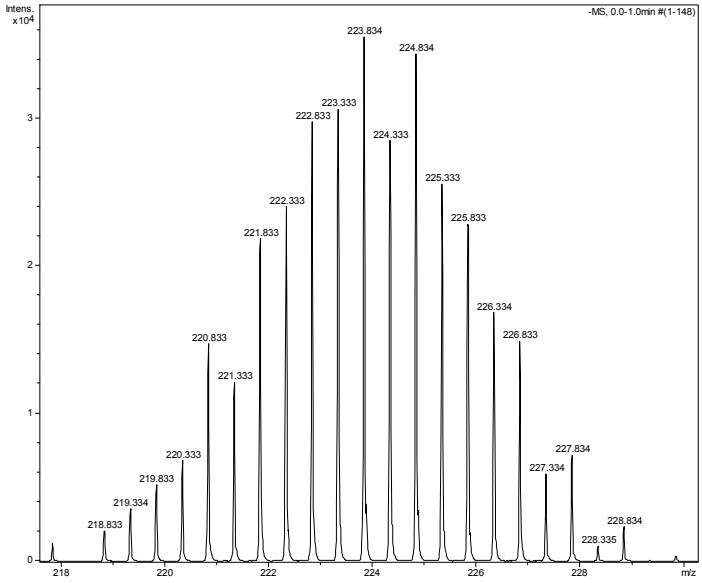

Figure 6 Mass spectral data from Run E showing the expanded envelope associated with the $[Mo_3O_{10}]^{2-}$ species at 223.83 m/z.

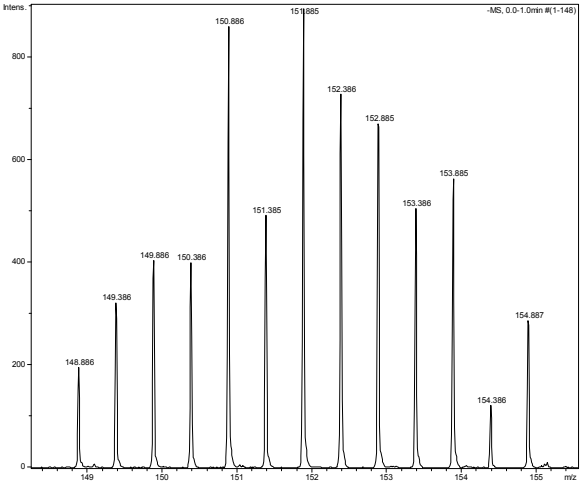

Figure 7 Mass spectral data from Run E showing the expanded envelope associated with the $[Mo_2O_7]^{2-}$ species at 151.88 m/z.

UNIVERSITAT ROVIRA I VIRGILI
ASSEMBLY AND PROPERTIES OF POLYOXOMETALATES: A THEORETICAL POINT OF VIEW
Laia Vilà Nadal
ISBN.978-84-694-2170-3/DL:T. 1039-2011

Table 3. Reaction energies (in kcal mol^{-1}) for Mechanism 2.

MECHANISM 2	ΔE (kcal mol^{-1})
1) **$[MoO_3(OH)]^-_{(aq)}$** + $[MoO_3(OH)]^-_{(aq)} \rightarrow [Mo_2O_6(OH)_2]^{2-}_{(aq)}$	0.4
2) $[Mo_2O_6(OH)_2]^{2-}_{(aq)} + H_3O^+_{(aq)} \rightarrow$ **$[Mo_2O_6(OH)]^-_{(aq)}$** + $2H_2O_{(aq)}$	-18.3
3) $[Mo_2O_6(OH)]^-_{(aq)} + [MoO_3(OH)]^-_{(aq)} \rightarrow [Mo_3O_9(OH)_2]^{2-}_{(aq)}$	-1.7
4) $[Mo_3O_9(OH)_2]^{2-}_{(aq)} + H_3O^+_{(aq)} \rightarrow$ **$[Mo_3O_9(OH)]^-_{(aq)}$** + $2H_2O_{(aq)}$	-6.7
5) $[Mo_3O_9(OH)]^-_{(aq)} + [MoO_3(OH)]^-_{(aq)} \rightarrow [Mo_4O_{12}(OH)_2]^{2-}_{(aq)}$	-10.2
6) $[Mo_4O_{12}(OH)_2]^{2-}_{(aq)} + H_3O^+_{(aq)} \rightarrow$ **$[Mo_4O_{12}(OH)]^-_{(aq)}$** + $2H_2O_{(aq)}$	-17.2
7) $[Mo_4O_{12}(OH)]^-_{(aq)} + [MoO_3(OH)]^-_{(aq)} \rightarrow [Mo_5O_{15}(OH)_2]^{2-}_{(aq)}$	16.9
8) $[Mo_5O_{15}(OH)_2]^{2-}_{(aq)} + H_3O^+_{(aq)} \rightarrow [Mo_5O_{15}(OH)]^-_{(aq)} + 2H_2O_{(aq)}$	-3.5
9) $[Mo_5O_{15}(OH)]^-_{(aq)} + [MoO_3(OH)]^-_{(aq)} \rightarrow [Mo_6O_{18}(OH)_2]^{2-}_{(aq)}$	-14.3
10) $[Mo_6O_{18}(OH)_2]^{2-}_{(aq)} \rightarrow$ **$[Mo_6O_{19}]^{2-}_{(aq)}$** + $H_2O_{(aq)}$	-12.3

Table 4. Relative energies (in kcal mol^{-1}) for dinuclear species with respect to the monomers.

Structure		ΔE (kcal mol^{-1})	
		M=W	M=Mo
$[M_2O_8H_2]^{2-}$	**1**	–7.5	+0.4
	2	+0.2	+7.4
	3	+10.2	+11.4
$[M_2O_7]^{2-}$	**1**	–5.4	–2.2

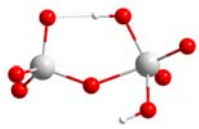

(a) $[M_2O_6(OH)_2]^{2-}$ **1**

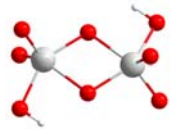

(b) $[M_2O_6(OH)_2]^{2-}$ **2**

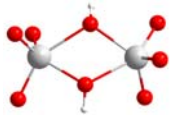

(c) $[M_2O_6(OH)_2]^{2-}$ **3**

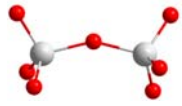

(d) $[M_2O_7]^{2-}$ **1**

Figure 8. Optimized structures for the most representative dinuclear species.

ISBN.978-84-694-2170-3/DL:T. 1039-2011

Table 5. Relative energies (in kcal mol^{-1}) species with respect to the monomers.

Structure		ΔE (kcal mol^{-1})	
		M=W	M=Mo
$[M_3O_{10}]^{2-}$	**1**	0.0	0.0
	2	+1.5	+4.8
	3	+7.1	+7.9
	4	+7.2	+15.4
	5	+16.5	+19.4
	6	+43.7	+49.5
$[M_3O_9(OH)]^{-}$	**1**	0.0	+1.0
	2	+2.3	0.0
	3	+11.9	+8.6
	4	+15.3	+12.7
	5	+16.3	+18.0
	6	+34.8	+38.6
$[M_3O_{10}(OH)]^{3-}$	**1**	0.0	0.0
	2	+4.7	+2.12
	3	+9.9	-
	4	+8.0	+0.5
$[M_3O_9(OH)_2]^{2-}$	**1**	0.0	+2.1
	2	+1.9	0.0
	3	+7.2	+0.9
	4	+8.4	+1.2

UNIVERSITAT ROVIRA I VIRGILI
ASSEMBLY AND PROPERTIES OF POLYOXOMETALATES: A THEORETICAL POINT OF VIEW
Laia Vilà Nadal
ISBN.978-84-694-0170-3/DL:T. 1039-2011

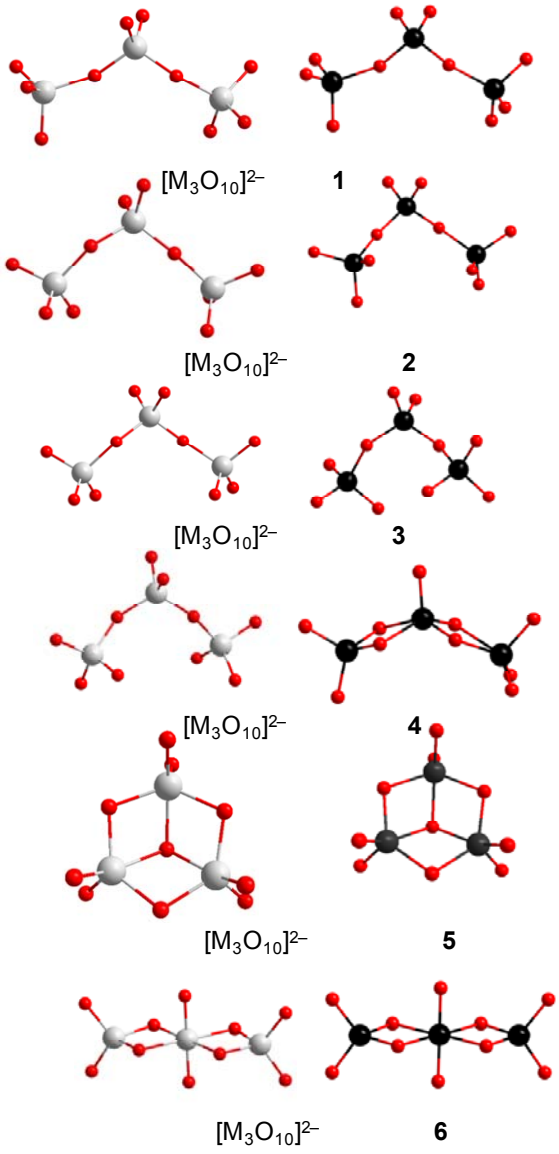

Figure 9. Optimized structures for the $[M_3O_{10}]^{2-}$ species.

UNIVERSITAT ROVIRA I VIRGILI
ASSEMBLY AND PROPERTIES OF POLYOXOMETALATES: A THEORETICAL POINT OF VIEW
Laia Vilà Nadal
ISBN.978-84-694-2070-3/DL:T. 1039-2011

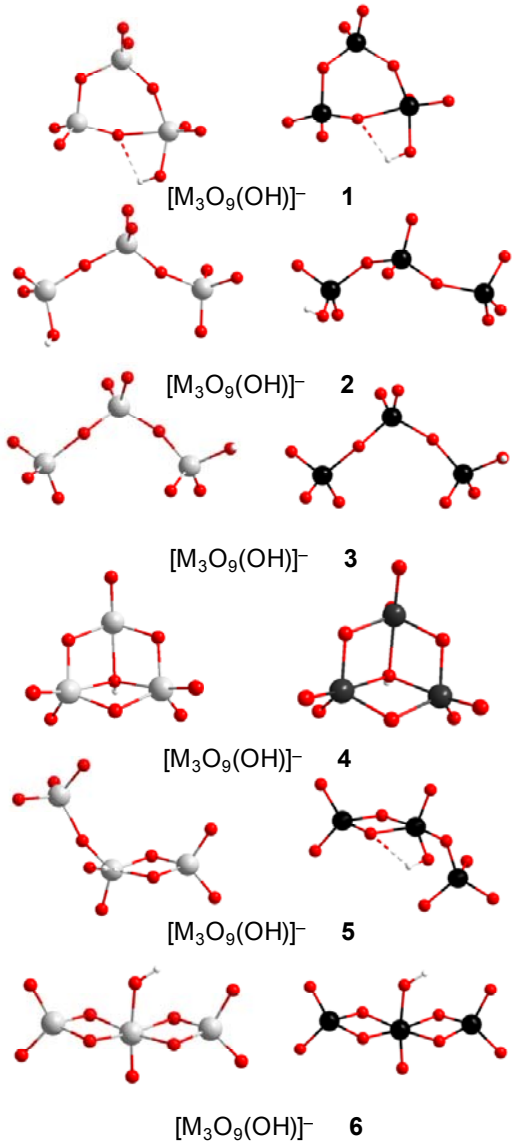

Figure 10. Optimized structures for the $[M_3O_9(OH)]^-$ species.

UNIVERSITAT ROVIRA I VIRGILI
ASSEMBLY AND PROPERTIES OF POLYOXOMETALATES: A THEORETICAL POINT OF VIEW
Laia Vilà Nadal
ISBN.978-84-694-2170-3/DL:T. 1039-2011

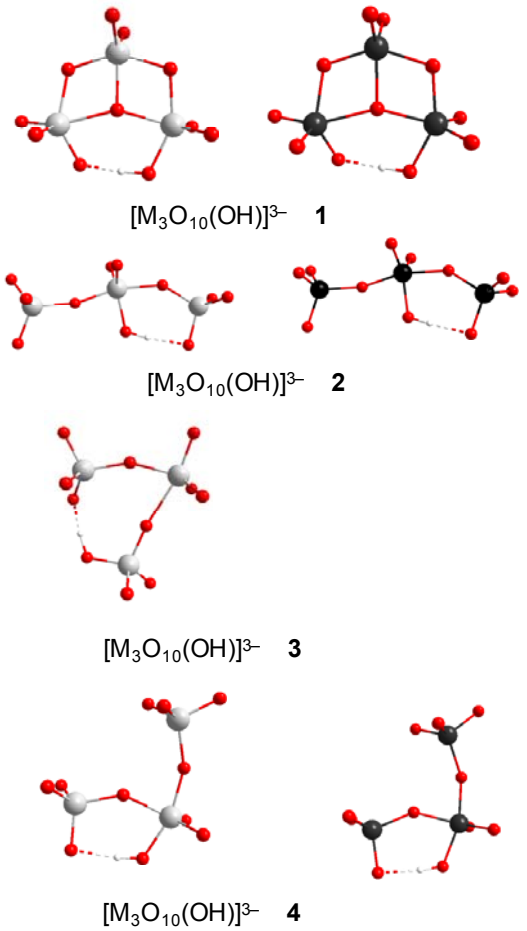

Figure 11. Optimized structures for the $[M_3O_{10}(OH)]^{3-}$ species.

UNIVERSITAT ROVIRA I VIRGILI
ASSEMBLY AND PROPERTIES OF POLYOXOMETALATES: A THEORETICAL POINT OF VIEW
Laia Vilà Nadal
ISBN.978-84-694-2270-3/DL:T. 1039-2011

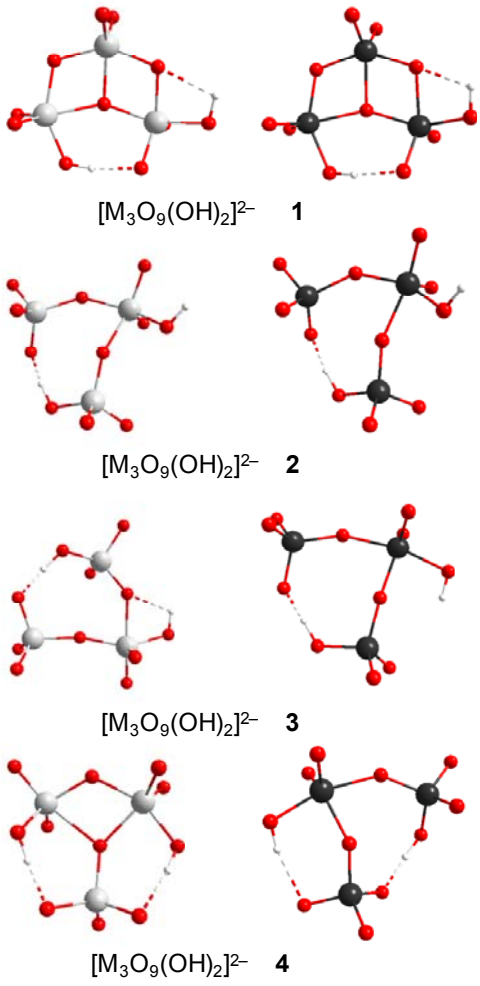

Figure 12. Optimized structures for the $[M_3O_9(OH)_2]^{2-}$ species.

UNIVERSITAT ROVIRA I VIRGILI
ASSEMBLY AND PROPERTIES OF POLYOXOMETALATES: A THEORETICAL POINT OF VIEW
Laia Vilà Nadal
ISBN.978-84-694-2170-3/DL:T. 1039-2011

Table 6. Relative energies (in kcal mol^{-1}) species with respect to the monomers.

Structure		ΔE (kcal mol^{-1})	
		M=W	M=Mo
$[M_4O_{13}]^{2-}$	**1**	0.0	0.0
	2	+10.4	+3.6
	3	+11.7	+3.9
	4	+19.7	+9.5
$[M_4O_{12}(OH)]^{-}$	**1**	0.0	0.0
	2	+10.2	+3.6
	3	+13.4	+8.3
	4	+13.2	+10.2
	5	+16.1	+10.6
$[M_4O_{13}(OH)]^{3-}$	**1**	0.0	+7.1
	2	+0.2	0.0
	3	+2.8	+1.1
	4	+4.6	+5.5
	5		+7.5
$[M_4O_{12}(OH)_2]^{2-}$	**1**	0.0	0.0
	2	+5.5	+4.3
	3	+8.5	+2.3
	4	+9.8	+7.2
	5	+13.7	+6.3
	6	+17.8	+10.7
	7	+19.1	+12.3

UNIVERSITAT ROVIRA I VIRGILI
ASSEMBLY AND PROPERTIES OF POLYOXOMETALATES: A THEORETICAL POINT OF VIEW
Laia Vilà Nadal
ISBN.978-84-694-2170-3/DL:T. 1039-2011

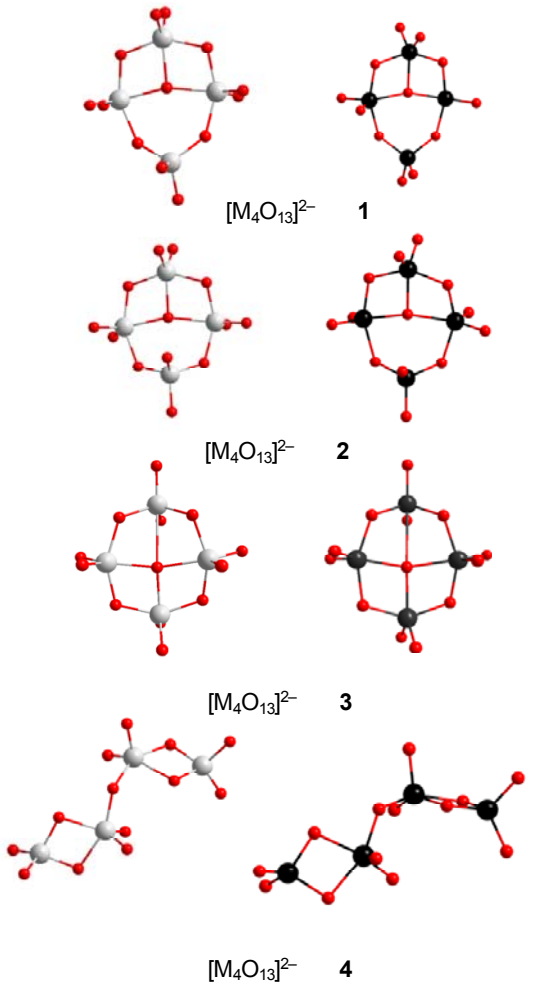

Figure 13. Optimized structures for the $[M_4O_{13}]^{2-}$ species.

UNIVERSITAT ROVIRA I VIRGILI
ASSEMBLY AND PROPERTIES OF POLYOXOMETALATES: A THEORETICAL POINT OF VIEW
Laia Vilà Nadal
ISBN.978-84-694-2570-3/DL:T. 1039-2011

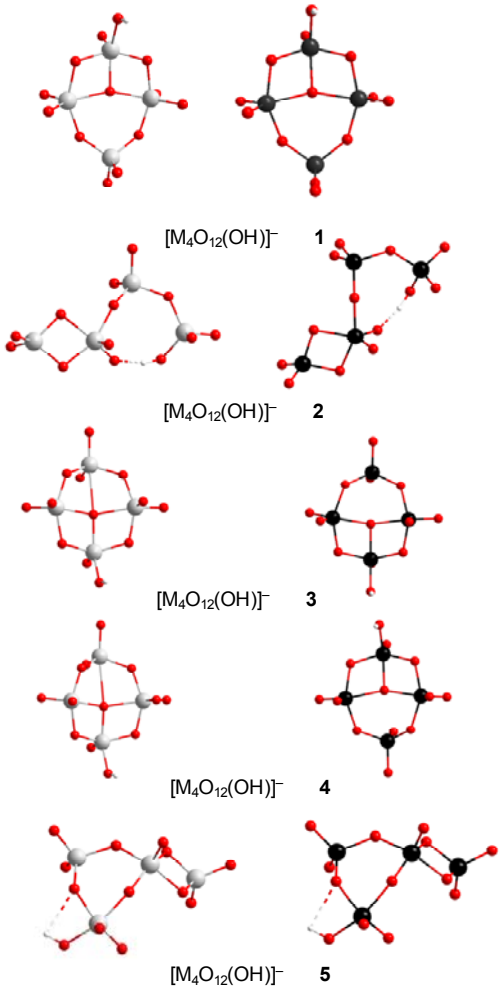

Figure 14. Optimized structures for the the $[M_4O_{12}(OH)]^-$ species.

UNIVERSITAT ROVIRA I VIRGILI
ASSEMBLY AND PROPERTIES OF POLYOXOMETALATES: A THEORETICAL POINT OF VIEW
Laia Vilà Nadal
ISBN.978-84-694-2670-3/DL:T. 1039-2011

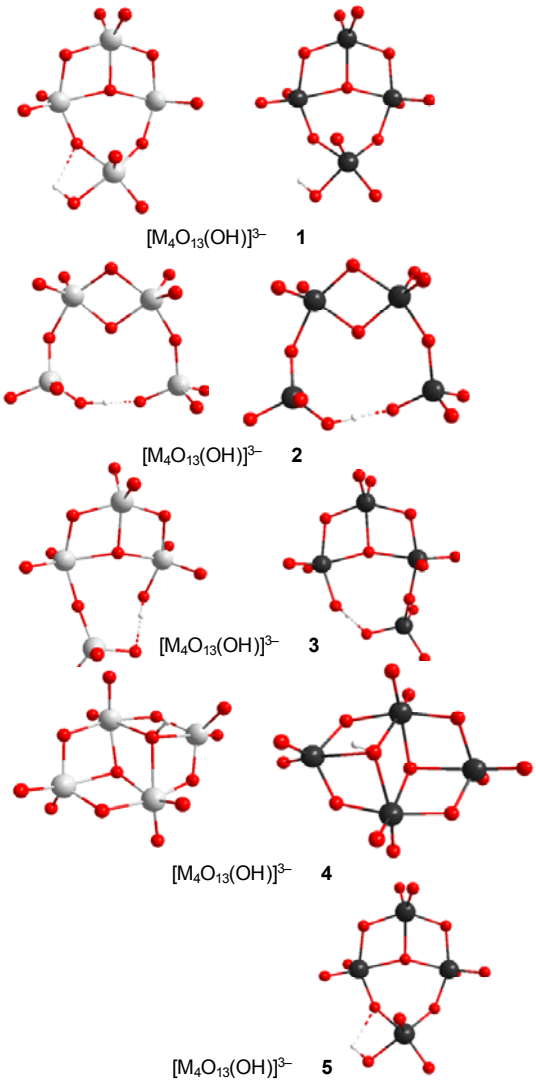

Figure 15. Optimized structures for the the $[M_4O_{13}(OH)]^{3-}$ species.

UNIVERSITAT ROVIRA I VIRGILI
ASSEMBLY AND PROPERTIES OF POLYOXOMETALATES: A THEORETICAL POINT OF VIEW
Laia Vilà Nadal
ISBN.978-84-694-2270-3/DL:T. 1039-2011

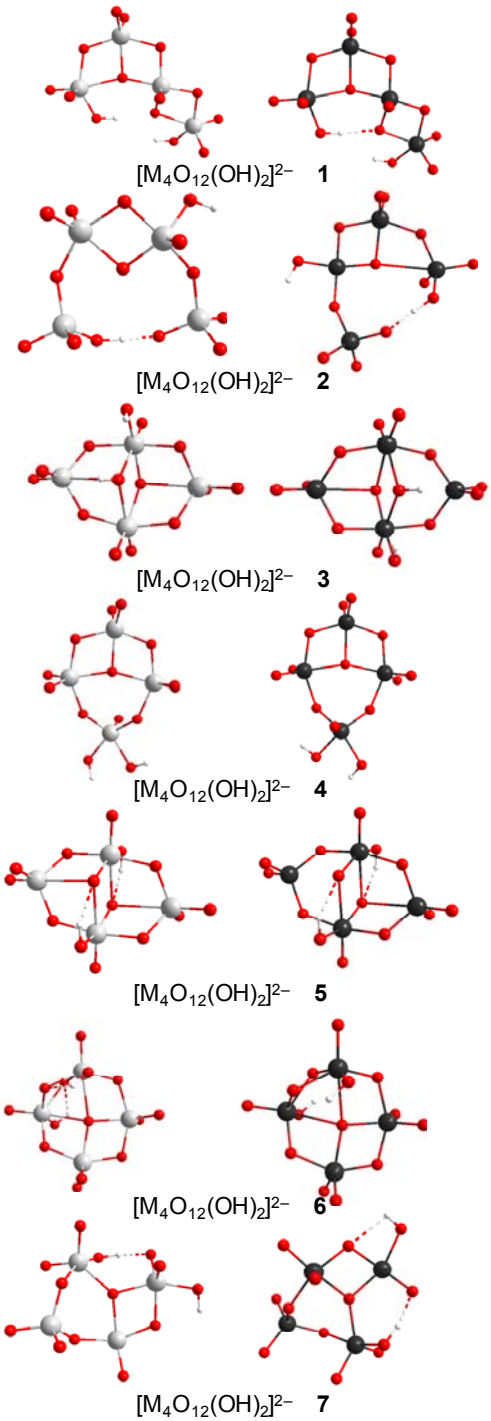

Figure 16. Optimized structures for the the $[M_4O_{12}(OH)_2]^{2-}$ species

UNIVERSITAT ROVIRA I VIRGILI
ASSEMBLY AND PROPERTIES OF POLYOXOMETALATES: A THEORETICAL POINT OF VIEW
Laia Vilà Nadal
ISBN.978-84-694-2870-3/DL:T. 1039-2011

Table 4. Relative energies (in kcal mol^{-1}) species with respect to the monomers.

Structure		ΔE (kcal mol^{-1})	
		M=W	M=Mo
$[M_5O_{16}]^{2-}$	**1**	0.0	0.0
	2	+3.2	+2.6
	3	+3.3	+3.6
	4	-	+1.0
	5	+15.7	+9.8
$[M_5O_{15}(OH)]^{-}$	**1**	0.0	0.0
	2	+7.8	+2.5
	3	+17.1	+1.2
	4	+22.2	+20.7
	5	-	+1.5
$[M_5O_{16}(OH)]^{3-}$	**1**	0.0	+1.2
	2	+6.1	-
	3	+22.0	+3.4
	4	+32.7	+4.7
	5	-	0.0
	6	-	+0.1
$[M_5O_{15}(OH)_2]^{2-}$	**1**	0.0	+4.0
	2	+3.0	0.0
	3	+3.3	+1.8
	4	+4.3	+2.4
	5	+6.5	+8.5
	6	+12.9	+11.3

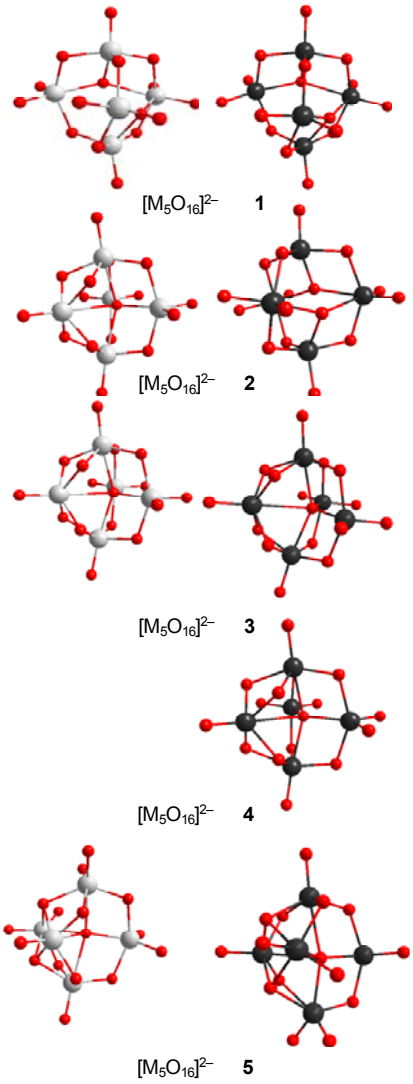

Figure 17. Optimized structures for the the $[M_5O_{16}]^{2-}$ species

UNIVERSITAT ROVIRA I VIRGILI
ASSEMBLY AND PROPERTIES OF POLYOXOMETALATES: A THEORETICAL POINT OF VIEW
Laia Vilà Nadal
ISBN.978-84-694-2170-3/DL:T. 1039-2011

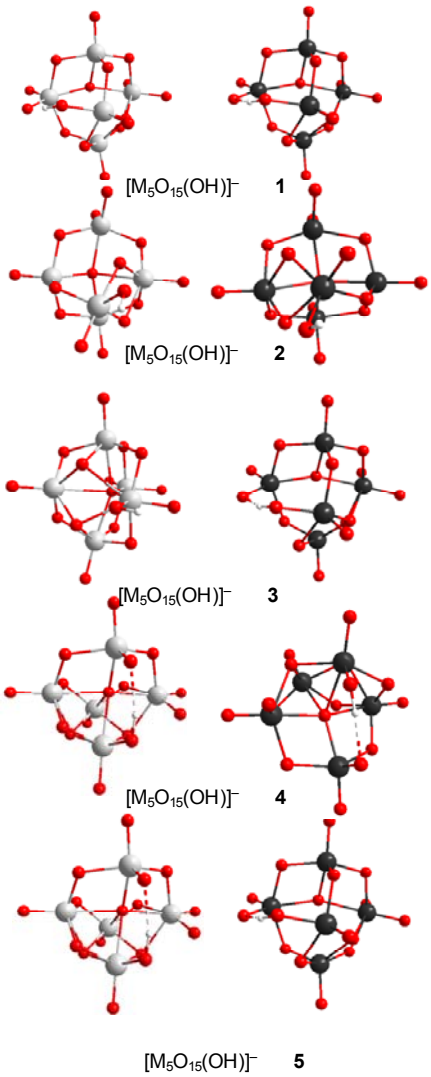

Figure 18. Optimized structures for the the $[M_5O_{15}(OH)]^-$ species.

UNIVERSITAT ROVIRA I VIRGILI
ASSEMBLY AND PROPERTIES OF POLYOXOMETALATES: A THEORETICAL POINT OF VIEW
Laia Vilà Nadal
ISBN.978-84-694-2170-3/DL:T. 1039-2011

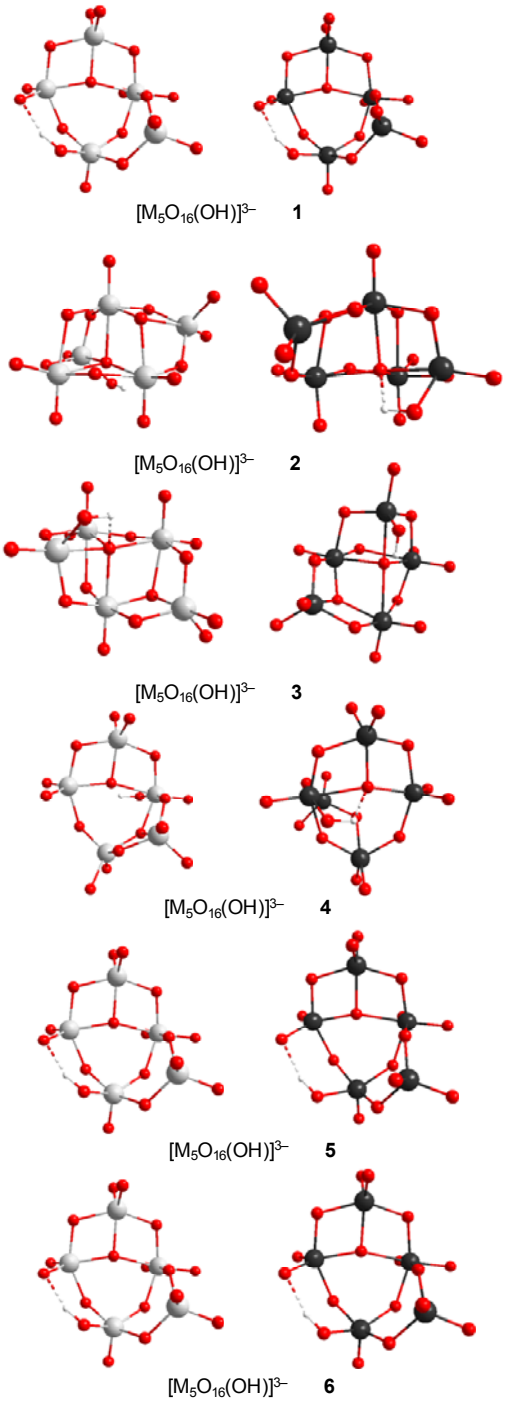

Figure 19. Optimized structures for the the $[M_5O_{16}(OH)]^{3-}$ species.

UNIVERSITAT ROVIRA I VIRGILI
ASSEMBLY AND PROPERTIES OF POLYOXOMETALATES: A THEORETICAL POINT OF VIEW
Laia Vilà Nadal
ISBN.978-84-694-2270-3/DL:T. 1039-2011

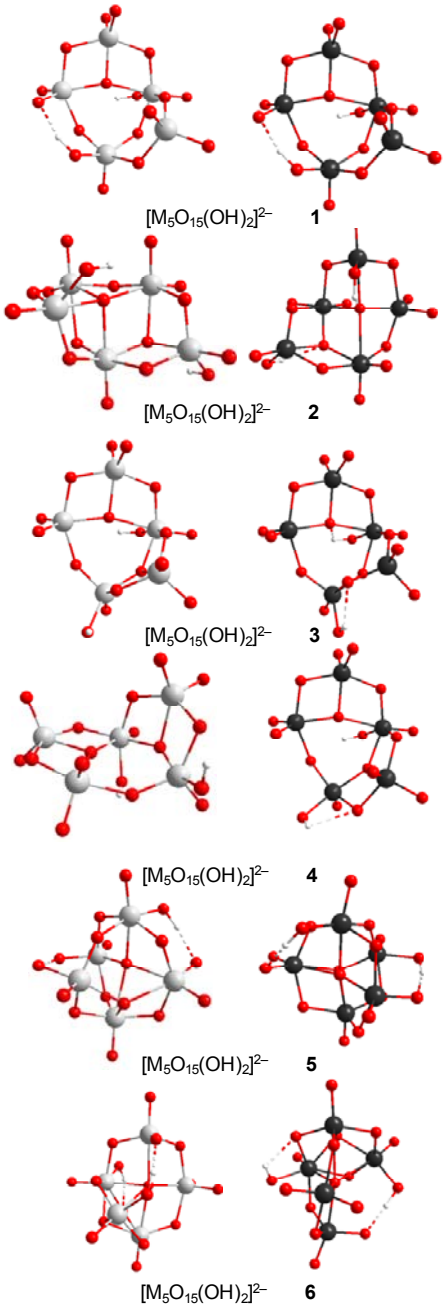

Figure 20. Optimized structures for the the $[M_5O_{15}(OH)_2]^{2-}$ species.

UNIVERSITAT ROVIRA I VIRGILI
ASSEMBLY AND PROPERTIES OF POLYOXOMETALATES: A THEORETICAL POINT OF VIEW
Laia Vilà Nadal
ISBN.978-84-694-2170-3/DL:T. 1039-2011

Table 7. Relative energies (in kcal mol^{-1}) hexameric species with respect to the monomers.

Structure		ΔE (kcal mol^{-1})	
		M=W	M=Mo
$[M_6O_{19}]^{2-}$	**1**	-97.1	-66.9
$[M_6O_{19}(OH)]^{3-}$	**2**	-62.4	-35.1
$[M_6O_{18}(OH)_2]^{2-}$	**3**	-81.4	-54.5

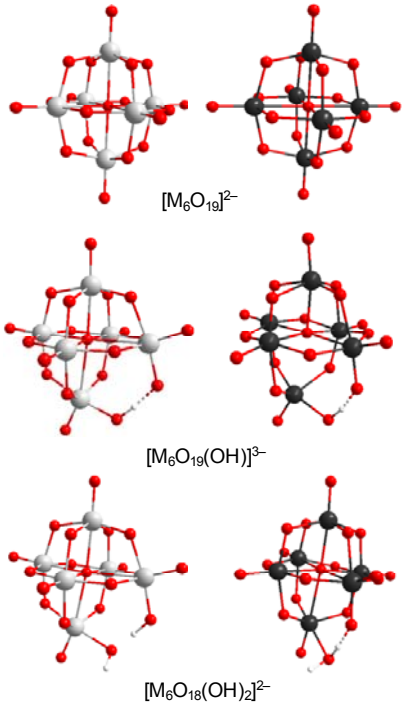

Figure 21. Optimized structures for the most representative hexamers.

UNIVERSITAT ROVIRA I VIRGILI
ASSEMBLY AND PROPERTIES OF POLYOXOMETALATES: A THEORETICAL POINT OF VIEW
Laia Vilà Nadal
ISBN.978-84-694-2170-3/DL:T. 1039-2011

UNIVERSITAT ROVIRA I VIRGILI
ASSEMBLY AND PROPERTIES OF POLYOXOMETALATES: A THEORETICAL POINT OF VIEW
Laia Vilà Nadal
ISBN.978-84-694-2170-3/DL:T. 1039-2011

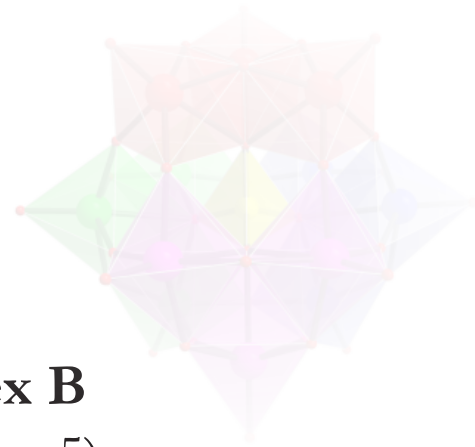

Annex B
(chapter 5)

UNIVERSITAT ROVIRA I VIRGILI
ASSEMBLY AND PROPERTIES OF POLYOXOMETALATES: A THEORETICAL POINT OF VIEW
Laia Vilà Nadal
ISBN.978-84-694-2170-3/DL:T. 1039-2011

UNIVERSITAT ROVIRA I VIRGILI
ASSEMBLY AND PROPERTIES OF POLYOXOMETALATES: A THEORETICAL POINT OF VIEW
Laia Vilà Nadal
ISBN.978-84-694-2170-3/DL:T. 1039-2011

Table 1. Reaction energies (in kcal mol^{-1}) for dinuclear species with respect to the monomers. Detected stoichiometries in ESI-MS are $[W_2O_7]^{2-}$, $[Mo_2O_7]^{2-}$ and $[W_2O_6(OH)]^-$ highlighted in boldface type.

Structure			ΔE (kcal mol^{-1})			
			M=W		M=Mo	
			X=P	X=As	X=P	X=As
$[M_2O_6(OH)_2]^{2-}$	**1**	a	–7.5		+0.4	
	2	b	+0.2		+7.4	
	3	c	+10.2		+11.4	
$[M_2O_7]^{2-}$	**1**	d	–4.4		–2.2	
	2	e	–3.3		–2.1	
$[M_2O_6(OH)]^-$	**1**	f	–21.9		–17.9	
$[XMO_5(OH)_3]^{2-}$	**1**	g	+2.4	+1.3	+4.2	+3.7
	2	h	+12.6	+13.2	+15.7	+14.0
	3	i	+3.0	+3.2	+5.5	+8.4
	4	j	+27.3	+10.3	+30.2	+12.9
$[XMO_6(OH)]^{2-}$	**1**	k	+0.8	+2.5	+1.6	+1.76
	2	l	+2.2	+0.6	+1.7	+0.92
	3	m	+1.5	–0.3	+1.5	+0.16
$[XMO_5(OH)_2]^-$	**1**	n	–18.6	–22.2	–17.2	–21.4

UNIVERSITAT ROVIRA I VIRGILI
ASSEMBLY AND PROPERTIES OF POLYOXOMETALATES: A THEORETICAL POINT OF VIEW
Laia Vilà Nadal
ISBN.978-84-694-2170-3/DL:T. 1039-2011

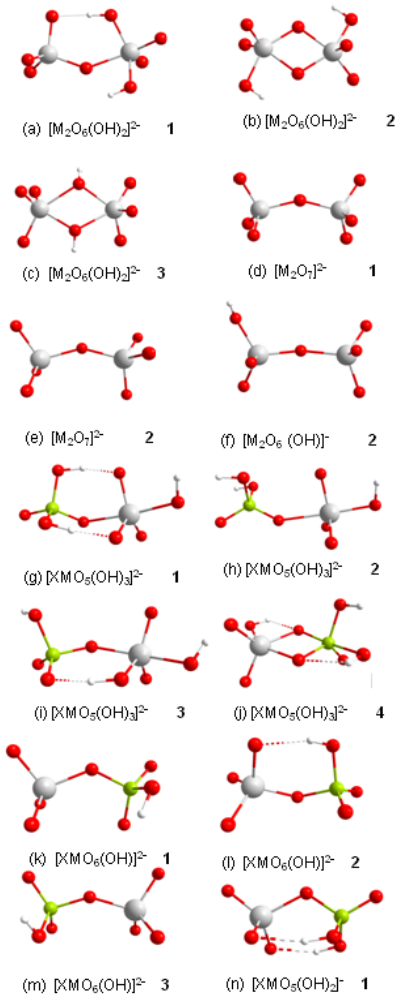

Figure 1. Optimized structures for the most representative dinuclear species.

UNIVERSITAT ROVIRA I VIRGILI
ASSEMBLY AND PROPERTIES OF POLYOXOMETALATES: A THEORETICAL POINT OF VIEW
Laia Vilà Nadal
ISBN.978-84-694-2170-3/DL:T. 1039-2011

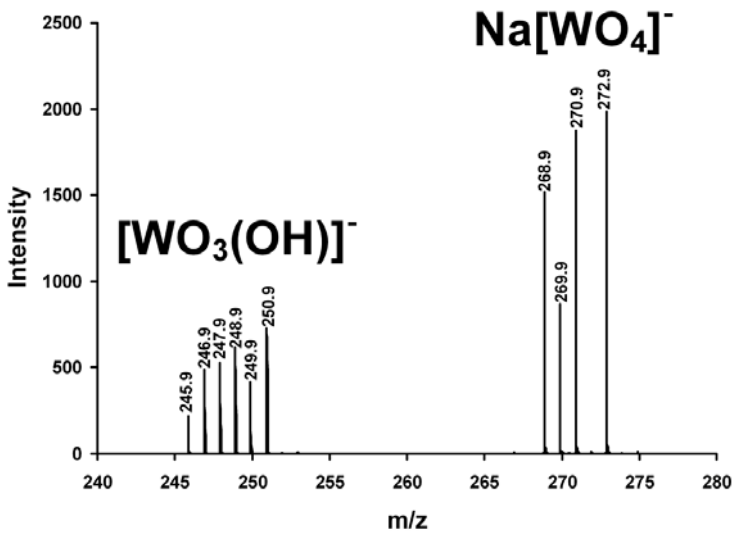

Figure 2. Monomeric fragments $[WO_3(OH)]^-$ (*m/z* 248.9) and $Na[WO_4]^-$ (*m/z* 270.9) observed in the assembly solution of $[(n\text{-}C_4H_9)_4N]_3AsW_{12}O_{40}$ in the Mass Spectrometer.

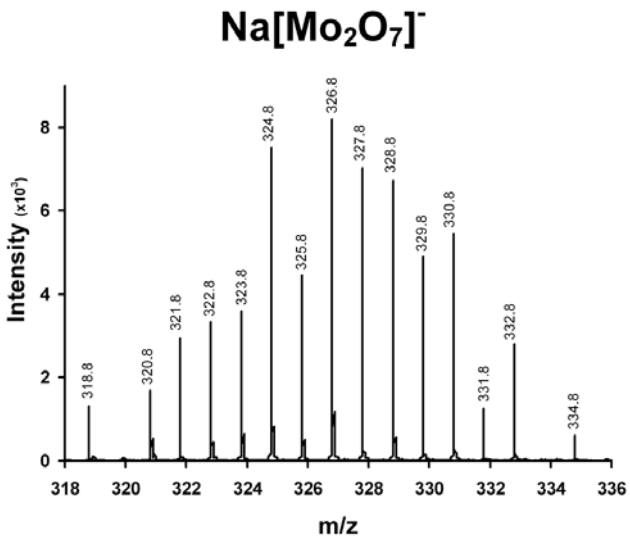

Figure 3. Isodimeric fragment $Na[Mo_2O_7]^-$ (*m/z* 326.8) observed in the assembly solution of $[(n\text{-}C_4H_9)_4N]_3PMo_{12}O_{40}$ in the Mass Spectrometer.

UNIVERSITAT ROVIRA I VIRGILI
ASSEMBLY AND PROPERTIES OF POLYOXOMETALATES: A THEORETICAL POINT OF VIEW
Laia Vilà Nadal
ISBN.978-84-694-2170-3/DL:T. 1039-2011

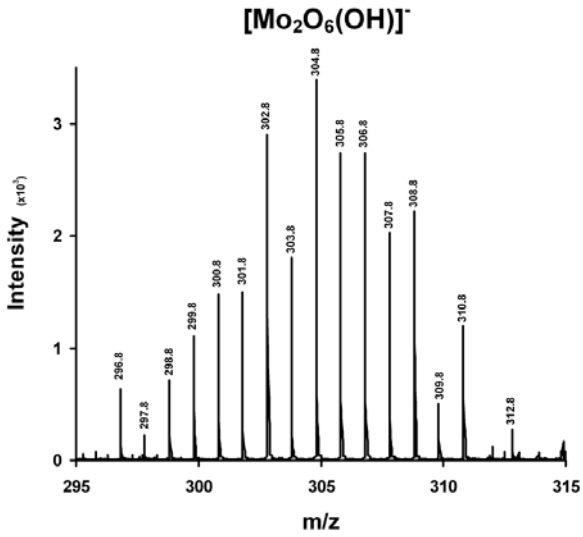

Figure 4. Protonated isodimeric fragment $[Mo_2O_6(OH)]^-$ (*m/z* 304.8) observed in the assembly solution of $[(n\text{-}C_4H_9)_4N]_3PMo_{12}O_{40}$ in the Mass Spectrometer.

UNIVERSITAT ROVIRA I VIRGILI
ASSEMBLY AND PROPERTIES OF POLYOXOMETALATES: A THEORETICAL POINT OF VIEW
Laia Vilà Nadal
ISBN.978-84-694-2170-3/DL:T. 1039-2011

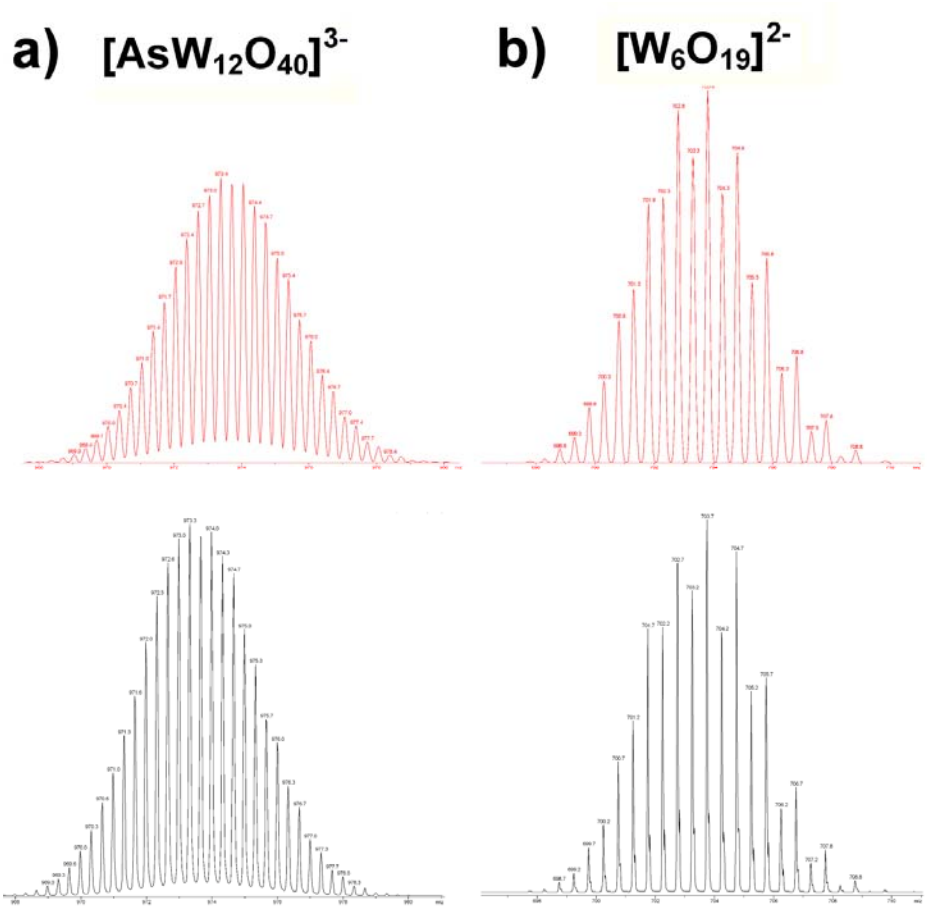

Figure 5. Comparison of experimental (top, red) and theoretical (bottom, black) mass spectra for (a) $[AsW_{12}O_{40}]^{3-}$ (*m/z* 973.3); and (b) $[W_6O_{19}]^{2-}$ (*m/z* 703.8). The experimental (red) isotope patterns shown above for the ion assigned peaks were generated from $[(n\text{-}C_4H_9)_4N]_3AsW_{12}O_{40}$ dissolved in acetonitrile solution and studies by ESI-MS.

UNIVERSITAT ROVIRA I VIRGILI
ASSEMBLY AND PROPERTIES OF POLYOXOMETALATES: A THEORETICAL POINT OF VIEW
Laia Vilà Nadal
ISBN.978-84-694-2170-3/DL:T. 1039-2011

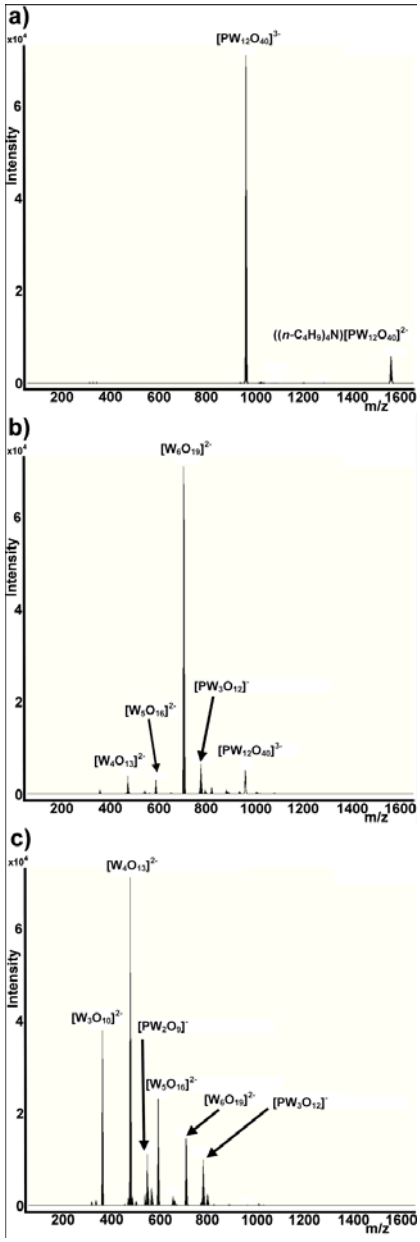

Figure 6. Electrospray Ionisation Mass Spectrometry data showing the collision induced dissociation (CID) of $[(n\text{-}C_4H_9)_4N]_3PW_{12}O_{40}$ in acetonitrile showing the major ions observed in the gas phase at collision energies (CE) a) 5 eV; b) 25 eV; c) 45 eV respectively.

UNIVERSITAT ROVIRA I VIRGILI
ASSEMBLY AND PROPERTIES OF POLYOXOMETALATES: A THEORETICAL POINT OF VIEW
Laia Vilà Nadal
ISBN.978-84-694-2170-3/DL:T. 1039-2011

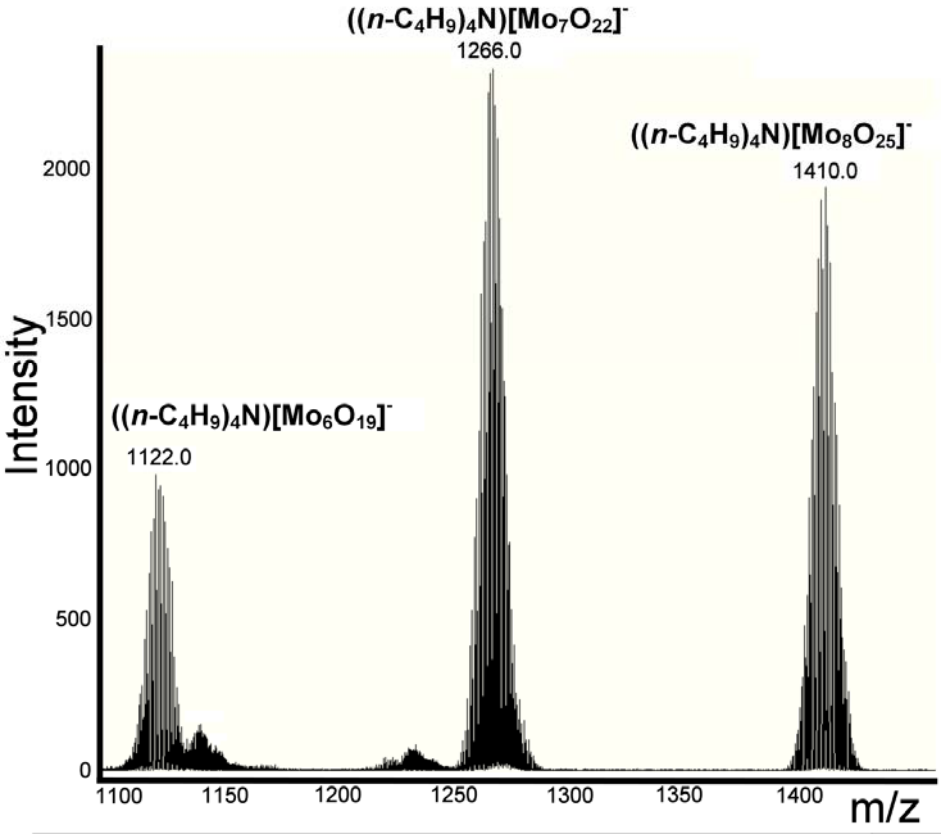

Figure 7. Electrospray Ionisation Mass Spectrometry data of collision induced dissociation (CID) of $[(n\text{-}C_4H_9)_4N]_3AsMo_{12}O_{40}$ in acetonitrile showing the presence of key ions in the gas phase $((n\text{-}C_4H_9)_4N)[Mo_6O_{19}]^-$ (*m/z* 1122.0); $((n\text{-}C_4H_9)_4N)[Mo_7O_{22}]^-$ (*m/z* 1266.0) and $((n\text{-}C_4H_9)_4N)[Mo_8O_{25}]^-$ (*m/z* 1410.0).

UNIVERSITAT ROVIRA I VIRGILI
ASSEMBLY AND PROPERTIES OF POLYOXOMETALATES: A THEORETICAL POINT OF VIEW
Laia Vilà Nadal
ISBN.978-84-694-2170-3/DL:T. 1039-2011

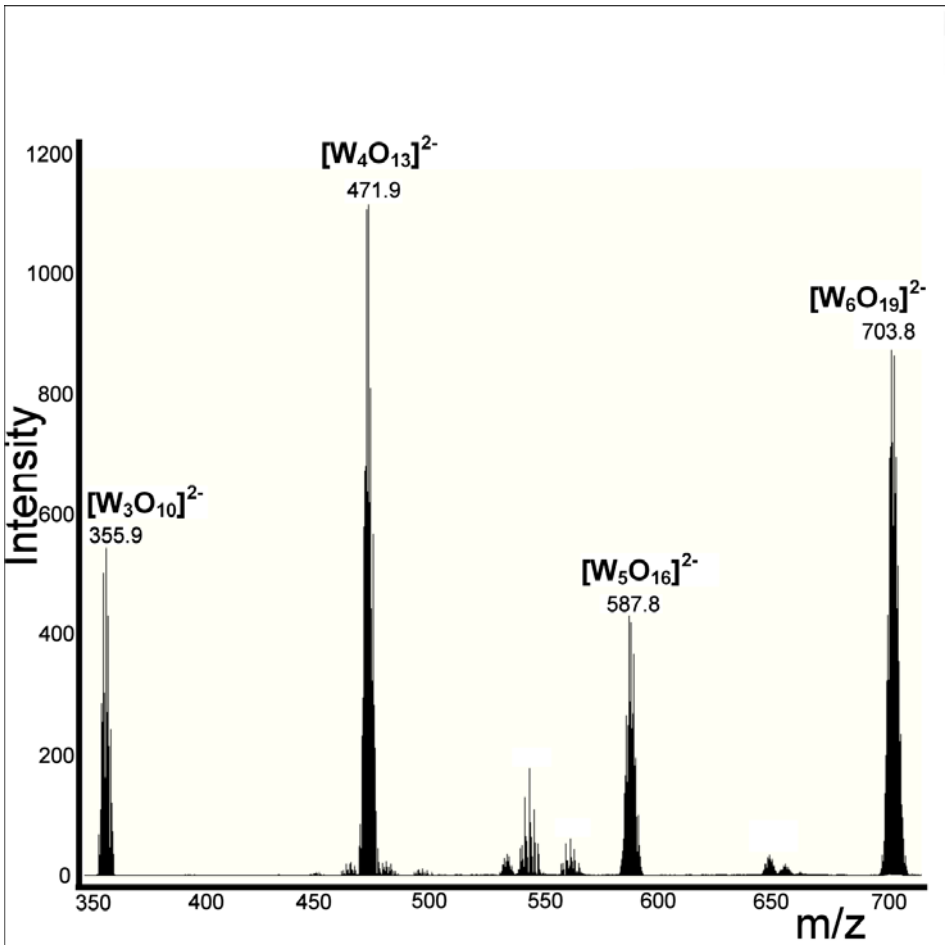

Figure 8. Electrospray Ionisation Mass Spectrometry data of collision induced dissociation (CID) of $[(n\text{-}C_4H_9)_4N]_3PW_{12}O_{40}$ in acetonitrile showing the presence of key doubly charged ions in the gas phase: $[W_3O_{10}]^{2-}$ (*m/z* 355.9); $[W_4O_{13}]^{2-}$ (*m/z* 471.9); $[W_5O_{16}]^{2-}$ (*m/z* 587.8) and $[W_6O_{19}]^{2-}$ (*m/z* 703.8)

UNIVERSITAT ROVIRA I VIRGILI
ASSEMBLY AND PROPERTIES OF POLYOXOMETALATES: A THEORETICAL POINT OF VIEW
Laia Vilà Nadal
ISBN.978-84-694-2170-3/DL:T. 1039-2011

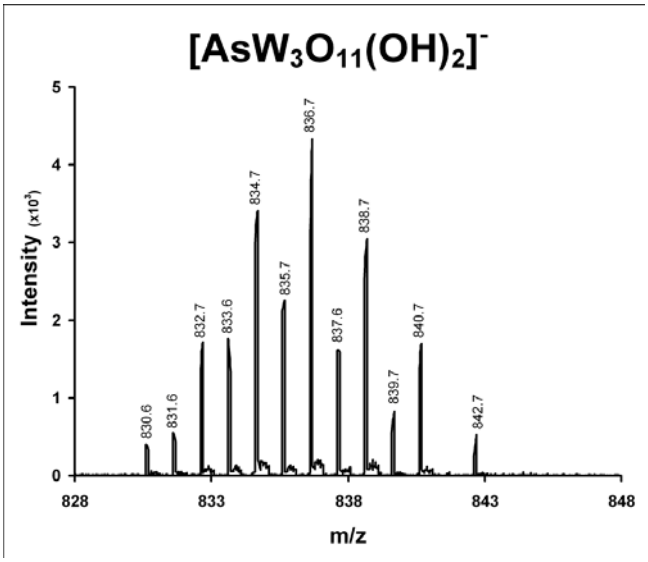

Figure 9. Heterotetrameric fragment $[AsW_3O_{11}(OH)_2]^-$ (*m/z* 836.7) observed in the fragmentation of $[(n\text{-}C_4H_9)_4N]_3AsW_{12}O_{40}$ in acetonitrile.

UNIVERSITAT ROVIRA I VIRGILI
ASSEMBLY AND PROPERTIES OF POLYOXOMETALATES: A THEORETICAL POINT OF VIEW
Laia Vilà Nadal
ISBN.978-84-694-2170-3/DL:T. 1039-2011

Table 2. A summary of the common fragments observed in the assembly and fragmentation of Keggin anions, $[XM_{12}O_{40}]^{3-}$ (X = P, As; M = W, Mo), transferred to the gas phase by electrospray ionization and analysed in the Mass Spectrometer.

Nucleation	Assembly		Fragmentation	
	W-Keggins[a]	Mo-Keggins	W-Keggins[a]	Mo-Keggins
Monomer	$Na[WO_4]^-$	$Na[MoO_4]^-$		
	$[WO_3(OH)]^-$	$[MoO_3(OH)]^-$		
Dimer	$Na[W_2O_7]^-$	$Na[Mo_2O_7]^-$ $((n\text{-}C_4H_9)_4N)[Mo_2O_7]^-$		
	$[W_2O_6(OH)_2]^{2-}$	$Na[Mo_2O_6(OH)_2]^-$ $Li[Mo_2O_6(OH)_2]^-$ $[Mo_2O_6(OH)]^-$		
Trimer			$[XW_2O_9]^-$	
			$[XW_2O_8(OH)_2]^-$	
			$[W_3O_{10}]^{2-}$	
Tetramer			$[W_4O_{13}]^{2-}$	$[Mo_4O_{13}]^{2-}$ $((n\text{-}C_4H_9)_4N)[Mo_4O_{13}]^-$
			$[XW_3O_{12}]^-$	$[XMo_3O_{12}]^-$
			$[XW_3O_{11}(OH)_2]^-$	
Pentamer			$[XW_4O_{15}]^-$	$[XMo_4O_{15}]^-$
			$[W_5O_{16}]^{2-}$	$[Mo_5O_{16}]^{2-}$
Hexamer			$[W_6O_{19}]^{2-}$	$[Mo_6O_{19}]^{2-}$ $((n\text{-}C_4H_9)_4N)[Mo_6O_{19}]^-$
Heptamer			$[W_7O_{22}]^{2-}$	$[Mo_7O_{22}]^{2-}$ $((n\text{-}C_4H_9)_4N)[Mo_7O_{22}]^-$
Octamer				$[Mo_8O_{25}]^{2-}$ $((n\text{-}C_4H_9)_4N)[Mo_8O_{25}]^-$
Dodecamer			$[XW_{12}O_{40}]^{3-}$	$H[PMo_{12}O_{40}]^{2-}$
			$((n\text{-}C_4H_9)_4N)[XW_{12}O_{40}]^{2-}$	$((n\text{-}C_4H_9)_4N)[XMo_{12}O_{40}]^{2-}$
			$((n\text{-}C_4H_9)_4N)_2[XW_{12}O_{40}]^{1-}$	$((n\text{-}C_4H_9)_4N)_2[XMo_{12}O_{40}]^{1-}$

UNIVERSITAT ROVIRA I VIRGILI
ASSEMBLY AND PROPERTIES OF POLYOXOMETALATES: A THEORETICAL POINT OF VIEW
Laia Vilà Nadal
ISBN.978-84-694-2170-3/DL:T. 1039-2011

Table 3. Relative energies, with respect to the most stable geometry, (in kcal mol^{-1}) for $[XM_2O_8(OH)_3]^{2-}$ and $[XM_2O_8(OH)_2]^{-}$ stoichiometries. The results are organized with respect the values from stoichiometries $[PW_2O_8(OH)_3]^{2-}$ and $[PW_2O_8(OH)_2]^{-}$ in order of decreasing stability. Detected stoichiometry in ESI-MS experiment is $[PW_2O_8(OH)_2]^{2-}$ highlighted in boldface type.

Structure			ΔE (kcal mol^{-1})			
			M=W		M=Mo	
			X=P	X=As	X=P	X=As
$[XM_2O_8(OH)_3]^{2-}$	**1**	a	0.0	0.0	0.0	0.0
	2	b	+7.9	+3.3	+5.2	-
	3	c	+8.4	+9.3	+9.7	-
	4	d	+11.4	+8.9	+9.8	-
	5	e	+11.7	+7.2	+8.6	+6.3
	6	f	+15.7	+7.5	+18.8	-
$[XM_2O_8(OH)_2]^{-}$	**1**	h	0.0	+0.1	0.0	0.0
	2	i	+2.9	0.0	+2.2	+4.8
	3	j	+3.4	+0.3	+1.7	+2.9
	4	k	+4.0	+1.0*	+1.6	+2.3*
	5	l	+6.1	+1.2	+5.7	+4.9

UNIVERSITAT ROVIRA I VIRGILI
ASSEMBLY AND PROPERTIES OF POLYOXOMETALATES: A THEORETICAL POINT OF VIEW
Laia Vilà Nadal
ISBN.978-84-694-2170-3/DL:T. 1039-2011

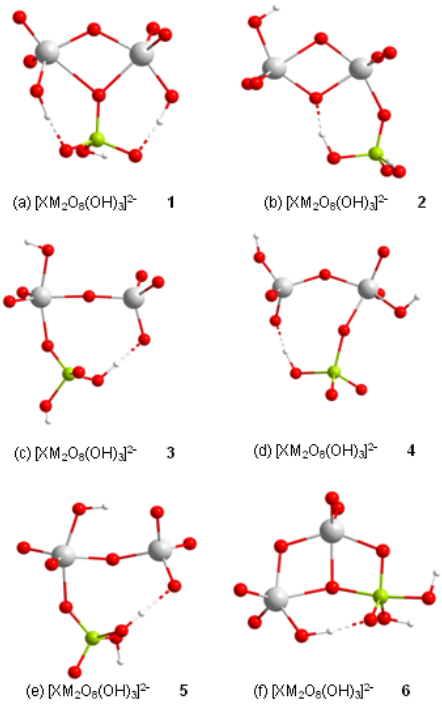

Figure 10. Optimized structures for the most representative trinuclear species. The str organized with respect the results of stoichiometry $[PW_2O_8(OH)_3]^{2-}$ in order of decreasing s

UNIVERSITAT ROVIRA I VIRGILI
ASSEMBLY AND PROPERTIES OF POLYOXOMETALATES: A THEORETICAL POINT OF VIEW
Laia Vilà Nadal
ISBN.978-84-694-2170-3/DL:T. 1039-2011

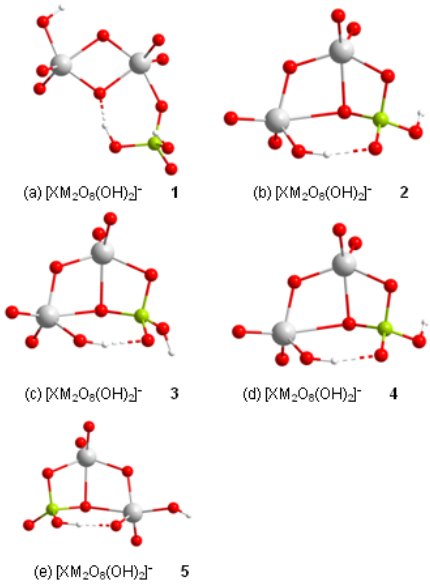

Figure 11. Optimized structures for the most representative trinuclear species. The str organized with respect to the results of stoichiometry $[PW_2O_8(OH)_2]^-$ in order of decreas There are minor geometrical differences between geometries 2 and 4, they are degenerate (~1 Kcal mol^{-1}).

*Optimized structures for the case of structure 5 $[AsM_2O_8(OH)_2]^-$

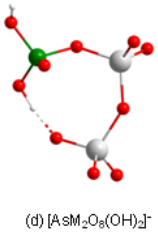

UNIVERSITAT ROVIRA I VIRGILI
ASSEMBLY AND PROPERTIES OF POLYOXOMETALATES: A THEORETICAL POINT OF VIEW
Laia Vilà Nadal
ISBN.978-84-694-2170-3/DL:T. 1039-2011

Table 4. Relative energies, with respect to the most stable geometry, (in kcal mol^{-1}) for [XM stoichiometry. The results are organized with respect the results of stoichiometry [PW_2C order of decreasing stability.

Structure			ΔE (kcal mol^{-1})			
			M=W		M=Mo	
			X=P	X=As	X=P	X=As
$[XM_2O_9(OH)_2]^{3-}$	**1**	a	0.0	+0.1	+2.0	+4.0
	2	b	+1.1	0.0	+0.6	+3.4
	3	c	+2.8	+1.7	0.0	0.0
	4	d	+4.1	0.0	+9.9	+7.5
	5	e	+5.5	+9.7*	+12.2	+11.8*
	6	f	+6.0	+4.4	+10.5	+9.4
	7	g	+6.2	+3.7	+8.8	+10.1
	8	h	+6.6	+3.9	-	-
	9	i	+7.0	+9.8	-	-
	10	j	+8.6	+3.0	-	-
	11	k	+9.5	+10.1	-	-
	12	l	+9.6	+8.2	-	-
	13	m	+9.8	+9.4	-	-
	14	n	+10.2	+7.0	-	-
	15	o	+10.3	+15.3	-	-
	16	p	+28.0	-	-	-

*Optimized structures for the case of structure 5 $[AsM_2O_9(OH)_2]^{3-}$

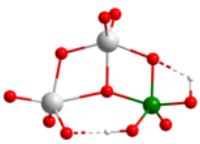

UNIVERSITAT ROVIRA I VIRGILI
ASSEMBLY AND PROPERTIES OF POLYOXOMETALATES: A THEORETICAL POINT OF VIEW
Laia Vilà Nadal
ISBN.978-84-694-2170-3/DL:T. 1039-2011

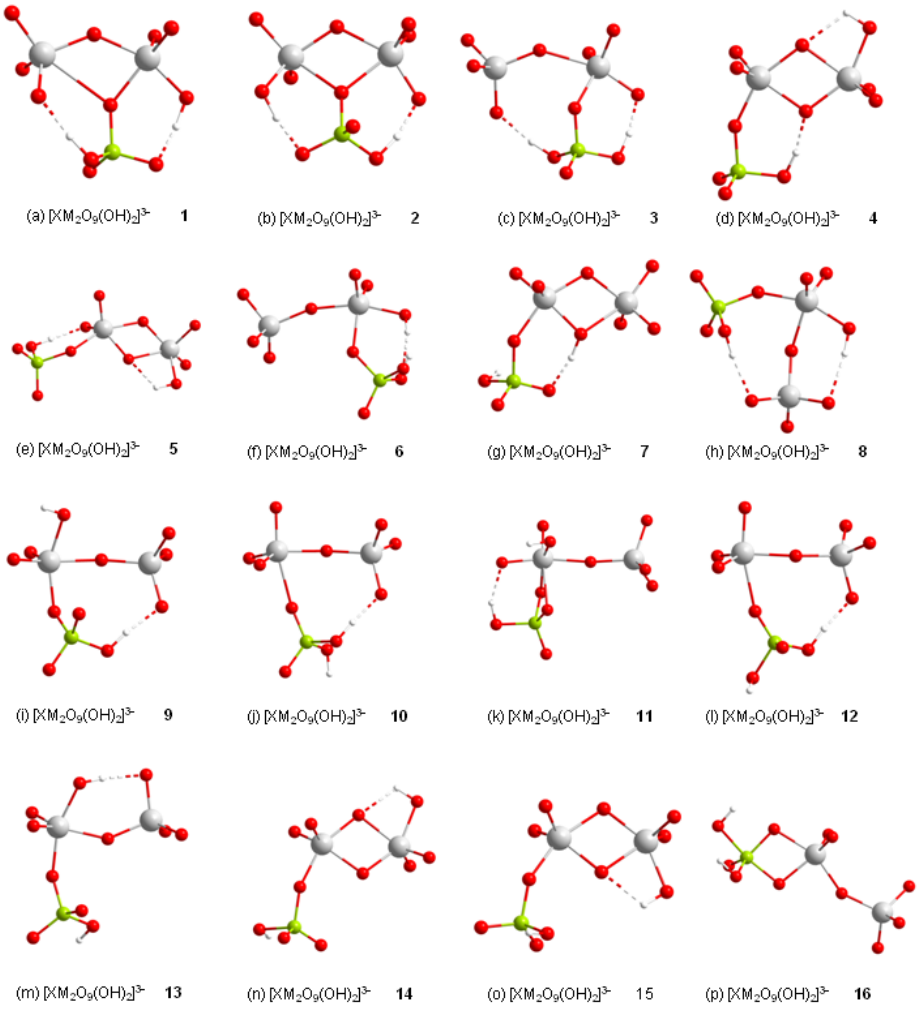

Figure 12. Optimized structures for the most representative trinuclear species. The str organized with respect the results of stoichiometry $[PW_2O_9(OH)_2]^{3-}$ in order of decreasing s

UNIVERSITAT ROVIRA I VIRGILI
ASSEMBLY AND PROPERTIES OF POLYOXOMETALATES: A THEORETICAL POINT OF VIEW
Laia Vilà Nadal
ISBN.978-84-694-2170-3/DL:T. 1039-2011

Table 5. Relative energies, with respect to the most stable geometry, (in kcal mol^{-1}) for $[XM_2O_9OH)]^{2-}$ and $[XM_2O_9]^-$ stoichiometries. Detected stoichiometries in ESI-MS experiment are $[PW_2O_9]^-$ and $[AsW_2O_9]^-$, highlighted in boldface type.

Structure			ΔE (kcal mol^{-1})			
			M=W		M=Mo	
			X=P	X=As	X=P	X=As
$[XM_2O_9(OH)]^{2-}$	**1**	a	0.0	+3.5	+1.5	+6.1
	2	b	+0.6	0.0	0.0	0.0
	3	c	+1.4	+2.4	+3.0	+1.1
	4	d	+2.6	+12.5	+4.6	+9.7
	5	e	+3.3	+2.9	+1.3	+1.3
	6	f	+4.6	+1.9	+5.8	+0.7
	7	g	+8.2	+9.7	+7.4	+8.5
	8	h	+11.3	+7.0	+12.6	+0.9
$[XM_2O_9]^-$	**1**	g	0.0	+4.7	0.0	+7.8
	2	h	+3.9	0.0	+0.3	0.0
	3	i	+4.1	+3.2	+4.8	+6.5
	4	j	+6.5	+1.0	+5.7	+2.3
	5	k	+18.3	+12.4	+16.7	+14.3
	6	l	+37.0	+20.3	+34.4	+23.3

UNIVERSITAT ROVIRA I VIRGILI
ASSEMBLY AND PROPERTIES OF POLYOXOMETALATES: A THEORETICAL POINT OF VIEW
Laia Vilà Nadal
ISBN.978-84-694-2170-3/DL:T. 1039-2011

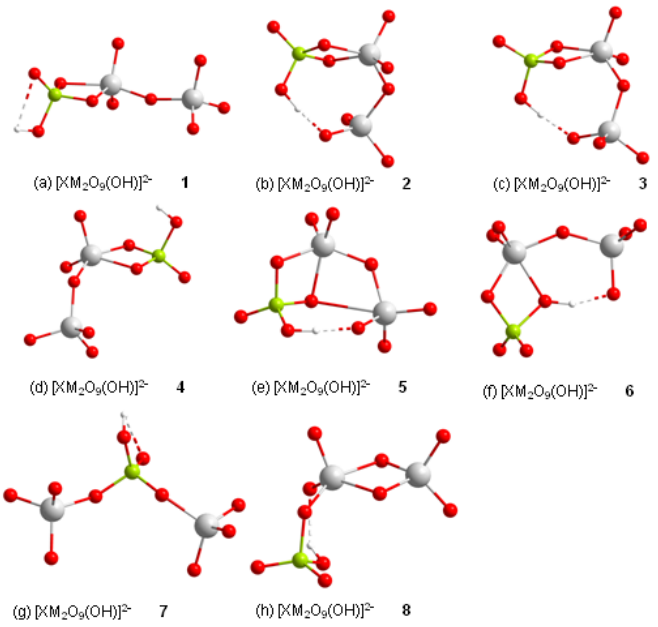

Figure 13. Optimized structures for the most representative trinuclear species. The organized with respect the results of stoichiometry $[PW_2O_9(OH)]^{2-}$ in order of decreasi Structures 1 and 2 are practically degenerated.

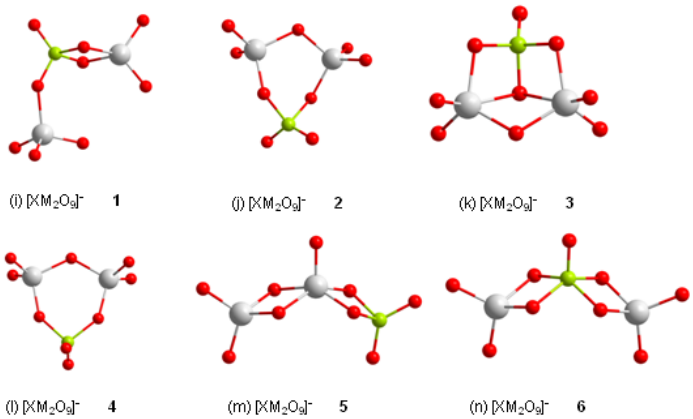

Figure 14. Optimized structures for the most representative trinuclear species. The organized with respect the results of stoichiometry $[PW_2O_9]^{-}$ in order of decreasing stability

UNIVERSITAT ROVIRA I VIRGILI
ASSEMBLY AND PROPERTIES OF POLYOXOMETALATES: A THEORETICAL POINT OF VIEW
Laia Vilà Nadal
ISBN.978-84-694-2170-3/DL:T. 1039-2011

Table 6. Relative energies, respect the most stable geometry, (in kcal mol^{-1}) for $[XM_3O_{11}(OH)_3]^{2-}$ stoichiometry. Geometry 4 is a trident-Keggin like structure.

Structure			ΔE (kcal mol^{-1})	
			M=W	
			X=P	X=As
$[XM_3O_{11}(OH)_3]^{2-}$	**1**	a	0.0	0.0
	2	b	+12.6	+19.5
	3	c	+14.8	+15.8
	4	d	+16.4	+19.1
	5	e	+20.7	-
	6	f	+23.5	-
	7	g	+23.7	-
	8	h	+24.0	-
	9	i	+24.8	-
	10	j	+25.7	-
	11	k	+26.0	-
	12	l	+27.2	

UNIVERSITAT ROVIRA I VIRGILI
ASSEMBLY AND PROPERTIES OF POLYOXOMETALATES: A THEORETICAL POINT OF VIEW
Laia Vilà Nadal
ISBN.978-84-694-2170-3/DL:T. 1039-2011

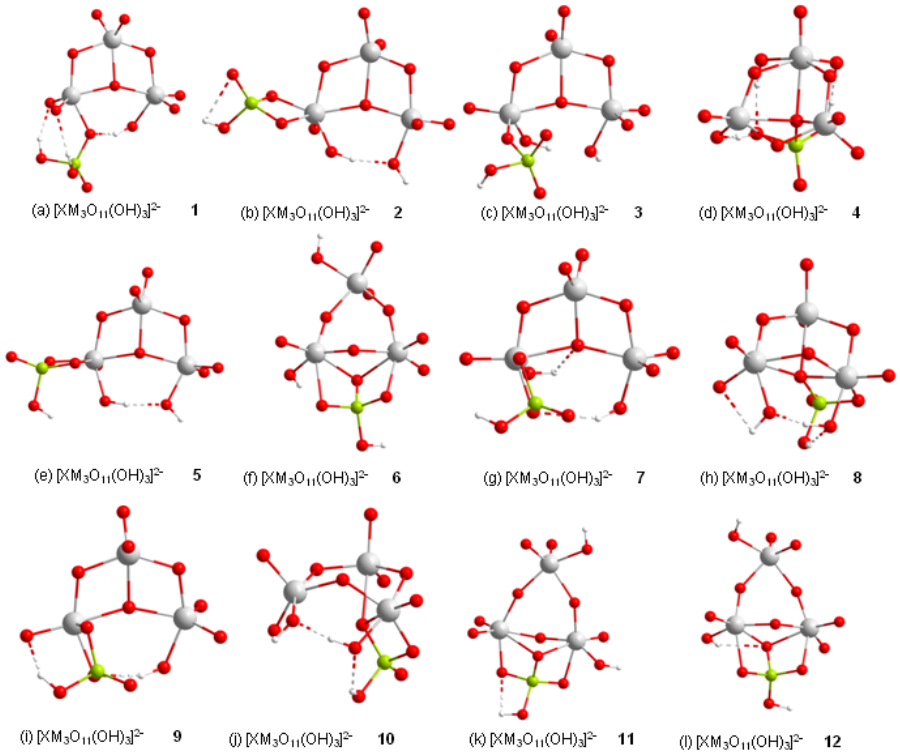

Figure 15. Optimized structures for $[XM_3O_{11}(OH)_3]^{2-}$ stoichiometry. The structures are c order of decreasing stability.

UNIVERSITAT ROVIRA I VIRGILI
ASSEMBLY AND PROPERTIES OF POLYOXOMETALATES: A THEORETICAL POINT OF VIEW
Laia Vilà Nadal
ISBN.978-84-694-2170-3/DL:T. 1039-2011

Table 7. Relative energies, respect the most stable geometry, (in kcal mol^{-1}) for $[XM_3O_{11}(OH)_2]^-$ stoichiometry. Structures 4 and 5 are degenerated. Detected stoichiometries in ESI-MS experiment are $[PW_3O_{11}(OH)_2]^-$ and $[AsW_3O_{11}(OH)_2]^-$, highlighted in boldface type.

Structure			ΔE (kcal mol^{-1})	
			M=W	
			X=P	X=As
$[XM_3O_{11}(OH)_2]^-$	**1**	a	0.0	0.0
	2	b	+4.2	+0.6
	3	c	+4.3	+5.5
	4	d	+6.4	+10.1
	5	e	+7.5	-
	6	f	+15.8	-
	7	g	+15.9	-
	8	h	+15.9	-
	9	i	+16.3	-
	10	j	+16.7	-
	11	k	+17.7	-
	12	l	+20.6	-
	13	m	+50.1	-

UNIVERSITAT ROVIRA I VIRGILI
ASSEMBLY AND PROPERTIES OF POLYOXOMETALATES: A THEORETICAL POINT OF VIEW
Laia Vilà Nadal
ISBN.978-84-694-2170-3/DL:T. 1039-2011

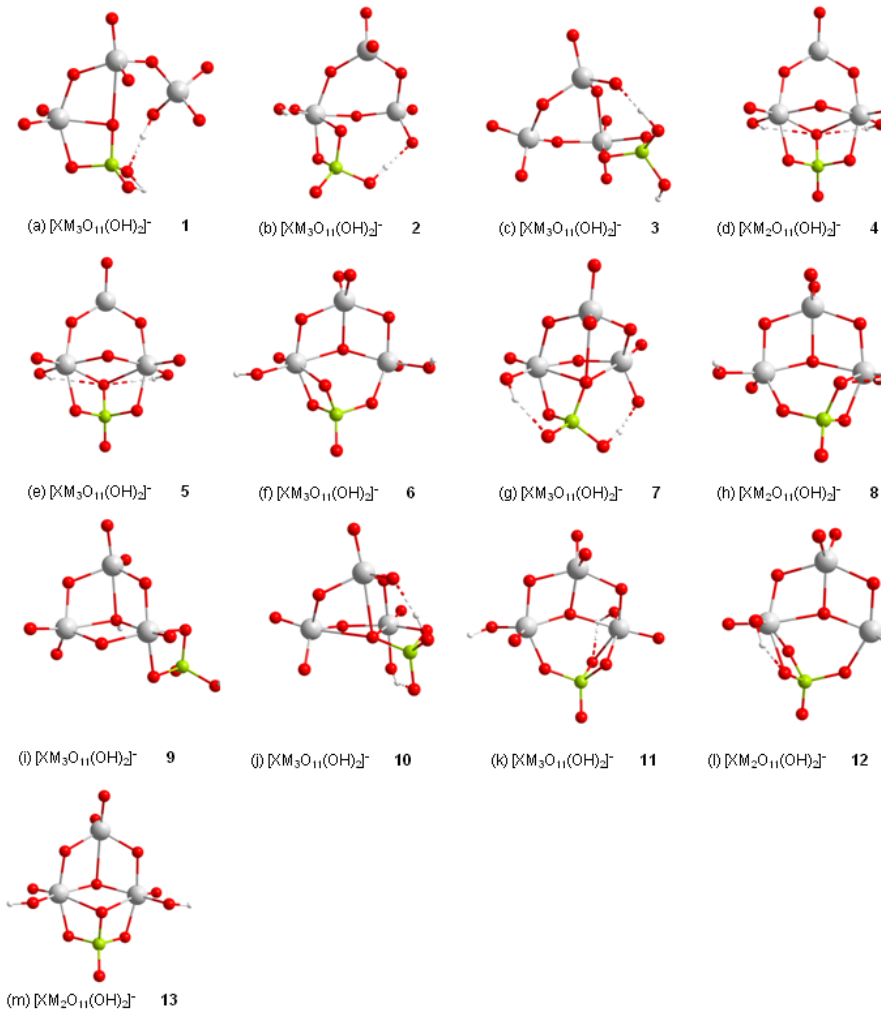

Figure 16. Optimized structures for $[XM_3O_{11}(OH)_2]^-$ stoichiometry. The structures are c order of decreasing stability.

UNIVERSITAT ROVIRA I VIRGILI
ASSEMBLY AND PROPERTIES OF POLYOXOMETALATES: A THEORETICAL POINT OF VIEW
Laia Vilà Nadal
ISBN.978-84-694-2170-3/DL:T. 1039-2011

Table 8. Relative energies, respect the most stable geometry, (in kcal mol^{-1}) for $[XM_3O_{12}(OH)]^{2-}$ stoichiometry.

Structure			ΔE (kcal mol^{-1})	
			M=W	
			X=P	X=As
$[XM_3O_{12}(OH)]^{2-}$	**1**	a	0.0	0.0
	2	b	+0.4	+2.5
	3	c	+0.4	+2.8
	4	d	+1.0	+4.2
	5	e	+1.2	+3.7
	6	f	+13.0	-
	7	g	+13.7	-
	8	h	+14.9	-
	9	i	+15.7	-

UNIVERSITAT ROVIRA I VIRGILI
ASSEMBLY AND PROPERTIES OF POLYOXOMETALATES: A THEORETICAL POINT OF VIEW
Laia Vilà Nadal
ISBN.978-84-694-2170-3/DL:T. 1039-2011

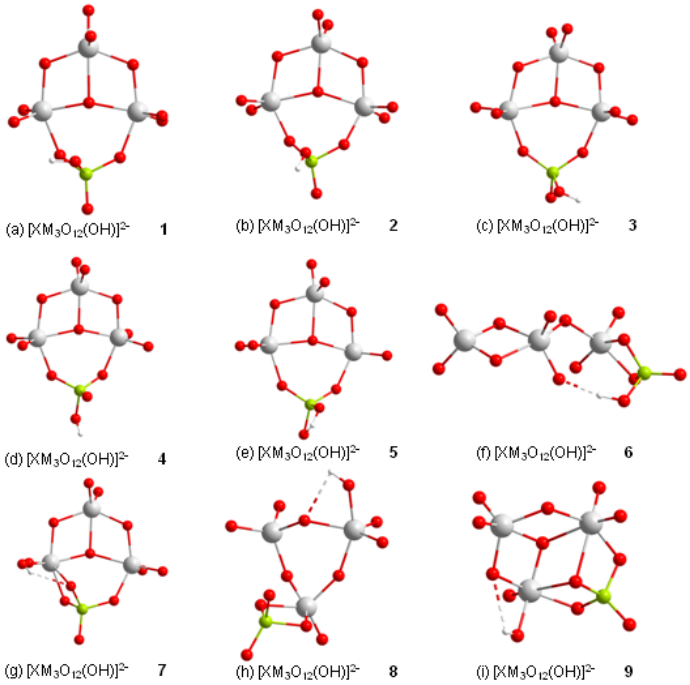

Figure 17. Optimized structures for $[XM_3O_{12}(OH)]^{2-}$ stoichiometry. The structures are c order of decreasing stability.

Table 9. Relative energies, respect the most stable geometry, (in kcal mol^{-1}) for

UNIVERSITAT ROVIRA I VIRGILI
ASSEMBLY AND PROPERTIES OF POLYOXOMETALATES: A THEORETICAL POINT OF VIEW
Laia Vilà Nadal
ISBN.978-84-694-2170-3/DL:T. 1039-2011

Structure			ΔE (kcal mol^{-1})	
			M=W	
			X=P	X=As
$[XM_3O_{12}]^-$	**1**	a	0.0	0.0
	2	b	+4.0	+5.1
	3	c	+6.5	+9.5
	4	d	+6.8	+6.1
	5	e	+8.6	-
	6	f	+11.0	-
	7	g	+12.4	-
	8	h	+12.6	-
	9	i	+13.3	-
	10	j	+13.6	-
	11	k	+14.0	-
	12	l	+31.0	-
	13	m	+38.7	-

UNIVERSITAT ROVIRA I VIRGILI
ASSEMBLY AND PROPERTIES OF POLYOXOMETALATES: A THEORETICAL POINT OF VIEW
Laia Vilà Nadal
ISBN.978-84-694-2170-3/DL:T. 1039-2011

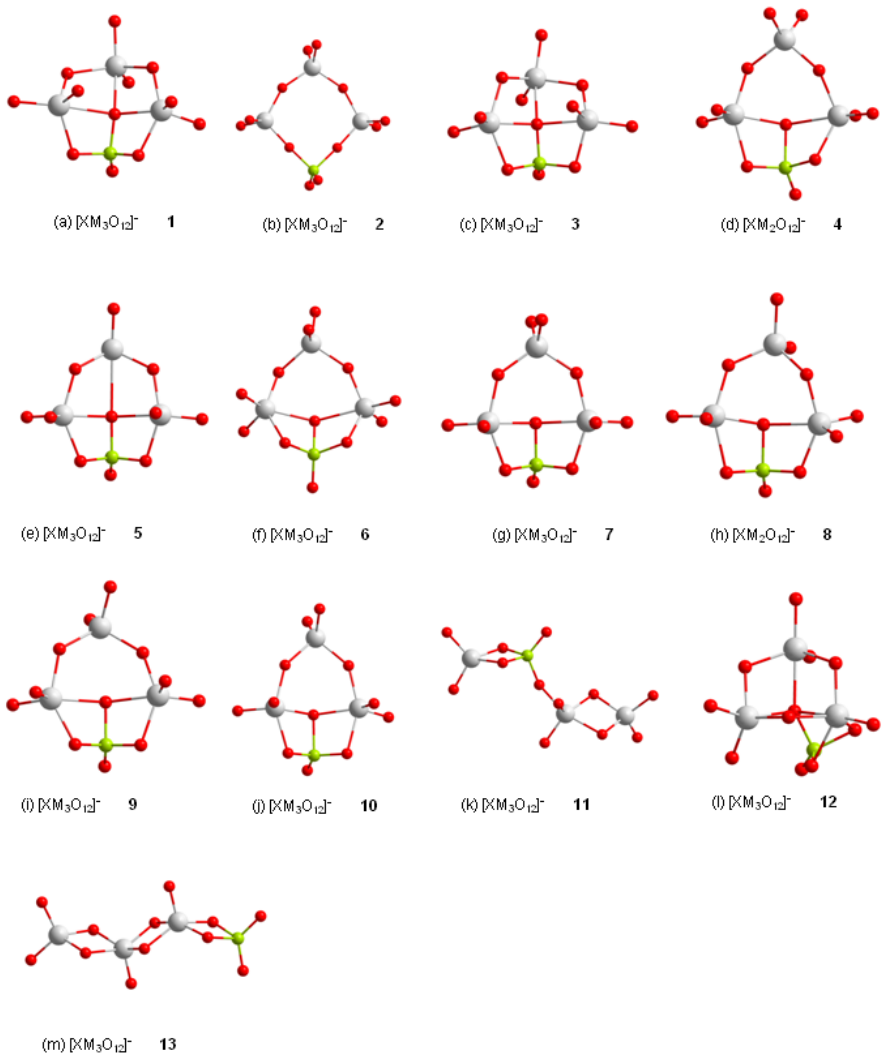

Figure 18. Optimized structures for $[XM_3O_{12}]^-$ stoichiometry. The structures are organized decreasing stability

UNIVERSITAT ROVIRA I VIRGILI
ASSEMBLY AND PROPERTIES OF POLYOXOMETALATES: A THEORETICAL POINT OF VIEW
Laia Vilà Nadal
ISBN.978-84-694-2170-3/DL:T. 1039-2011

UNIVERSITAT ROVIRA I VIRGILI
ASSEMBLY AND PROPERTIES OF POLYOXOMETALATES: A THEORETICAL POINT OF VIEW
Laia Vilà Nadal
ISBN.978-84-694-2170-3/DL:T. 1039-2011

Annex C
(chapter 6)

UNIVERSITAT ROVIRA I VIRGILI
ASSEMBLY AND PROPERTIES OF POLYOXOMETALATES: A THEORETICAL POINT OF VIEW
Laia Vilà Nadal
ISBN.978-84-694-2170-3/DL:T. 1039-2011

UNIVERSITAT ROVIRA I VIRGILI
ASSEMBLY AND PROPERTIES OF POLYOXOMETALATES: A THEORETICAL POINT OF VIEW
Laia Vilà Nadal
ISBN.978-84-694-2170-3/DL:T. 1039-2011

Table 1. Relative energies in kcal mol^{-1} with respect to the most stable $[As_2W_{18}O_{62}]^{6-}$ isomer, and the HOMO–LUMO gaps.

$[W_{18}O_{54}(AsO_4)_2]^{6-}$	HOMO (eV)	LUMO (eV)	GAP (eV)	Relative Energy (kcal mol^{-1})
alfa	-6.74	-4.43	-2.3	1.1
beta	-6.69	-4.47	-2.2	2.4
gamma	-6.66	-4.52	-2.1	0.6
alfa*	-6.57	-4.43	-2.1	16.5
beta*	-6.65	-4.45	-2.2	6.5
gamma*	-6.66	-4.47	-2.2	0.0

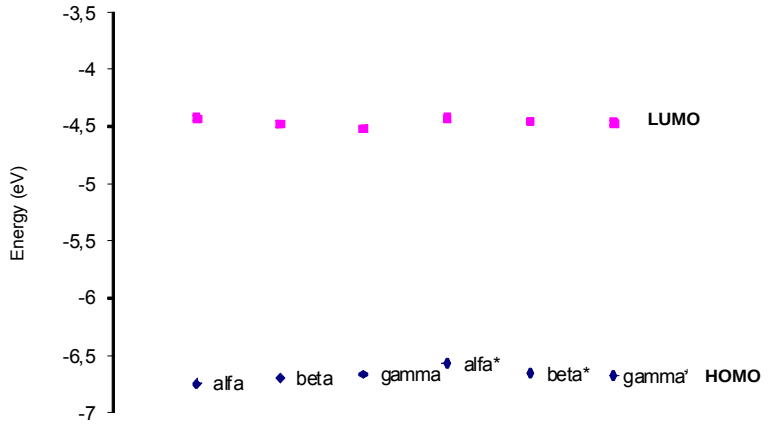

Figure 1. Graphical representation of HOMO and LUMO orbital energies for the six isomers α, β, γ, α*, β*, γ* when X=As, $[As_2W_{18}O_{62}]^{6-}$.

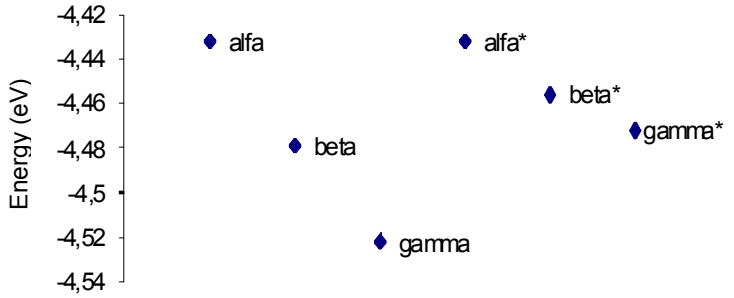

Figure 2. Graphical representation of LUMO orbital energies for the six isomers α, β, γ, α*, β*, γ* when X=As, $[As_2W_{18}O_{62}]^{6-}$.

UNIVERSITAT ROVIRA I VIRGILI
ASSEMBLY AND PROPERTIES OF POLYOXOMETALATES: A THEORETICAL POINT OF VIEW
Laia Vilà Nadal
ISBN.978-84-694-2170-3/DL:T. 1039-2011

Table 2. Relative energies in kcal mol^{-1} with respect to the most stable $[P_2W_{18}O_{62}]^{6-}$ isomer, and the HOMO–LUMO gaps.

$[W_{18}O_{54}(PO_4)_2]^{6-}$	HOMO (eV)	LUMO (eV)	GAP (eV)	Relative Energy (kcal mol^{-1})
alfa	-6.70	-4.38	-2.3	0.0
beta	-6.65	-4.43	-2.2	5.2
gamma	-6.62	-4.49	-2.1	5.4
alfa*	-6.50	-4.40	-2.1	22.1
beta*	-6.62	-4.44	-2.2	12.6
gamma*	-6.64	-4.47	-2.2	7.5

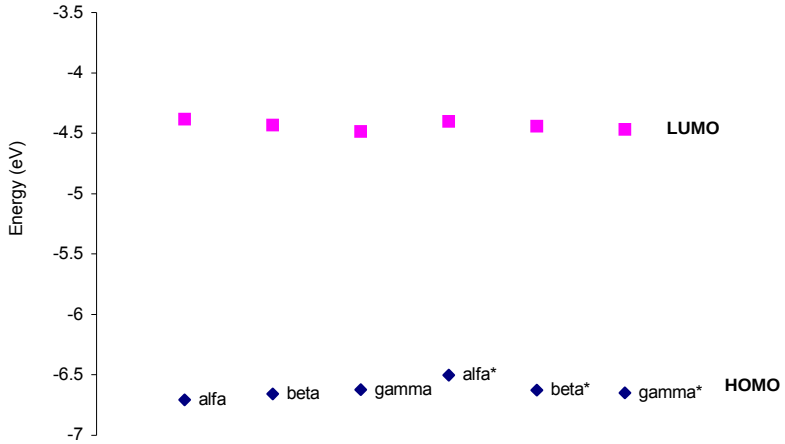

Figure 3. Graphical representation of HOMO and LUMO orbital energies for the six isomers α, β, γ, α*, β*, γ* when X=P, $[P_2W_{18}O_{62}]^{6-}$.

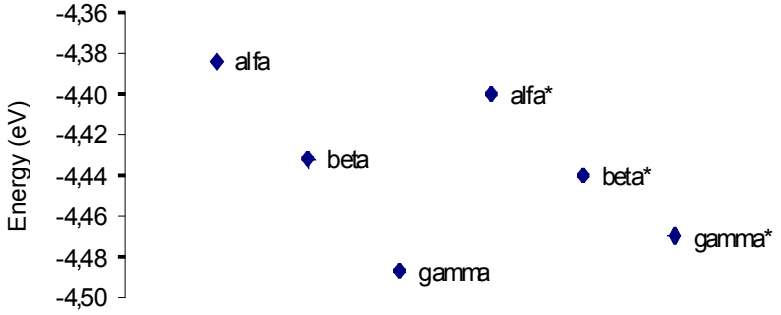

Figure 4. Graphical representation of LUMO orbital energies for the six isomers α, β, γ, α*, β*, γ* when X=P, $[P_2W_{18}O_{62}]^{6-}$.

UNIVERSITAT ROVIRA I VIRGILI
ASSEMBLY AND PROPERTIES OF POLYOXOMETALATES: A THEORETICAL POINT OF VIEW
Laia Vilà Nadal
ISBN.978-84-694-2170-3/DL:T. 1039-2011

Table 3. Relative energies in kcal mol^{-1} with respect to the most stable $[S_2W_{18}O_{62}]^{4-}$ isomer, and the HOMO–LUMO gaps.

$[W_{18}O_{54}(SO_4)_2]^{4-}$	HOMO (eV)	LUMO (eV)	GAP (eV)	Relative Energy (kcal mol^{-1})
alfa	-7.00	-4.72	-2.3	0.0
beta	-6.90	-4.76	-2.1	3.6
gamma	-6.90	-4.81	-2.1	3.7
alfa*	-6.82	-4.75	-2.1	16.7
beta*	-6.93	-4.76	-2.2	7.0
gamma*	-6.92	-4.78	-2.1	1.9

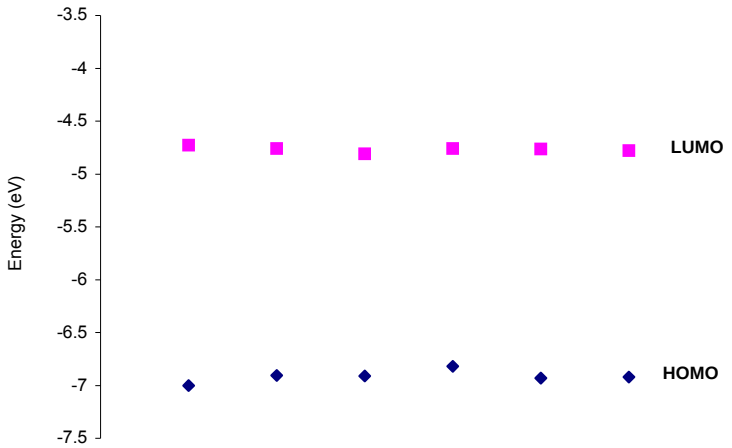

Figure 5. Graphical representation of HOMO and LUMO orbital energies for the six isomers α, β, γ, α*, β*, γ* when X=S, $[S_2W_{18}O_{62}]^{4-}$.

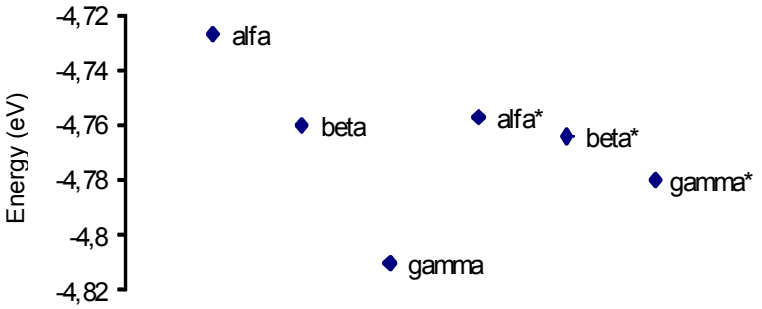

Figure 6. Graphical representation of LUMO orbital energies for the six isomers α, β, γ, α*, β*, γ* when X=As, $[S_2W_{18}O_{62}]^{4-}$.

UNIVERSITAT ROVIRA I VIRGILI
ASSEMBLY AND PROPERTIES OF POLYOXOMETALATES: A THEORETICAL POINT OF VIEW
Laia Vilà Nadal
ISBN.978-84-694-2170-3/DL:T. 1039-2011

UNIVERSITAT ROVIRA I VIRGILI
ASSEMBLY AND PROPERTIES OF POLYOXOMETALATES: A THEORETICAL POINT OF VIEW
Laia Vilà Nadal
ISBN.978-84-694-2170-3/DL:T. 1039-2011

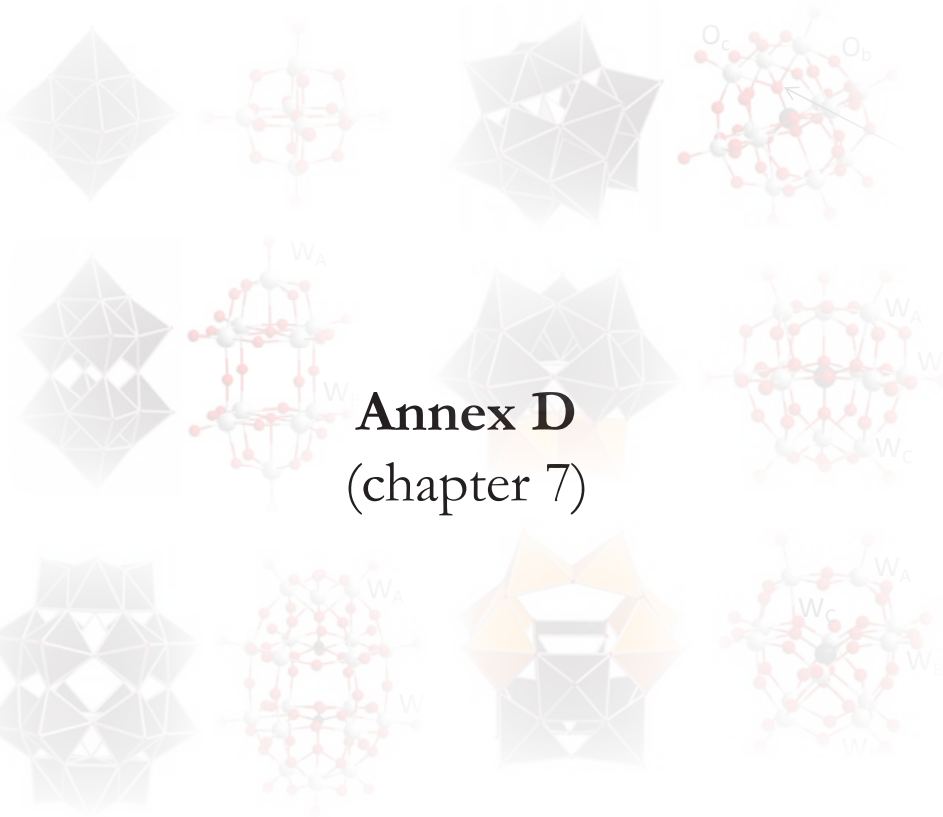

Annex D
(chapter 7)

UNIVERSITAT ROVIRA I VIRGILI
ASSEMBLY AND PROPERTIES OF POLYOXOMETALATES: A THEORETICAL POINT OF VIEW
Laia Vilà Nadal
ISBN.978-84-694-2170-3/DL:T. 1039-2011

UNIVERSITAT ROVIRA I VIRGILI
ASSEMBLY AND PROPERTIES OF POLYOXOMETALATES: A THEORETICAL POINT OF VIEW
Laia Vilà Nadal
ISBN.978-84-694-2170-3/DL:T. 1039-2011

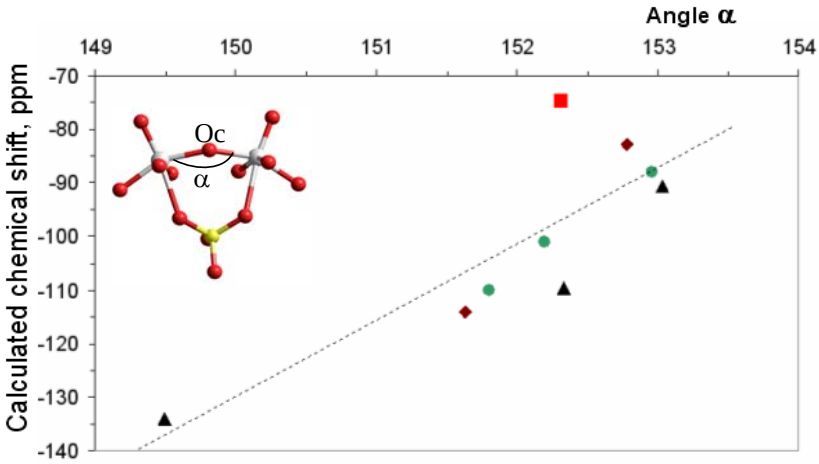

Figure 1. Plot between the calculated chemical shifts and angle α W-O_c-W at corner sharing oxygen atom for α-$XW_{12}O_{40}^{q-}$ (X: ◆ for P, As; ●: for Si, Si (DMF), Ge; ▲: B, Al, Ga; ■: Zn)

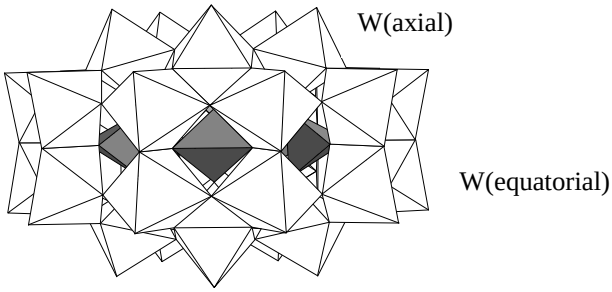

Figure 2. Polyhedral representation for Preyssler Anion $[MP_5W_{30}O_{110}]^{q-}$

UNIVERSITAT ROVIRA I VIRGILI
ASSEMBLY AND PROPERTIES OF POLYOXOMETALATES: A THEORETICAL POINT OF VIEW
Laia Vilà Nadal
ISBN.978-84-694-2170-3/DL:T. 1039-2011

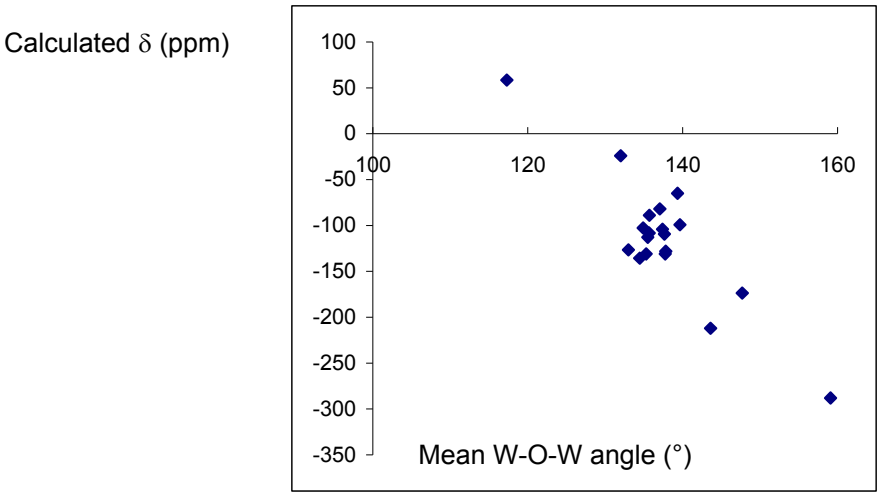

Anion	Mean angle[a]	Chemical Shift, δ (ppm)
α–GeW12	137.05	-82
α–AlW12	135.5	-113
α–PW12	139.65	-99
α–AsW12	139.35	-65
α–BW12	135.3	-131
α–GaW12	135.7	-89
α–SiW12	137.4	-104
β–SiW12	134.9	-102.6
	137.65	-109.5
	137.75	-130.9
γ–SiW12	114.3	Not considered
	135.68	-108.1
	133	-126.6
	134.45	-135.8
P2W18 (Wa)	137.8	-128.1
(Wb)	147.7	-173.8
W6	117.3	58.6
W10 (Wa)	117.3	
(Wb)	132	-24

[a] Average of the four equatorial W-O-W angles for each tungsten centre.

Figure 3. Correlation between mean equatorial W-O-W (computed) and ^{183}W NMR chemical shift (experimental).

UNIVERSITAT ROVIRA I VIRGILI
ASSEMBLY AND PROPERTIES OF POLYOXOMETALATES: A THEORETICAL POINT OF VIEW
Laia Vilà Nadal
ISBN.978-84-694-2170-3/DL:T. 1039-2011

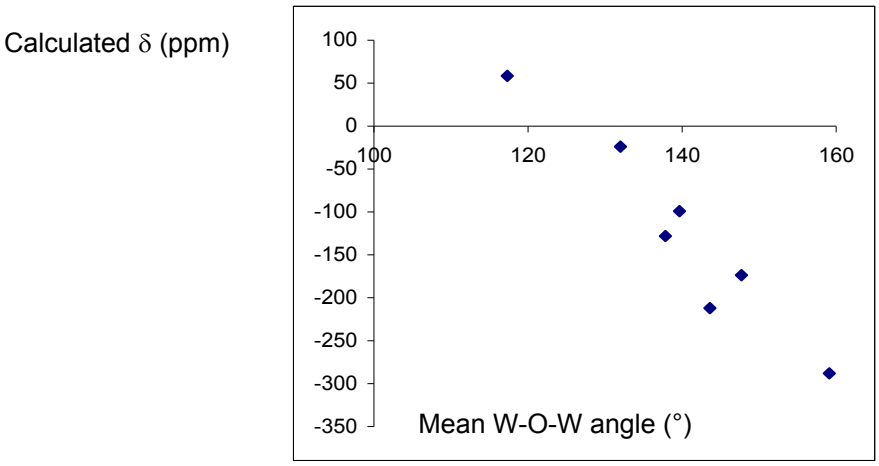

Figure 4. Correlation between mean equatorial W-O-W (computed) and ^{183}W NMR chemical shift (experimental) considering isopolyanions and only containing phosporous heteropolyanions.

Table 1. Structural parameters and ^{183}W NMR chemical shifts for several polyoxotungstates.

Anion[a]	Corner - sharing links	W-O-W[b]	δ-calc	δ-expt
W_6	0	117.3	+65.1	+58.9
W_{10} (belt)	1	132	-8.6	-23
α-PW_{12}	2	139.6	-114.6	-99
P_2W_{18} (cap)	2	137.8	-126.0	-128.1
P_2W_{18} (belt)	3	147.8	-170.0	-173.1
NaP_5W_{30} (equat)[c]	3	143.6	---	-212
NaP_5W_{30} (axial) [c]	4	159.1	---	-288

[a] Anions are given with the short-hand notation without oxygens and charge [b] Average of the four equatorial W-O-W angles for each tungsten centre. [c] Average angles for the Preyssler anion (Figure S2) were taken from a previous structure computed using TZP + COSMO geometry under the restrictions of D_{5d} symmetry group (40).

Table 2. The calculated ^{183}W shielding (σ), geometrical parameters and atomic charges.[a)]

X		B1	B2	B2 + COSMO
B	Σd_{W-O}	11.884	11.829	11.807
	q	2.331	2.379	2.389
	σ	2588.0	2657.7	2684.0
Al	Σd_{W-O}	11.820	11.767	11.752
	q	2.301	2.350	2.366
	σ	2557.7	2630.2	2660.4
Ga	Σd_{W-O}	11.803	11.762	11.743
	q	2.298	2.360	2.378
	σ	2509.5	2611.5	2641.3
Si	Σd_{W-O}	11.875	11.826	11.816
	q	2.322	2.364	2.377
	σ	2573.6	2632.1	2651.2
Ge	Σd_{W-O}	11.843	11.787	11.777
	q	2.319	2.356	2.372
	σ	2545.5	2605.3	2631.1
P	Σd_{W-O}	11.938	11.899	11.89
	q	2.322	2.358	2.369
	σ	2584.5	2634.3	2653.1
As	Σd_{W-O}	11.875	11.844	11.836
	q	2.310	2.340	2.352
	σ	2548.8	2600.6	2621.8
Zn	Σd_{W-O}	11.788	11.742	11.713
	q	2.270	2.316	2.333
	σ	2524.0	2595.0	2632.0

a) Total shielding σ computed with a TZP basis sets including SO (vacuum) using geometries obtained at different levels: B1 means geometry optimized with a TZP basis set; B2 with a QZ4P basis set and B2+ COSMO means that the geometry was computed with the QZ4P basis set in aqueous solution.

Table 3. Energies in eV at the B2+COSMO//B2+COSMO level.

Anion	Solvent	E (eV)
α–$[BW_{12}O_{40}]^{5-}$	H_2O	-448.467
α–$[AlW_{12}O_{40}]^{5-}$	H_2O	-447.269
α–$[GaW_{12}O_{40}]^{5-}$	H_2O	-473.208
	H_2O	-455.552
α–$[SiW_{12}O_{40}]^{4-}$	DMF	-473.985
α–$[GeW_{12}O_{40}]^{4-}$	H_2O	-451.115
α–$[PW_{12}O_{40}]^{3-}$	H_2O	-457.815
α–$[AsW_{12}O_{40}]^{3-}$	H_2O	-453.018
α–$[ZnW_{12}O_{40}]^{6-}$	H_2O	-431.354
	H_2O	-474.099
β–$[SiW_{12}O_{40}]^{4-}$	DMF	-473.820
γ–$[SiW_{12}O_{40}]^{4-}$	DMF	-473.302
$[P_2W_{18}O_{62}]^{6-}$	H_2O	-727.230
$[W_{10}O_{32}]^{4-}$	DMF	-379.452
$[W_6O_{19}]^{2-}$	DMF	-224.843

UNIVERSITAT ROVIRA I VIRGILI
ASSEMBLY AND PROPERTIES OF POLYOXOMETALATES: A THEORETICAL POINT OF VIEW
Laia Vilà Nadal
ISBN.978-84-694-2170-3/DL:T. 1039-2011

Table 4. Calculated 183W chemical shieldings for □-$[XW_{12}O_{40}]^{n-}$ Keggin anions. Calculated values at B1+SO+COSMO//B2+COSMO.

Shift ppm	α–$[BW_{12}O_{40}]^{5-}$	α–$[AlW_{12}O_{40}]^{5-}$	α–$[GaW_{12}O_{40}]^{5-}$	α–$[SiW_{12}O_{40}]^{4-}$	α–$[GeW_{12}O_{40}]^{5-}$	α–$[PW_{12}O_{40}]^{3-}$	α–$[AsW_{12}O_{40}]^{3-}$	α–$[ZnW_{12}O_{40}]^{5-}$	$[WO_4]^{2-}$
δ_{exp}	-131	-113	-89	-104	-82	-99	-65	-95.8	0
σ_p	-6773.2	-6799,2	-6818.3	-6791.2	-6815.4	-6782.5	-6816.9	-6841.9	-6944.9
σ_d	9655.6	9656.0	9656.0	9656.2	9656.3	9656.3	9656.5	9656.9	9661.9
σ_{so}	-207.2	-206.0	-206.0	-213.8	-211.8	-218.7	-215.6	-207.1	-175.8
σ_{total}	2675.2	2650.8	2631.7	2651.2	2629.1	2655.2	2624.0	2615.8	2541.1
δ_{cal}	-134.1	-109.7	-90.6	-110.1	-88.0	-114.1	-82.9	-74.7	0

Table 5. Calculated 183W chemical shieldings for several polianions. Calculated values at B1+SO+COSMO//B2+COSMO.

Shift ppm	α–$[SiW_{12}O_{40}]^{4-}$	α–$[SiW_{12}O_{40}]^{4-}$	β–$[SiW_{12}O_{40}]^{4-}$			β–$[SiW_{12}O_{40}]^{4-}$			γ–$[SiW_{12}O_{40}]^{4-}$			
Solvent	H_2O	DMF	H_2O			DMF			DMF			
			Wa	Wb	Wc	Wa	Wb	Wc	Wa	Wb	Wc	Wd
δ_{exp}	-104	-92.1	-129.8	-114.5	-110.0	-120.5	-104.0	-103.5	-160.1	-104.7	-116.8	-127.4
σ_p	-6791.2	-6799.3	-6768.4	-6784.1	-6800.9	-6768.4	-6784.5	-6801.2	-6772,0	-6788,9	-6775,0	-6756,9
σ_d	9656.2	9656.3	9656.4	9656.4	9656.1	9656.4	9656.4	9656.1	9657,0	9656,3	9656,4	9656,5
σ_{so}	-213.8	-214.3	-215.2	-220.4	-210.3	-215.2	-220.4	-210.3	-188,3	-217,3	-212,8	-221,8
σ_{total}	2651.2	2642.7	2672.7	2651.9	2644.9	2672.8	2651.5	2644.6	2696,7	2650,1	2668,6	2677,8
δ_{cal}	-110.1	-101.0	-133.3	-111.9	-103.0	-130.9	-109.5	-102.6	-154.7	-108.1	-126.6	-135.8

UNIVERSITAT ROVIRA I VIRGILI
ASSEMBLY AND PROPERTIES OF POLYOXOMETALATES: A THEORETICAL POINT OF VIEW
Laia Vilà Nadal
ISBN.978-84-694-2170-3/DL:T. 1039-2011

Table 6. Calculated ^{183}W chemical shieldings for several polianions. Calculated values at B1+SO+COSMO//B2+COSMO.

Shift ppm	$[P_2W_{18}O_{62}]^{6-}$		$[W_{10}O_{32}]^{4-}$		$[W_6O_{19}]^{2-}$	$[WO_4]^{2-}$	
Solvent	H_2O		DMF		DMF	H_2O	DMF
	Wa	Wb	Wa	Wb			
δ_{exp}	-128.1	-173.8	-166	-23	+58.9	0	0
σ_p	-6773.2	-6710.3	-6777.9	-6904.4	-7021.4	-6944.9	-6944.1
σ_d	9656.4	9655.9	9657.5	9656.6	9657.1	9661.9	9661.9
σ_{so}	-215.5	-233.7	-166.2	-201.6	-158.8	-175.8	-175.8
σ_{total}	2667.8	2711.8	2713.4	2550.6	2476.9	2541.1	2542.0
δ_{cal}	-126.0	-170.0	-171.4	-8.6	+65.1	0	0

Table 7. Calculated ^{183}W chemical shieldings for α–$[SiW_{12}O_{40}]^{4-}$ at B1+SO+COSMO//Exp. level. The experimental structure is deposited at CCDB under the code KIDWIE (J. Liu, Y. Li, E. Wang, D. Xiao, L. Fan, Z. Zhang, Y. Wang *J. Mol. Struct.*, **2007**, 837, 237-244.)

	σ_p	σ_d	σ_{so}	σ_{total}	δ_{cal}	δ_{exp}	δ_{exp}–δ_{cal}
W1	-6665,7	9655,5	-206,5	2783,2	-242.1	-104	138.3
W2	-6618,1	9655,3	-207,6	2829,5	-288.4	-104	184.6
W3	-6698,7	9655,7	-210,1	2746,9	-205.8	-104	102.0
W4	-6698,6	9655,6	-209,4	2747,6	-206.5	-104	102.7
W5	-6718,1	9655,8	-208,5	2729,2	-188.1	-104	84.3
W6	-6691,3	9655,9	-208,8	2755,8	-214.7	-104	110.9
W7	-6700,3	9655,8	-212,0	2743,5	-202.3	-104	98.5
W8	-6720,0	9655,3	-210,0	2725,3	-184.2	-104	80.4
W9	-6748,9	9655,9	-209,4	2697,6	-156.4	-104	52.6
W10	-6650,9	9655,5	-210,6	2793,9	-252.8	-104	149.0
W11	-6674,5	9655,5	-209,4	2771,6	-230.5	-104	126.7
W12	-6633,9	9655,6	-208,2	2813,4	-272.3	-104	168.5
				$\bar{X}$ (δ_{cal})	-220.3	$\bar{X}$ (δ_{cal})–δ_{exp}	116.5

UNIVERSITAT ROVIRA I VIRGILI
ASSEMBLY AND PROPERTIES OF POLYOXOMETALATES: A THEORETICAL POINT OF VIEW
Laia Vilà Nadal
ISBN.978-84-694-2170-3/DL:T. 1039-2011

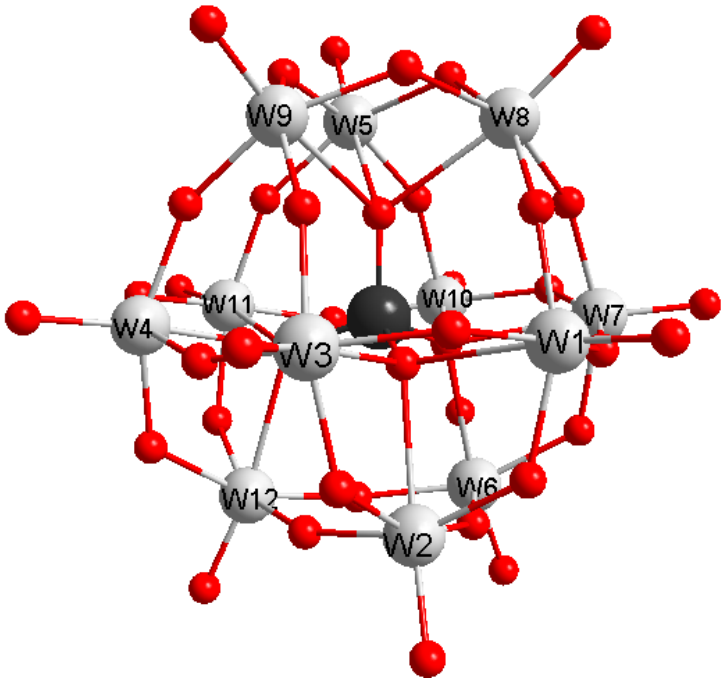

Figure 5. Ball-and-stick representation for α–$[SiW_{12}O_{40}]^{4-}$. Tungsten atoms labels correspond to σ and δ signals in Table 1.

UNIVERSITAT ROVIRA I VIRGILI
ASSEMBLY AND PROPERTIES OF POLYOXOMETALATES: A THEORETICAL POINT OF VIEW
Laia Vilà Nadal
ISBN.978-84-694-2170-3/DL:T. 1039-2011

UNIVERSITAT ROVIRA I VIRGILI
ASSEMBLY AND PROPERTIES OF POLYOXOMETALATES: A THEORETICAL POINT OF VIEW
Laia Vilà Nadal
ISBN.978-84-694-2170-3/DL:T. 1039-2011